



Poznan University of Medical Sciences
Poland

JMS *Journal of Medical Science*

previously *Nowiny Lekarskie*

Founded in 1889

2022
Vol. 91, No. 4

QUARTERLY

Indexed in:

DOAJ, Crossref, Google Scholar,
Polish Medical Bibliography, Index Copernicus,
Ministry of Education and Science

eISSN 2353-9801
ISSN 2353-9798
DOI: 10.20883/ISSN.2353-9798

www.jms.ump.edu.pl

EDITOR-IN-CHIEF

Jarosław Walkowiak

EDITORIAL BOARD

David Adamkin, USA
Sofio Bakhtadze, Georgia
Adrian Baranchuk, Canada
Paolo Castiglioni, Italy
Ewelina Chawłowska, Poland
Agata Czajka-Jakubowska, Poland
Jan Domaradzki, Poland
Piotr Eder, Poland
Michael Gekle, Germany
Krzysztof Greberski, Poland
Karl-Heinz Herzig, Finland
Mihai Ionac, Romania
Paweł P. Jagodziński, Poland
Jerzy Jankun, USA
Lucian Petru Jiga, Germany
Nataliya Kashirskaya, Russia
Berthold Koletzko, Germany
Stan Kutcher, Canada
Tadeusz Malinski, USA
Piotr Myśliwiec, Poland
Talgat Nurgozhin, Kazakhstan
Marcos A. Sanchez-Gonzalez, USA
Georg Schmidt, Germany
Mitsuko Seki, Japan
Puneet Sindhvani, USA
Elżbieta Skorupska, Poland
Rafał Staszewski, Poland
Tomasz Szczapa, Poland
Jerzy P. Szaflarski, USA
Sebastian Szubert, Poland
Natallia Tsikhan, Belarus
Dariusz Walkowiak, Poland
Przemysław Zalewski, Poland

ASSOCIATE EDITORS

Agnieszka Bienert
Ewa Mojs
Adrianna Mostowska
Nadia Sawicka-Gutaj

SECTION EDITORS

Jaromir Budzianowski – Pharmaceutical Sciences
Paweł P. Jagodziński – Basic Sciences
Joanna Twarowska-Hauser – Clinical Sciences

LANGUAGE EDITORS

Margarita Lianeri, Canada
Jacek Żywiczka, Poland

STATISTICAL EDITOR

Magdalena Roszak, Poland

SECRETARIAT ADDRESS

27/33 Szpitalna Street, 60-572 Poznań, Poland
phone: +48 618491432, fax: +48 618472685
e-mail: jms@ump.edu.pl
www.jms.ump.edu.pl

DISTRIBUTION AND SUBSCRIPTIONS

70 Bukowska Street, 60-812 Poznań, Poland
phone/fax: +48 618547414
e-mail: sprzedazwydawnictw@ump.edu.pl

PUBLISHER

Poznan University of Medical Sciences
10 Fredry Street, 61-701 Poznań, Poland
phone: +48 618546000, fax: +4861852 04 55
www.ump.edu.pl

© 2022 by respective Author(s). Production and hosting
by Journal of Medical Science (JMS)

This is an open access journal distributed under
the terms and conditions of the Creative Commons
Attribution (CC BY-NC) licence

eISSN 2353-9801

ISSN 2353-9798

DOI: 10.20883/ISSN.2353-9798

Publishing Manager: Grażyna Dromirecka

Technical Editor: Bartłomiej Wąsiel



WYDAWNICTWO NAUKOWE
UNIWERSYTETU MEDYCZNEGO
IM. KAROLA MARCINKOWSKIEGO
W POZNANIU

60-812 Poznań, ul. Bukowska 70
tel./fax: +48 618547151
www.wydawnictwo.ump.edu.pl

Ark. wyd. 15,4. Ark. druk. 13,5.
Zam. nr 186/23.

The Editorial Board kindly informs that since 2014 *Nowiny Lekarskie* has been renamed to *Journal of Medical Science*.

The renaming was caused by using English as the language of publications and by a wide range of other organisational changes. They were necessary to follow dynamic transformations on the publishing market. The Editors also wanted to improve the factual and publishing standard of the journal. We wish to assure our readers that we will continue the good tradition of *Nowiny Lekarskie*.

You are welcome to publish your basic, medical and pharmaceutical science articles in *Journal of Medical Science*.

Ethical guidelines

The Journal of Medical Science applies the ethical principles and procedures recommended by COPE (Committee on Conduct Ethics), contained in the Code of Conduct and Best Practice Guidelines for Journal Editors, Peer Reviewers and Authors available on the COPE website: <https://publicationethics.org/resources/guidelines>

CONTENTS

ORIGINAL PAPERS

- Moath Refat, Anes A.M., Hesham Siddick, Abdul-Rahman, Mohammed Sharah, Abdul-baqi A. Thabet, Manar Refat, Aiman Saleh A. Mohammed, Ahmed Al-Sabati*
Formulation and evaluation of Yemeni potash alum as hydrophilic topical preparations against bacterial skin infections 235
- Dženan Kovačić, Adna Salihović*
Multi-epitope mRNA Vaccine Design that Exploits Variola Virus and Monkeypox Virus Proteins for Elicitation of Long-lasting Humoral and Cellular Protection Against Severe Disease 247
- Polo-Ma-Abiele Hildah Mfengwana*
Mutagenic and antimutagenic evaluation of *Asparagus larycinus* Burch., *Senecio asperulus* DC., and *Gunnera perpensa* L. to hepatic cells 266
- Martin Pola, Hana Kolarova, Robert Bajgar*
Generation of singlet oxygen by porphyrin and phthalocyanine derivatives regarding the oxygen level 278
- Oluwaseyi Bamisaye, Anthony Fashina, Fatai Abdulraheem, Olufemi Emmanuel Akanni, Fadiora S. Olufemi*
Genotoxic and chemopreventive potentials of ethanol leaves extract of *Annona muricata* on *N-Ethyl-N-Nitrosourea*-induced pro-leukaemia carcinogen in mice model by bone marrow micronucleus assay 287

REVIEW PAPERS

- Piotr Włodarczyk, Mikołaj Witczak, Agnieszka Gajewska, Tomasz Chady, Igor Piotrowski*
The role of TDP-43 protein in amyotrophic lateral sclerosis 296
- Chi-Kwan Leung*
An overview of cord blood stem cell transplantation in Hong Kong. 309
- Dawid Łażewski, Marek Murias, Marcin Wierzychowski*
Pegylation – in search of balance and enhanced bioavailability 321

IMAGES IN CLINICAL MEDICINE

- Sweta Subhadarshani, Anisha P. Valluri*
A case of symmetrical drug-related intertriginous and flexural exanthema 333
- Instructions for Authors 335

Formulation and evaluation of Yemeni potash alum as hydrophilic topical preparations against bacterial skin infections

Moath Refat

Department of Biochemistry and Molecular Biology, The Key Laboratory of Environment and Genes Related to Disease of Ministry of Education, Health Science Center, Xi'an Jiaotong, University, China

College of Pharmacy, University of Science and Technology, Al-Hodeidah, Yemen

 <https://orcid.org/0000-0003-4017-9052>

Corresponding author: moath.refat@hotmail.com

Anes A.M.

Thabit College of Pharmacy, University of Science and Technology, Al-Hodeidah, Yemen

Pharmacy department, Al-Razi University, Sana'a, Yemen

 —

Hesham Siddick

College of Pharmacy, University of Science and Technology, Al-Hodeidah, Yemen

 —

Abdul-Rahman

Maqbol College of Pharmacy, University of Science and Technology, Al-Hodeidah, Yemen

 —

Mohammed Sharah

College of Pharmacy, University of Science and Technology, Al-Hodeidah, Yemen

 —

Abdul-baqi A. Thabet

College of Medical Sciences, University of Science and Technology, Al-Hodeidah, Yemen

 —

Manar Refat

College of Medical Sciences, University of Science and Technology, Al-Hodeidah, Yemen

 —

Aiman Saleh A. Mohammed

Department of Pharmacology, Faculty of Pharmacy, University of Aden, Aden, Yemen

 —

Ahmed Al-Sabati

College of Pharmacy, University of Science and Technology, Al-Hodeidah, Yemen

College of Pharmacy, Sana'a University, Sana'a, Yemen

 —

 doi: 10.20883/medical.e713

Keywords: Potassium Alum, Yemen's Alum, Anti-bacterial, Topical Preparations, Skin and soft tissue infections

Published: 2022-11-14

How to Cite: Refat M, Thabit AA, Siddick H, Sharah M, Thabet AA, Refat M, Mohammed ASA, Al-Sabati A. Formulation and evaluation of Yemeni potash alum as hydrophilic topical preparations against bacterial skin infections: Yemeni potash alum's topical preparations against bacterial skin infections. Journal of Medical Science. Ahead of Print. doi:10.20883/medical.e713



© 2022 by the author(s). This is an open access article distributed under the terms and conditions of the Creative Commons Attribution (CC BY-NC) license. Published by Poznan University of Medical Sciences

ABSTRACT

Skin and soft tissue infections are common. *Staphylococcus aureus*, *Streptococcus pyogenes*, *Escherichia coli*, and *Pseudomonas aeruginosa* cause most bacterial skin infections. Yemen's alum is a natural mineral with potent antibacterial and antifungal activity. The current study aimed to verify Yemen alum's antibacterial activity against chosen bacterial strains to formulate a valuable topical preparation. We formulated twenty-three formulations involving four non-adjusted aqueous solutions, eight adjusted pH aqueous solutions, three Oil/Water cream formulations, and eight glycerin solutions, all with different alum con-

centrations. After that, we evaluated the antibacterial efficacy against the selected bacterial strains. Additionally, we performed stability testing (almost six weeks) to determine the chosen preparations' estimated shelf life (t90). Alum showed antibacterial activity against *Staphylococcus aureus*, *Streptococcus pyogenes*, *Escherichia coli*, and *Pseudomonas aeruginosa*. Finally, it was concluded that Oil/Water cream (10% alum) is viable preparation for large-scale production.

Introduction

Skin and soft tissue infections (SSTIs) are common. It ranges from uncomplicated superficial infections to severe necrotizing infections of the skin and the underlying subcutaneous tissues and muscles. Its incidence exceeds approximately 7% of patients admitted to hospitals, two folds of urinary tract infections, and tenfold of pneumonia, counting around 6.3 million medical consultations annually [1, 2]. Despite SSTIs being often superficial and mild, it may be just a matter of days to turn into a systemic infection, extremely invasive or potentially lethal, particularly in immunosuppressed patients [1, 3]. Given the variety and multiplicity of pathogenic strains [4] in SSTIs, clinicians utilize broad-spectrum antimicrobials to ensure the most effective eradication. However, incorrect diagnosis, which accounts for 35.2% of cases reported by specialists compared to 30.2% of patients confirmed to have dermatoses such as skin infections, can dramatically exacerbate antibiotic resistance [5]. In addition, overusing antimicrobials for unconfirmed cases may produce multidrug-resistant bacteria [6, 7].

The infectious incidence of several bacterial species has increased, and some species are resistant to antibacterial drugs. The risk of acute infections is associated with substantial morbidity and death, especially in diabetes individuals [8]. *Staphylococcus aureus* and *Streptococcus pyogenes* are the most common gram-positive bacteria to infect the skin. They cause impetigo, erysipelas, and cellulitis [9]. *Klebsiella pneumonia* is a gram-negative bacterium that apart from skin infections also causes eye, brain, lung, liver, and genitourinary infections [10]. *Pseudomonas aeruginosa* is also gram-negative bacteria. It is associated with ear, lung, urinary tract, and skin infections [11].

Alum is a naturally occurring sulfate mineral rock that generally forms from the oxidation

of potassium- and sulfide-containing minerals [12–14]. Using alum at a concentration of 4% can provide astringent effects [15, 16]. In addition, it is believed to shrink pores and minimize fluid discharges, thus used to relieve nosebleeds, haemorrhoids, and internal organ bleeding [15, 17, 18]. As FDA awarded alum category I ingredient in mouthwashes [20, 21], it has been used as an antiseptic mouthwash [17–19] to treat oral and gingival ulcers, gingivitis, and mucositis.

Alum can be found abundantly in the form of white sedimentary rocks containing aluminium in numerous mountain caves across Yemen governorates, including Amran. Yemeni natives have utilized alum as a deodorant, an astringent, and an aftershave. Furthermore, it has been used to purify water in rural areas due to its antibacterial properties, which help rid the water of bacterial contamination and make it suitable for drinking and bathing. In our previous study [22], we formulated topical skin preparations utilizing Aluminium Potassium Sulphate (Yemen's Alum), which were evaluated against various topical fungal infections. In this study, we will evaluate the effectiveness of these preparations against various topical bacterial infections.

Materials and Methods

Materials

Yemen's alum was gathered from its source. It occurs naturally as a rock-form precipitate in some mountains' caves in "Amran Governorate – Maswar District" and various governorates and districts in Yemen. Bacterial specimens of *Staphylococcus aureus* (SH1000), *Streptococcus pyogenes* (M1T1), *Klebsiella pneumonia* (ATCC 700603), and *Pseudomonas aeruginosa* (PAO1) have been brought from the central research Laboratory at Sana'a University. Other materials were: Mueller Hinton agar, sodium hydroxide

pellets, sodium sulfide, tartaric acid, dithizone, sodium lauryl sulfate and sodium acetate (Himedia, India), blood agar base (Conda, Spain), hydrochloric acid, sodium carbonate, paraffin wax (Uni-Chem, Serbia), barium chloride, ammonium hydroxide, zinc sulfate (ngec chemicals), EDTA disodium salt (acme-chemicals, India), ammonium acetate (E. Merck, India), glacial acetic acid (Al-Arifi medical, Yemen), ethanol (YSCO, Yemen), boric acid (El.nasr pharmaceutical chemicals co, Egypt), glycerin (Qualikems, India), paraffin oil (YSCO, Yemen), white petrolatum jelly (Optika, Yemen), ciprofloxacin cream 0.5 % (Ciplox®, Cip-

la, India, b.n.:g588), ciprofloxacin infusion 2 mg/mL (ciplox®, Cipla, India, b.n.:zc2051).

Methods

A flowchart in **Figure 1** makes it easier to understand this research better. The figure is recreated based on a comparable one in the previous research, considering any necessary modifications. There were four stages of experimentation, each of which was broken into multiple sub-stages. As numerous experiments were discussed in our previous study, and as they were fully detailed in our previous article [22], we will not detail them

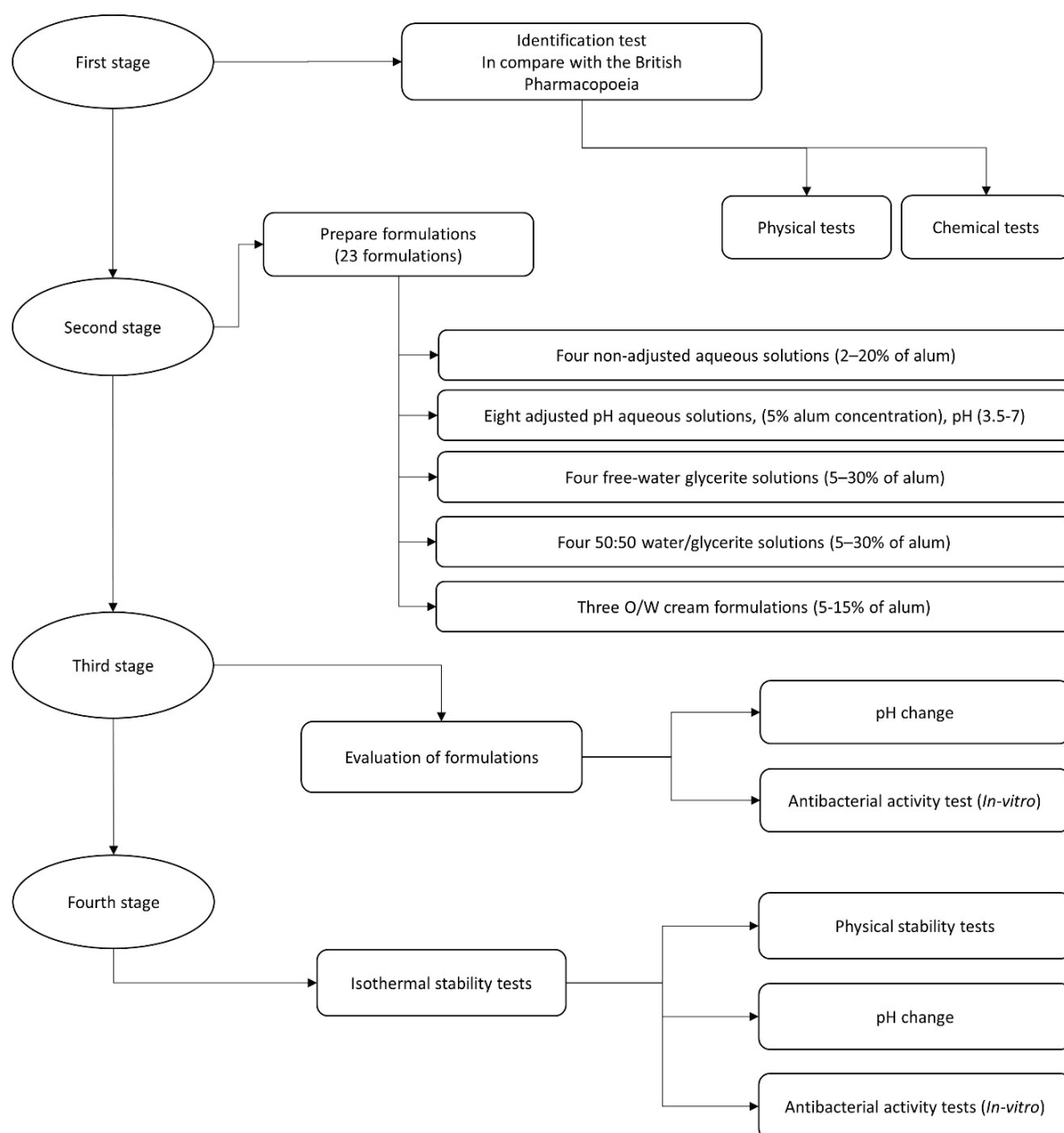


Figure 1. Experimental work flowchart

again here. We have chosen only to discuss the new experiments. Please refer to our previous article for further details.

Formulation of Alum preparations

Non-adjusted pH aqueous solutions

Alum powder with a particle size ranging between 180–250 μm was dissolved in water with continuous stirring and filtering (the simple solution method) to prepare four aqueous solutions with various alum concentrations, including A1 (2%), A2 (5%), A3 (10), and A4 (20%), as shown in **Table 1**.

Table 1. Ingredients and their quantities to prepare 100 ml of non-adjusted pH aqueous alum solutions

Ingredient	A ₁	A ₂	A ₃	A ₄
Alum (g)	2	5	10	20
Water up to (mL)	100	100	100	100

Adjusted pH aqueous solutions

A similar concentration of alum (5%) was used to make eight aqueous alum solutions, as was previously stated. As stated in **Table 2**, borate buffer was used to adjust the pH between 3.5 to 7. The primary goal of adjusting the pH of the solutions was to find the pH of maximal alum activity at different pH levels.

Glycerin solutions

Eight alum's glycerin solutions were prepared using a shaker water bath at 70°C with different (water: glycerin) co-solvent ratios. The preparations included four water-free glycerin solutions: G1(5%), G2(10%), G3(20%) and G4(30%), as well as

four 50:50 (water: glycerin) solutions: Gw1(5%), Gw2(10%), Gw3(20%), Gw4(30%). **Table 3** indicates all formulations' concentrations.

O/W creams

Three O/W cream formulations with various alum concentrations were prepared by the fusion method; the formulations were C1 (5%), C2 (10%), and C3 (15%). **Table 4** refers to the amount of each formulation in detail.

Table 4. Ingredients and their quantities (g) to prepare 100 g of semisolid O/W cream formulation of alum

Ingredient	C ₁	C ₂	C ₃
Alum	5	10	15
Glycerin	12.3	11.7	11.05
liquid paraffin	0.95	0.90	0.85
Sodium lauryl sulfate	0.95	0.90	0.85
Paraffin wax	9.5	9	8.5
White petrolatum jelly	23.75	22.50	21.25
Water	47.55	45	42.5

Evaluation of the antibacterial activity of the alum preparations

Culture medium preparation

Mueller Hinton agar

Molar Hinton agar powder (38 g) was added to 1000 mL of water, which was heated until boiling over a flame and then cooled at room temperature (around 5 minutes). The heating/cooling cycle has been done thrice to obtain total solubility and proper sterilization. Finally, the mixture was cooled to 40°C, and then 25 mL of it was

Table 2. Ingredients and their quantities to prepare 100 ml of adjusted pH aqueous alum solutions

Formulation	A _{A1}	A _{A2}	A _{A3}	A _{A4}	A _{A5}	A _{A6}	A _{A7}	A _{A8}
pH	3.5	4	4.5	5	5.5	6	6.5	7
Ingredient								
Alum (g)	5	5	5	5	5	5	5	5
Boric acid buffer pH 10.4 (mL)	-	7.5	17.5	22.5	26.5	30	33.5	35
Water Up to (mL)	100	100	100	100	100	100	100	100

Table 3. Ingredients and their quantities to prepare 100 mL of glycerin-alum solutions

Ingredient	G ₁	G ₂	G ₃	G ₄	G _{w1}	G _{w2}	G _{w3}	G _{w4}
Alum (g)	5	10	20	30	5	10	20	30
Water	-	-	-	-	50	50	50	50
Glycerin up to (mL)	100	100	100	100	100	100	100	100

poured into separate sterile Petri dishes, carefully capped, and left to solidify.

Blood agar

Blood agar powder (40 g) was added to 1000 mL of water, boiled using a flame, and then cooled at room temperature (about 5 minutes). The heating/cooling cycle has been done thrice to obtain complete solubility and proper sterilization. Eventually, the mixture was cooled to 40°C, and then 25 mL of it was poured into separate sterile Petri dishes, carefully capped, and left to solidify.

Specimen collection and culturing

Four pathogenic bacterial specimen types were collected, including *Staphylococcus aureus*, *Streptococcus pyogenes*, *Klebsiella pneumoniae*, and *Pseudomonas aeruginosa*. *Escherichia coli*, *Staphylococcus aureus*, and *Pseudomonas aeruginosa* were cultured in the Mueller Hinton agar, But *Streptococcus pyogenes* were cultured in Blood agar. For culturing on plate culture, a sterile loop was used to spread bacterial specimens as parallel lines on a plate culture, with the plate being rotated to facilitate spreading.

Testing for the antibacterial activity

The antibacterial activity of the twenty-four formulations prepared previously was investigated on four different bacteria, including *staphylococcus aureus*, *Streptococcus pyogenes*, *Escherichia coli*, and *Pseudomonas aeruginosa*. The standard cup plate method [23] was utilized to investigate the antibacterial effect of alum in the formulation. We also tested positive control formulations with 150 µL ciprofloxacin 5% solution and 0.2 g ciprofloxacin 0.5% O/W cream throughout the inspection process and compared them to the aqueous and glycerin alum solutions or alum O/W cream formulations, respectively. The MIC of the antibacterial-containing preparation was determined utilizing the broth dilution method; then, MIC was estimated depending on the presence or absence of bacterial growth. Please check our prior research [22] for more details on this part..

Isothermal accelerated stability study

Alike the previously mentioned study, the successful three preparations A2 (5% alum aqueous solution), G2 (10% alum water-free glycerin solutions), and C2 (10% O/W cream) underwent an

isothermal stress stability test in an oven at 37°C, 50°C, and 75°C [25] for six weeks. Then, samples were taken from the stored preparations and assessed at 0, 1, 3, 4, and 6 weeks of storage. The assessment only assessed physical appearance, pH, and antibacterial activity against *Streptococcus pyogenes*. The degradation kinetics has been done previously in the former study. Please refer to our previously mentioned study [22] for more details.

Data analysis

All data were analyzed, and graphs were generated using GraphPad Prism 8 software. The data were presented with appropriate replicates of each experiment, and one-way analysis of variance (ANOVA) with LSD posthoc test was used to compare statistical differences between the groups. Results are shown as (mean ± S.D., n = 3) compared with the control group. ***P ≤ 0.001, **P ≤ 0.01, *P ≤ 0.05, ns > 0.05.

Results and Discussion

With an increased need to find more powerful, and safe antibacterial drugs, many studies have been performed to reveal alum's activity against some types of bacterial infections [15, 17, 20, 21, 26–28], fungal infections [29, 30], and viral infections. Moreover, as a vaccine adjuvant [31, 32], the leishmania vaccine [33–36], and hepatitis vaccine [37, 38]. In their study, Kelber et al. [39] suggest various potential modes of action regarding alum antifungal and antibacterial activity. However, the alum's mechanism of action behind its fungicidal and bactericidal properties is still unclear [28].

In their study, K. Alzomor et al. aimed to formulate and evaluate different preparations of alum, including deodorant lotion and after-shaving astringent as cream and gel [21]. As shown in **Figure 1**, throughout the four stages of the study, we aimed to formulate and evaluate effective topical preparations of Yemen's potash alum against bacterial skin infections. We considered all the time that bacterial species in this study could cause invasive systemic bacterial infections. However, the relationship between these species is that they could begin as topical/mild infections and then transmit via the bloodstream into multiple tissues, including the brain, liver, lungs, kid-

ney, soft tissues, and others. Finally, this might cause life-threatening illness or patient death, with an overall case mortality rate overtaking 27% [40].

First of all – alum's verification – all findings met the British Pharmacopeia specifications, as depicted in **Table 5**. Kindly refer to our previously mentioned research [22] for more details.

Table 5. Potash alum identification tests

Test	Result
Physical aspects	Granular powder or translucent, colourless, crystalline bulk.
Solubility	Freely soluble in water, highly soluble in boiling water, soluble in glycerol, and almost insoluble in ethanol (96%).
Potassium detection	White precipitation crystals developed.
Sulfates detection	A white-coloured precipitate was formed.
Aluminium detection	A gelatinous, white precipitate that was insoluble in the excess reagent was produced.
Melting point (°C) range	93–95°C
pH Average (± S.D.; C.V.%)	3.2 (± 0.103; 3.22)

In the second stage, we prepared twenty-three formulations involving: four alum non-adjusted pH aqueous solutions (concentration between 2–20%); eight adjusted pH aqueous solutions (5% alum concentration and pH between 3.5–7); eight glycerin solutions (four water-free solutions, and four 50:50 water\glycerin solutions, alum concentration 5 to 30%); and three alum O/W cream preparations (concentration between 5–15%). Please refer to **Tables 1–4** in our earlier research for extra information on the second-stage results.

The evaluation of formulations was the topic of interest in the third research stage. The antibacterial activity of all the formulations was tested; accordingly, because of their antibacterial efficacy, only three preparations were involved in this stage. Concerning preparations pH, as the alum concentrations increased, a decrement of pH was observed in non-adjusted pH aqueous preparations and the glycerin solutions in water-free and water-contain glycerin, attributed to the acidic nature of the materials. As alum content rose from 5 to 10, the rate of pH decrement in water-free glycerin solutions varied, particularly compared to other preparations. In contrast, the pH of the O/W cream preparations was almost identical regardless of the alum concentration differences. For further details on the results of the third stage, kindly refer to **Tables 7–8** in our earlier research for more details.

The antibacterial activity of the twenty-four formulations prepared previously was investigated on four different bacteria, including *staphylococcus aureus*, *Streptococcus pyogenes*, *Escherichia coli*, and *Pseudomonas aeruginosa*. Alzomor et al. [21] reported that the MIC varied between 0.9 and 2 based on the bacterial type. However, as shown in **Figure 2**, for non-pH adjusted aque-

ous solutions, the 5% alum concentration (A2 formulation) had the lowest value of (MIC) with inhibition zones of ≥ 20 mm diameter in comparison to the ciprofloxacin (the positive control.). For adjusted pH aqueous alum solutions **Figure 3**, the antibacterial activity had dramatically declined at pH > 3.5 and almost vanished over pH 4. That was noticed against all the tested bacteria, where there was little action, demonstrating a clear relationship between the medium's pH and the alum's antibacterial effectiveness.

Likewise, among water-free glycerin solution in **Figure 4**, G2 (10% alum concentration) showed the MIC with inhibition zones of ≥ 20 mm diameter against all the tested bacteria. However, because of the instability of water-containing glycerin solutions, as alum crystals were remarkably observed shortly after the following storage at room temperature, all water-containing glycerin preparation was neglected despite MIC values. Conversely, the optimum MIC of the O/W cream formulations is shown with C2 (10 % alum concentration). As in **Figure 5**, the inhibition zone is ≥ 20 mm in diameter against all bacteria.

Similar to our former antifungal study, as referred to in the related **Tables 10–12** and **Figures 7–8, Supp. Fig. 2**, three preparations (A2, G2, and C2) were selected for the last stage to undergo isothermal stability testing. The physical stability and general appearance are incon-

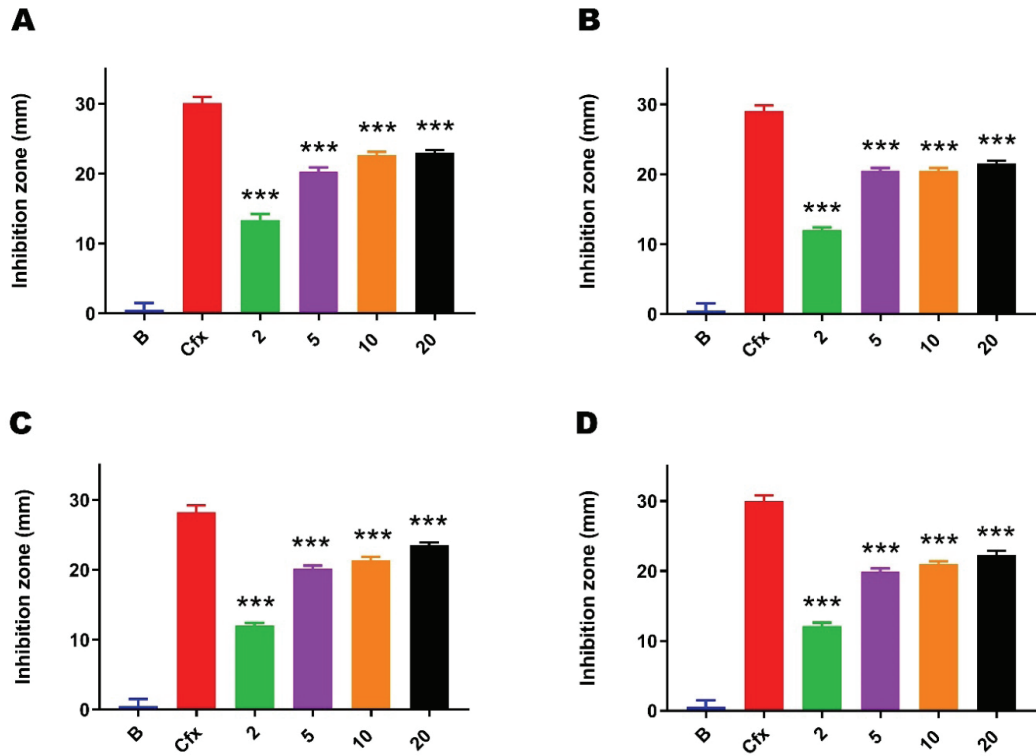


Figure 2. Antibacterial activity of non-adjusted pH aqueous alum solutions on (A) staphylococcus aureus, (B) Streptococcus pyogenes, (C) Escherichia coli, (D) Pseudomonas aeruginosa. Preparations included blank formulation, ciprofloxacin positive control, and alum formulations with different concentrations ranging (from 2%–20%). Results are shown as (mean \pm S.D., n=3) compared with the control group. ***P \leq 0.001, **P \leq 0.01, *P \leq 0.05, ns 0.05

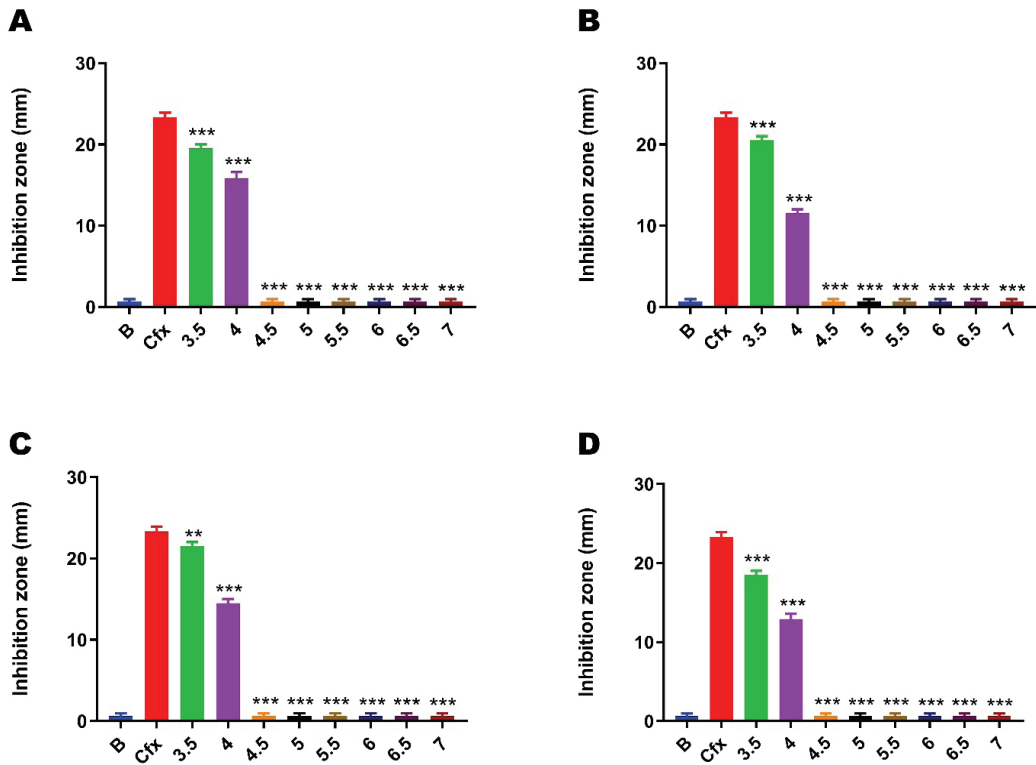


Figure 3. Antibacterial activity of adjusted pH (5%) aqueous solutions on (A) staphylococcus aureus, (B) Streptococcus pyogenes, (C) Escherichia coli, (D) Pseudomonas aeruginosa. Preparations included blank preparation, ciprofloxacin positive control, and alum formulation with eight different pH values ranging from 3.5–7. Results are shown as (mean \pm S.D., n=3) compared with the control group. ***P \leq 0.001, **P \leq 0.01, *P \leq 0.05, ns 0.05

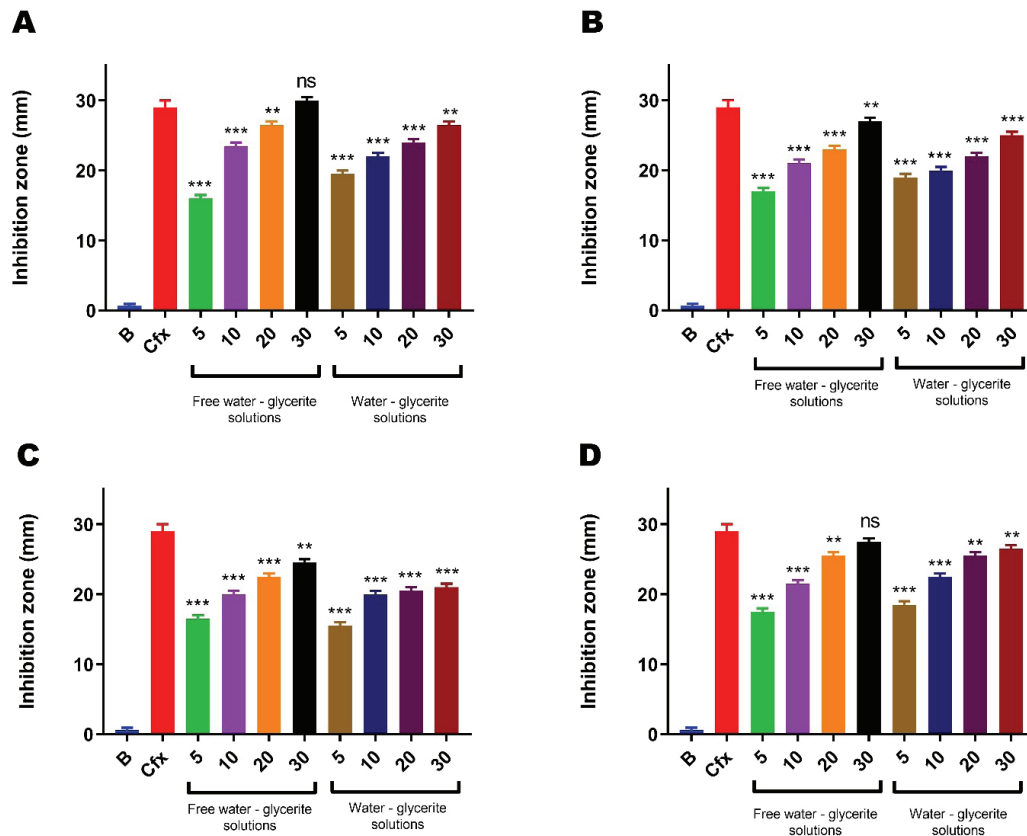


Figure 4. Antibacterial activity of glycerin preparations on (A) *Staphylococcus aureus*, (B) *Streptococcus pyogenes*, (C) *Escherichia coli*, (D) *Pseudomonas aeruginosa*. Preparations included blank formulation, ciprofloxacin positive control, and alum formulations with different concentrations ranging (from 5%–30%). Results are shown as (mean \pm S.D., n=3) compared with the control group. ***P \leq 0.001, **P \leq 0.01, *P \leq 0.05, ns 0.05

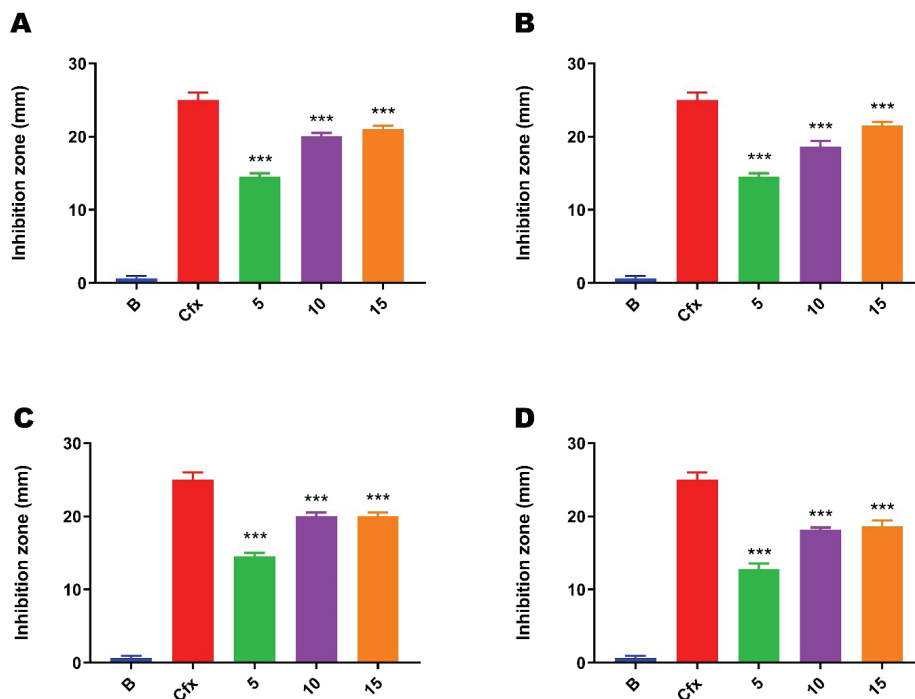


Figure 5. Antibacterial activity of cream preparations (A) *Staphylococcus aureus*, (B) *Streptococcus pyogenes*, (C) *Escherichia coli*, (D) *Pseudomonas aeruginosa*. Preparations included blank formulation, ciprofloxacin positive control, and alum formulations with different concentrations ranging (from 5%–15%). Results are shown as (mean \pm S.D., n=3) compared with the control group. ***P \leq 0.001, **P \leq 0.01, *P \leq 0.05, ns 0.05

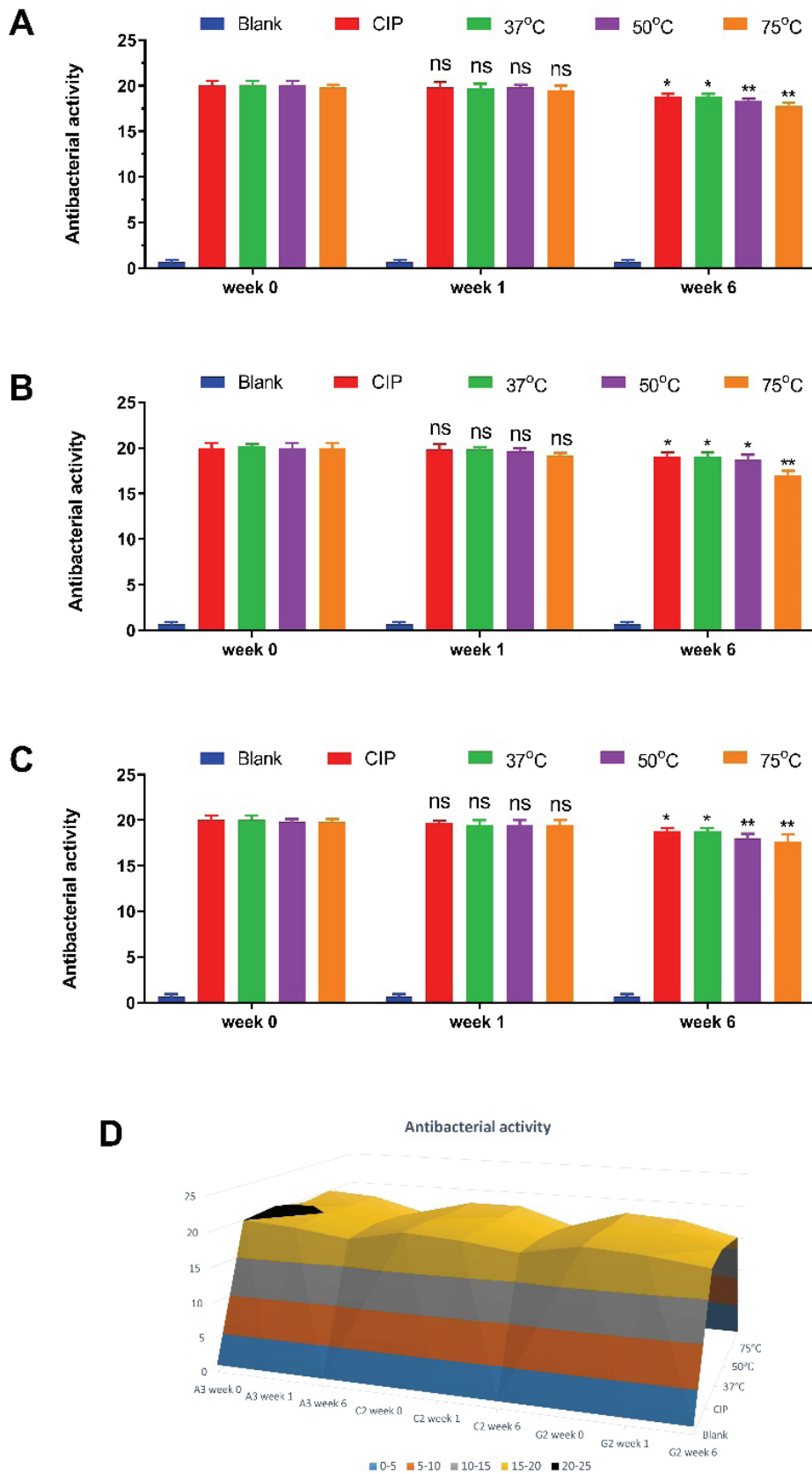


Figure 6. Stability study testing. Figures (A-C) show the antibacterial activity of aqueous formulations 5% (A2), O/W cream formulations 10% (C2), and glycerin formulations 10% (G2) on *Streptococcus pyogenes* during the stability study. Results are shown as (mean \pm S.D., n=3) compared with the control group. *** $P \leq 0.001$, ** $P \leq 0.01$, * $P \leq 0.05$, ns 0.05

sistent with what was observed by K. Alzomor et al. [21], no valuable changes were observed in all formulations at 37°C, as reported in **Table 6**. However, at 50°C and 75°C, the glycerin formulation and cream formulation exhibited patterns of physical instability as colour and odour change, in addition to phase separation for the latest one.

For preparations' pH, neither the cream preparations nor the aqueous solution exhibited a remarkable variation – for more details, please refer to **Figure 7** in our earlier research. In contrast, a considerable decrement in pH was seen in the glycerin preparation at the three-storage temperature. Furthermore, as in **Figure 6**, the antibacterial activity of the preparations showed no significant changes as expressed by the variation in the inhibition zone.

Regarding the degradation kinetics of alum in the stored formulation, as we discussed in our earlier study, the content (%) of alum remained in the aqueous solution, and its kinetic parameter revealed that alum exhibited first-order degradation with higher R^2 . Furthermore, the predicted shelf-life (t_{90}) of alum in that formulation determined from the Arrhenius plot was approximately two years. Similar findings were observed with the cream formulation and the glycerin formulation. According to the Arrhenius plot, the cream formulation predicted shelf-life (t_{90}) approximated 1.52 years. However, for the glycerin formulation, the t_{90} of alum was significantly shorter (0.16 years) – please refer to our earlier research for more details on this part.

Conclusion

To conclude, alum proved to have antibacterial activity. Therefore, the 10% alum O/W cream and 5% alum aqueous solution presented by this study are promising preparations for large-scale production as safe, stable hydrophilic topical preparations of Yemen's alum preparations owing to remarkable antibacterial activity. However, increasing the pH over 3.5 of the medium in aqueous alum solutions can significantly reduce the alum's antibacterial activity.

This study had some potential limitations; first, the bacterial species included in this study were limited to four species because the

scope of the study was prone to formulate an effective antibacterial preparation regardless of bacterial species. Bacterial species covered in this study have been chosen upon their prevalence and spreading among the local community. Second, no topical routes of administration were considered in this study except the dermal preparations because working on other dosage forms might consume much more time and need more funds.

In addition, inhibitory zones and minimum inhibitory concentration (MIC) values were used to evaluate the antibacterial activity of alum in preparations. However, the MIC was visually determined utilizing the broth dilution method. If we had utilized a statistical method including MIC range, MIC50, and MIC90 values, the evaluation might have been more accurate; however, this would have required the testing of more than 100 isolates, which was not possible considering the limited funds we had.

Depending on the stated limitations, we suggest covering more bacterial strains in addition to fungal strains as well. This study will significantly impact considering natural product preparations as an acceptable choice for treating dermal infections. Furthermore, we aim to broaden the scope of this study to include more administration routes, including eyes and nose washes or douches, the same for the mouth, and a gargle and rinse. Burn and injury dermal washes also could be considered for further studies.

Acknowledgements

CRedit authorship contribution statement

Moath Refat: Methodology, Conceptualization, Investigation, Formal analysis, Visualization, Software, Data curation, Writing – original draft, Writing – review & editing. **Anes A.M. Thabit:** Supervision, Methodology, Conceptualization, Formal analysis, Writing – review & editing. **Hesham Siddick:** Investigation, Formal analysis, Data curation, Writing – original draft. **Abdul-Rahman Maqboli:** Investigation, Formal analysis, Data curation, Writing – original draft. **Mohammed Sharah:** Investigation, Formal analysis, Data curation, Writing – original draft. **Abdul-baqi A. Thabet:** Conceptualization, Methodology, Supervision. **Manar Refat:** Investigation. **Ahmed Al-Sabati:** Supervision, Methodology, Conceptualization, Resources, Funding acquisition.

Conflict of interest statement

The authors declare no conflict of interest.

Funding sources

This work was supported by "The University of Science and Technology", Hodeidah, Yemen.

References

1. Ki V, Rotstein C. Bacterial skin and soft tissue infections in adults: A review of their epidemiology, pathogenesis, diagnosis, treatment and site of care. *Can J Infect Dis Med Microbiol.* 2008 Mar;19(2):173-84. doi: 10.1155/2008/846453.
2. Stevens DL, Bisno AL, Chambers HF, Dellinger EP, Goldstein EJ, Gorbach SL, Hirschmann JV, Kaplan SL, Montoya JG, Wade JC; Infectious Diseases Society of America. Practice guidelines for the diagnosis and management of skin and soft tissue infections: 2014 update by the Infectious Diseases Society of America. *Clin Infect Dis.* 2014 Jul 15;59(2):e10-52. doi: 10.1093/cid/ciu444.
3. Gonzalez Santiago TM, Pritt B, Gibson LE, Comfere NI. Diagnosis of deep cutaneous fungal infections: correlation between skin tissue culture and histopathology. *J Am Acad Dermatol.* 2014 Aug;71(2):293-301. doi: 10.1016/j.jaad.2014.03.042.
4. Esposito S, Noviello S, De Caro F, Boccia G. New insights into classification, epidemiology and microbiology of SSTIs, including diabetic foot infections. *Infez Med.* 2018 Mar 1;26(1):3-14. PMID: 29525792.
5. Tay LK, Lee HY, Thirumoorthy T, Pang SM. Dermatology referrals in an East Asian tertiary hospital: a need for inpatient medical dermatology. *Clin Exp Dermatol.* 2011 Mar;36(2):129-34. doi: 10.1111/j.1365-2230.2010.03923.x
6. Sears D, Schwartz BS. *Candida auris*: An emerging multidrug-resistant pathogen. *Int J Infect Dis.* 2017 Oct;63:95-98. doi: 10.1016/j.ijid.2017.08.017.
7. Guo R, Liu Y, Li K, Tian B, Li W, Niu S, Hong W. Direct interactions between cationic liposomes and bacterial cells ameliorate the systemic treatment of invasive multidrug-resistant *Staphylococcus aureus* infections. *Nanomedicine.* 2021 Jun;34:102382. doi: 10.1016/j.nano.2021.102382.
8. Falcone M, Meier JJ, Marini MG, Caccialanza R, Aguado JM, Del Prato S, Menichetti F. Diabetes and acute bacterial skin and skin structure infections. *Diabetes Res Clin Pract.* 2021 Apr;174:108732. doi: 10.1016/j.diabres.2021.108732.
9. Corso R, Jones RM. Common cutaneous infections. *Medicine.* 2021;49(6):387-393. doi: <https://doi.org/10.1016/j.mpmed.2021.03.010>.
10. Zhang S, Zhu K, Zhang C. Successful treatment of a patient with cutaneous co-infection caused by *Mucor irregularis* and *Klebsiella pneumoniae*. *An Bras Dermatol.* 2020 Sep-Oct;95(5):623-626. doi: 10.1016/j.abd.2020.03.004.
11. Aragonese J, Suárez A, Algar J, Rodríguez C, López-Valverde N and Aragonese JM. Oral Manifestations of COVID-19: Updated Systematic Review With Meta-Analysis. *Front Med.* 2021;8:726753. doi: 10.3389/fmed.2021.726753.
12. Marszałek M, Gaweł A, Włodek A. Pickeringite from the Stone Town Nature Reserve in Ciezkowice (the Outer Carpathians, Poland). *Minerals.* 2020;10(2):187. doi: 10.3390/min10020187.
13. Jambor J, Nordstrom D, Alpers C. 6. Metal-sulfate Salts from Sulfide Mineral Oxidation. In: Alpers C, Jambor J, Nordstrom D (ed.) *Sulfate Minerals: Crystallography, Geochemistry, and Environmental Significance.* Berlin, Boston: De Gruyter; 2001. p. 303-350. doi: 10.1515/9781501508660-008.
14. Zimbelman DR, Rye RO, Breit GN. Origin of secondary sulfate minerals on active andesitic stratovolcanoes. *Chem Geol.* 2005;215(1-4):37-60. doi: 10.1016/j.chemgeo.2004.06.056.
15. Ali MA, Siwan H. Shubb-e-yamani (alum) a unique drug and its utilization in Unani medicine: A physicochemical and pharmacological review. *Int. J. Res. Ayurveda Pharm.* 2017;8(2):17-22. doi: 10.7897/2277-4343.08255
16. Pharmacopoeia B. Her majesty's stationery office. *Parliam. Aff.* 1954;8(2):205-214. doi: 10.1093/oxfordjournals.pa.a053040.
17. Al-Huwaizi RF, Al-Alousi WS. The Effects of Different Concentrations of Alum Solutions on Mutans Streptococci: In Vitro Study. *J. Baghdad Coll. Dent.* 2013;325(2210):1-6. doi: 10.12816/0015131.
18. Hussein AA. The effects of different concentration of Alum solutions on plaque and bleeding levels. *J. Pharm. Sci. Res.* 2019;11(3):1078-1081.
19. Altaei TS, Al-Jubouri RH. Evaluation of the efficacy of alum suspension in treatment of recurrent ulcerative ulceration. *J. Baghdad Coll. Dent.* 2005;17:45-48.
20. Faraj BM. Evidence for feasibility of aluminum potassium sulfate (alum) solution as a root canal irrigant. *J. Baghdad Coll. Dent.* 2012;24(Special Issue 1).
21. Alzomor AK, Moharram AS, Al Absi NM. Formulation and evaluation of potash alum as

- deodorant lotion and after shaving astringent as cream and gel. *Int. Curr. Pharm. J.* 2014;3(2):228–233. doi: 10.3329/icpj.v3i2.17512.
22. Refat M et al. Formulation and Evaluation of Yemeni Potash Alum as Hydrophilic Topical Preparations against Candidiasis and Aspergillosis. *Clin. Complement. Med. Pharmacol.* 2022: 100044. doi: 10.1016/j.ccmp.2022.100044.
 23. Olowosulu AK, Ibrahim YKE, Bhatia PG. Studies on the antimicrobial properties of formulated creams and ointments containing *Baphia nitida* heartwood extract. *J. Pharm. Biore-sour.* 2005;2(2):124–130. doi: 10.4314/jpb.v2i2.32075.
 24. Refat M et al. Formulation and Evaluation of Yemeni Potash Alum as Hydrophilic Topical Preparations Against Candidiasis and Aspergillosis. *Clinical Complementary Medicine and Pharmacology.* 2022;2:100044. doi: 10.1016/j.ccmp.2022.100044.
 25. Chow S-C, Shao J. *Statistics in drug research: methodologies and recent developments.* CRC press, 2002. doi: 10.1201/9780203910146.
 26. Khurshid H et al. 14. Antimicrobial properties of hydrogen peroxide and potash alum alone and in combination against clinical bacterial isolates. *Pure Appl. Biol.* 2019;8(4):2238–2247. doi: 10.19045/bspab.2019.80169.
 27. Putt MS, Kleber CJ, Smith CE. Evaluation of an alum-containing mouthrinse in children for plaque and gingivitis inhibition during 4 weeks of supervised use. *Pediatr. Dent.* 1996;18:139–144.
 28. Mourughan K, Suryakanth MP. Evaluation of an alum-containing mouthrinse for inhibition of salivary streptococcus mutans levels in children--a controlled clinical trial. *J. Indian Soc. Pedod. Prev. Dent.* 2004;22(3):100–105. Available at: <http://europepmc.org/abstract/MED/15573655>.
 29. Manzoor M, Sadiq S, Shahzad N. Efficacy of Amla (*Emblica officinensis*) and Shibe yamani (potash alum) in the management of Candida vaginitis: a randomized standard controlled trial. *Int J Reprod Contracept Obstet Gynecol.* 2016;5:1601–6. doi: 10.18203/2320-1770.ijrcog20161333.
 30. Babadi F, Malekzadeh H, Mansour A, Soweyti F. An in vitro Evaluation of Antifungal Effectiveness of Alum on the Growth of *Candida Albicans* and *Candida Tropicalis* Growth. *Jundishapur Sci. Med. J.* 2019;18(4):403–414.
 31. Layton RC, Gigliotti A, Armijo P, Myers L, Knight J, Donart N, Pyles J, Vaughan S, Plourde J, Fomukong N, Harrod KS, Gao P, Koster F. Enhanced immunogenicity, mortality protection, and reduced viral brain invasion by alum adjuvant with an H5N1 split-virion vaccine in the ferret. *PLoS One.* 2011;6(6):e20641. doi: 10.1371/journal.pone.0020641.
 32. Gupta OJ, Singh A. Optimizing the utilization of aluminum adjuvants in vaccines you might just get what you want. 2019;8(1):43–57.
 33. Misra A, Dube A, Srivastava B, Sharma P, Srivastava JK, Katiyar JC, Naik S. Successful vaccination against *Leishmania donovani* infection in Indian langur using alum-precipitated autoclaved *Leishmania major* with BCG. *Vaccine.* 2001 May 14;19(25-26):3485–92. doi: 10.1016/s0264-410x(01)00058-5.
 34. Khezri P, Shahabi S, Abasi E, Mohammadzadeh H. Comparison of immunogenicity of *Leishmania major* (MRHO/IR/75/ER) antigens prepared by 3 different methods in conjunction with Alum-Naltrexone adjuvant in BALB / c mice. *Alexandria J. Med.* 2018;4(54):503–510. doi: 10.1016/j.ajme.2018.10.004.
 35. Goyal DK, Keshav P, Kaur S. Immune induction by adjuvanted *Leishmania donovani* vaccines against the visceral leishmaniasis in BALB/c mice. *Immunobiology.* 2021 Mar;226(2):152057. doi: 10.1016/j.imbio.2021.152057.
 36. Barati M, Mohebbali M, Alimohammadian MH, Khmesipour A, Keshavarz H, Akhoun-di B, Zarei Z. Double-Blind Randomized Efficacy Field Trial of Alum Precipitated Autoclaved *Leishmania major* (Alum-ALM) Vaccine Mixed With BCG Plus Imiquimod Vs. Placebo Control Group. *Iran J Parasitol.* 2015 Jul-Sep;10(3):351–9.
 37. Hyer RN, Janssen RS. Immunogenicity and safety of a 2-dose hepatitis B vaccine, HBsAg/CpG 1018, in persons with diabetes mellitus aged 60–70 years. *Vaccine.* 2019 Sep 16;37(39):5854–5861. doi: 10.1016/j.vaccine.2019.08.005.
 38. Diaz-Mitoma F, Popovic V, Spaans JN. Assessment of immunogenicity and safety across two manufacturing lots of a 3-antigen hepatitis B vaccine, Sci-B-Vac®, compared with Engerix-B® in healthy Asian adults: A phase 3 randomized clinical trial. *Vaccine.* 2021 Jun 29;39(29):3892–3899. doi: 10.1016/j.vaccine.2021.05.067.
 39. Kleber CJ, Putt MS. Aluminum and dental caries. A review of the literature. *Clin Prev Dent.* 1984 Nov-Dec;6(6):14–25.
 40. von Lilienfeld-Toal M, Wagener J, Einsele H, Cornely OA, Kurzai O. Invasive Fungal Infection. *Dtsch Arztebl Int.* 2019 Apr 19;116(16):271–278. doi: 10.3238/arztebl.2019.0271.

Multi-epitope mRNA Vaccine Design that Exploits Variola Virus and Monkeypox Virus Proteins for Elicitation of Long-lasting Humoral and Cellular Protection Against Severe Disease

Dženan Kovačić

Department of Genetics and Bioengineering, Faculty of Engineering and Natural Sciences, International Burch University, Ilidža, Bosnia and Herzegovina

 <https://orcid.org/0000-0003-3218-5073>

Corresponding author: dzenan.kovacic@stu.ibu.edu.ba

Adna Salihović

Department of Genetics and Bioengineering, Faculty of Engineering and Natural Sciences, International Burch University, Ilidža, Bosnia and Herzegovina

 <https://orcid.org/0000-0003-0482-1861>

Keywords: smallpox, monkeypox, monkeypox outbreak, monkeypox vaccine, mRNA vaccines, poxviruses

Published: 2022-11-28

How to Cite: Kovačić D, Salihović A. Multi-epitope mRNA Vaccine Design that Exploits Variola Virus and Monkeypox Virus Proteins for Elicitation of Long-lasting Humoral and Cellular Protection Against Severe Disease. *Journal of Medical Science*. Ahead of Print. doi:10.20883/medical.e750

 doi: 10.20883/medical.e750



© 2022 by the author(s). This is an open access article distributed under the terms and conditions of the Creative Commons Attribution (CC BY-NC) license. Published by Poznan University of Medical Sciences

ABSTRACT

Human monkeypox represents a relatively underexplored infection that has received increased attention since the reported outbreak in May 2022. Due to its clinical similarities with human smallpox, this virus represents a potentially tremendous health problem demanding further research in the context of host-pathogen interactions and vaccine development. Furthermore, the cross-continental spread of monkeypox has reaffirmed the need for devoting attention to human poxviruses in general, as they represent potential bioterrorism agents. Currently, smallpox vaccines are utilized in immunization efforts against monkeypox, an unsurprising fact considering their genomic and phenotypic similarities. Though it offers long-lasting protection against smallpox, its protective effects against human monkeypox continue to be explored, with encouraging results. Taking this into account, this work aims at utilizing *in silico* tools to identify potent peptide-based epitopes stemming from the variola virus and monkeypox virus proteomes, to devise a vaccine that would offer significant protection against smallpox and monkeypox. In theory, a vaccine that offers cross-protection against variola and monkeypox would also protect against related viruses, at least in severe clinical manifestation. Herein, we introduce a novel multi-epitope mRNA vaccine design that exploits these two viral proteomes to elicit long-lasting humoral and cellular immunity. Special consideration was taken in ensuring that the vaccine candidate elicits a Th1 immune response, correlated with protection against clinically severe disease for both viruses. Immune system simulations and physicochemical and safety analyses characterize our vaccine candidate as antigenically potent, safe, and overall stable. The protein product displays high binding affinity towards relevant immune receptors. Furthermore, the vaccine candidate is to elicit a protective, humoral and Th1-dominated cellular immune response that lasts over five years. Lastly, we build a case about the rapidity and convenience of circumventing the live attenuated vaccine platform using mRNA vaccine technology.

Background

A currently ongoing outbreak of the monkeypox virus (MPXV), a zoonotic orthopoxvirus, was reported by the World Health Organization in May 2022, with the initial cluster identified in the United Kingdom. Though characterized as a rare zoonosis, over 10,000 cases have been reported thus far across the world. Two well-characterized clades of MPXV exist (West African and Central African). However, the clade responsible for the 2022 outbreak is genomically distinct from the two clades. Additionally, monkeypox is clinically indistinguishable from smallpox, though the transmissibility and severity of monkeypox disease are lower than the latter. The distinction between monkeypox and smallpox arose only in the 1970s during the smallpox eradication program when the virus was isolated from a suspected smallpox patient. Considering that the causative agent of smallpox – the variola virus – was eradicated from the human population in the 1980s, surveilling and studying other zoonotic orthopoxviruses with similar or identical clinical manifestations is justifiably garnering increased attention. Currently approved monkeypox vaccines are not specifically targeted to the MPXV orthopoxvirus but to human variola. The fact is sensible, considering the overlapping clinical manifestations between these human infec-

tions and their genomic similarity. Observational studies have revealed that the smallpox vaccine derived from the Vaccinia virus is 85% effective at preventing monkeypox. A novel attenuated Vaccinia virus vaccine was approved for the prevention of monkeypox in 2019. However, the vaccine is modestly available across the world.

The host innate immune response against poxviruses can be generally described as a classic antiviral response; interferon (IFN), the complement system, natural killer, and inflammatory cells are all engaged, upon which a greater inflammatory response typically ensues. Humoral and cell-mediated immunity, in the case of MPXV infected cells, mount the adaptive immune response via antibody-dependent cell-mediated cytotoxicity, virus neutralization, opsonization, and cytotoxic T-lymphocyte (CTL) effector functions through a myriad of pattern recognition receptor (PRR) families [1]. Specifically, effective viral control correlates strongly with the generation of neutralizing antibodies; it has been shown that CD4+/CD8+ T lymphocytes are not necessary for recovery from secondary poxvirus infection and are depleted after 8–15 years upon vaccination (**Figure 1**) [2]. Furthermore, MPXV-infected cells are believed to be able to trigger a state of unresponsiveness of T cells and thus evade CTL effector functions in a major histocompatibility complex (MHC)-independent fashion [3].

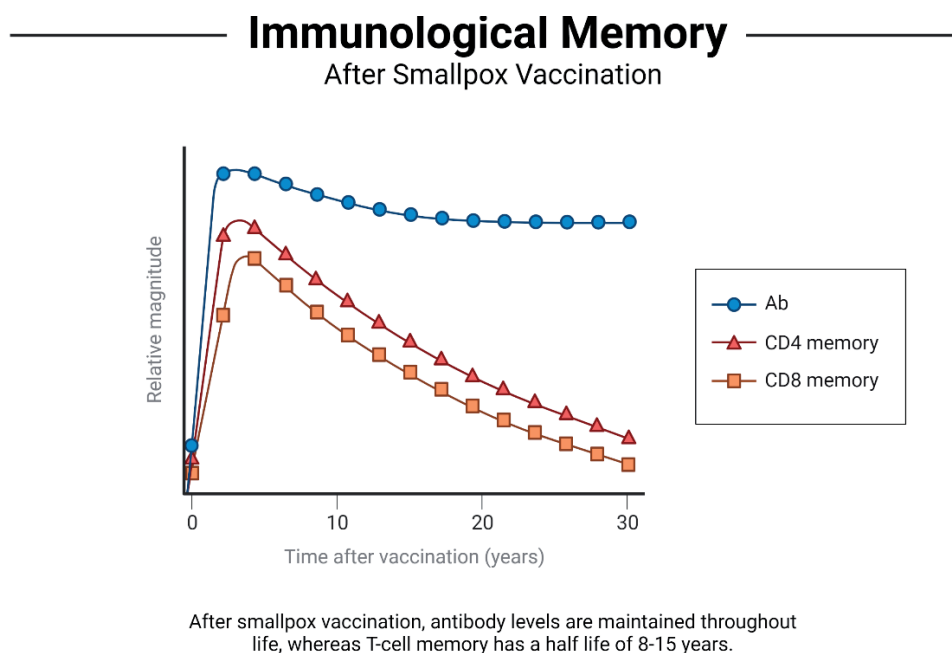


Figure 1. The canonical immune response to smallpox vaccination. Prepared based on data from [4–6]

The ability of poxviruses, primarily, to inhibit pro-inflammatory cytokines that regulate MHC expression (such as tumour necrosis factor (TNF) and IFN) may explain the indirect mechanisms at play that downplay the role of MHC. Considering the MPXV-infected intracellular environment, the inhibition of apoptosis via caspases and the protein kinase R (PKR) signalling pathway employs anti-IFN strategies. Indeed, the abrogation of IFN signalling was explored in further detail as a critical factor in promoting MPXV pathogenesis in humans [7]. MPXV encodes several PKR antagonists, notably, the MPXV F3 protein encoded by host genes F3L, a homolog of the VACV E3 protein homolog) that inhibits the PKR pathway [8]. Generally, the PRRs PKR and 2'-5'-oligoadenylate synthetase (OAS)/RNase L as the double-stranded RNA-activated sensors overarch the IFN-induced systems in response to MPXV infection [9]. The diverse crosstalk between several immune pathways with multiple PRRs targeting the same viral proteins mirrors the cascades of the viral antagonists, as alluded on the E3 sequestering dsRNA inhibiting PKR, OAS/RNase L, and Toll-like receptors (TLRs).

Ultimately, the importance of antibodies in MPXV infection was further heightened in a study realizing the insufficient protection from MPXV in immunodeficient macaques upon smallpox (Dryvax vaccine) immunization due to antibody-mediated depletion of B cells. To this end, utilisation of humoral immunity by using antigens that are targets of intracellular mature virions in neutralising antibodies is believed to warrant an effective monkeypox vaccine with an improved safety profile. Furthermore, smallpox vaccines' strong T and B cell responses target various viral proteins and offer cross-protective immunity against significant human infections, including variola and MPXV [4].

With mRNA vaccine technology recently finding its real-world applicational affirmation, utilizing this technology to devise more efficient vaccines has become an attractive notion. Though traditional vaccines garner a safety and efficiency profile solidified with decades of clinical data, optimizing how vaccines are designed to educate the immune system is becoming increasingly relevant with the emergence of zoonoses and other pathogens. Furthermore, the mRNA vaccine platform would allow for manipulating intracellular machinery involved in antigen processing and

presentation to optimise this process. Antigen processing is surprisingly inefficient in humans, even for high-affinity MHC-I ligands. Strikingly, only 1 in every 10,000 antigens gets presented by MHC-I, leaving a tremendous and somewhat underexplored opportunity for optimization via mRNA vaccine technology [10]. The most relevant aspect of this technology concerning emerging zoonoses is that designing mRNA vaccine constructs generally outpaces the traditional developmental process based on other vaccine platforms, e.g., employing attenuated or inactivated pathogens, due to the availability of software-based tools. It is also less time-consuming than developing subunit protein vaccines, as evidenced during the COVID-19 pandemic and the unseen pace at which mRNA vaccine candidates were manufactured (approx. one month since the whole sequence of SARS-CoV-2 genome was made publicly available).

In line with this, in the present study, we employed many freely available and commercial computational tools to identify and analyze antigenic peptides that belong to the variola virus and MPXV. The most antigenic peptides were incorporated into the conventional mRNA vaccine design, eventuating in a vaccine construct comprised of epitopes stemming from both viruses. The final construct was computationally evaluated for its ability to elicit an immune response, with encouraging predictions regarding antibody production, T cell response longevity, and adequate cytokine production recorded during immune response simulations. Other elements within the construct served as stabilizers, adjuvants, and signalling peptides that should theoretically guide the epitopes into their designated antigen-processing compartments in the context of MHC-I/II. Additional computations were performed regarding stereochemical quality, toxicity, allergenicity, mRNA and mRNA protein product stability, antigenic processing of the construct, as well as its interactions with toll-like receptors (TLRs) and MHC molecules.

Methods

Protein Sequences and Sequence Alignment

Protein sequences of MPXV (strain: Congo 8, accession: KJ642613) and the variola virus

(strain: Isolate Human/India/Ind3/1967, accession: X69198) were retrieved from UniProt. After that, the two proteomes were aligned using the National Center for Biotechnology Information (NCBI) BLASTp algorithm. It was done to identify whether any proteins crucial in pathogenicity or virulence overlap in amino acid sequence to avoid oversaturation of the mRNA construct with genomically identical antigenic elements.

Furthermore, the Pipeline builder for target identification (PBIT) was employed to assess whether the mRNA vaccine protein product shared homology with proteomes belonging to gut microbiome members [11]. Given the emerging body of evidence accumulated in recent years regarding the relevance of the gut microbiome for human homeostasis, vaccines and therapeutics should ideally avoid disrupting the delicate niche in which commensal microorganisms thrive.

CD4+ T Cell Epitope Identification and Selection

Identification of helper T cell (HTL) epitopes was performed using the MHC-II Binding Tool available from the Immune Epitope Database (IEDB) (www.iedb.org). Individual variola and MPXV proteins were screened using the Consensus method, where epitopes with a computed percentile rank ≤ 0.25 were considered for further evaluation [12]. Other computed properties deemed relevant for CD4+ T cell epitope identification included inducibility of TNF, interleukin 4 (IL-4), IL-10 production, allergenicity, and toxicity.

CD8+ T Cell Epitope Identification and Selection

Individual MPXV and variola proteins were screened for cytotoxic T cell (CTL) epitopes using the NetCTL-1.2 server (<https://services.healthtech.dtu.dk/service.php?NetCTL-1.2>) [13]. The approach incorporates predictions for the efficiency of TAP transport, proteasomal C terminal cleavage, and peptide MHC class I binding. The server supports CTL epitope predictions limited to 12 MHC class I supertypes. Artificial neural networks are used to carry out the proteasomal cleavage and MHC class I binding processes. TAP transport efficiency is predicted with a weight matrix. The NetCTL v1.2 server now supports 12 MHC-I supertypes (A1, A2, A3, A24, A26, B7, B8, B27, B39, B44, and B58), all of which were employed in the first screening pro-

cedure, with an epitope identification threshold of 0.75. The IEDB MHC-I immunogenicity tool was then used to test the immunogenicity of each anticipated epitope [14]. Subsequently, the peptides with the highest immunogenicity score were analyzed in terms of MHC binding partners via the IEDB MHC-I binding tool. Peptide sequences with a percentile rank ≤ 2 were considered for further evaluation in the context of allergenicity, toxicity, and probable protective antigenicity.

B Cell Epitopes

The production of long-lasting antibodies that neutralise various virus components hallmarks the immune response to smallpox and, presumably, monkeypox. Ergo, any novel vaccine tailored for these viruses should ensure a humoral immune response of sufficient quality and longevity. In line with this, we screened MPXV and variola virus proteins with antagonistic functions towards the immune response's relevant molecular elements. One such viral protein is the variola virus cytokine response-modifying protein B (Crmb). It binds to host TNF and numerous cytokines, followed by the variola virus B cell lymphoma 2 (Bcl2) homolog F1L, and the MPXV bifunctional 21 KDa precursor protein of 18 KDa membrane fusion protein (B8R). The BepiPred 2.0 server for predicting linear and discontinuous antibody epitopes (<https://services.healthtech.dtu.dk/service.php?BepiPred-2.0>) was used To identify opportunistic linear B cell (LBL) epitopes derived from the variola and MPXV antigenic proteins [15]. The selected LBL epitopes were then screened for allergenicity, toxicity, and antigenicity.

Prediction of Cytokine Inducibility

The ability of the vaccine to elicit cytokine secretion and antigenic response characterizes the vaccine construct's immune response, specifically, the effective stimulation and activation of CD4+. Thus, after antigenicity, toxicity, and allergenicity assessment, the HTL epitopes were screened for the simultaneous response of the cytokines IFN- γ , IL-10, and IL-4 to ensure induction of the adaptive cellular immune response. Therefore, the IL-4Pred [16], IL-10Pred [17], and IFNepitope [18] servers were used to filter the opportunistic HTL epitopes.

Computing Antigenicity, Allergenicity, Toxicity and Physicochemical Properties

Along with the screening of LBL and HTL epitopes, the CTL epitopes initially screened using the IEDB server with an immunogenic score of the 99th percentile were directly screened with the Aller-catPro v2.0 server to predict allergenicity potential [19]. Then, the ToxinPred server was used to predict the toxicity potential of the non-allergenic epitopes by applying the Quantitative Matrix method (mono-peptide) [20]. Finally, the non-toxic and non-allergenic epitopes were screened through the VaxiJen v2.0 server to predict the protective antigen potential of each epitope for subunit vaccine validation using a threshold ≥ 0.5 [21]. Upon completion of the construct design, the antigenicity of the translated open reading frame (ORF) was evaluated using both VaxiJen and ANTIGENpro [22]. The criteria for immunogenic epitope selection rely on them being computed as non-toxic, non-allergenic, and effectually antigenic, screened solely by their physicochemical properties.

The physicochemical properties of the mRNA open reading frame were analysed using the Prot-Param tool in order to compute the overall stability, half-life, and general compositional properties (<https://web.expasy.org/protparam/>) [23]. Prot-Param computes the physicochemical properties from the input protein sequence, independent of performing sequence alignment.

Structure prediction and Molecular Docking

Before performing representative molecular docking simulations between MHC-I/II alleles and their binding partners, binding affinities and bond lengths were computed between each filtered antigenic peptide and their corresponding MHC allele using the Protein-Ligand Interaction Analyzer tool through SAMSON-Connect (OneAngstrom) (<https://www.samson-connect.net>). Then, molecular docking simulations between MHC-I/II alleles and their binding partners were performed using the GalaxyPepDock molecular docking server [24]. MHC-I/II crystal structures were retrieved from the RCSB Protein Data Bank (PDB). If a specific MHC-I/II crystal structure was unavailable, homology modelling was performed using the SWISS-MODEL server. Finally, the sequences were retrieved from the IPD-IMGT/HLA database (<https://www.ebi.ac.uk/ipd/imgt/hla/>). Before molecular docking,

all crystal structures were processed using SAMSON by removing unnecessary ligands, followed by energy minimization through the Swiss-PDB Viewer. Once the 3D structure of the mRNA ORF was predicted using the Phyre2 web server (<http://www.sbg.bio.ic.ac.uk/phyre2/>) for *de novo* protein folding prediction, molecular docking between the mRNA protein product and MHC-I/II and TLR3 was performed using the ClusPro 2.0 protein-protein docking server (<https://cluspro.bu.edu/>) [25]. Docking the protein to MHC-II is particularly relevant, as MHC-II binding is the first step in the cathepsin processing of exogenous antigenic proteins [26]. Before docking the 3D structure of the construct, however, refinement was performed using GalaxyRefine (<https://galaxy.seoklab.org/cgi-bin/submit.cgi?type=REFINE>) [27].

Lastly, the minimum-free energy (MFE) secondary structure of the entire mRNA construct was predicted using the RNAfold web server [28]. The secondary structure of an RNA sequence that contributes the least free energy is the MFE structure. A loop-based energy model and the dynamic programming approach were used to forecast this structure [29]. An RNA secondary structure can be uniquely divided into loops and external bases. Thus the loop-based energy model views the free energy $F(s)$ of an RNA secondary structure s as the total of the contributing free energies FL of the loops L included in s . The secondary structure s that minimizes $F(s)$ is calculated using the selected energy parameter set and the specified temperature (37 °C by default).

Population Coverage Analysis of HLA Variants

The quality of the human immune response to pathogenic microbes and viruses is strongly correlated with the host's immunogenetic constitution. Genetic variants of genes relevant to the immune response determine host susceptibility and allow for either a beneficial or detrimental immunopathologic course to ensue upon infection [30–46]. Among this immune response, genes are those that encode HLA proteins. Polymorphisms within these genes have been strongly correlated with infection outcome and vaccine response. The substantial number of documented HLA variants across different populations suggests that the vaccine design process must factor in HLA variant distribution. Thus, their global distribution was determined once the cor-

responding HLA-I/II alleles were identified during epitope selection. Ensuring that the identified alleles are geographically widely distributed allows the vaccine to protect more individuals. The IEDB Population Coverage Tool was used to compute global allele coverage by factoring in 16 geographical regions [47].

Vaccine Construct Design: Linkers, Trafficking Sequences and Stabilizers

The profiled LBL, HTL, and CTL epitopes, respectively, are part of the open reading frame of the mRNA vaccine construct. The construct upstream and downstream untranslated regions (UTRs), which flank the ORF, generally increase the epitopes' stability, translatability, and adjuvanticity. Moreover, they characterise eukaryotic mRNA. Linkers were used to concatenate the subunits of the 5' UTR, ORF, and 3' UTR for stabilization and have further utility in ensuring that each subunit behaves independently. Furthermore, the linkers are both flexible and rigid enough to allow differentiation between each independent element within the construct.

The N terminus comprises a 7-methylguanosine 5' cap structure and the human β -globin sequence in increasing translational efficiency [48–50]. Correspondingly, the 3' UTR is flanked downstream with the α -globin sequence and a poly(A) tail, respectively, before which a STOP codon is put in place [48]. Additionally, the incorporation of poly(A) tail has been shown to

increase protein expression level with increased length; therefore, the length of the poly(A) tail was extended to 150 residues [48].

The ORF, apart from the epitopes, begins with the Kozak sequence to initiate translation [51]. Following the start codon, a cleavage signal sequence belonging to the tissue plasminogen activator (tPa) was added in order to guide the translational machinery toward product cleavage [52–54]. The tPa sequence is followed by a portion of the human β -defensin protein to increase adjuvanticity (UniProt: A0A7I2-YQ93) [48, 49]. The Signal.P-5.0 web server was employed (<https://services.healthtech.dtu.dk/service.php?SignalP-5.0>) to ensure that the signal sequence would be recognised upon incorporation [55]. As LBLs are located towards the N terminus of the construct, the pan HLA DR-binding epitope (PADRE) sequence was added. Previous work has demonstrated that the incorporating of a PADRE sequence in vaccine designs provides T-cell-aided induction of protective antibodies [56–58]. In order to identify the signal sequence within the tPA protein, the Signal.P-6.0 server was used (Supplementary File 1) [55]. Towards the C terminus, after the final CTL, an AAY-linked MHC Class I trafficking signal domain (MITD) was added in order to guide CTL epitopes toward MHC-I processing (UniProt: Q8WV92) [10]. A schematic representation of the vaccine construct may be found in **Figure 2**.

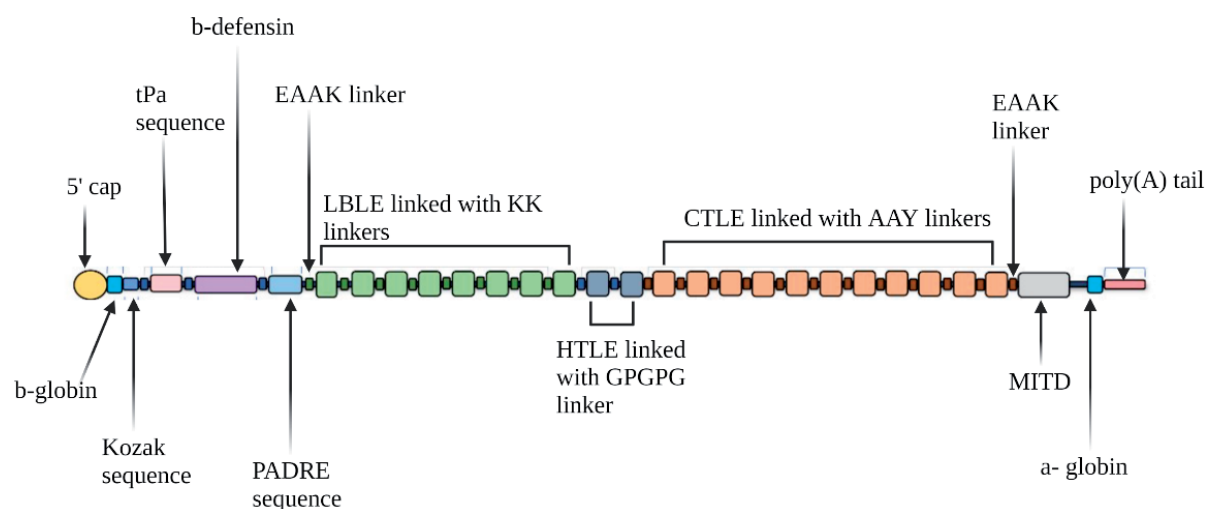


Figure 2. Schematic representation of the mRNA construct design. Abbreviations: tPa – tissue plasminogen activator; LBLE – linear B cell epitopes; HTLE – helper T cell epitopes; CTLE- cytotoxic t cell epitopes; MITD – MHC-I trafficking domain; PADRE – pan HLA DR-binding epitope

Molecular Dynamics Simulations

Upon docking the mRNA vaccine protein product with TLR3, MHC-I, and MHC-II, molecular dynamics (MD) simulations were performed for each complex in order to assess complex stability, using the GROMACS Wizard for SAMSON-Connect [59]. Each complex was placed in a water-containing octahedral box according to the SPC/E water model to achieve this. The boundary was set to at least 10Å from the protein atoms. The addition of Cl⁻ ions performed neutralisation of the solvated structures. The LINCS technique was used to restrict covalent bonds involving hydrogen atoms, while particle-mesh Ewald handled long-range electrostatic interactions using a real-space cutoff of 10Å. In order to eliminate near interactions, the system was first momentarily reduced with the system atoms restricted to the original coordinates (no jumping atoms). The restrained system was then gradually heated to 300 K under constant volume at 0.01ns. Finally, each system was brought into equilibrium for 0.01 ns for NVT and NPT equilibration, using the continuous isothermal-isobaric ensemble at 1 atm and 300 K without constraints. With a 2fs integration time step, the Parrinello-Rahman barostat and a Brendsen thermostat were employed. Production mode for 0.5 ns was applied to run MD simulations, with coordinates recorded every 1000fs. The OPLS-AA/L force field was used for all simulations. mRNA protein product stability was assessed using identical parameters.

Immune System Simulations

The C-Immsim server was employed using the Celada-Seiden model to simulate the vaccine construct humoral and cellular immune response [60, 61]. C-Immsim considers cells as individual agents (agent-based modelling), representing polyclonal models thereof, and quantitatively depicts immune response at the cellular scale. In setting the parameters, the simulation time frame was set to approximately five years (5000-time-steps). Two doses (50 µL simulation volume) were administered, one at time-step 1 and a booster dose at time-step 1095 (one year apart). One advantage of implementing C-Immsim is that an individual simulation may be set up to simulate the immune with user-selected HLA-I/II alleles taken into consideration. In line with this, we

selected HLA alleles that correspondingly to the peptides based on the HLA-I/II epitope screening results, namely *HLA-A02:01*, *HLA-A02:61*, *HLA-B07:02*, *HLA-B39:01*, *HLA-DRB1-07:01*, and *HLA-DRB1-03:01*.

Results

Identification, Evaluation and Selection of T cell and B Cell Epitopes

Considering that the entirety of the available MPXV and variola proteomes underwent screening for potential CTL epitopes, it is not surprising that the initial NetCTL v.1.2. analysis returned thousands of potential CTLs (Supplementary File 1). Only after further computations involving MHC class I immunogenicity and MHC-I binding was further selection possible (Table 1). A similar situation was observed upon initial screening for MHC-II epitopes (see Table 1). Molecular docking results are available in Supplementary File 1.

Corresponding HLA Alleles Are Widely Distributed

The IEDB Population Coverage tool computed a global coverage of 91.33%. In terms of regional coverage, out of the 16 geographical regions included in the computation, all but one (Central America) had a computed coverage score >50% (Figure 2).

The Vaccine Construct: RNA secondary structure, Components, Protein Product and Physicochemical Properties

A total of 23 antigenic peptides were incorporated into the construct; 7 LBL epitopes, 6 HTL epitopes and 10 CTL epitopes. Secondary structure prediction by RNAfold computed a structure whose free thermodynamic ensemble energy is -840.86 kcal/mol (Figure 3). The formulation of the construct is as follows:

5' Cap – human β globin 5' UTR – Kozak context – GPGPG linker – tPa signal sequence – GPGPG linker – human β defensin sequence – GPGPG linker – PADRE sequence – EAAK linker – YSNNEYTPFNK (LBL) – KK linker – CDVGFDSIDI (LBL) – KK linker – TIDSSTIQRRE (LBL) – KK linker – IDDDIDDIDDIDDIDDKASNNDDHN (LBL) – KK linker – NKSTNILDYLSTE (LBL) – KK linker – DISPPDNTIPNISTRE (LBL) – KK linker – YYCLLKSSGCKACVSQTKGIGYGVSGHTSVGDV ICSPCGFTYSHTVSSADKCEPVPNNFTFNYIDVEITLYPVNDTSCRTTTTGLSESILTSELITMNHDCNPVFREEYFVSLNKVATSGFF

Table 1. Summarization of identified cytotoxic, helper T cell and B epitopes, according to VaxiJen score and the most likely HLA variant binders. Peptides with a VaxiJen score ≥ 0.5 were considered potential protective antigens

T Cell Epitopes	VaxiJen Score	HLA Variant
CD4⁺		
KIILISDVRSKRGGN	1.1520	HLA-DRB1*03:01
LDTVNIYISILINHR	0.9376	HLA-DRB1*15:01
VIFYFISIYSRPKIK	0.8242	HLA-DRB5*01:01
SRLIHFSISFSISLM	1.2229	HLA-DRB1*07:01
RLIHFSISFSISLMQ	1.2158	HLA-DRB1*07:01
MSRLIHFSISFSISL	1.1653	HLA-DRB1*07:01
CD8⁺		
KRRNVEWEL	2.1466	HLA-B*27:05
RGSIIFINY	1.1953	HLA-B*58:01, HLA-B*58:02
FAIIAIVFV	1.3444	HLA-A*02:01, HLA-A*02:06
STIHYYWVK	1.2641	HLA-A*03:01, HLA-A*26:01
SHVRWRDIW	1.5510	HLA-B*39:01
ATRIEFGPL	2.6960	HLA-B*07:02
NFKIEFEAV	1.8963	HLA-B*08:01
YTNWAIILL	1.3359	HLA-A*01:01, HLA-A*02:01, HLA-A*02:06, HLA-A*26:01, HLA-B*39:01, HLA-B*58:01, HLA-B*58:02
KDEAIEIGL	1.6384	HLA-B*44:02, HLA-B*44:03
FKIEFEAVY	1.3717	HLA-A*26:01, HLA-B*27:02, HLA-B*27:05
B Cell Epitopes		
CDVGFDSIDI	1.4667	
IDDIDDIDDIDDIDDIDDKASNNDDHN	1.0407	
DISPPDNTIPNISTRE	0.9703	
TIDSSTIQRRE	0.8453	
YYCLLKSSGCKACVSQTKCGIGYGVSGHTSVGDVICSPCGFTYSHT-VSSADKCEPVPNNTFNIDVEITLYPVNDTSCRTTTTGLSESILTSELT-ITMNHTDCNPVFREEYFVNLNKVATSGFFTGENRYQNISKVCTLNFEIK-CNNKGSSFKQLTKAKND	0.7414	
YSNNEYTPFNK	0.6185	
NKSTNILDYLSSTE	0.5738	

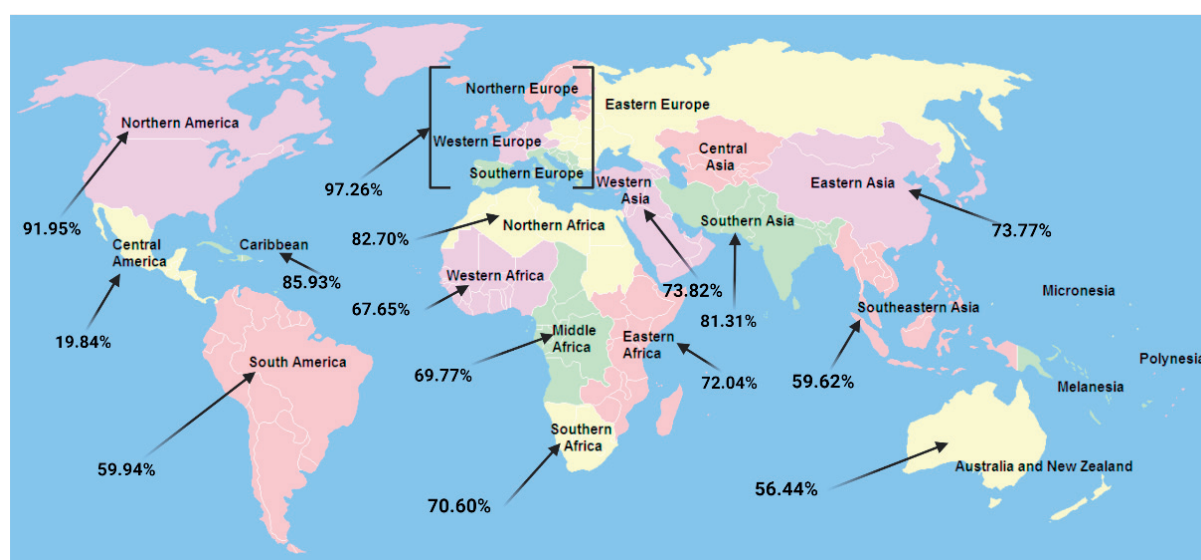


Figure 3. Geographical distribution of HLA allele variants that have been predicted to bind with the identified epitopes

TGENTRYQISKVCTLNFEIKCNNGKSSFKQLTKAKND (LBL) – GPGPG linker – KIILISDVRSKRGGN (HTL) – GPGPG linker – LDTVNIYISILINHR (HTL) – GPGPG linker – VIFYFISIYSRPKIK (HTL) – GPGPG linker – SRLIHFSISFISLSM (HTL) – GPGPG linker – RLIHFSISFISLSMQ (HTL) – GPGPG linker – MSRLIHFSISFISLS (HTL) – AAY linker – KRRNVEWEL (CTL) – AAY linker – RGSIIIFINY (CTL) – AAY linker – FAIIAIVFV (CTL) – AAY linker – STIHIYWGK (CTL) – AAY linker – ATRIEFGPL (CTL) – AAY linker – NFKIEFEAV (CTL) – AAY linker – YTNWAIILL (CTL) – AAY linker – KDEAIEIGL (CTL) – AAY linker – FKIEFEAVY (CTL) – EAAK linker – MIT trafficking signal sequence – GPGPG linker – STOP codon – human α globin 3' UTR – Poly(A) tail.

Toxicity and allergenicity computations estimated that the protein product of the ORF is both non-toxic and non-allergenic, further supplemented with findings of no significant homology between the amino acid sequence of the construct and proteomes belonging to commensal microbes (Supplementary File 1). Physicochemical evaluation of the mRNA protein product computed the protein as stable, with a long-lasting half-life (Table 2). Antigenicity predictions conducted by VaxiJen and ANTIGENpro computed that the mRNA product is a probable protective antigen, with scores of 0.7143 and 0.826646 for VaxiJen and ANTIGENpro, respectively. The Signal.P-6.0 evaluation of the ORF appropriately recognized the incorporated tPa sequence as a signal sequence, indicating a high degree of probability that it will be recognized appropriately during translation (Figure 4).

After the *de novo* protein folding using the Pyhre2 server, the generated PDB structure was

refined using the GalaxyRefine tool, followed by stereochemical evaluation using the Ramachandran plot extension available within the SAMSON-Connect software package. Evaluation of the refined construct returned 90.381% highly preferred observations, followed by 7.463% preferred and 2.156% questionable observations (Figure 5).

The mRNA Product Elicits a Protective and Long-lasting T and B Cell Immune Response

Upon administering the initial dose containing 1000 construct (Ag) units (simulation details in Supplementary File 1), high IgM and, subsequently, IgG antibody titers were documented within the first ten days post-immunization (Figure 6). The observed production of IgG1 corresponds with the predicted solubility-associated computations that classified the protein product as water-soluble, considering that IgG1 is predominantly primed toward hydrophilic antigenic proteins. IgG2 is also simultaneously produced in the primary and secondary immune response. The Ig production as described above corresponds adequately with the observed B cell clonal expansion, where IgM isotype B cells demonstrate high stability across the simulated period, with no tendency to decline. This insight is encouraging, as IgMs are the first responder to foreign organisms and viruses [62]. Though IgG production peaks approximately ten days upon primary and secondary immunization,

Table 2. Summarization of physicochemical, allergenicity, toxicity, and antigenicity properties of the mRNA protein product

Computed Property	Result	Interpretation
Number of amino acids	698	Adequate
Molecular weight	76731.62	Average
Chemical formula	C ₃₄₁₉ H ₅₃₆₄ N ₉₂₂ O ₁₀₂₂ S ₃₁	/
Computed theoretical pI	8.7	Basic
Negatively charged residues (Asp+Glu)	74	/
Positively charged residues (Arg + Lys)	87	/
Number of atoms	10758	/
Instability Index (II)	37.65	Protein is stable
Aliphatic index (AI)	80.82	Protein is thermostable
Grand average of hydropathicity (GRAVY)	-0.256	Protein is hydrophilic
Antigenicity evaluation based on sequence data	0.7143 (VaxiJen)	Construct is predicted as a strong protective antigen
	0.826646 (ANTIGENpro)	
AllerCatPro Evaluation	Probable non-allergen	Protein is a non-allergen
ToxinPred Evaluation	Non-toxin	Protein is non-toxic

A)



B)

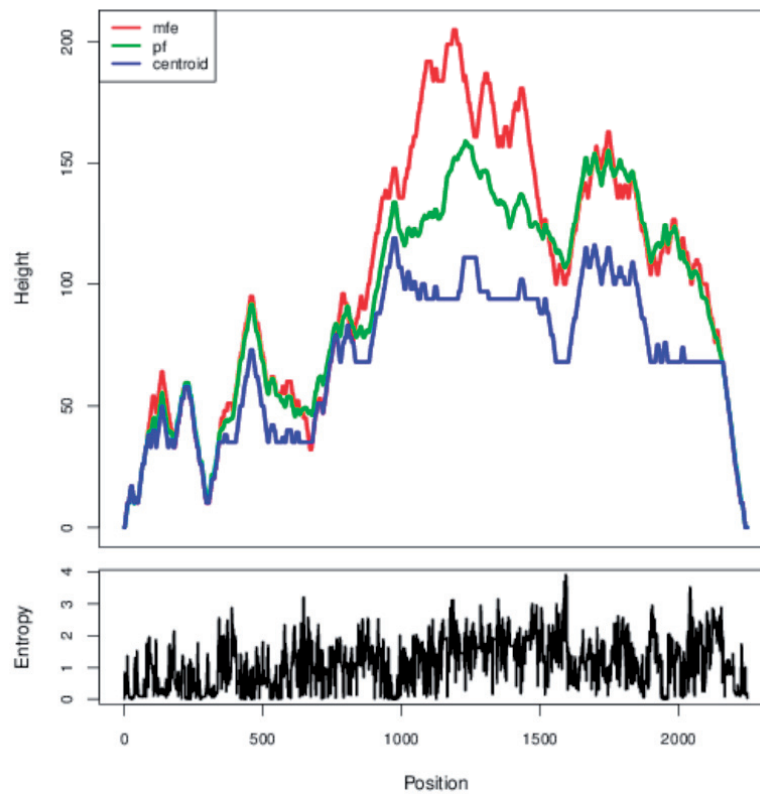


Figure 4. A) RNAfold minimum free energy (MFE) secondary structure prediction of the entire mRNA vaccine construct. B) A mountain plot representation of the MFE structure, the thermodynamic ensemble of RNA structures, and the centroid structure

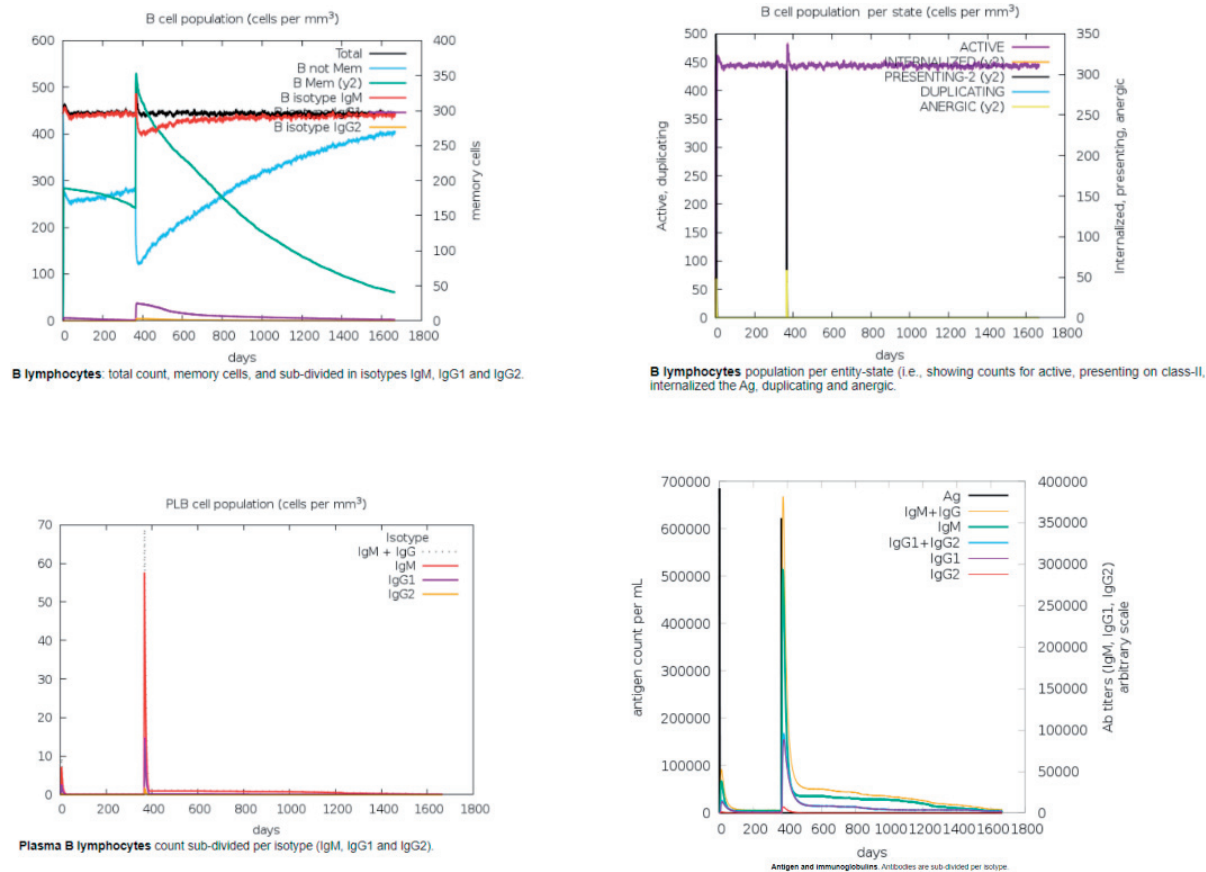


Figure 7. The predicted humoral response to the protein product of the mRNA vaccine construct over five years

differentiated memory HTL pool peaks approximately one month after immunization, followed by a steady decline and subsequent stabilization approximately four years after the second dose. Though active HTLs peak at around day 20 after the initial dose, the amount of active and resting HTLs declines rapidly and stabilises around day 60. Upon the second dose, a robust proliferation of active HTLs is observed, followed by their steady decline and stabilization through conversion towards a resting state some 2.5 years after the second injection. Interestingly, the proliferation of regulatory T cells (Tregs) was significantly more potent after the first dose than the second one. Active and resting Tregs seem to decline significantly and plateau 140 days after the first dose. However, these cells' presence remains consistent despite their minute quantities after the plateau phase. Despite the second dose not offering a significant increase in the resulting repertoire of differentiated Tregs, it maintains detection-worthy counts even five years after the second dose. Perhaps the most encouraging finding is that the immune response to the

vaccine construct is primed towards Th1 immunity, further supported by the predicted cytokine production induced after immunization. The observably high and stable counts of differentiated CD8+ T cells, followed by increased activation in natural killer (NK) cell production and innate immune cell engagement (dendritic cells and macrophages), demonstrated the above.

Molecular Dynamics Simulations

We used GROMACS to simulate the docked complexes (vaccine and TLR-3, MHC-I, and MHC-II) to determine the vaccine-receptor complex's stability. Furthermore, the overall stability of the mRNA protein product was assessed using the same MD parameters. Analyses regarding energy minimization, pressure evaluation, temperature, and estimates of potential energy were carried out. A stable system and a successful MD run were indicated by the simulation system's temperature and pressure during the simulation run and were stable throughout the entire simulation. The overall structural variation of the complex of the

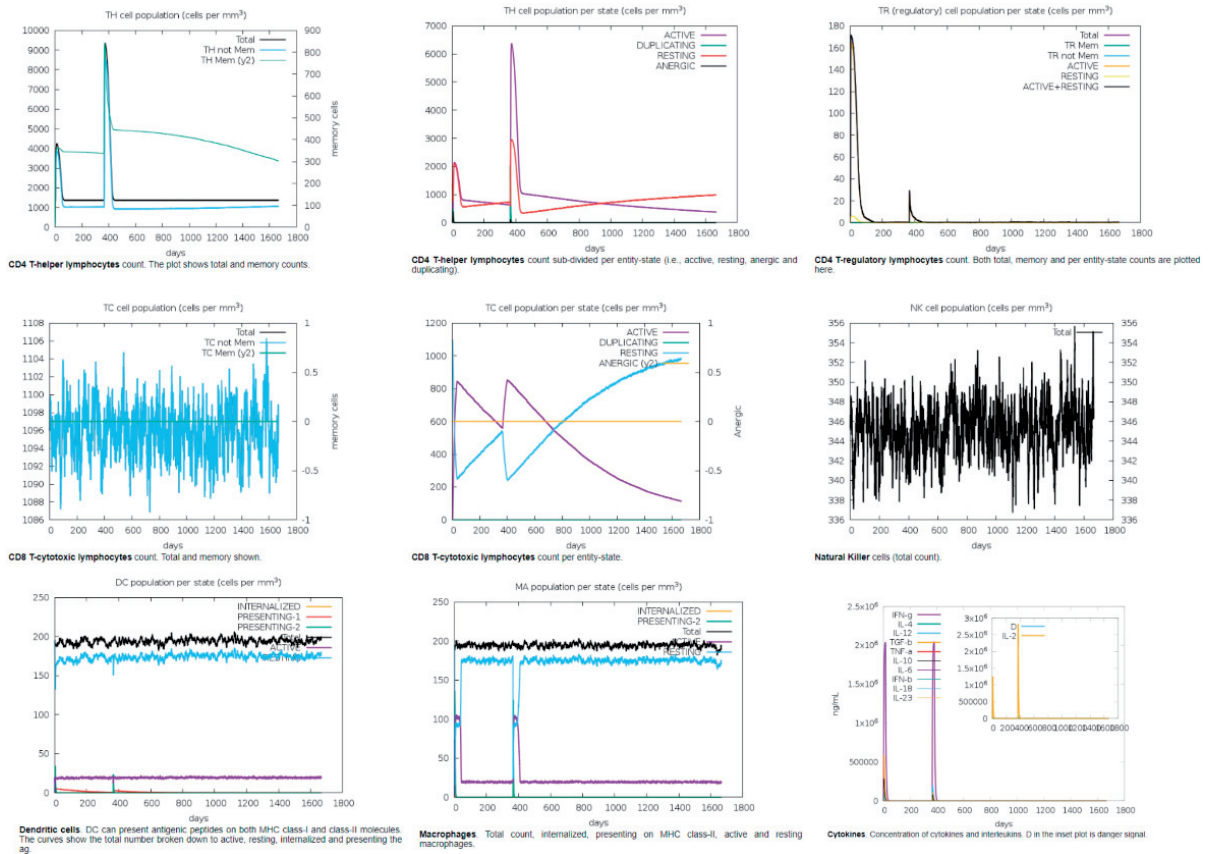


Figure 8. The predicted T cell immune response to the vaccine construct, supplemented with dendritic cell (DC) and macrophage (MA) engagement, supplemented with cytokine secretion profiles

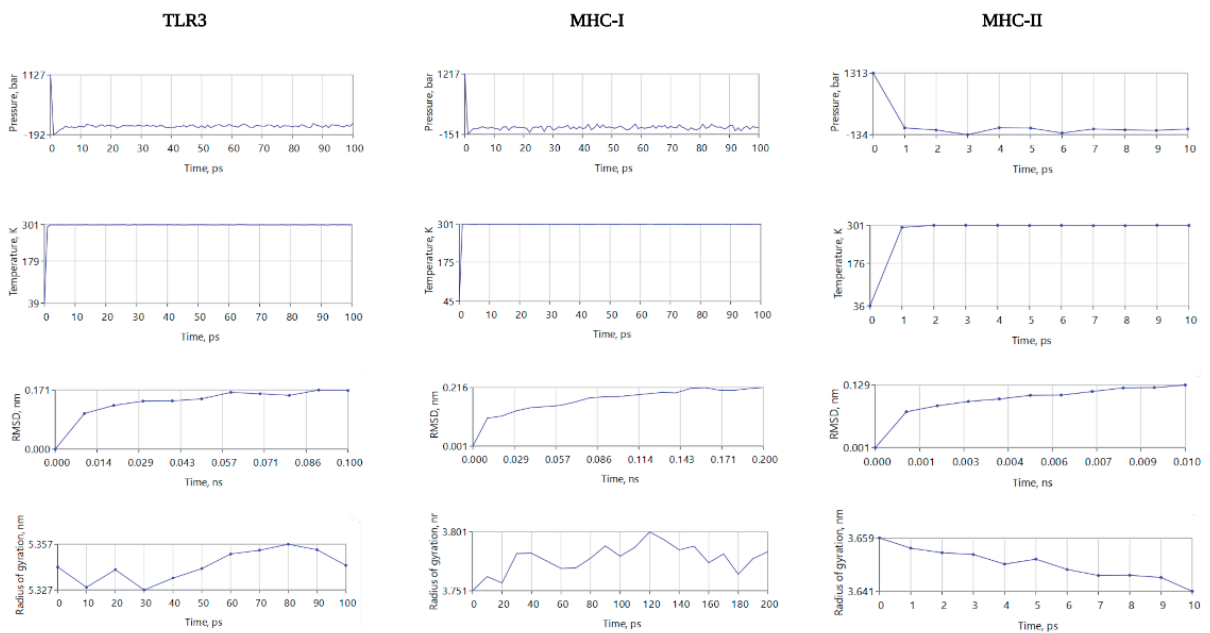


Figure 9. Molecular Dynamics (MD) simulation results for toll-like receptor 3 (TLR3), major histocompatibility complex I (MHC-I), and major histocompatibility complex II (MHC-II) docked with the folded protein product of the vaccine construct. The image displays results in the context of system pressure, temperature, and root mean square deviation (RMSD) of the docked complexes, along with the gyration radius

vaccine and immune receptor is depicted by the complex root mean square deviation (RMSD) (See **Figure 8, A**). The protein product alone has also been computed as stable when simulated under the same MD production run parameters (see Supplementary File 1).

Discussion

Though human smallpox was eradicated from the human population in the 1980s, the notion that an intentional variola virus release may occur has helped maintain the relevance of studying human orthopoxviruses. With this in mind, it is not all surprising that the majority of smallpox-related data stems from research conducted on the human Vaccinia virus rather than variola, as variola is classified as a level 4 biological agent stored in only a small number of laboratories. On the other hand, the recent outbreak of MPXV gave rise to a rather indicative body of research regarding the virus's genomics, proteomics and host-pathogen immunobiology, which may be opportunistically used for better understanding of variola as well. A very useful body of immunological data pertaining to T cell and B cell immunity is therefore available. An opportunity lies in merging these insights with computational tools to more accurately understand MPXV and variola, particularly with vaccine design. Though much remains to be uncovered, the currently-available data on MPXV infection offers clues into what sort of protective immune response profile should be elicited by a novel vaccine.

During severe MPXV infection, the cytokine profile suggests a dominant Th2 response associated with cytokine storm development [64]. Th2 cytokines (IL-10, IL-4, IL-13, IL-5, IL-6) are elevated during clinically severe infections, of which IL-10 and IL-4 dampen Th1 response [64], [65]. IL-10 downregulates Th1 cytokines (IL-2, TNF- α , IL-12, IFN- γ), indicating the cytokine storm's onset. Our immune response simulation results display a favourable, Th1-orientated response upon vaccination, suggesting T regulatory cell response and prolonged B cell and effector T cell survival. The process is further supplemented with the vaccine-induced cytokine secretion profile recorded within this work, indicating an IFN-mediated immune response. During the innate

immune response against MPXV, it has been observed that the impairment in NK cells causes the dysregulation of IFN- γ and TNF- α secretion [4, 5, 64–66]. Though monocytes play a critical role in shaping the adaptive immune response, subsequent cytokine release that induces monocyte apoptosis for viral dissemination is insufficient in countering cytokine storm-induced toxemia [67]. Moreover, the inability to induce an effective IFN response was associated with disease severity; adaptive immune response in eradicating virus-infected monocytes via IFN- γ secreting CD8+ cells was proven for sufficient protection, independent of CD4+ and B cells [68]. Considering our implementation of LBL epitopes, the incorporation of the apoptosis inhibitor F1L, IFN- γ binding proteins B8R, and the TNF and chemokine binding protein CrmB may effectively encompass the specific viral evasion strategies to host immune response in both intrinsic and extrinsic pathways for leveraging secreted antibodies [69–71]. Thus, the inclusion of characterized B cell epitopes and systematically defined HTL and CTL epitopes help accurately profile MPXV infection. This beneficial immunological response was recorded for our vaccine design, suggesting that the vaccine would most likely offer sufficient protection within this context. Following stimulation of T cells and subsequent antibody development, B cells and antibody production have notably indicated that protective IgG+ memory B cells highlight protection alone [67]. While this insight warrants further investigation in a population-specific context, it is encouraging that our vaccine design elicits IgG+-specific B cell production, along with stable and long-lasting IgG antibody titers. Overall, the predicted immunological response to the protein product of the vaccine construct would theoretically induce a beneficial Th1-mediated protective immune response. Stimulation of Th1 immunity is also a key protective factor against variola [4–6, 72]. With this in mind, the proposed vaccine design may protect against human smallpox, considering that the immune response simulation results satisfy the necessary criteria that hallmark protective immunity against the virus. The above is not surprising considering the genomic and host-pathogen similarities between variola and MPXV. An attractive hypothesis that may be drawn from this work is that this vaccine would offer cross-protection against other orthopox-

viruses, considering the number of diverse antigens incorporated into the construct.

Safety and antigenicity computations have classified the mRNA protein product as a non-allergenic, non-toxic, and highly-antigenic protein with no significant homology with the human gut microbiota. In terms of homology between human-derived signalling and trafficking elements incorporated within the construct, homology prediction was not performed, as these sequences are expected to be cleaved during translation.

Despite the encouraging results obtained from this study, its limitations should be adequately addressed. Namely, whilst epitope identification using the IEDB analysis toolkit has been broadly used for theoretical vaccine design in the past, their accuracy entirely relies on the quality of the datasets used to train the implemented algorithms. However, IEDB still stands as an acceptable tool for epitope identification. MHC-I processing prediction, on the other hand, is a complex and inefficient system, leaving room for algorithm improvement and forming the need for experimental validation in terms of antigenic processing. Furthermore, computational tools currently need to be available to predict the interaction between the host's cellular machinery and an introduced exogenous mRNA construct in a reliable fashion. Thus, all of our simulation results stem from analyzing the specific protein product encoded by the mRNA ORF rather than considering the process of mRNA translation or validating whether the translational machinery will recognize the cleavage/trafficking sequences *in vivo*. To compensate for this shortcoming, we employed SignalP-5.0, which detects the presence of signal sequences based on a protein's amino acid code. The tPA signal sequence was adequately detected upon incorporation within the construct, allowing us to hypothesize that the translational machinery would most likely recognize its presence. However, the major drawback of this study is the lack of *in vivo* data regarding our vaccine design, coupled with the fact that there are no computational tools for evaluating mRNA vaccines on a cellular level. Analyses of the protein product revealed encouraging results, even when the various partitions of the mRNA construct would not be guided by replication machinery towards different antigen processing compart-

ments (MHC-I/II). All this was revealed through molecular docking and subsequent molecular dynamics simulations between the mRNA product complexed with MHC-I/II and TLR3. Furthermore, the C-Immsim server, although the gold standard for open-source *in silico* immune response predictions, does not take into account the delivery method used and suffers from the inability for a greater number of HLA alleles to be specified within the input parameters. Additionally, the degree to which the statement of quantity is near that quantity's actual (true) value is known as the forecast's accuracy. Because the forecast is a statement about the future, the actual value is typically impossible to measure when issued, which should be considered when interpreting results from such forecasting tools. In line with this, another C-Immsim simulation was carried out for one year, with the second dose being omitted (Supplementary File 1). Considering that TLR3 can detect virus-associated nucleic acid and peptide sequences, a molecular dynamics simulation was performed on the docked mRNA-TLR3 complex in order to determine the stability of this complex. Furthermore, the overall stability of the mRNA protein product was further assessed using MD simulations. Though MD simulations and molecular docking have drawbacks regarding the accuracy and *in vitro* and *in vivo* translatability, they still represent well-accepted methods for *in silico* biophysical analysis of large molecular structures.

Overall, this work describes a novel conventional mRNA-based vaccine design, which incorporates various potential antigenic targets stemming from the variola virus and MPXV, in an attempt to design a vaccine that would elicit a protective immune response against these and other orthopoxviruses. In the confines of *in silico* evaluation, the vaccine design satisfies all safety, antigenicity and immune response longevity criteria. Furthermore, according to previous works, the Th1-oriented immune response elicited by the vaccine would offer sufficient protection against both viruses. Choosing the mRNA vaccine platform stems from the added potential of increasing antigen presentation to increase vaccine efficiency, safety and design speed. Yet the specific relationship between the mRNA construct and the intracellular machinery warrants *in vivo* validation. Taken altogether, our work elegantly dem-

onstrates the immense potential that computational tools hold for fast and relatively accurate streamlining of vaccine design, as this approach may be extrapolated to peptide-based and protein subunit vaccines.

Lastly, in terms of biosafety aspects, this design and pipeline represent a potentially fruitful avenue to pursue. They allow the rapid development of protective vaccines based on genomic or proteomic data. Furthermore, due to the opportunity to enhance antigen processing via the incorporation of trafficking and signal domains and predict various potential biophysical and immunological outcomes, this technology may be a valuable tool in the case of biological threats.

Acknowledgements

Supplementary Materials: All supplementary materials from Supplementary File 1 can be found on the following link: <https://doi.org/10.5281/zenodo.7264789>

Author Contributions: Conceptualization, Dženan Kovačić; methodology, Dženan Kovačić.; software, Dženan Kovačić.; validation, Dženan Kovačić.; formal analysis, Dženan Kovačić and Adna Salihović.; investigation, Dženan Kovačić and Adna Salihović.; resources, Dženan Kovačić and Adna Salihović.; data curation, Dženan Kovačić.; writing—original draft preparation, Dženan Kovačić.; writing—review and editing, Adna Salihović and Dženan Kovačić.; visualization, Dženan Kovačić and Adna Salihović.; supervision, Dženan Kovačić.; project administration, Dženan Kovačić. All authors have read and agreed to the published version of the manuscript.

Data Availability Statement: The epitope screening and identification data are freely available from public repositories, with sequence and proteome names clearly stated within the manuscript. All other data generated through commercial software is available within the Supplementary Files.

Acknowledgements: We appreciate professors Andrej A. Gajić, Riad Hajdarević, PhD, and Damir Marjanović, PhD, for their continuous support during the conceptualisation and preparation of this manuscript.

Conflict of interest statement

The authors declare no conflict of interest.

Funding sources

There are no sources of funding to declare.

References

1. McFadden G. Poxvirus tropism. *Nat Rev Microbiol.* 2005 Mar;3(3):201-13. doi: 10.1038/nrmicro1099.
2. Panchanathan V, Chaudhri G, Karupiah G. Protective immunity against secondary poxvirus infection is dependent on antibody but not on CD4 or CD8 T-cell function. *J Virol.* 2006 Jul;80(13):6333-8. doi: 10.1128/JVI.00115-06.
3. Hammarlund E, Dasgupta A, Pinilla C, Norori P, Früh K, Slifka MK. Monkeypox virus evades antiviral CD4+ and CD8+ T cell responses by suppressing cognate T cell activation. *Proc Natl Acad Sci U S A.* 2008 Sep 23;105(38):14567-72. doi: 10.1073/pnas.0800589105.
4. Kennedy RB, Ovsyannikova IG, Jacobson RM, Poland GA. The immunology of smallpox vaccines. *Curr Opin Immunol.* 2009 Jun;21(3):314-20. doi: 10.1016/j.coi.2009.04.004.
5. Amanna IJ, Slifka MK, Crotty S. Immunity and immunological memory following smallpox vaccination. *Immunol Rev.* 2006 Jun;211:320-37. doi: 10.1111/j.0105-2896.2006.00392.x.
6. Hammarlund E, Lewis MW, Hansen SG, Strelow LI, Nelson JA, Sexton GJ, Hanifin JM, Slifka MK. Duration of antiviral immunity after smallpox vaccination. *Nat Med.* 2003 Sep;9(9):1131-7. doi: 10.1038/nm917.
7. Stabenow J, Buller RM, Schriewer J, West C, Sagaritz JE, Parker S. A mouse model of lethal infection for evaluating prophylactics and therapeutics against Monkeypox virus. *J Virol.* 2010 Apr;84(8):3909-20. doi: 10.1128/JVI.02012-09.
8. Arndt WD, Cotsmire S, Trainor K, Harrington H, Hauns K, Kibler KV, Huynh TP, Jacobs BL. Evasion of the Innate Immune Type I Interferon System by Monkeypox Virus. *J Virol.* 2015 Oct;89(20):10489-99. doi: 10.1128/JVI.00304-15
9. Yu H, Bruneau RC, Brennan G, Rothenburg S. Battle Royale: Innate Recognition of Poxviruses and Viral Immune Evasion. *Biomedicines.* 2021 Jul 1;9(7):765. doi: 10.3390/biomedicines9070765.
10. Kreiter S, Selmi A, Diken M, Sebastian M, Osterloh P, Schild H, Huber C, Türeci O, Sahin U. Increased antigen presentation efficiency by coupling antigens to MHC class I trafficking signals. *J Immunol.* 2008 Jan 1;180(1):309-18. doi: 10.4049/jimmunol.180.1.309.
11. Shende G, Haldankar H, Barai RS, Bharmal MH, Shetty V, Idicula-Thomas S. PBIT: Pipeline Builder for Identification of drug Targets for infectious diseases. *Bioinformatics.* 2017 Mar 15;33(6):929-931. doi: 10.1093/bioinformatics/btw760.
12. Wang P, Sidney J, Kim Y, Sette A, Lund O, Nielsen M, Peters B. Peptide binding predictions for HLA DR, DP and DQ molecules. *BMC Bioinformatics.* 2010 Nov 22;11:568. doi: 10.1186/1471-2105-11-568.
13. Larsen MV, Lundegaard C, Lamberth K, Buus S, Lund O, Nielsen M. Large-scale validation of methods for cytotoxic T-lymphocyte epitope prediction. *BMC Bioinformatics.* 2007 Oct 31;8:424. doi: 10.1186/1471-2105-8-424.
14. Calis JJ, Maybeno M, Greenbaum JA, Weiskopf D, De Silva AD, Sette A, Keşmir C, Peters B. Properties of MHC class I presented peptides that enhance immunogenicity. *PLoS Comput Biol.* 2013 Oct;9(10):e1003266. doi: 10.1371/journal.pcbi.1003266.
15. Jespersen MC, Peters B, Nielsen M, Marcatili P. BepiPred-2.0: improving sequence-based B-cell epitope prediction using conformational epitopes. *Nucleic*

- Acids Res. 2017 Jul 3;45(W1):W24-W29. doi: 10.1093/nar/gkx346.
16. Dhanda SK, Gupta S, Vir P, Raghava GP. Prediction of IL4 inducing peptides. *Clin Dev Immunol.* 2013;2013:263952. doi: 10.1155/2013/263952.
 17. Nagpal G, Usmani S, Dhanda S, et al. Computer-aided designing of immunosuppressive peptides based on IL-10 inducing potential. *Sci Rep.* 2017;7:42851. doi: 10.1038/srep42851.
 18. Dhanda SK, Vir P, Raghava GP. Designing of interferon-gamma inducing MHC class-II binders. *Biol Direct.* 2013 Dec 5;8:30. doi: 10.1186/1745-6150-8-30.
 19. Nguyen MN, Krutz NL, Limviphuvadh V, Lopata AL, Gerberick GF, Maurer-Stroh S. AllerCatPro 2.0: a web server for predicting protein allergenicity potential. *Nucleic Acids Res.* 2022 Jul 5;50(W1):W36-W43. doi: 10.1093/nar/gkac446. PMID: 35640594; PMCID: PMC9252832.
 20. Sharma N, Naorem LD, Jain S, Raghava GPS. Toxin-Pred2: an improved method for predicting toxicity of proteins. *Brief Bioinform.* 2022 Sep 20;23(5):bbac174. doi: 10.1093/bib/bbac174.
 21. Doytchinova IA, Flower DR. VaxiJen: a server for prediction of protective antigens, tumour antigens and subunit vaccines. *BMC Bioinformatics.* 2007;8:4 doi: 10.1186/1471-2105-8-4.
 22. Magnan CN, Zeller M, Kayala MA, Vigil A, Randall A, Felgner PL, Baldi P. High-throughput prediction of protein antigenicity using protein microarray data. *Bioinformatics.* 2010 Dec 1;26(23):2936-43. doi: 10.1093/bioinformatics/btq551.
 23. Gasteiger E et al. Protein Identification and Analysis Tools on the ExPASy Server. *The Proteomics Protocols Handbook*, 2005:571–607. doi: 10.1385/1-59259-890-0:571. doi: 10.1385/1-59259-890-0:571.
 24. Lee H, Heo L, Lee MS, Seok C. GalaxyPepDock: a protein-peptide docking tool based on interaction similarity and energy optimization. *Nucleic Acids Res.* 2015 Jul 1;43(W1):W431-5. doi: 10.1093/nar/gkv495.
 25. Kelley LA, Mezulis S, Yates CM, Wass MN, Sternberg MJ. The Phyre2 web portal for protein modeling, prediction and analysis. *Nat Protoc.* 2015 Jun;10(6):845-58. doi: 10.1038/nprot.2015.053.
 26. Sadegh-Nasseri S, Kim A. Exogenous antigens bind MHC class II first, and are processed by cathepsins later. *Mol Immunol.* 2015 Dec;68(2 Pt A):81-4. doi: 10.1016/j.molimm.2015.07.018.
 27. Ko J, Park H, Heo L, Seok C. GalaxyWEB server for protein structure prediction and refinement. *Nucleic Acids Res.* 2012 Jul;40(Web Server issue):W294-7. doi: 10.1093/nar/gks493.
 28. Lorenz R, et al. ViennaRNA Package 2.0. *Algorithms for Molecular Biology.* 2011 Nov.;6(1):1–14. doi: 10.1186/1748-7188-6-26.
 29. Hofacker IL, Stadler PF. Memory efficient folding algorithms for circular RNA secondary structures. *Bioinformatics.* 2006 May 15;22(10):1172-6. doi: 10.1093/bioinformatics/btl023.
 30. Delanghe J, Speckaert M, De Buyzere M. COVID-19 infections are also affected by human ACE1 D/I polymorphism. *Clinical Chemistry and Laboratory Medicine (CCLM).* 2020;58(7):1125-1126. <https://doi.org/10.1515/cclm-2020-0425>
 31. Itoyama S, Keicho N, Quy T, Phi NC, Long HT, Ha LD, Ban VV, Ohashi J, Hijikata M, Matsushita I, Kawana A, Yanai H, Kirikae T, Kuratsuji T, Sasazuki T. ACE1 polymorphism and progression of SARS. *Biochem Biophys Res Commun.* 2004 Oct 22;323(3):1124-9. doi: 10.1016/j.bbrc.2004.08.208.
 32. Harishankar M, Selvaraj P, Bethunaickan R. Influence of Genetic Polymorphism Towards Pulmonary Tuberculosis Susceptibility. *Front Med (Lausanne).* 2018 Aug 16;5:213. doi: 10.3389/fmed.2018.00213.
 33. Anoosheh S, Farnia P, Kargar M. Association between TNF-Alpha (-857) Gene Polymorphism and Susceptibility to Tuberculosis. *Iran Red Crescent Med J.* 2011 Apr;13(4):243-8.
 34. Ng MW, Zhou G, Chong WP, Lee LW, Law HK, Zhang H, Wong WH, Fok SF, Zhai Y, Yung RW, Chow EY, Au KL, Chan EY, Lim W, Peiris JS, He F, Lau YL. The association of RANTES polymorphism with severe acute respiratory syndrome in Hong Kong and Beijing Chinese. *BMC Infect Dis.* 2007 Jun 1;7:50. doi: 10.1186/1471-2334-7-50.
 35. Oral HB et al. Interleukin-10 (IL-10) gene polymorphism as a potential host susceptibility factor in tuberculosis. *Cytokine.* 2006 Aug.;35(3-4):143-147. doi: 10.1016/j.cyto.2006.07.015.
 36. Selvaraj P, Alagarasu K, Harishankar M, Vidyanani M, Nisha Rajeswari D, Narayanan PR. Cytokine gene polymorphisms and cytokine levels in pulmonary tuberculosis. *Cytokine.* 2008 Jul;43(1):26-33. doi: 10.1016/j.cyto.2008.04.011.
 37. Chan KY, Xu MS, Ching JC, So TM, Lai ST, Chu CM, Yam LY, Wong AT, Chung PH, Chan VS, Lin CL, Sham PC, Leung GM, Peiris JS, Khoo US. CD209 (DC-SIGN) -336A>G promoter polymorphism and severe acute respiratory syndrome in Hong Kong Chinese. *Hum Immunol.* 2010 Jul;71(7):702-7. doi: 10.1016/j.humimm.2010.03.006.
 38. Yi YX, Han JB, Zhao L, Fang Y, Zhang YF, Zhou GY. Tumor necrosis factor alpha gene polymorphism contributes to pulmonary tuberculosis susceptibility: evidence from a meta-analysis. *Int J Clin Exp Med.* 2015 Nov 15;8(11):20690-700.
 39. Akahoshi M, Nakashima H, Miyake K, Inoue Y, Shimizu S, Tanaka Y, Okada K, Otsuka T, Harada M. Influence of interleukin-12 receptor beta1 polymorphisms on tuberculosis. *Hum Genet.* 2003 Mar;112(3):237-43. doi: 10.1007/s00439-002-0873-5.
 40. Chan KY, Xu MS, Ching JC, Chan VS, Ip YC, Yam L, Chu CM, Lai ST, So KM, Wong TY, Chung PH, Tam P, Yip SP, Sham P, Lin CL, Leung GM, Peiris JS, Khoo US. Association of a single nucleotide polymorphism in the CD209 (DC-SIGN) promoter with SARS severity. *Hong Kong Med J.* 2010;16(5 Suppl 4):37-42.
 41. Yuan FF, Tanner J, Chan PK, Biffin S, Dyer WB, Geczy AF, Tang JW, Hui DS, Sung JJ, Sullivan JS. Influence of Fc gammaRIIA and MBL polymorphisms on severe acute respiratory syndrome. *Tissue Antigens.* 2005 Oct;66(4):291-6. doi: 10.1111/j.1399-0039.2005.00476.x.

42. Remus N, El Baghdadi J, Fieschi C, Feinberg J, Quintin T, Chentoufi M, Schurr E, Benslimane A, Casanova JL, Abel L. Association of IL12RB1 polymorphisms with pulmonary tuberculosis in adults in Morocco. *J Infect Dis.* 2004 Aug 1;190(3):580-7. doi: 10.1086/422534.
43. Bukhari M, Aslam MA, Khan A, Iram Q, Akbar A, Naz AG, Ahmad S, Ahmad MM, Ashfaq UA, Aziz H, Ali M. TLR8 gene polymorphism and association in bacterial load in southern Punjab of Pakistan: an association study with pulmonary tuberculosis. *Int J Immunogenet.* 2015 Feb;42(1):46-51. doi: 10.1111/iji.12170.
44. Prabhu Anand S, Selvaraj P, Jawahar MS, Adhilakshmi AR, Narayanan PR. Interleukin-12B & interleukin-10 gene polymorphisms in pulmonary tuberculosis. *Indian J Med Res.* 2007 Aug;126(2):135-8.
45. Adam KM. Immunoinformatics approach for multi-epitope vaccine design against structural proteins and ORF1a polyprotein of severe acute respiratory syndrome coronavirus-2 (SARS-CoV-2). *Trop Dis Travel Med Vaccines.* 2021 Jul 8;7(1):22. doi: 10.1186/s40794-021-00147-1.
46. Monteiro-Maia R, Ortigão-de-Sampaio MB, Pinho RT, Castello-Branco LR. Modulation of humoral immune response to oral BCG vaccination by *Mycobacterium bovis* BCG Moreau Rio de Janeiro (RDJ) in healthy adults. *J Immune Based Ther Vaccines.* 2006 Sep 6;4:4. doi: 10.1186/1476-8518-4-4.
47. Bui HH, Sidney J, Dinh K, Southwood S, Newman MJ, Sette A. Predicting population coverage of T-cell epitope-based diagnostics and vaccines. *BMC Bioinformatics.* 2006 Mar 17;7:153. doi: 10.1186/1471-2105-7-153.
48. Schlake T, Thess A, Fotin-Mleczek M, Kallen KJ. Developing mRNA-vaccine technologies. *RNA Biol.* 2012 Nov;9(11):1319-30. doi: 10.4161/rna.22269. Epub 2012 Oct 12.
49. Pardi N, Hogan MJ, Porter FW, Weissman D. mRNA vaccines - a new era in vaccinology. *Nat Rev Drug Discov.* 2018 Apr;17(4):261-279. doi: 10.1038/nrd.2017.243.
50. Ahammad I, Lira SS. Designing a novel mRNA vaccine against SARS-CoV-2: An immunoinformatics approach. *Int J Biol Macromol.* 2020 Nov 1;162:820-837. doi: 10.1016/j.ijbiomac.2020.06.213.
51. Kozak M. Possible role of flanking nucleotides in recognition of the AUG initiator codon by eukaryotic ribosomes. *Nucleic Acids Res.* 1981 Oct 24;9(20):5233-52. doi: 10.1093/nar/9.20.5233.
52. Wang JY, Song WT, Li Y, Chen WJ, Yang D, Zhong GC, Zhou HZ, Ren CY, Yu HT, Ling H. Improved expression of secretory and trimeric proteins in mammalian cells via the introduction of a new trimer motif and a mutant of the tPA signal sequence. *Appl Microbiol Biotechnol.* 2011 Aug;91(3):731-40. doi: 10.1007/s00253-011-3297-0.
53. Seillier C, Hélie P, Petit G, Vivien D, Clemente D, Le Mauff B, Docagne F, Toutirais O. Roles of the tissue-type plasminogen activator in immune response. *Cell Immunol.* 2022 Jan;371:104451. doi: 10.1016/j.cellimm.2021.104451.
54. Kou Y, Xu Y, Zhao Z, Liu J, Wu Y, You Q, Wang L, Gao F, Cai L, Jiang C. Tissue plasminogen activator (tPA) signal sequence enhances immunogenicity of MVA-based vaccine against tuberculosis. *Immunol Lett.* 2017 Oct;190:51-57. doi: 10.1016/j.imlet.2017.07.007.
55. Teufel F, Almagro Armenteros JJ, Johansen AR, Gíslason MH, Pihl SI, Tsirigos KD, Winther O, Brunak S, von Heijne G, Nielsen H. SignalP 6.0 predicts all five types of signal peptides using protein language models. *Nat Biotechnol.* 2022 Jul;40(7):1023-1025. doi: 10.1038/s41587-021-01156-3.
56. Franke ED, Hoffman SL, Sacci JB Jr, Wang R, Charoenvit Y, Appella E, Chesnut R, Alexander J, Del Guercio MF, Sette A. Pan DR binding sequence provides T-cell help for induction of protective antibodies against *Plasmodium yoelii* sporozoites. *Vaccine.* 1999 Mar 5;17(9-10):1201-5. doi: 10.1016/s0264-410x(98)00341-7.
57. Alexander J, del Guercio MF, Maewal A, Qiao L, Fikes J, Chesnut RW, Paulson J, Bundle DR, DeFrees S, Sette A. Linear PADRE T helper epitope and carbohydrate B cell epitope conjugates induce specific high titer IgG antibody responses. *J Immunol.* 2000 Feb 1;164(3):1625-33. doi: 10.4049/jimmunol.164.3.1625.
58. Ghaffari-Nazari H, Tavakkol-Afshari J, Jaafari MR, Tahaghoghi-Hajghorbani S, Masoumi E, Jalaali SA. Improving Multi-Epitope Long Peptide Vaccine Potency by Using a Strategy that Enhances CD4+ T Help in BALB/c Mice. *PLoS One.* 2015 Nov 10;10(11):e0142563. doi: 10.1371/journal.pone.0142563.
59. Van Der Spoel D, Lindahl E, Hess B, Groenhof G, Mark AE, Berendsen HJ. GROMACS: fast, flexible, and free. *J Comput Chem.* 2005 Dec;26(16):1701-18. doi: 10.1002/jcc.20291.
60. Celada F, Seiden PE. A computer model of cellular interactions in the immune system. *Immunol Today.* 1992 Feb;13(2):56-62. doi: 10.1016/0167-5699-(92)90135-T.
61. Puzone R, Kohler B, Seiden P, F. Celada. IMMSIM, a flexible model for in machina experiments on immune system responses. *Future Generation Computer Systems.* 2002 Aug;18(7):961-972. doi: 10.1016/S0167-739X(02)00075-4.
62. S. Gong and RM Ruprecht. Immunoglobulin M: An Ancient Antiviral Weapon – Rediscovered. *Front Immunol.* 2020 Aug;11:1943. doi: 10.3389/FIMMU.2020.01943/BIBTEX. doi: 10.3389/fimmu.2020.01943.
63. BP O'Connor, MW Gleeson, RJ Noelle, and LD Erickson. The rise and fall of long-lived humoral immunity: terminal differentiation of plasma cells in health and disease. *Immunol Rev.* 2003 Aug;194:61. doi: 10.1034/J.1600-065X.2003.00055.X. doi: 10.1034/j.1600-065X.2003.00055.x
64. Lum FM, Torres-Ruesta A, Tay MZ, Lin RTP, Lye DC, Rénia L, Ng LFP. Monkeypox: disease epidemiology, host immunity and clinical interventions. *Nat Rev Immunol.* 2022 Oct;22(10):597-613. doi: 10.1038/s41577-022-00775-4.
65. Johnston SC, Johnson JC, Stonier SW, Lin KL, Kisalu NK, Hensley LE, Rimoin AW. Cytokine modula-

- tion correlates with severity of monkeypox disease in humans. *J Clin Virol.* 2015 Feb;63:42-5. doi: 10.1016/j.jcv.2014.12.001.
66. Lum FM, Torres-Ruesta A, Tay MZ, Lin RTP, Lye DC, Rénia L, Ng LFP. Monkeypox: disease epidemiology, host immunity and clinical interventions. *Nat Rev Immunol.* 2022 Oct;22(10):597-613. doi: 10.1038/s41577-022-00775-4.
67. Pittman PR, Martin JW, Kingebeni PM, et al. Clinical characterization of human monkeypox infections in the Democratic Republic of the Congo. *medRxiv*; 2022. doi: 10.1101/2022.05.26.22273379.
68. Goulding J, Abboud G, Tahiliani V, Desai P, Hutchinson TE, Salek-Ardakani S. CD8 T cells use IFN- γ to protect against the lethal effects of a respiratory poxvirus infection. *J Immunol.* 2014 Jun 1;192(11):5415-25. doi: 10.4049/jimmunol.1400256.
69. Alvarez-de Miranda FJ, Alonso-Sánchez I, Alcamí A, Hernaez B. TNF Decoy Receptors Encoded by Poxviruses. *Pathogens.* 2021 Aug 22;10(8):1065. doi: 10.3390/pathogens10081065.
70. Verardi PH, Jones LA, Aziz FH, Ahmad S, Yilma TD. Vaccinia virus vectors with an inactivated gamma interferon receptor homolog gene (B8R) are attenuated *In vivo* without a concomitant reduction in immunogenicity. *J Virol.* 2001 Jan;75(1):11-8. doi: 10.1128/JVI.75.1.11-18.2001.
71. Marshall B, Puthalakath H, Caria S, Chugh S, Doerflinger M, Colman PM, Kvensakul M. Variola virus F1L is a Bcl-2-like protein that unlike its vaccinia virus counterpart inhibits apoptosis independent of Bim. *Cell Death Dis.* 2015 Mar 12;6(3):e1680. doi: 10.1038/cddis.2015.52.
72. Simon WL, Salk HM, Ovsyannikova IG, Kennedy RB, Poland GA. Cytokine production associated with smallpox vaccine responses. *Immunotherapy.* 2014;6(10):1097-112. doi: 10.2217/imt.14.72.

Mutagenic and antimutagenic evaluation of *Asparagus larycinus* Burch., *Senecio asperulus* DC., and *Gunnera perpensa* L. to hepatic cells

Polo-Ma-Abiele Hildah Mfengwana

Department of Health Sciences, Central University of
Technology, Free State, Bloemfontein, South Africa

 <https://orcid.org/0000-0002-4208-8026>

Corresponding author: pntsoeli@cut.ac.za

Published: 2022-12-27

How to Cite: Mfengwana P-M-AH. Mutagenic and antimutagenic evaluation of *Asparagus larycinus* Burch., *Senecio asperulus* DC., and *Gunnera perpensa* L. to hepatic cells. *Journal of Medical Science*. 2022;91(4):e745. doi:10.20883/medical.e745

 doi: 10.20883/medical.e745



Keywords: neutral red uptake, VITOTOX, Alkaline Comet assay, VITOTOX, Alkaline Comet assay, DNA mutation toxicity

© 2022 by the author(s). This is an open access article distributed under the terms and conditions of the Creative Commons Attribution (CC BY-NC) licence. Published by Poznan University of Medical Sciences

ABSTRACT

Introduction. The use of traditional medicinal plant concoctions to cure or treat different diseases daily in African folk medicine. However, the effects of most medicinal plants on human health or genetic material remain unknown. This study thus aimed to evaluate the mutagenic and antimutagenic potentials of *Asparagus larycinus* Burch. cladodes, *Senecio asperulus* DC., and *Gunnera perpensa* L. roots extract *in vitro*.

Material and methods. Neutral red uptake assay, alkaline comet assay, and the VITOTOX test was used with plant extract dilutions of 4, 20, 50, and 100 µg/ml, respectively, on hepatic (C3A) cells and *Salmonella Typhimurium* TA104 strains. Ethyl methane-sulfonate and 4-nitroquinoline oxide were used as positive controls for the comet and VITOTOX assays, respectively.

Results. *In vitro* cytotoxicity and genotoxicity were not observed from all tested extracts, except for the two dichloromethane (DCM) extracts of *S. asperulus* and *G. perpensa*, which appeared to be cytotoxic with S9 metabolic activation, but not genotoxic or mutagenic. From the VITOTOX test results, none of the extracts appeared to have antimutagenic properties after treating *S. Typhimurium* strains with a known mutagen.

Conclusions. These results confirm that previously reported anticarcinogenic properties of *A. larycinus*, *S. asperulus*, and *G. perpensa* did not result from the protective mechanism against genotoxicity but from other ones. Moreover, the negative mutagenic and cytotoxic activities of the tested plants highlighted the safe use of these medicinal plants *in vitro*. Therefore, *S. asperulus* and *G. perpensa* DCM extracts require further investigation for their possible *in vivo* cytotoxic effects on humans.

Introduction

Medicinal plants play an essential role in African communities' folk medicine as they are used as remedies for minor ailments and even severe and significant ailments such as cancer [1–3]. Never-

theless, medicinal plants with mutagenic activity can induce deoxyribonucleic acid (DNA) damage in human body cells. Plants' chemical agents may directly or indirectly damage the cell's genetic information in the DNA, cause mutations, or

even lead to cancer when not repaired [4]. When mutations occur in the cell division genes, oncogenes are formed, and a cell may begin to proliferate abnormally [5]. The process occurs when cells with mutations escape repairs by a regular cellular repair system, then uncontrollably divide when they were not supposed to, thus ultimately becoming cancerous. The affected cancerous cell will either undergo programmed cell death or the damage to its oncogene will be passed on to descendant cancer cells as they divide. Moreover, gene mutations can result from chromosomal abnormalities and re-arrangements through deletion, translocation, and inversion. However, cells can protect themselves from a genotoxic mutation by triggering DNA repair or a programmed cell death process (apoptosis); failure to commit to one of these two options leads to mutagenicity. Medicinal plants can sometimes have genotoxic effects that are mutagenic or could even have antimutagenic effects that reverse and prevent or reverse or prevent mutation, which usually leads to oncogene formation [6]. Medicinal plants can be helpful in the development of new anticancer drugs.

Africa is blessed with rich flora. This abundance, especially in medicinal plants, contributes to the growing number of people using traditional medicinal plants. Other factors for the increased dependence on medicinal plants are easy accessibility even at local markets, affordability, and a belief that they have few or no side effects [7]. Local people use the medicinal plants selected for this study to treat different ailments. However, their mutagenicity has not been reported. *Asparagus larycinus* Burch. is native to the Southern African region and is used to treat cancer, tuberculosis, sores, red water, uterine infection, general alignments, and umbilical cord inflammation, and it serves as a diuretic [8–9]. Previous studies on the leaves of *Asparagus larycinus* showed the presence of tannins, saponins, terpenes, steroids, flavonoids, glycosides, steroids, and carbohydrates [10–11]. However, this plant showed the absence of alkaloids. The leaves of *Asparagus larycinus* also demonstrated antioxidant, antibacterial, and anticarcinogenic activities [11–12].

Senecio asperulus is ethnomedicinally used in Lesotho to treat back pain, swollen feet [13], colic, flu, colds, sore throat, mouth ulcers, and sore joints and to improve blood circulation

[14]. Moreover, Kose et al., in their ethnobotanical study [15], further reported on the use of this plant for the treatment of tuberculosis, herpes, syphilis, and itchy feet by the Lesotho community. *Senecio asperulus* infusion has also been used as a remedy for internal poisoning [16]. Mugomeri et al. [13] identified phytochemicals, such as flavonoids, glycosides, and phytosterols, with beneficial medicinal properties from *Senecio asperulus*. *Gunnera perpensa* is widely known for its high medicinal importance in several traditional medicine systems. The plant treats cancer, regulates the menstrual cycle, treats impotence, induces labour, treats stomachache, eases period pains, and relieves colic during pregnancy [17–18]. Some phytochemicals, including saponins, phenols, alkaloids, tannins, steroids, cardiac glycosides, flavonoids, and proanthocyanins and flavonols, have been identified from *Gunnera perpensa* [19–20]. Khan et al. [21] further isolated and identified Z-venusol as a significant component of *Gunnera perpensa*.

Many active compounds used to develop drugs come from medicinal plants. Even pharmaceutical companies show an increased interest in plant-derived drugs mainly because of the current widespread belief that 'green medicine' is safe, with fewer side effects [22–23]. However, there are still challenging tasks for drug research scientists, including investigating the safety of herbal medicine [23]. To distinguish favourable from adverse effects and to ban poisonous plants or contaminations from herbal mixtures, the assessment of the effect of plant-derived products' toxicity on the tissue or organs of mammalian recipients is still required. Most plants used in traditional medicine have *in vitro* mutagenic properties [24–25]; therefore, it is important to evaluate their mutagenic potency. Plants with mutagenic properties must thus be considered potentially unsafe and require further testing before their continued use is recommended. To evaluate the potential of tested sample to cause mutations to the DNA of cells, the use of high throughput assays such as Neutral red uptake assay, alkaline comet assay, and the VITOTOX tests are valuable as they provide information on the genotoxicity and cytotoxicity of the sample. The study aimed to investigate the mutagenic and antimutagenic properties of *Asparagus larycinus* Burch., *Senecio asperulus* DC., and *Gunnera perpensa* L.

Materials and methods

Plant material

The study received plant collection and export permits from the Ministry of Tourism Environment and Culture, Lesotho, and from the Department of Economic Development, Tourism and Environmental Affairs, South Africa (NC.553/2017), for import approval. The plant materials were collected from the mountains of Lesotho (Mohale's Hoek district, Mpharane). Then, they were authenticated by scientists at the National Botanical Gardens in Bloemfontein, South Africa. Their voucher specimens were deposited at the National Botanical Gardens with herbarium numbers MAS001 for *Asparagus larycinus*, PHM01 for *Senecio asperulus*, and PHM02 for *Gunnera perpensa*. Roots of *Senecio asperulus* DC. and *Gunnera perpensa* L., and *Asparagus larycinus* Burch. cladodes were washed, air-dried at room temperature (22°C), then grounded into a fine powder using an electric blender and weighed. They were then stored in a cool place until analysis. The crude extracts were used in this study as lay people frequently use these plants to treat different ailments and use concoctions prepared from the whole part of the plant, not the isolated compound.

Extraction method

The extraction was done using maceration [6]. Plant material (10 g of the dried powdered roots, and cladodes, respectively) were weighed, pulverised, and soaked in distilled water (DH₂O), methanol (MeOH), and dichloromethane (DCM), for 72 hours with occasional stirring using a mechanical shaker. The extracts were filtered, and new solvents were added again, respectively, for more extraction until the solvents remained clear (this process was repeated three times). The extracts were then filtered, and aqueous extracts were concentrated with a freeze-drier and organic solvents with a rocket evaporator. Percentage yields were calculated.

C3A cell culture

The toxicology of the studied plant extracts was determined using mycoplasma-free human hepatocyte cells (C3A). C3A cells are a sensitive model for *in vitro* predictive of human genotoxic exposure. Cell suspensions of human C3A cells in Dulbecco's modified Eagle's culture medium sup-

plemented with 10% fetal calf serum were seeded into each well of a 96-well microtiter plate, so the cell density was 40,000 cells/well. Plates were incubated overnight (24 hours) at 37°C and 5% carbon dioxide (CO₂). Humidity was maintained using a water bath containing distilled water inside the incubator.

The neutral red uptake (NRU) test

The NRU test estimates the dose of medicinal extracts that is not cytotoxic to human hepatic cells (C3A). The NRU test is based on the ability of live cells to take up and bind the 3-amino-7-dimethyl-2-methylphenazine hydrochloride (NR) dye. This dye is known to accumulate in the lysosomes of the viable cell after penetrating the cell membranes through non-ionic diffusion. Increased unabsorbed NR dye shows increased cell death. Therefore, viable cells can be distinguished from dead or dying cells based on their NRU, and quantitative measurement of the number of viable cells can be undertaken. In this study, the neutral red uptake (NRU) test was performed using the method described by Repetto et al. [26]. After overnight incubation, the cells were then treated with dilutions of the extracts, which were 4 µg/ml, 20 µg/ml, 50 µg/ml, and 100 µg/ml. Cells were further incubated for another 24 hours to allow the extracts to work. Then cells were washed in phosphate-buffered saline (PBS), after which 200 µl of a 0.625 mg/ml neutral red (NR)-solution was added. Cells were rewashed with PBS after being incubated for three hours to remove excess dye. Two hundred microlitres of a 50:1 ethanol-acetic acid solution were then added, and cells could mix with this solution for 1.5 hours on the shaker to remove the dye from the cells. The absorbances were measured with a microplate spectrophotometer at 540 nm wavelength. The absorption of non-treated cells (negative control) was given a 100% value to which data from treated cells were compared. Sodium dodecyl sulfate was used as a positive control.

The comet assay

The protocol by Olive and Banáth [27], was followed to evaluate the DNA damaging and protective effects of the three-plant species. Microscope slides were pre-coated by spreading 300 µl 1% standard melting point agarose in water evenly over the slides and allowing the agarose to

harden. Hepatic (C3A) cells at a density of 200000 cells/ml were treated with different concentrations of the test sample in 24-well plates and incubated for 24 hours at 37°C in a 5% CO₂ incubator. The plant extracts were tested at 250, 100, 50, and 4 µg/ml concentrations. Ethyl methane-sulfonate (EMS) at 1 mM was used as a positive control/mutagen. The cells were exposed to plant extracts alone for mutagenicity testing, and for antimutagenicity testing, the cells were exposed to a combination of the plant extracts and 1 mM EMS. After incubation, cells were trypsinized, and 10 µl of a 10 000-cell suspension was added to 300 µl of 0.8% low melting point agarose at 37°C.

The mixture was spread on the pre-coated slides and hardened under a coverslip on ice. Once the agarose had been prepared, the coverslips were removed. The microscope slides were placed in a lysis buffer overnight. First, denaturation was conducted using the electrophoresis buffer at 17°C for 40 minutes. Next, electrophoresis was conducted using the same solution at 25V, and the current was adjusted to 300 mA for 20 minutes. After electrophoresis, the microscope slides were neutralised in a Tris buffer (pH 7.5), and dried. The slides were then placed in ice-cold ethanol for 10 minutes and dried at room temperature. Finally, the gels were stained with 100 µl of 20 µg/ml ethidium bromide, left for 10 minutes, and rinsed in distilled water. The slides were analyzed using a fluorescence microscope supplied with a camera. The tail length, percentage DNA in the tail, and tail moment were determined using the computer image-analysis program Tri-Tek CometScore™. This program allows the measurement of tail length, percentage of DNA in the tail, and tail moment as parameters to measure DNA damage in the comet assay.

Moreover, for mutagenicity testing, differences in parameters used to measure DNA damage (i.e. tail length, percentage DNA in tail and tail moment) were compared between sample concentration and solvent blank (negative control). For antimutagenicity testing, the same parameters used for genotoxicity testing were used. In this case, the measurements in the test samples were compared to the positive control (EMS).

The VITOTOX® test

The VITOTOX® test is performed following the method described by Verschaeve [28], with *Sal-*

monella Typhimurium bacteria that lack the necessary oxidative enzyme systems for the metabolism of foreign compounds as they can react with DNA. As for most other in vitro assays, the bacteria were treated with the test compound in the presence and absence of a post-mitochondrial supernatant ('S9'). Micro-organisms were incubated overnight and then a dilution of the bacterial suspension was incubated for an hour on a rotative shaker. Multiwell plates were used to contain the solvent, different concentrations of the test compound, or the positive control for genotoxicity testing (4-Nitroquinoline 1-oxide (4-NQO) with S9 or 4-NQO without S9). Genotoxicity and toxicity measurements were performed using a microplate luminometer that enabled online measurements of emitted light (e.g., every five minutes over four hours). After completion of the measurements, the data were transferred into a Microsoft Excel macro sheet, and the signal-to-noise (S/N) ratio, i.e., the light production of exposed bacteria divided by the light production of non-exposed bacteria, was calculated for each measurement. The S/N ratio was calculated for the *recN2-4* and *pr1* strains separately. So was the ratio between the maximum S/N values of the *recN2-4* and *pr1* strains. All calculations occurred automatically and were based on measurements between 60 and 240 minutes of incubation. Based on experimental grounds, a compound was considered genotoxic when the following criteria were met:

- › max S/N (*recN2-4*) / max S/N (*pr1*) (to be indicated as: *rec/pr1*) was greater than 1.5,
- › max S/N in *recN2-4* must show a good dose-dependent effect.

Statistical analysis

All experiments per sample were repeated in triplicates. The Mann-Whitney U test was used for the statistical analysis, and $p < 0.05$ was considered significant.

Results

The results from this study showed that the viability of cells treated with different concentrations (4 µg/ml, 20 µg/ml, 50 µg/ml, and 100 µg/ml) of *Asparagus larycinus*, *Senecio asperulus*, and *Gunnera perpensa* plant extracts to be dose-dependent as shown in **Figure 1 (A-I)**. DCM extracts of *Aspar-*

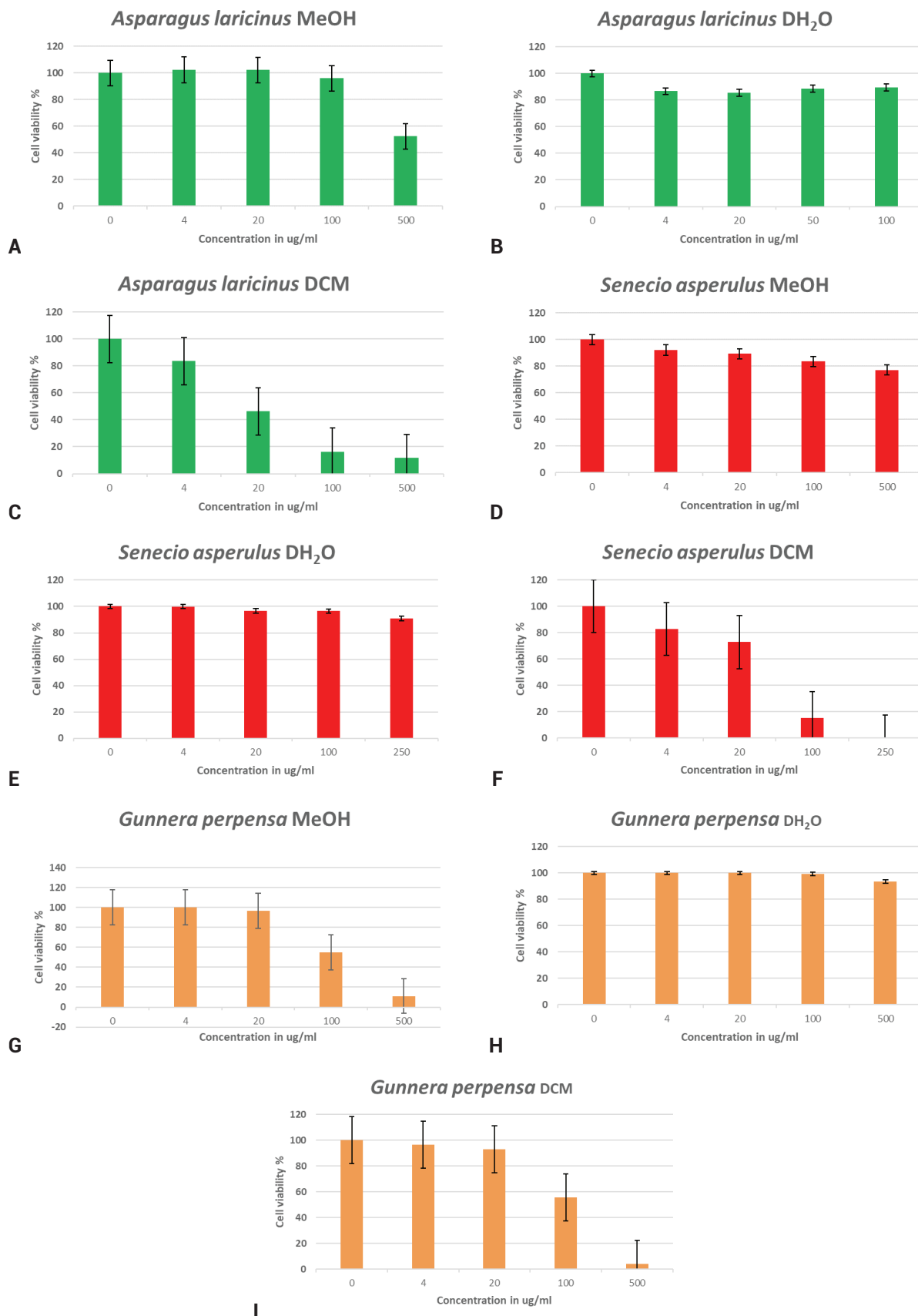


Figure 1. Neutral Red Uptake test results of *Asparagus larycinus* (A: methanol, B: water, and C: dichloromethane), *Senecio asperulus* (D: methanol, E: water, and F: dichloromethane) and *Gunnera perpensa* (G: methanol, H: water and I: dichloromethane) plant extracts. On the x-axis, 0 represents the negative control. Cells were treated with different concentrations of the extracts between 4 µg/ml and 500 µg/ml, then treated with a dye to differentiate between live and dead cells. Live cells took up the dye, and their viability was measured and presented by red bars

agus laricinus and *Senecio asperulus* showed proliferation inhibition to C3A cells in a dose-dependent manner from the 50 µg/ml concentrations. *Gunnera perpensa* MeOH and DCM extracts showed cytotoxic effects from the 100 µg/ml concentrations. The remaining extracts had no significant cell proliferation inhibition effects even at the higher concentration of 100 µg/ml compared to the untreated (negative control) C3A cells.

The concentration of the tail formed (due to damaged/broken pieces of DNA) relative to the head (intact DNA), reflecting the number of DNA breaks and the extent of DNA damage, was calculated automatically by the use of imaging software. **Figure 2 (A-I)** shows the results. Deviations that were statistically significant for *Asparagus laricinus* were found at as low as 4 µg/ml for aqueous extracts, 20 µg/ml for methanolic extracts, and 250 µg/ml for DCM extracts. After that, concentration showed increased DNA damage due to the observed percentage of the tail (**Figure 2: A-I**). Nonetheless, these effects were low compared to DNA damage caused by the well-known mutagen EMS. *Senecio asperulus* extracts did not show any formation of statistically significant comets nor *Gunnera perpensa* aqueous extracts. However, *Gunnera perpensa* organic extracts showed statistically significant DNA damage at the highest tested concentration of 500 µg/ml for MeOH extracts and 100 µg/ml for DCM extracts. However, there was no significant DNA damage increase for the latter as the concentrations increased.

Table 1 reports the summarized results of the toxicological properties of *Asparagus laricinus*, *Senecio asperulus*, and *Gunnera perpensa* plant extracts. These plants were assessed using the VITOTOX assay by investigating both genotoxicity and cytotoxicity effects with and without S9. The tested concentrations were guided by the NRU results reported in **Figure 1 (A-I)**.

With the VITOTOX assay, the plant extracts' genotoxicity and cytotoxicity are assayed simultaneously to identify false-positive results caused by non-specific light production induced by other mechanisms besides the genotoxic effect [27]. Both the genotoxic strain with luciferase operon (TA104 recN2-4) and Cytox strain expressing the lux operon (TA104 pr1) were used with and without metabolic activation by the S9 enzyme. The light production showed the genotoxicity of the plant extract after the genotoxic extract had activated the recN promoter in the TA104 recN2-4 strain. Non-specific light production when the compound activates the pr1 in the TA104 pr1 strain was indicative of the cytotoxicity of the plant extract. The genotoxicity and cytotoxicity of each extract at concentrations of 100 µg/ml, 250 µg/ml, and 500 µg/ml were investigated and reported in **Table 1**. The positive control, 4-nitroquinoline 1-oxide, is known to have mutagenic and carcinogenic effects. For the validity of the test, 4-NQO showed genotoxicity with an S/N ratio greater than 1.5. Yet no cytotoxicity with an S/N ratio greater than 0.8 (**Table 1**).

Table 1. The genotoxicity and cytotoxicity performed with the highest tested concentration (as guided by the neutral red uptake results) of *Asparagus laricinus* (*A. laricinus*), *Senecio asperulus* (*S. asperulus*), and *Gunnera perpensa* (*G. perpensa*) with, and without S9 activation

Extract and concentration	Genotoxicity (S/N ratio)	Genotoxicity with S9 (S/N ratio)	Cytotoxicity (S/N ratio)	Cytotoxicity with S9 (S/N ratio)
<i>A. laricinus</i> MeOH [500 µg/ml]	<0.6	>0.8 but <1.0	<0.8	>0.8 but <1.0
<i>A. laricinus</i> DH ₂ O [100 µg/ml]	0.0	0.0	0.0	0.0
<i>A. laricinus</i> DCM [500 µg/ml]	>1.5	1.0	>1.6	<1.2 but >1.0
<i>S. asperulus</i> MeOH [500 µg/ml]	>1.5	1.0	>0.8	1.0
<i>S. asperulus</i> DH ₂ O [250 µg/ml]	0.0	<0.6	0.0	<0.6
<i>S. asperulus</i> DCM [250 µg/ml]	<0.6	>0.8 but <1.5	>0.8	<0.8
<i>G. perpensa</i> MeOH [500 µg/ml]	>1.5	<1.0	<0.8	>0.8
<i>G. perpensa</i> DH ₂ O [500 µg/ml]	1.5	0.8	<0.8	<0.8
<i>G. perpensa</i> DCM [500 µg/ml]	<0.8	<0.6	<0.8	<0.8
4-NQO 100 µg/ml	>1.5	>1.5	>0.8	>0.8

Abbreviations: S9, hepatic post-mitochondrial supernatant; S/N, signal-to-noise; MeOH, methanol; DH₂O, distilled water; DCM, dichloromethane; 4-NQO, 4-Nitroquinoline 1-oxide; <, less than; >, greater than.

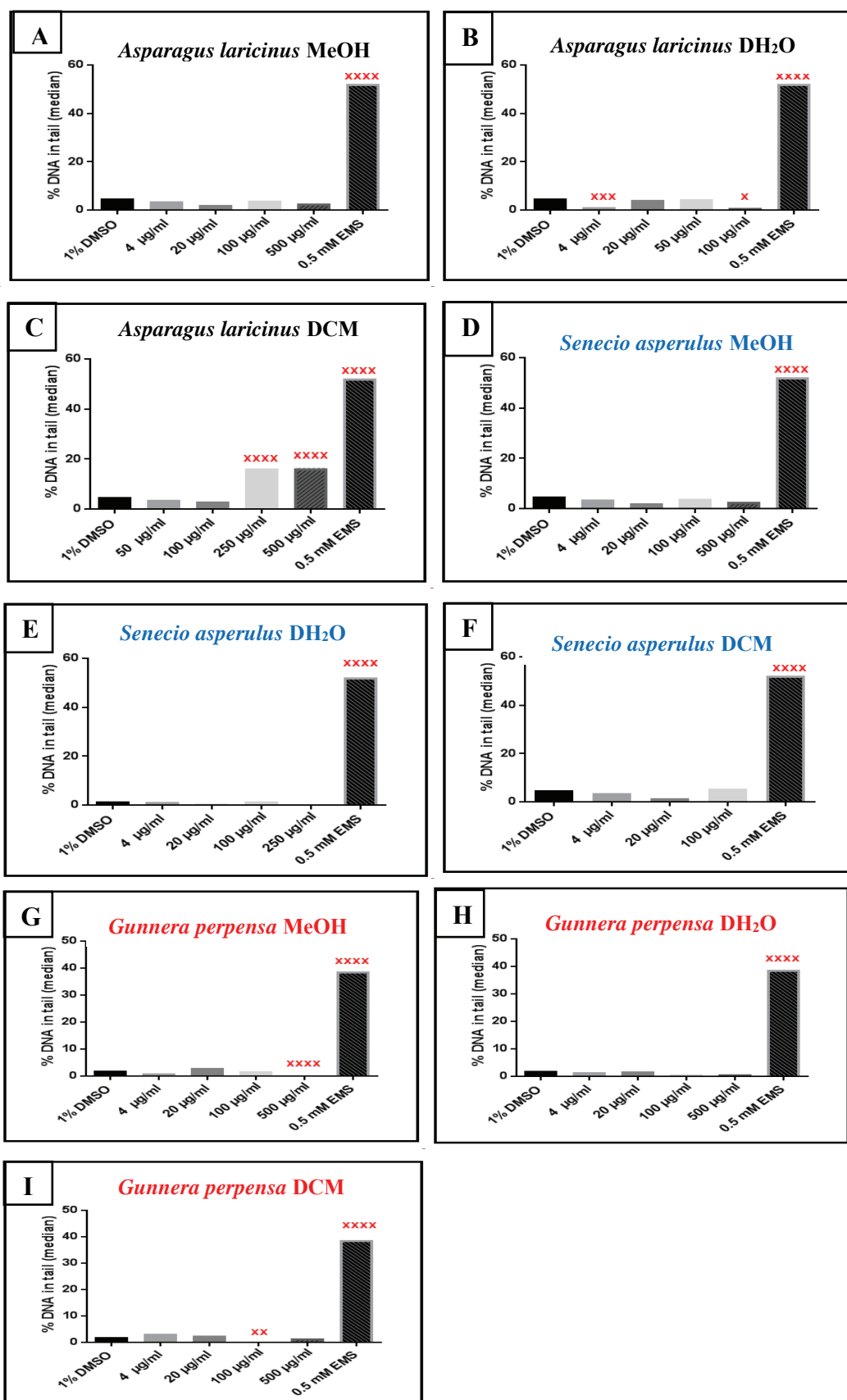


Figure 2. Comet test results of *Asparagus larycinus* (A-C), *Senecio asperulus* (D-F) and *Gunnera perpensa* (G-I) plant extracts. The statistically significant increases above background levels when compared with cells treated with 1% dimethyl sulfoxide(DMSO), and this was indicated as **x** = $P < 0.05$; **xx** = $P < 0.01$, and **xxx** = $P < 0.005$ and **xxxx** = $P < 0.001$. Abbreviations: MeOH, methanol; DH₂O, distilled water; DCM, dichloromethane; EMS, Ethyl methane-sulfonate

Discussion

For the continuous use of medicinal plants with a history of being used for the treatment of various ailments and cancer to be recommended, their safety to mammal cells must be evaluated. Although medicinal plant users believe they are safe by their users, research has proven that natural products, including medicinal plants, can be mutagenic [24–25]. Mutagenicity is the ability of a chemical agent to cause mutations to the DNA of cells, and these agents are said to be genotoxic [4, 29]. Genotoxic compounds from medicinal plants can cause mutations that are mutagenic. All mutagens are thus genotoxic, but not all genotoxic agents are mutagenic.

Moreover, mutations are known to be significant contributors to carcinogenesis; mutagens are thus most likely considered carcinogens [30]. However, plants with antimutagenic potential are considered interesting sources for new therapeutic uses [28]. The paper reports how the mutagenicity and antimutagenicity of *Asparagus larycinus*, *Senecio asperulus*, and *Gunnera perpensa* affect mycoplasma-free human hepatocyte (C3A) cells using two tests, namely the bacterial VITOTOX test, and the alkaline comet assay.

The VITOTOX test is a high throughput bacterial genotoxicity test that is very fast, sensitive, and uses only tiny quantities of a sample. This test uses two different *Salmonella Typhimurium* TA104 recombinant test strains that carry a luciferase operon to determine the genotoxicity and cytotoxicity of the sample. Furthermore, the assay correlates well with the Ames test or the SOS chromotest [4, 31]. SOS gene response is triggered when there is cell DNA damage in which the cell cycle is arrested, and DNA repair and mutagenesis are induced [32]. Thus genotoxic compounds are considered SOS-inducing compounds. The VITOTOX test is based on the induction of SOS function transcription by inserting an operon-less "lux" gene next to recN, resulting in light production when the bacterial DNA is damaged. Infusing luxCDABE on the multicopy plasmid to recN promoter allows genotoxicity to be detected. On the other hand, its fusion with the pr1 promoter allows cytotoxicity to be detected. According to Verschaeve et al. [4], when recN-luxCDABE fusion occurs, the sample genotoxicity at sublethal will increase light production. In con-

trast, this light production decreases as a function of the sample toxicity due to the infusion of Pr1-luxCDABE. Therefore, a signal-to-noise (S/N) ratio greater than 1.5 indicates genotoxicity. An S/N ratio <0.8 shows cytotoxicity.

The comet assay is a single-cell gel electrophoresis assay that is simple to perform, versatile and sensitive for single- and double-strand break measurements in damaged DNA [29, 33]. The comet assay was performed only in the absence of S9 as the cells used (liver cells, C3A) could already retain their metabolic activity. **Figure 1 (A-I)** demonstrates concentrations used in this test guided by the results obtained from the NRU test as demonstrated, as well as the solubility of the extracts. Moreover, overly toxic concentrations will influence the percentages of DNA fragments in the tail of the formed comets. Thus, their DNA damage properties were assessed at lower concentrations for extracts that reduced the viability of cells at higher concentrations, such as *Senecio asperulus* dichloromethane extracts.

Furthermore, the comet assay was performed in the dark to prevent light-induced DNA damage [34]. According to Chang et al. [35], this migration results when the structural loop of the DNA break loses its supercoiling and is pulled towards the anode under the electrophoresis field. These formed comets were observed by fluorescence microscopy after the DNA was stained with DNA-specific fluorescent dyes such as ethidium bromide or propidium iodide.

Asparagus larycinus methanol and *Senecio asperulus* aqueous extracts were neither genotoxic nor cytotoxic with or without S9. Their S/N ratio in response to the Genox strain was less than 1.5 and to the Cyttox strain was below 0.8 in a dose-dependent manner (**Table 1**). *Asparagus larycinus* water and *Gunnera perpensa* dichloromethane extracts were neither genotoxic nor cytotoxic with or without S9. The *Asparagus larycinus* dichloromethane extracts were cytotoxic and genotoxic, with or without S9 activation, which was in line with the NRU test and comet assay results. Furthermore, the results coincided with findings by Mfengwana et al. [12]. *Asparagus larycinus* dichloromethane extracts were reported to be cytotoxic after nuclear morphological changes, and their cytotoxicity was due to induced apoptosis. VITOTOX test results in this study showed *Asparagus larycinus* to be non-mu-

tagenic. The outcome correlated with the Ames test findings reported by Mashele and Fuku36. The test evaluated the mutagenic and antimutagenic properties of *Asparagus laricus* aqueous root extracts. The *Asparagus laricus* leaf aqueous extracts were reported to be cytotoxic to Vero cells at the concentration of 200 µg/ml, which contradicts the finding by Mashele and Kolesnikova [8] as the roots of the same plant showed no cytotoxic effect. However, the study by Mfengwana [37] showed the presence of nine compounds from the leaves of *Asparagus laricus* (publication on the identification of these compounds is in progress), while only a few compounds were isolated from the roots of *Asparagus laricus*: indole-3-carbinol, α-sitosterol, and ferulic acid [10]. Thus, certain compounds are present in the leaves that are absent from the root part of this plant, which could be why the leaf extracts were cytotoxic at higher concentrations. It indicates the importance of determining the correct dose that will not lead to cytotoxicity or genotoxicity before medicinal plant application. The *in vivo* toxicity of the *Asparagus laricus* leaves has not been evaluated yet, as only the toxicological evaluation of the roots has been reported [38].

Mutagenicity is the ability of a chemical agent to cause mutations that result in cell death. Then, those agents are genotoxic [4, 29]. *Senecio asperulus* MeOH extract was genotoxic and cytotoxic without the presence of S9. However, this extract remained cytotoxic but was not genotoxic after adding S9. Literature reports show the *in vitro* cytotoxicity of *Senecio asperulus* DCM extracts on kidney epithelial cells extracted from an African green monkey (Vero cells) The cytotoxicity of this extract was thus observed without S9 activation when the (3-(4, 5-dimethylthiazolyl-2)-2, 5-diphenyltetrazolium bromide) MTT assay was used (11). The study findings also confirmed the cytotoxicity of the *Senecio asperulus* DCM extract as it was not genotoxic or cytotoxic without S9, then its toxicity was reversed by the presence of S9 as this extract became cytotoxic. This indicates that *Senecio asperulus* DCM extract is not a direct mutagen (inactive without S9) but becomes cytotoxic after metabolism (mutagenic in the presence of S9). It suggests that diverse assays (VITOTOX and MTT in this case) have different specificities and sensitivity against

certain mutagens. Plant mutagenicity, therefore, cannot be based on one test result [39].

Both the methanol and water extract of *Gunnera perpensa* were genotoxic but could not produce an S/N ratio above 0.8 for the cytox strain. They were thus genotoxic but not cytotoxic. However, these extracts were not genotoxic but cytotoxic when S9 was present. The presence of S9 reversed the mutagenicity or even blocked the induced mutagenic activity of these extracts and made them genotoxic agents that are not mutagenic, that is, some of the compounds present in this extract are mutagens. The isolation of pure compounds and the re-analysis of those will, therefore, assist in highlighting unknown mutagens from these plant extracts. The study results indicate that the presence of the S9 enzyme (from both comet and VITOTOX assays) reduced *Gunnera perpensa* extract genotoxicity, which means that the safety of this plant is modified when the liver cells metabolise the plant. However, this could only be concluded after *in vivo* work on this plant has been completed (work in progress).

Antimutagens counteract mutagens by inactivating or preventing the Mutagen-DNA reaction or mutagenic compound transformation into mutagen. These can be natural or synthetic compounds rendering certain mechanisms, such as (i) directly interacting with mutagens, (ii) inhibiting the activation of mutagens, (iii) blocking the mutagen binding to the target, and (iv) through the generation of antioxidant mechanism [40]. These mechanisms prove that antimutagens have the potential to eliminate or reduce the mutagenic effects of potentially harmful substances. Therefore, the investigation of antimutagenic compounds provides new possibilities in anticancer drug discovery, and this quest is expanding hastily in cancer research [41–42]. DNA damage in cells exposed to the test substance was investigated to evaluate the mutagenicity and antimutagenicity of *Asparagus laricus*, *Senecio asperulus*, and *Gunnera perpensa*. For satisfactory evaluation of the genotoxic potential of a compound, 3 endpoints need to be assessed: gene mutation, DNA damage, and structural and numerical chromosome aberrations [26]. Accordingly, many *in vitro* and *in vivo* toxicology test methods including the VITOTOX test, mammal cell micronucleus test, and comet assay, have been developed to

assess the potential of substances to cause mutagenicity that may lead to cancer.

Extracts were tested to assess the antimutagenic effects of the selected medicinal plants with 4-NQO and with and without S9. The same concentrations and conditions were set as in the case of the genotoxicity test. 4-nitroquinoline-N-oxide (4-NQO) is a base substitution agent that causes direct DNA damage by acting at G residues, which leads to the induction of GC to AT transitions [43]. Based on the study results, all extracts tested could not significantly decrease or improve the genotoxicity of 4-NQO. They were thus considered as not having antigenotoxic activities. Hence the implication is that the observed anticarcinogenic activity of *Asparagus larycinus* and *Senecio asperulus* on breast cancer cells did not result from plant genotoxicity protection but other mechanisms, such as apoptosis [12]. *Gunnera perpensa* has been characterized before, and five compounds are identified from its methanolic extract: 3,3',4'-tri-O-methyl ellagic acid lactone, ellagic acid lactone, 1,1'-biphenyl-4,4'-diacetic acid, p-hydroxybenzaldehyde and Z-methyl lespedezate [44]. Some of these compounds are known as antihemorrhagic, antimutagenic and anticarcinogenic agents. Contrary to the compounds reported by Brookes and Dutton [44], none of the *Gunnera perpensa* extracts showed antimutagenic properties. Only *Gunnera perpensa* DCM extracts proved anticarcinogenic properties in vitro [12].

Conclusions

Asparagus larycinus, *Senecio asperulus*, and *Gunnera perpensa* have been used as traditional medicines to treat several diseases, including cancer. However, the safety of these plants has yet to be investigated before with comet and VITOTOX assays, especially using liver cells to mimic how the liver will metabolise the plant. Nevertheless, *S. asperulus* and *Asparagus larycinus* water extracts are potentially safe as they demonstrate no mutagenicity or cytotoxicity. Moreover, *G. perpensa* is genotoxic but not cytotoxic; however, its genotoxic and cytotoxic effects are reversed when the S9 enzyme is present. Thus, this proves that the genotoxicity properties are lost during the metabolism of this plant.

Thus, it does not cause DNA damage after being metabolized but becomes cytotoxic. This plant is, therefore, still questionable and should not be used further until its cytotoxic mechanism is well understood. Unfortunately, none of the tested extracts showed any antimutagenic effects and thus cannot be used to reverse DNA damage caused by mutagens.

Acknowledgements

Conflict of interest statement

The authors declare no conflict of interest.

Funding statement

The National Research Fund (117961), Thuthuka Grant, funded the study.

Ethical considerations

The author has observed ethical issues (including plagiarism, data fabrication, and double publication). The Faculty of Health and Environmental Sciences research committee at the Central University of Technology, Free State in South Africa (CUT-208012729) evaluated and approved the protocol.

Significance

This research emphasises the safety of *Asparagus larycinus*, *Senecio asperulus*, and *Gunnera perpensa* medicinal plants, which are common cancer treatment methods. This information can support further uses of these plants in human health as they are not carcinogenic.

Acknowledgements

The author would like to thank the Central University of Technology, the Free State (CUT) research office, the National Research Fund, the Department of Higher Education and Training, and the next generation of the academic program for their financial and other support. An appreciation to Luc Verschaeve and Roel Anthonissen from the Institute of Public Health, Brussels, for assisting with the data analysis. An expression of genuine gratitude to the "Ha Morena Motlatsi's" Chieftaincy, Mpharane, Mohale's Hoek district, Lesotho, for their warm welcome and permission for plant collection from their land. Special thanks to the indigenous plants' knowledge holder, Ms T.R Mochochoko, for sharing her knowledge with the CUT research team.

References

1. Mohd-Fuat AR, Kofi EA, Allan GG. Mutagenic and cytotoxic properties of three herbal plants from Southeast Asia. *Trop Biomed*. 2007 Dec;24(2):49-59. PMID: 18209708.
2. Roy A, Attre T, Bharadvaja N. Anticancer agent from medicinal plants: a review. In book: *New aspects in medicinal plants and pharmacognosy*, 1st edition. 2017;1(3):54-73. https://www.researchgate.net/profile/Arpita-Roy-3/publication/318721809_Anti-

- cancer_agent_from_medicinal_plants_a_review/links/597ace074585151e35aea568/Anticancer-agent-from-medicinal-plants-a-review.pdf
3. Verschaeve L, Edziri H, Anthonissen R, Boujnah D, Skhiri F, Chehab H, Aouni M, Mastouri M. In vitro Toxicity and Genotoxic Activity of Aqueous Leaf Extracts From Four Varieties of *Olea europea* (L). *Pharmacogn Mag.* 2017 Jan;13(Suppl 1):S63-S68. doi: 10.4103/0973-1296.203980.
 4. Verschaeve L, Van Gompel J, Thilemans L, Regniers L, Vanparys P, van der Lelie D. VITOTOX bacterial genotoxicity and toxicity test for the rapid screening of chemicals. *Environ Mol Mutagen.* 1999;33(3):240-8.
 5. Griffiths AJ, Miller JH, Suzuki DT, Lewontin RC, Gelbart WM. Quantifying heritability. In Freeman WH, ed. *An Introduction to Genetic Analysis*, 7th edition. 2000. http://lgb.rc.unesp.br/biomol/literatura/Griffiths_8th.pdf
 6. Bouguellid G, Russo C, Lavorgna M, Piscitelli C, Ayouni K, Wilson E, Kim HK, Verpoorte R, Choi YH, Kilani-Atmani D, Atmani D, Isidori M. Antimutagenic, antigenotoxic and antiproliferative activities of *Fraxinus angustifolia* Vahl. leaves and stem bark extracts and their phytochemical composition. *PLoS One.* 2020 Apr 16;15(4):e0230690. doi: 10.1371/journal.pone.0230690.
 7. Mustapha AA. Medicinal plants with possible anti-HIV activities: A review. *Int J Med Plants.* 2014;106:439-53. <https://clinphytoscience.springeropen.com/articles/10.1186/s40816-015-0004-1>.
 8. Mashele SS, Kolesnikova N. In vitro anticancer screening of *Asparagus larycinus* extracts. *Pharmacologyonline.* 2010;2(1):246-252. <https://pharmacologyonline.silae.it/files/archives/2010/vol2/023.Mashele.pdf>.
 9. Mfengwana PH, Mashele SS. Medicinal Properties of Selected *Asparagus* Species: A Review. In: Roa V, Mans D, Roa L, eds. *Phytochemicals in Human Health*. London 2019. Intechopen. <https://www.intechopen.com/chapters/67855>.
 10. Fuku S, Al-Azzawi AM, Madamombe-Manduna IT, Mashele S. Phytochemistry and free radical scavenging activity of *Asparagus larycinus*. *Int J Pharmacol.* 2013;9(5):312-17. <https://scialert.net/fulltext/?doi=ijp.2013.312.317>.
 11. Ntsoelinyane PH, Mashele SS. Phytochemical screening, antibacterial and antioxidant activities of *Asparagus larycinus* leaf and stem extracts. *Bangladesh J Pharmacol.* 2014;9:10-4. <https://www.semanticscholar.org/paper/Phytochemical-screening%2C-antibacterial-and-of-leaf-Ntsoelinyane-Mashele/72c699d9275e4802f2b92e998e2c9222ca29db8d>.
 12. Mfengwana PH, Mashele SS, Manduna IT. Cytotoxicity and cell cycle analysis of *Asparagus larycinus* Burch. and *Senecio asperulus* DC. on breast and prostate cancer cell lines. *Heliyon.* 2019 May 11;5(5):e01666. doi: 10.1016/j.heliyon.2019.e01666.
 13. Mugomeri E, Chatanga P, Hlapisi S, Rahlao L. Phytochemical characterization of selected herbal products in Lesotho. *Lesotho Med Asso J.* 2014;12:38-47. <https://www.ajol.info/index.php/ajtcam/article/view/130715>.
 14. Moteetee A, Van Wyk B. The medical ethnobotany of Lesotho: a review. *Bothalia.* 2011;41(1):209-228. <http://www.ethnopharmacologia.org/prelude2020/pdf/biblio-hm-44-moteetee.pdf>.
 15. Seleteng Kose L, Moteetee A, Van Vuuren S. Ethnobotanical survey of medicinal plants used in the Maseru district of Lesotho. *J Ethnopharmacol.* 2015 Jul 21;170:184-200. doi: 10.1016/j.jep.2015.04.047.
 16. Quattrocchi U. *CRC World Dictionary of Medicinal and Poisonous Plants. Common Names, Scientific Names, Eponyms, Synonyms, and Etymology.* Boca Raton: Taylor & Francis Group, 2016. <https://doi.org/10.1201/b16504>.
 17. Mammo F, Mohanlall V, Shode F. *Gunnera perpensa* L.: a multi-use ethnomedicinal plant species in South Africa. *Afr J Sci Technol Innov Dev.* 2017. doi: 10.1080/20421338.2016.1269458.
 18. Maroyi A. From Traditional Usage to Pharmacological Evidence: Systematic Review of *Gunnera perpensa* L. *Evid Based Complement Alternat Med.* 2016;2016:1720123. doi: 10.1155/2016/1720123.
 19. Simelane MB, Lawal OA, Djarova TG, Musabayane CT, Singh M, Opoku AR. Lactogenic activity of rats stimulated by *Gunnera perpensa* L. (Gunneraceae) from South Africa. *Afr J Tradit Complement Altern Med.* 2012 Jul 1;9(4):561-73. doi: 10.4314/ajtcam.v9i4.14.
 20. Chigor CB. Development of conservation methods for *Gunnera perpensa* L.: an overexploited medicinal plant in the Eastern Cape, South Africa. PhD Thesis, University of Fort Hare 2014. <https://core.ac.uk/download/pdf/145034661.pdf>.
 21. Khan F, Peter XK, Mackenzie RM, et al. Venusol from *Gunnera perpensa*: structural and activity studies. *Phytochemistry.* 2004 Apr;65(8):1117-1121. doi: 10.1016/j.phytochem.2004.02.024. PMID: 15110692.
 22. Ndhkala AR, Finnie JF, Van Staden J. Plant composition, pharmacological properties and mutagenic evaluation of a commercial Zulu herbal mixture: *Imbiza ephuzwato*. *J Ethnopharmacol.* 2011 Jan 27;133(2):663-74. doi: 10.1016/j.jep.2010.10.053.
 23. Efferth T, Kaina B. Toxicities by herbal medicines with emphasis to traditional Chinese medicine. *Curr Drug Metab.* 2011 Dec;12(10):989-96. doi: 10.2174/138920011798062328.
 24. Cardoso CR, de Syllos Cólus IM, Bernardi CC, Sannomiya M, Vilegas W, Varanda EA. Mutagenic activity promoted by amentoflavone and methanolic extract of *Byrsonima crassa* Niedenzu. *Toxicology.* 2006 Aug 1;225(1):55-63. doi: 10.1016/j.tox.2006.05.003.
 25. Déciga-Campos M, Rivero-Cruz I, Arriaga-Alba M, Castañeda-Corral G, Angeles-López GE, Navarrete A, Mata R. Acute toxicity and mutagenic activity of Mexican plants used in traditional medicine. *J Ethnopharmacol.* 2007 Mar 21;110(2):334-42. doi: 10.1016/j.jep.2006.10.001.
 26. Repetto G, del Peso A, Zurita JL. Neutral red uptake assay for the estimation of cell viability/cytotoxicity. *Nat Protoc.* 2008;3(7):1125-31. doi: 10.1038/nprot.2008.75.
 27. Olive PL, Banáth JP. The comet assay: a method to measure DNA damage in individual cells. *Nat Protoc.* 2006;1(1):23-9. doi: 10.1038/nprot.2006.5.

28. van der Lelie D, Regniers L, Borremans B, Provoost A, Verschaeve L. The VITOTOX test, an SOS bioluminescence *Salmonella typhimurium* test to measure genotoxicity kinetics. *Mutat Res.* 1997 Mar 17;389(2-3):279-90. doi: 10.1016/s1383-5718(96)00158-1.
29. Collins AR. The use of bacterial repair endonucleases in the comet assay. *Methods Mol Biol.* 2011;691:137-47. doi: 10.1007/978-1-60761-849-2_8.
30. Makhuvele R, Foubert K, Apers S, Pieters L, Verschaeve L, Elgorashi E. Antimutagenic constituents from *Monanthes caffra* (Sond.) Verdc. *J Pharm Pharmacol.* 2018 Jul;70(7):976-984. doi: 10.1111/jphp.12918.
31. Vaghasiya Y, Dave R, Chanda S. Phytochemical analysis of some medicinal plants from western region of India. *Res J Medicinal Plant.* 2011;5(5):567-76. <https://www.cabdirect.org/globalhealth/abstract/20123177659>.
32. Biran A, Yoav HB, Yagur-Kroll S, Pedahzur R, Buchinger S, Shacham-Diamand Y, Reifferscheid G, Belkin S. Microbial genotoxicity bioreporters based on *sulA* activation. *Anal Bioanal Chem.* 2011;400(9):3013-24. <https://link.springer.com/article/10.1007/s00216-011-5007-2>.
33. Słoczyńska K, Powroźnik B, Pękala E, Waszkiewicz AM. Antimutagenic compounds and their possible mechanisms of action. *J Appl Genet.* 2014 May;55(2):273-85. doi: 10.1007/s13353-014-0198-9.
34. Azqueta A, Collins AR. The essential comet assay: a comprehensive guide to measuring DNA damage and repair. *Arch Toxicol.* 2013 Jun;87(6):949-68. doi: 10.1007/s00204-013-1070-0.
35. Chang JB, Wu MF, Lu HF, Chou J, Au MK, Liao NC, Chang CH, Huang YP, Wu CT, Chung JG. Toxicological evaluation of *Andropogon cinnamomea* in BALB/c mice. *In Vivo.* 2013 Nov-Dec;27(6):739-45.
36. Mashele SS, Fuku S. Evaluation of the antimutagenic and mutagenic properties of *Asparagus laricinus*. *J Med Technol.* 2011;2:33-36. <https://www.semanticscholar.org/paper/Evaluation-of-the-antimutagenic-and-mutagenic-of-Mashele-Fuku/a9e076d98f8993f79a0dac125ad4669986adf268>.
37. Mfengwana P. Evaluation of Pharmacological Properties of Traditional Medicinal Plants Used For The Treatment Of Cancer By South African And Lesotho Communities. 2019. <http://hdl.handle.net/11462/2032>.
38. Mokgawa SD. Toxicology of *Asparagus laricinus* in rats. 2016. <http://ir.cut.ac.za/bitstream/handle/11462/1332/Mokgawa%2C%20Sekobane%20Daniel.pdf?sequence=1&isAllowed=y>.
39. Edziri H, Mastouri M, Mahjoub A, Anthonissen R, Mertens B, Cammaerts S, Gevaert L, Verschaeve L. Toxic and mutagenic properties of extracts from Tunisian traditional medicinal plants investigated by the neutral red uptake, VITOTOX and alkaline comet assays. *S Afr J Bot.* 2011;77:703-710. <https://www.sciencedirect.com/science/article/pii/S0254629911000214>.
40. Gautam S, Saxena S, Kumar S. Fruits and vegetables as dietary sources of antimutagens. *J Food Chem Nanotechnol.* 2016;2(3):97-114. <https://foodchemistryjournal.com/jfcn/articles/v2n3/jfcn-018-satyendra-gautam.pdf>.
41. El-Sayed WM, Hussin WA. Antimutagenic and antioxidant activity of novel 4-substituted phenyl-2,2'-bichalcophenes and aza-analogs. *Drug Des Devel Ther.* 2013;7:73-81. doi: 10.2147/DDDT.S40129.
42. Ferguson LR, Philpott M. Nutrition and mutagenesis. *Annu Rev Nutr.* 2008;28:313-29. doi: 10.1146/annurev.nutr.28.061807.155449.
43. Fronza G, Campomenosi P, Iannone R, Abbondandolo A. The 4-nitroquinoline 1-oxide mutational spectrum in single stranded DNA is characterized by guanine to pyrimidine transversions. *Nucleic Acids Res.* 1992 Mar 25;20(6):1283-7. doi: 10.1093/nar/20.6.1283.
44. Brookes KB, Dutton MF. Bioactive Components of the Uteroactive Medicinal Plant, *Gunnera perpensa* (or Ugobo). *S Afr J Sci.* 2007;103(5):187-189. <http://www.scielo.org.za/pdf/sajs/v103n5-6/07.pdf>

Generation of singlet oxygen by porphyrin and phthalocyanine derivatives regarding the oxygen level

Martin Pola

Department of Medical Biophysics, Faculty of Medicine and Dentistry, Palacky University in Olomouc, Olomouc, Czech Republic

 <https://orcid.org/0000-0002-8939-3941>

Hana Kolarova

Department of Medical Biophysics, Faculty of Medicine and Dentistry, Palacky University in Olomouc, Olomouc, Czech Republic

 <https://orcid.org/0000-0002-6156-4841>

Robert Bajgar

Department of Medical Biophysics, Faculty of Medicine and Dentistry, Palacky University in Olomouc, Olomouc, Czech Republic

 <https://orcid.org/0000-0003-4854-4114>

Corresponding author: robert.bajgar@upol.cz

 doi: 10.20883/medical.e752

Keywords: photodynamic therapy, photosensitizers, hyperoxia, singlet oxygen

Published: 2022-12-27

How to Cite: Pola M, Kolarova H, Bajgar R. Generation of singlet oxygen by porphyrin and phthalocyanine derivatives regarding the oxygen level. *Journal of Medical Science*. 2022;91(4);e752. doi:10.20883/medical.e752



© 2022 by the author(s). This is an open access article distributed under the terms and conditions of the Creative Commons Attribution (CC BY-NC) licence. Published by Poznan University of Medical Sciences

ABSTRACT

Background. The principle of photodynamic effect is based on the combined action of photosensitizer, molecular oxygen and light, which produce various reactive oxygen species and are associated with significant cellular damage. Singlet oxygen is one of the most serious representatives, which is characterised by powerful oxidising properties. Moreover, concomitant hyperbaric oxygen treatment can support these effects. Therefore, the subject of our study was to compare the yields of singlet oxygen for four different photosensitizers in dependency on the oxygen concentration.

Material and methods. Four different photosensitizers 5,10,15,20-tetrakis(1-methyl-4-pyridinio)porphyrin tetra(p-toluenesulfonate), tetramethylthionine chloride, 5,10,15,20-tetrakis(4-sulfonatophenyl)porphyrin zinc(II) and zinc phthalocyanine disulfonate were investigated to determine the yield of singlet oxygen in PBS by Singlet Oxygen Sensor Green reagent under different partial pressures of oxygen (0.4 and 36 mg/l).

Results. There were no noticeable shifts in the excitation and emission fluorescence spectra regarding the oxygen concentration. Concerning the same molar concentration of photosensitizers the production of singlet oxygen was highest for 5,10,15,20-tetrakis(4-sulfonatophenyl)porphyrin zinc(II), where the rate of the fluorescence change was more than 3 times higher than that obtained for 5,10,15,20-tetrakis(1-methyl-4-pyridinio)porphyrin tetra(p-toluenesulfonate). On the other hand, zinc phthalocyanine disulfonate showed the lowest yield in singlet oxygen production.

Conclusions. Singlet oxygen production, within the range of oxygen concentrations achievable in tissues under normoxia or hyperoxia, does not depend on these concentrations. However, the singlet oxygen generation is significantly influenced by the type of photosensitizer, with the highest yield belonging to 5,10,15,20-tetrakis(4-sulfonatophenyl)porphyrin zinc(II).

Introduction

The principal of the photodynamic effect (PDE) is the light absorption by a specific compound known as a photosensitizer. After absorption, the excited photosensitizer can release the excess energy by fluorescence or undergoes a transition to a triplet state via intersystem crossing. Close contact with surrounding molecules can subsequently lead to an electron transfer, forming free radicals or radical ions. Which, in turn, may finally interact with other molecules producing superoxide anion radicals, hydrogen peroxides and hydroxyl radicals (type I reaction) Alternatively, the excited photosensitizer can transfer the energy to a molecule of oxygen to form singlet oxygen (type II reaction). Although both reactions can co-occur, their proportion depends on the chemical structures of photosensitizers and substrate molecules and on the oxygen level [1, 2].

The production of reactive oxygen species (ROS) by PDE is the basis of photodynamic therapy (PDT), which is becoming an alternative method in treating oncological, cardiovascular, skin, and eye diseases. PDT is also used to treat chronic inflammation and drug-resistant bacterial infections [3]. Photosensitizers used in PDT represent diverse chemical compounds, including porphyrins, chlorophylls, bacteriochlorins, phthalocyanines, pheoforbides, purpurines, 5-aminolevulinic acid (ALA), texaphirines. Porphyrin derivatives belong to the first generation of photosensitizers. This group shows high absorption in the Soret band and poor solubility in polar solvents, which disadvantages the use for clinical purposes [4, 5].

On the other hand, the second generation of photosensitizers, such as phthalocyanines, chlorins and purpurins, absorbs light in the red region allowing better tissue penetration. It also has a higher potential to accumulate in the target cells [5]. An increase in solubility of hydrophobic photosensitizers can be achieved, for example, by sulfonation. Further, the formation of a complex with zinc and aluminium increases the yield and lifetime of the photosensitizer's triplet state, and thus singlet oxygen can be promoted [6–9].

The oxygen molecule is the third key component in PDT (besides photosensitizer and light). The type II oxygen-dependent reaction is primarily responsible for the biological PDT effect [10].

Oxygen partial pressure (pO_2) in normal tissues ranges from 30 to 60.0 mmHg (i.e. 1.2 to 2.4 mg/l of dissolved oxygen at 37°C, 0.9% salinity, and normal atmospheric pressure) [11, 12]. Hyperbaric oxygen (HBO) treatment causes a several-fold increase in the cerebral tissue pO_2 [13]. A recent study aimed at tissue oxygenation in the head and limbs revealed that transcutaneous pO_2 during HBO can be increased even 8–15 times [14]. Thus, our presented study aimed to investigate the significance of the different concentrations of oxygen on the production of singlet oxygen for four different photosensitizers.

Material and methods

Photosensitizers, hypoxia and hyperoxia

Four different photosensitizers were investigated to determine the yield of singlet oxygen in PBS under different partial pressures of oxygen. 5,10,15,20-tetrakis(1-methyl-4-pyridinio)porphyrin tetra(p-toluenesulfonate) (TmPyP) and tetramethylthionine chloride (methylene blue, MB) were purchased from Sigma-Aldrich (Sigma-Aldrich, MO, USA). Whereas Jiří Mosinger (Department of Inorganic Chemistry, Charles University in Prague, Czech Republic) and Jan Rakušan (Centre for Organic Chemistry Ltd, Rybitví, Czech Republic) synthesised and donated 5,10,15,20-tetrakis(4-sulfonatophenyl)porphyrin zinc(II) (ZnTPPS) and zinc phthalocyanine disulfonate (ZnPcS), respectively. Their synthesis was described previously [15, 16]. **Figure 1** shows chemical structures of these photosensitizers. Different partial pressures of oxygen related to dissolved oxygen concentrations of approximately 0.4 and 36 mg/l (measured by oximeter Greisinger 3630, Germany) were achieved by pure nitrogen and oxygen bubbling via injection needles into hermetically sealed cuvettes filled with 3 ml of PBS for 20 minutes.

Fluorescence spectroscopy

Photosensitizers' excitation and emission spectra were measured with the fluorescence spectrometer FLS980 (Edinburgh Instruments, UK). The resulting concentration of all photosensitizers in PBS was 1 μ M. The emission spectra for ZnTPPS and TmPyP were obtained at 420 nm excitation (at excitation and emission bandwidths of 1 nm). In contrast, MB and ZnPcS were excited by

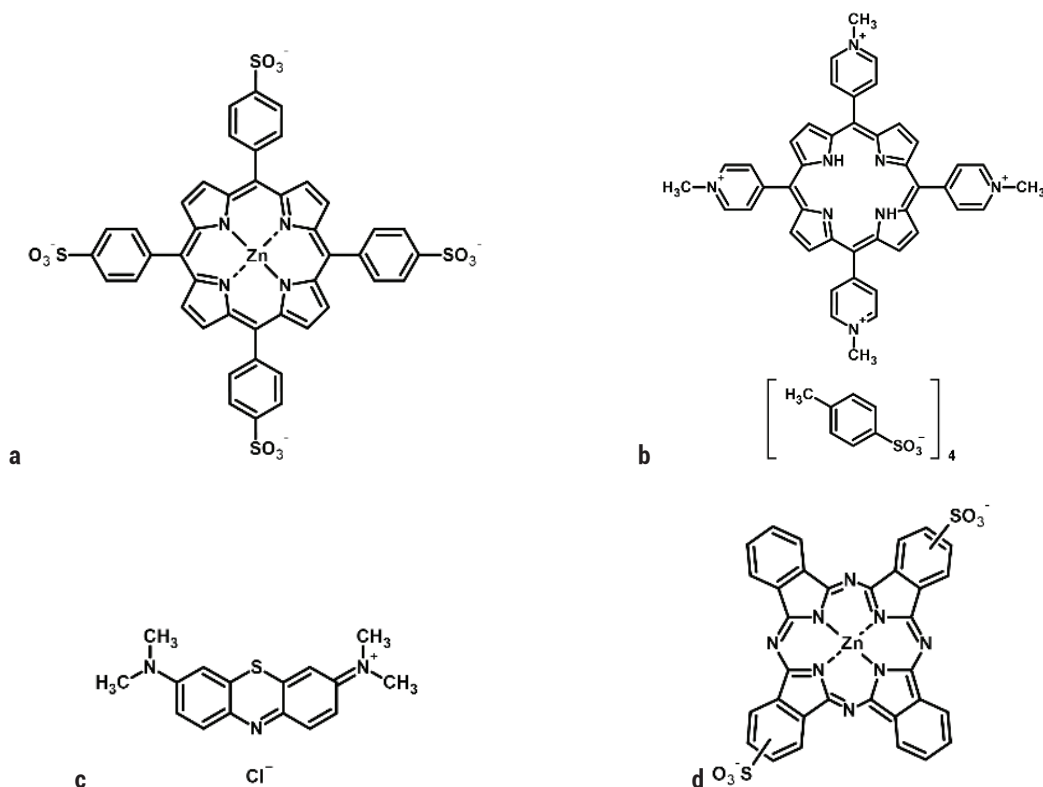


Figure 1. Chemical structure of photosensitizers: 5,10,15,20-tetrakis(4-sulfonatophenyl)porphyrin zinc(II) (ZnTPPS, a); 5,10,15,20-tetrakis(1-methyl-4-pyridinio)porphyrin tetra(p-toluenesulfonate) (TmPyP, b); tetramethylthionine chloride (methylene blue, MB, c); zinc phthalocyanine disulfonate (ZnPcS, d)

a wavelength of 663 nm (at excitation and emission bandwidths of 1 nm). The excitation spectra of photosensitizers were collected for their emission maxima, i.e. 607 nm for ZnTPPS, 715 nm for TmPyP, 689 nm for MB and 681 nm for ZnPcS.

Singlet oxygen measurement

The singlet oxygen sensor green reagent (SOSG, Invitrogen by Thermo Fisher Scientific, MA, USA) was used to detect singlet oxygen production in PBS buffer under different oxygen levels. First, the SOSG was added to the PBS buffer to reach the final $3\mu\text{M}$ concentration in each cuvette. Then the cuvettes were placed in the temperature-controlled holder of the spectrofluorometer. A generation of singlet oxygen was monitored as an increase in fluorescence emission intensity at 530 nm. An external source equipped with a mercury lamp, an optical bandpass filter of 460–480 nm, and optical fibre attached to the cuvette holder was used to excite SOSG. Singlet oxygen production was initiated by manually opening the shutter of the spectrofluorometer lamp. ZnTPPS and

TmPyP were activated by light with an excitation wavelength of 420 nm and a slit width of 2.6 nm, whereas MB and ZnPcS were activated by light with an excitation wavelength of 663 nm and a slit width of 3.3 nm. The different slit widths were chosen so that the reference detector showed the same number of registered photons (500,000 cps). The appropriate irradiances measured by the IL 1705 radiometer system using the SED033 sensor (International Light Technologies, USA) were $4.1 \times 10^{-4} \text{ W/cm}^2$ for the light of 420 nm and $2.1 \times 10^{-4} \text{ W/cm}^2$ for the light of 663 nm. The rate of change in fluorescence determined the quantification of the singlet oxygen production during the first 7 seconds and the difference in fluorescence values after 4 minutes of the sample irradiation.

Data analysis

The data presented illustrate either representative traces or means \pm standard errors of at least four independent measurements. The one-way analysis of variance (ANOVA) was used to compare experimental groups.

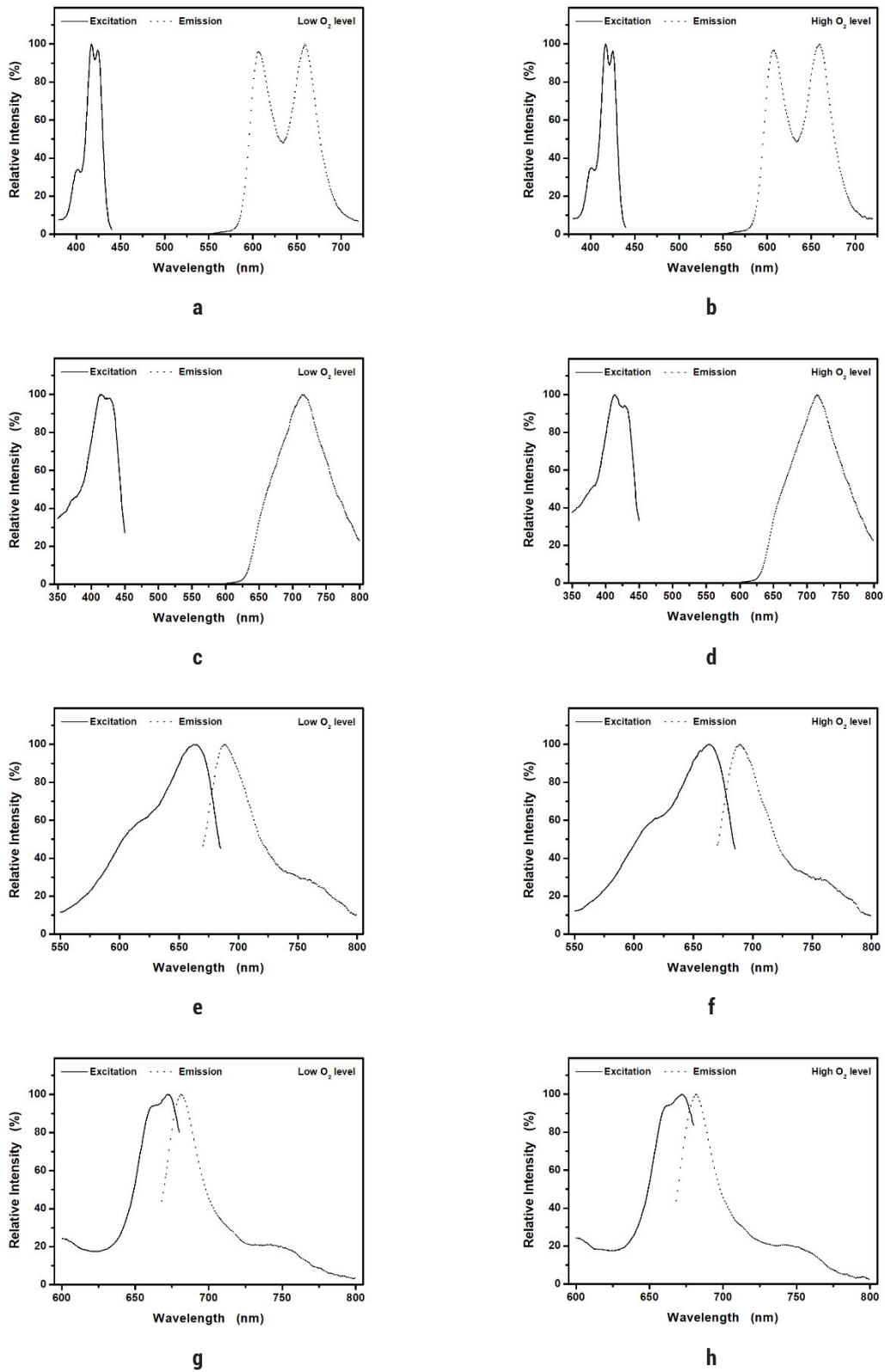


Figure 2. Normalized fluorescence spectra: ZnTPPS (a, b); TmPyP (c, d); MB (e, f); ZnPcS (g, h); under low (0.4 mg/ml, a, c, e, f) and high (36 mg/ml, b, d, f, h) oxygen concentration in PBS

Results

Fluorescence spectroscopy

To compare the yields in the production of singlet oxygen for different photosensitizers it was necessary to find the optimal conditions, i.e. their excitation maxima. The porphyrin derivatives are known for their absorption maxima in the Soret band. The excitation peak of the synthesized zinc complex of porphyrin ZnTPPS was located at about 420 nm with two maxima at 417 and 425 nm and a shoulder at 401 nm (**Figure 2a-b**). The commercially available derivative TmPyP showed an excitation peak at about 2 nm shorter wavelength, with the maximum at 414 nm and a shoulder at 428 nm (**Figure 2c-d**). A much more significant spectral difference for these 2 porphyrins was found in the peak width. Whereas the full width at the half maximum (FWHM) for

TmPyP was 58 nm, the excitation peak of ZnTPPS was significantly narrower with the FWHM of 20 nm. MB and non-commercial phthalocyanine derivative ZnPcS have their excitation spectra in the red region with a dominance around 660 nm (**Figure 2e-f and 2 g-h**, respectively). Compared to ZnPcS, the excitation spectrum of MB is wider. **Table 1** summarises the values of the excitation and emission maxima. In addition, there were not any noticeable shifts in the spectral characteristics regarding the difference in the oxygen concentration.

Singlet oxygen measurement

The generation of singlet oxygen by PDE using different photosensitizers at two different concentrations of oxygen in PBS was measured continuously for 4 minutes from the start of irradiation of the solution (**Figure 3**). The porphyrin

Table 1. Excitation and emission maxima of photosensitizers in PBS with low (0.4 mg/ml) and high (36 mg/ml) oxygen concentrations

Photosensitizer	Oxygen level	Excitation λ_{max} (nm)	Emission λ_{max} (nm)
ZnTPPS	Low	401, 417, 425	607, 659
	High	401, 417, 425	607, 659
TmPyP	Low	414, 428	715
	High	414, 428	715
MB	Low	621, 663	689, 758
	High	621, 663	689, 758
ZnPcS	Low	663, 672	681, 744
	High	663, 672	681, 744

Shoulders are in italics.

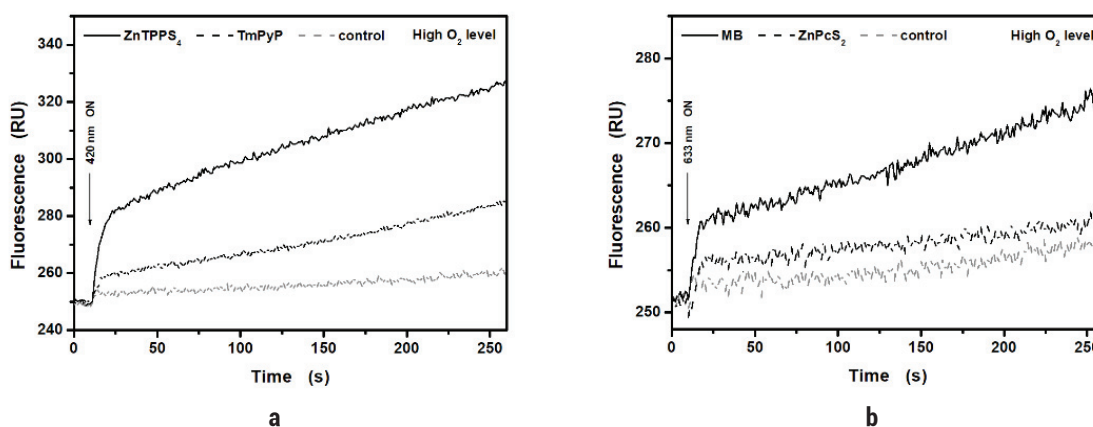


Figure 3. Representative traces of singlet oxygen production reflect the formation of high fluorescent SOSG endoperoxide from SOSG in the presence of singlet oxygen generated by: ZnTPPS and TmPyP during exposition to the light of 420 nm (a); MB and ZnPcS during exposition to the light of 663 nm (b)

Table 2. Singlet oxygen production quantification by different photosensitisers in PBS with low (0.4 mg/ml) and high (36 mg/ml) oxygen concentrations. Due to the significantly different response in SOSG fluorescence over time, the change in fluorescence intensity per unit of time in the first 7 seconds ($\Delta F/\Delta t$) and the total change in fluorescence intensity (ΔF) after 4 minutes of irradiation were evaluated. The one-way analysis of variance (ANOVA) was used to compare the means of these data differing in oxygen concentration, and the p-value is the significance level of the analysis.

Photosensitizer	Oxygen level	$\Delta F/\Delta t$ (RU·s ⁻¹)		ΔF (RU)	
		in the first 7 seconds		after 4 minutes	
ZnTPPS	Low	4.0 ± 0.3	p = 0.588	96 ± 15	p = 0.257
	High	3.9 ± 0.2		83 ± 15	
TmPyP	Low	1.2 ± 0.2	p = 0.972	42 ± 5	p = 0.734
	High	1.2 ± 0.1		40 ± 5	
MB	Low	1.0 ± 0.1	p = 0.549	32 ± 5	p = 0.847
	High	1.1 ± 0.1		31 ± 6	
ZnPcS	Low	0.68 ± 0.06	p = 0.291	13 ± 4	p = 0.899
	High	0.75 ± 0.09		12 ± 2	

derivatives were excited by a light wavelength of 420 nm at 4.1×10^{-4} W/cm² irradiance, whereas MB and ZnPcS were by 663 nm at 2.1×10^{-4} W/cm² irradiance. SOSG was added into the buffer as a sensor of singlet oxygen generation, which undergoes a chemical structure change producing high fluorescent SOSG endoperoxide. From the kinetic measurements, we evaluated the rates of that fluorescence increase during the first 7 seconds and the total change in fluorescence intensity in 4 minutes (Table 2). Concerning the same molar concentration of photosensitizers, the singlet oxygen production was highest for ZnTPPS, where the rate of fluorescence change was more than 3 times higher than that obtained for TmPyP. A similar yield in the singlet oxygen production, as was observed for TmPyP, was achieved for MB, but the irradiance value was halved there. In addition, the MB rate was about 30 % higher than was calculated for ZnPcS. Relatively similar results of the singlet oxygen production were achieved if we evaluated the changes in fluorescence after 4 minutes of measurement. Surprisingly, we did not observe statistically significant changes in singlet oxygen production relative to the different oxygen concentrations 0.4 and 36 mg/l (Table 2).

Discussion

2 types of reactions mediate PDE. It depends on many factors, including the photosensitiser's chemical structure, light wavelength and intensity, oxygen concentration, composition, dielectric constant and pH of the treated medium [17]. It

is assumed that the reaction of type II generating singlet oxygen is the most crucial process conditioning the efficiency of PDE in PDT [10]. Thus, our study was focused on whether it is possible to achieve higher singlet oxygen yields by increasing the oxygen concentration. Four different sensitizers passed this assessment. Nyman and Hynninen reported that the diamagnetic cation complex formation, for example, with Al³⁺, Zn²⁺ and Ga³⁺, increases the yield and lifetime of the triplet state of photosensitisers [9]. So the production of singlet oxygen can be supported. Therefore, we compared two porphyrin derivatives ZnTPPS and commercially available TmPyP. Our results showed that the production of singlet oxygen under similar conditions was about 3 times higher in the case of the zinc complex.

In the case of comparing two representatives of the second generation of photosensitizers with absorption maxima in the red region of the visible electromagnetic spectrum, the zinc complex of the synthesized phthalocyanine ZnPcS showed a yield of only about 30 % greater than the non-metal photosensitizer MB.

Typical values of cellular pO₂ are in the range 9.9–19 mm Hg (i.e. about 0.4–0.8 mg/l) [18]. During hyperbaric oxygen therapy, these values may increase several times. However, our measurements in PBS did not show that increasing the oxygen concentration from 0.4 to 36 mg/l would lead to higher singlet oxygen production in the presence of various light-activated photosensitizers. Several experimental and clinical studies have shown that hyperbaric oxygen increases the efficacy of PDT in cancer [19, 20]. On the other hand, protoporphyrin IX precursors at high-

er oxygen concentrations did not induce significant enhancement in phototoxicity of human squamous carcinoma cells [21]. Consistent with our current and previously obtained results [22], the yield of singlet oxygen via PDT at typical physiological pO_2 values is already reaching its maximum. With certain simplification, each oxygen molecule could be considered a cube with a size equal to the molecule's size (i.e. approximately 0.3 nm). The total number of these cubes per volume of 1 l is 3.7×10^{25} ($1 / (0.3 \times 10^{-8})^3$). At the oxygen concentration of 0.4 mg/l, the number of oxygen molecules per 1 l is 7.5×10^{18} ($4 \times 10^{-7} / (32 \times 1.66 \times 10^{-27})$). Thus, there are 4.9×10^6 ($3.7 \times 10^{25} / 7.5 \times 10^{18}$) cubes per one molecule of oxygen in a space which corresponds to a mutual distance between two neighbouring oxygen molecules of approximately 50 nm ($(4.9 \times 10^6)^{1/3} \times 0.3$). At the photosensitizer concentration of 1 μ M, the mutual distance between two neighbouring photosensitizer molecules is, on average, longer. When considering the homogenous distributions of photosensitizer and oxygen molecules, the maximum mutual distance between photosensitizer and oxygen molecule is halved (i.e. 25 nm), and the average distance equals 12.5 nm. In the case of an oxygen concentration of 36 mg/l, similar calculations give the average mutual distance of 2.5 nm. The excited triplet state of photosensitizer can transfer energy to the triplet state of the oxygen molecule because both electrons involved in the energy transfer process have the same spin. Therefore, mutual distance remains a crucial factor. According to the Förster theory [23], resonance energy transfer is inversely proportional to the sixth power of the distance. However, depending on the interacting molecules, this type of energy transfer can be maximally effective at mutual distances up to 5 or more nanometers [24]. In our simplification, we have omitted the fact that an oxygen molecule dissolved in water forms an induced dipole, which can electrostatically interact with the charged photosensitizer and thus significantly shorten their mutual distance. A relatively long lifetime of the photosensitizer triplet state, together with a high diffusion rate of oxygen, can also contribute to shortening distance. TMPyP and MB triplet states decay with a lifetime of about 2 μ s in an air-saturated aqueous solution [25, 26]. The sulfonated zinc derivatives of phthalocyanines are known for their long triplet lifetimes

and high singlet oxygen quantum yield [27]. In water, these lifetimes can reach up to 190 μ s [28]. The average distance travelled by a diffusing molecule in a time t is given by $(2 \times D \times t)^{1/2}$, where D is the diffusion coefficient of the molecule in the medium [29]. Since typical diffusion coefficients in water at 298 K are about 2×10^{-9} m²/s [30], each dissolved molecule can move 90 nm in 2 μ s.

According to the above facts, photosensitizer selection can achieve PDT enhancement under normoxic conditions. Furthermore, a complex with metal ions such as Zn²⁺ can increase singlet oxygen production. MB is a tricyclic phenothiazinium, and it is used in medical practice to primarily treat methemoglobinemia, carbon monoxide or cyanide poisoning, and malaria [31, 32]. Moreover, our results confirmed that MB could also be a promising photosensitizer inducing higher singlet oxygen production. MB was already applied in the PDT for anticancer treatment [33]. It was reported as an ideal photosensitizer for its adequate hydrophilic/lipophilic balance, high purity, stable composition, low cost, and strong absorption in the red region of the spectrum [34].

In conclusion, PDT represents an alternative treatment modality that can be very effective if it deals with specific issues such as photosensitizer selection, light dosage, and, most importantly, tissue hypoxia [35]. The use of oxygen carriers can achieve an increase of the oxygen pressure level in a tissue, improvement of blood flow, application of hyperbaric oxygen therapy, combining other therapies with PDT and fractionation of light, reducing oxygen consumption [35, 36]. Such approaches will be effective if the therapy aims at a hypoxic tissue, e.g. a developed (solid) tumour. However, our measurements showed that these solutions are unnecessary if PDT is used under normoxic conditions when the oxygen level is already sufficient to induce the maximum yield of singlet oxygen. According to our calculation, the lower oxygen availability can also be compensated by a longer interaction of the excited photosensitizer with the oxygen molecule, e.g. due to the longer triplet lifetime of the photosensitizer.

Acknowledgements

Conflict of interest statement

The authors declare no conflict of interest.

Funding sources

The Ministry of Health of the Czech Republic grant nr NU21-09-00357 supported this work.

References

1. Dolmans DE, Fukumura D, Jain RK. Photodynamic therapy for cancer. *Nat Rev Cancer*. 2003 May; 3(5):380-7. doi: 10.1038/nrc1071. PMID: 12724736.
2. Berg K, Selbo PK, Weyergang A, Dietze A, Prasmickaite L, Bonsted A, Engesaeter BØ, Angell-Petersen E, Warloe T, Frandsen N, Høgset A. Porphyrin-related photosensitizers for cancer imaging and therapeutic applications. *J Microsc*. 2005 May; 218(Pt 2):133-47. doi: 10.1111/j.1365-2818.2005.01471.x. PMID: 15857375.
3. Kharkwal GB, Sharma SK, Huang YY, Dai T, Hamblin MR. Photodynamic therapy for infections: clinical applications. *Lasers Surg Med*. 2011 Sep; 43(7):755-67. doi: 10.1002/lsm.21080. PMID: 22057503; PMCID: PMC3449167.
4. Gomes ATPC, Neves MGPMS, Cavaleiro JAS. Cancer, Photodynamic Therapy and Porphyrin-Type Derivatives. *An Acad Bras Cienc*. 2018; 90(1 Suppl 2):993-1026. doi: 10.1590/0001-3765201820170811. PMID: 29873666.
5. Roguin LP, Chiarante N, García Vior MC, Marino J. Zinc(II) phthalocyanines as photosensitizers for antitumor photodynamic therapy. *Int J Biochem Cell Biol*. 2019 Sep; 114:105575. doi: 10.1016/j.biocel.2019.105575. Epub 2019 Jul 27. PMID: 31362060.
6. Paquette B, Boyle RW, Ali H, MacLennan AH, Truscott TG, van Lier JE. Sulfonated phthalimidomethyl aluminum phthalocyanine: the effect of hydrophobic substituents on the in vitro phototoxicity of phthalocyanines. *Photochem Photobiol*. 1991 Mar; 53(3):323-7. doi: 10.1111/j.1751-1097.1991.tb03635.x. PMID: 2062879.
7. Margaron P, Grégoire MJ, Scasnár V, Ali H, van Lier JE. Structure-photodynamic activity relationships of a series of 4-substituted zinc phthalocyanines. *Photochem Photobiol*. 1996 Feb; 63(2):217-23. doi: 10.1111/j.1751-1097.1996.tb03017.x. PMID: 8657735.
8. Colussi VC, Feyes DK, Mulvihill JW, Li YS, Kenney ME, Elmets CA, Oleinick NL, Mukhtar H. Phthalocyanine 4 (Pc 4) photodynamic therapy of human OVCAR-3 tumor xenografts. *Photochem Photobiol*. 1999 Feb; 69(2):236-41. PMID: 10048316.
9. Nyman ES, Hynninen PH. Research advances in the use of tetrapyrrolic photosensitizers for photodynamic therapy. *J Photochem Photobiol B*. 2004 Jan; 73(1-2):1-28. doi: 10.1016/j.jphotobiol.2003.10.002. PMID: 14732247.
10. Pineiro M, Pereira MM, Gonsalves A, Arnaut LG, Formosinho SJ. Singlet oxygen quantum yields from halogenated chlorins. *J Photochem Photobiol A*. 2001 Jan; 38(2):147-57. doi: 10.1016/S1010-6030(00)00382-8.
11. Daruwalla J, Christophi C. Hyperbaric oxygen therapy for malignancy: a review. *World J Surg*. 2006 Dec;30(12):2112-31. doi: 10.1007/s00268-006-0190-6. PMID: 17102915.
12. Kizaka-Kondoh S, Inoue M, Harada H, Hiraoka M. Tumor hypoxia: a target for selective cancer therapy. *Cancer Sci*. 2003 Dec; 94(12):1021-8. doi: 10.1111/j.1349-7006.2003.tb01395.x. PMID: 14662015.
13. Niklas A, Brock D, Schober R, Schulz A, Schneider D. Continuous measurements of cerebral tissue oxygen pressure during hyperbaric oxygenation - HBO effects on brain edema and necrosis after severe brain trauma in rabbits. *J Neurol Sci*. 2004 Apr; 219(1-2):77-82. doi: 10.1016/j.jns.2003.12.013. PMID: 15050441.
14. Yamamoto N, Takada R, Maeda T, Yoshii T, Okawa A, Yagishita K. Microcirculation and tissue oxygenation in the head and limbs during hyperbaric oxygen treatment. *Diving Hyperb Med*. 2021 Dec 20;51(4):338-344. doi: 10.28920/dhm51.4.338-344. PMID: 34897598; PMCID: PMC8920905.
15. Kubat P, Mosinger J. Photophysical properties of metal complexes of meso-tetrakis (4-sulphonatophenyl) porphyrin. *J Photochem Photobiol A*. 1996 May; 96(1-3):93-97. doi: 10.1016/1010-6030(95)04279-2.
16. Griffiths J, Schofield J, Wainwright M, Brown SB. Some observations on the synthesis of polysubstituted zinc phthalocyanine sensitizers for photodynamic therapy. *Dyes Pigment*. 1997 33:65-78.
17. Kwiatkowski S, Knap B, Przystupski D, Saczko J, Kędzierska E, Knap-Czop K, Kotlińska J, Michel O, Kotowski K, Kulbacka J. Photodynamic therapy - mechanisms, photosensitizers and combinations. *Biomed Pharmacother*. 2018 Oct;106:1098-1107. doi: 10.1016/j.biopha.2018.07.049. Epub 2018 Jul 17. PMID: 30119176.
18. Gleadle J, Ratcliffe PJ. Hypoxia. In: Wiley J, editor. *Encyclopedia of life sciences*. Chichester: John Wiley & Sons; 2001.
19. Maier A, Tomaselli F, Anegg U, Rehak P, Fell B, Luznik S, Pinter H, Smolle-Jüttner FM. Combined photodynamic therapy and hyperbaric oxygenation in carcinoma of the esophagus and the esophago-gastric junction. *Eur J Cardiothorac Surg*. 2000 Dec;18(6):649-54; discussion 654-5. doi: 10.1016/s1010-7940(00)00592-3. PMID: 11113670.
20. Jirsa M Jr, Poucková P, Dolezal J, Pospíšil J, Jirsa M. Hyperbaric oxygen and photodynamic therapy in tumour-bearing nude mice. *Eur J Cancer*. 1991;27(1):109. doi: 10.1016/0277-5379(91)90075-o. PMID: 1826432.
21. Blake E, Allen J, Curnow A. The effects of protoporphyrin IX-induced photodynamic therapy with and without iron chelation on human squamous carcinoma cells cultured under normoxic, hypoxic and hyperoxic conditions. *Photodiagnosis Photodyn Ther*. 2013 Dec;10(4):575-82. doi: 10.1016/j.pdpdt.2013.06.006. Epub 2013 Aug 8. PMID: 24284114.
22. Pola M, Kolarova H, Ruzicka J, Zholobenko A, Modriansky M, Mosinger J, Bajgar R. Effects of zinc porphyrin and zinc phthalocyanine derivatives in photodynamic anticancer therapy under different partial pressures of oxygen in vitro. *Invest New*

- Drugs. 2021 Feb;39(1):89-97. doi: 10.1007/s10637-020-00990-7. Epub 2020 Aug 24. PMID: 32833137.
23. Förster T. Zwischenmolekulare Energiewanderung und Fluoreszenz. *Ann Phys.* 1948, 437, 55-75.
 24. Hu W, Yang F, Pietraszak N, Gu J, Huang J. Distance dependent energy transfer dynamics from a molecular donor to a zeolitic imidazolate framework acceptor. *Phys Chem Chem Phys.* 2020, 22, 25445-9.
 25. Lang K, Mosinger J, Wagnerová DM. Photophysical properties of porphyrinoid sensitizers non-covalently bound to host molecules; models for photodynamic therapy. *Coord Chem Rev.* 2004 Feb;248(3-4):321-50. doi: 10.1016/j.ccr.2004.02.004.
 26. Ashkenazi S. Photoacoustic lifetime imaging of dissolved oxygen using methylene blue. *J Biomed Opt.* 2010 Jul-Aug;15(4):040501. doi: 10.1117/1.3465548. PMID: 20799768.
 27. Beeby A, FitzGerald S, Stanley CF. A photophysical study of protonated (tetra-tert-butylphthalocyaninato)zinc. *J Chem Soc Perkin Trans.* 2001 Aug;2:1978-82.
 28. Ogunsipe A, Chen JY, Nyokong T. Photophysical and photochemical studies of zinc(ii) phthalocyanine derivatives - effects of substituents and solvents. *New J Chem.* 2004 Jun;28:822-7.
 29. Alwattar AH, Lumb MD, Birks, JB. Diffusion-controlled rate processes. In: Birks JB, editor. *Organic Molecular Photophysics.* New York: John Wiley & Sons; 1973. p. 403-454.
 30. Quina FH, Silva GTM. The photophysics of photosensitization: A brief overview. *J Photochem Photobiol.* 2021 Sep; 7:100042. doi: 10.1016/j.jpap.2021.100042.
 31. Haouzi P, Gueguinou M, Sonobe T, Judenherc-Haouzi A, Tubbs N, Trebak M, Cheung J, Bouillaud F. Revisiting the physiological effects of methylene blue as a treatment of cyanide intoxication. *Clin Toxicol (Phila).* 2018 Sep; 56(9): 828-840. doi: 10.1080/15563650.2018.1429615. Epub 2018 Feb 16. PMID: 29451035; PMCID: PMC6086742.
 32. Lu G, Nagbanshi M, Goldau N, Mendes Jorge M, Meissner P, Jahn A, Mockenhaupt FP, Müller O. Efficacy and safety of methylene blue in the treatment of malaria: a systematic review. *BMC Med.* 2018 Apr; 16(1):59. doi: 10.1186/s12916-018-1045-3. PMID: 29690878; PMCID: PMC5979000.
 33. Zhang LZ, Tang GQ. The binding properties of photosensitizer methylene blue to herring sperm DNA: a spectroscopic study. *J Photochem Photobiol B.* 2004 May; 74(2-3):119-25. doi: 10.1016/j.jphotobiol.2004.03.005. PMID: 15157907.
 34. Klosowski EM, de Souza BTL, Mito MS, Constantin RP, Mantovanelli GC, Mewes JM, Bizerra PFV, Menezes PVMDC, Gilglioni EH, Utsunomiya KS, Marchiosi R, Dos Santos WD, Filho OF, Caetano W, Pereira PCS, Gonçalves RS, Constantin J, Ishii-Iwamoto EL, Constantin RP. The photodynamic and direct actions of methylene blue on mitochondrial energy metabolism: A balance of the useful and harmful effects of this photosensitizer. *Free Radic Biol Med.* 2020 Jun; 153:34-53. doi: 10.1016/j.freeradbiomed.2020.04.015. Epub 2020 Apr 18. PMID: 32315767.
 35. Pucelik B, Sułek A, Barzowska A, Dąbrowski JM. Recent advances in strategies for overcoming hypoxia in photodynamic therapy of cancer. *Cancer Lett.* 2020 Nov; 492:116-135. doi: 10.1016/j.canlet.2020.07.007.
 36. Larue L, Myrzakhmetov B, Ben-Mihoub A, Moussaron A, Thomas N, Arnoux P, Baros F, Vanderesse R, Acherar S, Frochot C. Fighting Hypoxia to Improve PDT. *Pharmaceuticals.* 2019; 12(4): 163. doi: 10.3390/ph12040163.

Genotoxic and chemopreventive potentials of ethanol leaves extract of *Annona muricata* on *N*-Ethyl-*N*-Nitrosourea-induced pro-leukaemia carcinogen in mice model by bone marrow micronucleus assay

Oluwaseyi Bamisaye

Department of Biomedical Laboratory Science, Faculty of Basic Medical Science, College of Medicine, University of Ibadan

 <https://orcid.org/0000-0003-2741-2809>

Corresponding author:

eo.bamisaye@mail1.ui.edu.ng; bamisayeseyi@gmail.com

Anthony Fashina

Department of Medical Laboratory Science, Faculty of Basic Medical Sciences, College of Health Sciences, Ladoko Akintola University of Technology, Ogbomoso, Nigeria

 —

Fatai Abdulraheem

Department of Medical Laboratory Science, Faculty of Basic Medical Sciences, College of Health Sciences, Ladoko Akintola University of Technology, Ogbomoso, Nigeria

 —

Olufemi Emmanuel Akanni

Department of Medical Laboratory Science, College of Health Sciences, Osun State University, Osogbo, Nigeria

 <https://orcid.org/0000-0003-4572-7986>

Fadiora S. Olufemi

Department of Surgery, College of Health Sciences, Osun State University, Osogbo, Nigeria

 <https://orcid.org/0000-0002-6784-6196>

 doi: 10.20883/medical.e760

Keywords: Genotoxicity, Leukaemia, *Annona muricata*

Published: 2022-12-30

How to Cite: Bamisaye O, Fashina A, Abdulraheem F, Akanni OE, Olufemi FS. Genotoxic and chemopreventive potentials of ethanol leaves extract of *Annona muricata* on *N*-Ethyl-*N*-Nitrosourea-induced pro-leukaemia carcinogen in mice model by bone marrow micronucleus assay. *Journal of Medical Science*. 2022;91(4);e760. doi:10.20883/medical.e760



© 2022 by the author(s). This is an open access article distributed under the terms and conditions of the Creative Commons Attribution (CC BY-NC) license. Published by Poznan University of Medical Sciences

ABSTRACT

Background. Studies have proven the effect of several agents, including natural products, to induce, prevent and treat genotoxicity through experimental models and clinical trials. In this study, the genotoxic preventive potential of *Annona muricata* ethanol extract on *N*-Ethyl-*N*-Nitrosourea (ENU)-induced pro-leukaemia in mice models using micronuclei formation in bone marrow was assessed.

Materials and methods. Forty-eight mice weighing 18-24g were randomly divided into six groups of eight mice. The mice were intravenously administered 20mg/kg of NEU 48 hourly 3 times, 80mg/kg of NEU 48 hourly 3 times. The negative control was fed with feed and water only. We introduced 0.2ml (0.1g/ml) ethanolic extract of *Annona muricata* for 3 weeks prior to NEU low dosage administration, 0.2ml (0.1g/ml) ethanolic extract of *Annona muricata* for 3 weeks prior to ENU high dosage and *Annona muricata* (ethanolic extract) administration, and gave commercial diet to the adverse/ toxicity group. The bone marrow was harvested, smeared and stained using MayGrumwald. The procedure enabled the determination of micronucleus polychromatic erythrocytes (MNPCEs) microscopically.

Results. Groups exposed to various dosages of the ENU yielded significantly increased MNPCEs, with group B producing higher MNPCEs. The groups treated with the extract displayed a significant reduction in the MNPCEs despite prior exposure to concentrations of NEU. The adverse group displayed no difference in MNPCEs compared with the negative control.

Conclusions. The ENU induced genotoxicity depending on its concentration. The extract displayed a profound capacity to prevent genotoxicity and alleviate leukaemia with good tolerance.

Introduction

Leukaemia, the eighth to twelfth most common cancer generally, with an increasing incidence trend, is a global public health concern as more than 420,000 new cases and over 300,000 cancer deaths from leukaemia occur worldwide [1–3]. Notable geographical disparities evidence this as a result of significant factors such as quality health system with adequate accessibility and some etiological factors like gene-environment interaction [4].

Genotoxicity is a series of irritation to a cell's genetic makeup, which can result in adverse outcomes such as cancer, inherited mutation, ageing/other developmental toxicity and several diseased states [5]. The major classes of genotoxic materials include mutagens, carcinogens and teratogens. Their genotoxic effects could be categorized as mutational, clastogenic and aneuploidic [5, 6]. The most common chemical carcinogens identified in studying the progression of leukaemia are N-ethyl-*N*-nitrosourea (ENU), *N*-methyl-*N*-nitrosourea (MNU), dimethyl benzanthracene (DMBA), benzo (a) pyrene (BaP), amongst others [7]. *N*-ethyl-*n*-nitrosourea (ENU) (C₃H₇N₃O₂), a potent mutagen, acts by transferring its alkyl (ethyl or methyl) group to the nucleobases in nucleic acids in the bone marrow, thereby generating leukaemogenesis [8, 9].

Furthermore, the internationally accepted genotoxicity assessment methods are some in-vitro and in-vivo assays, including the mouse lymphoma gene mutation assay (MLA), the micronucleus assay, the Ames bacterial mutagenicity test, the Comet assay, the chromosome aberration test and sister chromatid exchange assays. All the methods assess DNA damage by diverse mechanisms, like intragenic mutations, chromosomal rearrangements or deletions, loss or gain of whole chromosomes (aneuploidy) or chromosomal segments and other genotoxic effects [10–12].

Herbal supplements and formulations have been experimented on severally to have beneficial, prevention, and therapeutic effects on the physiological function and reversal of diseased states in the body system [12–14]. There are several reports depicting their beneficial effects. The recently discussed ones include boosting the immune system, regulating oxidation, enhancing memory, acting as an antidepressant and an antidiabetic means, and chemotherapeutic agents in cancer [15–18]. We have identified the active ingredients in the aqueous or ethanolic forms of plants and herbs and their potencies. The toxicity tendencies of these herbs have also been examined. Studies are still emerging to depict the efficacy of more herbal products in treating carcinogen-induced genotoxicity and their systemic effects.

Annona muricata, also known as soursop, guanabana and commonly graviola, is an efficacious medicinal tree. Indigenous communities of Africa and South America use different parts of the plant extensively to perform numerous ethnomedicinal activities. Phytochemical analysis has identified annonaceous acetogenins as the major constituents of the leaves, bark, roots and fruits [19]. In addition, several studies have distinguished the anti-arthritic, hepatoprotective, anti-malarial, antidiabetic, anticancer, and anticonvulsant effects [20, 21].

Despite reported evidence of the efficacy of *A. muricata* in some cancers, there is a need to determine the effects on ENU-induced pro-leukaemia in experimental models as an in-vivo study. Furthermore, the study should use a micronucleus assay to determine genotoxicity and any other stage of transformation for possible future application in cancer prevention, therapy, control, and eradication. Hence there is a reason for this study.

Materials and Methods

Procurement, Identification and Extraction of *Annona muricata* leaves.

The leaf samples of *Annona muricata*, locally called Apekan, Tuwon biri and Sawansop in Yoruba, Hausa and Igbo languages of Nigeria, respectively, were gotten from a local farm at Osogbo city, Osun state, Nigeria. It was further identified and authenticated at the Department of Pharmacology, Obafemi Awolowo University Ile-Ife, Nigeria.

Ethanol Extraction of the leaves

Fresh matured leaves of *Annona muricata* were separated from the stalk, air-dried at room temperature (24°C), pulverized and crushed into a fine powder using a grinding machine and weighed. Ethanolic (Absolute) extracts of the plant were prepared by soaking 500 g of the dry powdered plant material in two (2) litres of absolute ethanol and then kept at room temperature for 48 hours (for thorough extraction). At the end of the 48 hours, the extracts were filtered first using a Whatman filter paper No.42 (125 mm) and cotton wool. The harvested ethanol extract of *Annona muricata* leaves was then dried off in an oven at 37°C and stored at 4°C. Subsequently, on each day of the experiment, an aliquot portion (1 g) of the crude plant extract residue was weighed and dissolved in distilled water (10 ml) for use.

Experimental Models

The experimental models included forty-eight (48) young Swiss Albino mice weighing between 18 g and 24 g and purchased from the animal house of Ladoke Akintola University of Technology (LAUTECH), Mercyland, Osogbo, Nigeria. The mice were divided into six (6) groups of eight (8) mice each, made to acclimatize to the new animal house conditions for one week at the department of Medical Laboratory Science, Ladoke Akinto-

la University of Technology (LAUTECH), Mercyland, Osogbo, Nigeria before the commencement of the experiment. They were fed with a standard commercial pellet with clean water *ad libitum*. The animal house was ascertained to be pathogen-free, room temperature maintained at 28 ± 2°C, and adequate ventilation ensured with 12 hours light/dark cycle.

Experimental procedures involving the experimental animals and their care were conducted in compliance with the Guidelines for Care and Use of Laboratory Animals in Biomedical Research promulgated by the Canadian Council on Animal Care (2003) [23]. Accordingly, the Animal Care and Use Ethical Committee of the College of Medicine and Health Science, Ladoke Akintola University of Technology (LAUTECH), Osogbo, Nigeria, granted the Ethical Approval.

Preparation and Administration of ENU for Leukaemia Induction

The *n*-ethyl-*n*-nitrosourea (ENU) was procured from Sigma Aldrich (Germany) and stored at -20°C as indicated by the manufacturer. It was reconstituted daily with normal saline by measurement of the average body weight (kg) of each mouse with corresponding carcinogen weight (mg) across all groups except the negative control and adverse reaction group (**Table 1**). The mice were administered twenty (20) mg/kg and eighty (80) mg/kg body weights of the solutions intraperitoneally (IP) with a sterile 26-gauge – needle 48 hourly three times (**Table 1**). The mice were then monitored closely to determine the induction of a pro-leukaemia state and other reactions on the administration of extracts.

Administration of Ethanolic Extract and Acute toxicity

One gram of *A. muricata* (ethanolic crude extract) was dissolved in 10 ml of distilled water to make

Table 1. Experimental Protocol

Groups (6 mice/group, 18–24kg)	Treatment	Inference
A	20mg/kg NEU 48 hourly thrice	Leukaemia induction by low dosage
B	80mg/kg of NEU 48 hourly thrice	Leukaemia Positive by high dosage
C	Feed and Water	Negative Control
D	0.2ml (0.1g/ml) extract +20mg/kg NEU 48 hourly thrice	Preventive group on low dosage of NEU
E	0.2ml (0.1g/ml) extract + 80mg/kg of NEU 48 hourly thrice	Preventive group on high dosage of NEU
F	0.2ml (0.1g/ml) extract + Feed and Water	Adverse Group

a concentration of 0.1 g/ml of the prepared extract. The mice in the preventive groups D and E (**Table 1**) were administered the *A. muricata* with 0.2 ml volume orally by gavage once daily with the aid of oral cannula and sterile syringes for 3 weeks. The adverse group F mice were administered the same concentration and volume of extracts for 3 weeks along with feed and water. They were then observed toxicity, behavioural changes and mortality the administration period. The ethanol leaf extract lethal dose (LD50) had been determined to be above 5000 mg/kg [23].

Sample Collection and Animal Sacrifice

Sample collection commenced precisely three weeks after the last exposure to ENU in each induction group A and B, the negative control group C, and the adverse/toxicity group F. Also, the sample collection commenced in the preventive at the fifth week after three weeks of the last exposure to ENU administration in groups D and F. At the end of the ninth week of the experiment, the animals from each group were terminated ethically by cervical dislocation, and both femurs were surgically removed and placed in a petri dish containing normal saline. The bone marrow was flushed with 1 ml of fetal calf serum (FCS) into 1.5 ml Eppendorf Tubes, centrifuged at 2000 rpm for 5 minutes and the supernatant removed. The pellets were then suspended in another 1 ml of FCS in Eppendorf Tubes, well-mixed, and centrifuged at the same rate. Finally, the supernatant was removed and discarded; 0.05 ml of FCS was added to the pellet and mixed properly to form a viscous suspension. The smear was made from the suspension on a clean, grease-free slide with drops of the viscous suspension and air-dried overnight.

Staining for Micronucleus (MN) test

Staining was performed as described by Schmidt (1976), Alabi and Bakare (2011), and Oyeyemi *et al.* (2015) [24–26]. First, the smear was fixed in 70% methanol for 3 min and air-dried for 24 hours. It was then stained with 0.4% May-Grumwald stain for 3 min. It was immediately transferred into another Coplin Jar containing an equal volume of May-Grumwald and distilled water to allow further staining for 3 min. Next, the stained slides were rinsed in distilled water and air-dried for 24 hours. After 24 hours, the air-dried slides were stained in 5% Giemsa stain for 5 minutes, rinsed

in distilled water and air-dried for 24 hours, after which it was dipped in Xylene and mounted in DPX at 45°C.

Enumeration of micronuclei cells in MN test

The slides were scored under 100X (oil immersion) objective using a light microscope to score the number of micronucleus polychromatic erythrocyte (MNPCEs) out of 1000 polychromatic erythrocytes per mice. The differential staining of the bluish–purple polychromatic erythrocytes (PCEs) and pinkish normochromatic erythrocytes (NCEs), as well as the relative size of the erythrocytes, were indices for differentiating them (Schmidt 1976; Alabi and Bakare 2011; Oyeyemi *et al.*, 2011).

Statistical Analysis

Data obtained were analyzed using IBM SPSS for Windows, version 25.0 (SPSS Inc., Chicago, IL), and the results were expressed as mean \pm SEM (standard error of the mean). PCE, NCE, and MNPCE values were calculated to derive percentages, and significant differences were tested using analysis of variance (ANOVA). Values considered significant at $p \leq 0.05$

Results

Pro-Leukaemia Induction by Micronucleus Assay

The number of micronucleus polychromatic erythrocytes per polychromatic erythrocytes was counted, as seen in **Figure 1**, and displayed the resultant pro-leukaemia induction effect of the ENU in the animal. It was visible as a simultaneously increased trend in the low and high ENU dosage groups A and B (**Table 2** and **Figure 2**) between weeks 2 and 5, which are distinctly significant and farther from the other groups in the diagrammatic representation. Also, groups D and E, where ENU was administered after the extract administration, displayed an increase in their mean MNPCE values in the line graph according to the administered ENU dosage (**Figure 2**).

In **Table 2**, significant differences were observed when group A was compared with the other 5 groups ($p < 0.05$) with a more significant increase in group B compared with the other 5 groups. Despite their preventive design, this observation is similar in groups D and E.

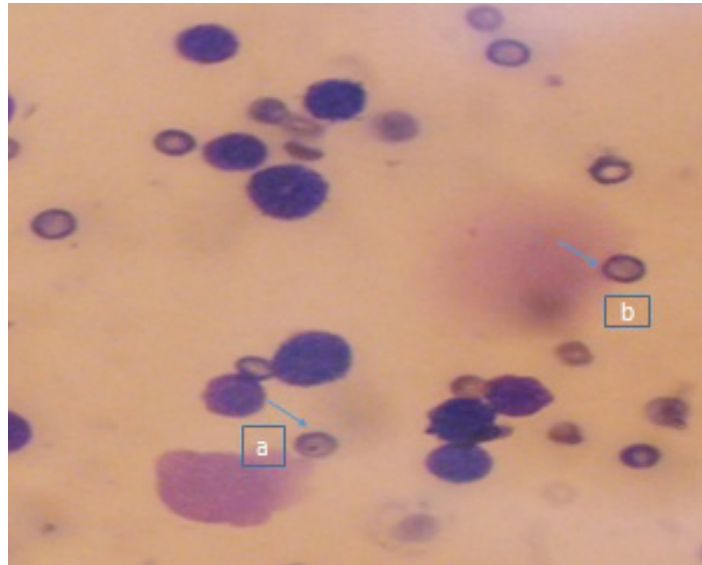


Figure 1. Micronuclei in mice administered *A. murricata* after exposure to *n*-ethyl-*n*-nitrosourea. A: Micronuclei polychromatic erythrocyte; B: Normal polychromatic erythrocyte

Table 2. Mean \pm Standard deviation of micronucleus polychromatic erythrocyte cells (MNPCE) population among the groups across the weeks of exposure

Week Number	Groups (Mean \pm Standard deviation of MNPCE)					
	A	B	C	D	E	F
1	-	-	-	-	-	-
2	14.13 \pm 0.56	50.45 \pm 2.31	4.52 \pm 0.34	-	-	4.53 \pm 0.45
3	15.01 \pm 0.18	53.77 \pm 1.95	4.61 \pm 0.67	-	-	4.62 \pm 0.23
4	16.11 \pm 0.22	56.95 \pm 2.01	4.91 \pm 0.88	-	-	5.63 \pm 0.45
5	19.64 \pm 1.68	68.23 \pm 1.56	4.82 \pm 0.75	6.15 \pm 0.49	17.11 \pm 1.11	5.92 \pm 0.67
6	-	-	-	7.85 \pm 0.98	20.34 \pm 2.34	-
7	-	-	-	8.01 \pm 1.01	25.11 \pm 1.67	-
8	-	-	-	10.07 \pm 0.67	30.54 \pm 2.34	-

Group A – Leukaemia induction by a low dosage; Group B – Leukaemia induction by a high dosage; Group C – Negative Control; Group D – Preventive group on a low dosage of N-Nitroso-N-ethylurea; Group E – Preventive group on a high dosage of N-Nitroso-N-ethylurea; Group F – Adverse/Toxicity group.

Acute Toxicity of *A. murricata*

The oral administration of 0.2 ml of 0.1 g/ml concentration of the ethanolic extract of *A. murricata* for 3 weeks continuously in group F did not yield behavioural changes, toxicity signs or mortality. Furthermore, the mean \pm SD MNPCE values for group F were not significantly different from the negative group C ($p > 0.05$), which proved good extract tolerance.

A. murricata preventive effect on genotoxicity

The chemopreventive potential of *A. murricata* ethanolic extract was displayed based on the ENU concentration administered in groups D and E. An increase in MNPCE level in both groups

was lower than in groups A and B because of the extract administration (**Figure 2**). Also, there was a significant decrease when group D was compared with A and B ($P < 0.05$) and an increase when compared with other groups ($P > 0.05$), and the same observation was recorded when group E was compared across other groups.

Discussion

Several studies have proven the use of herbal or plant extracts in the control and management of diseases efficient. Coupled with the cheap and affordable nature of such products, especially in

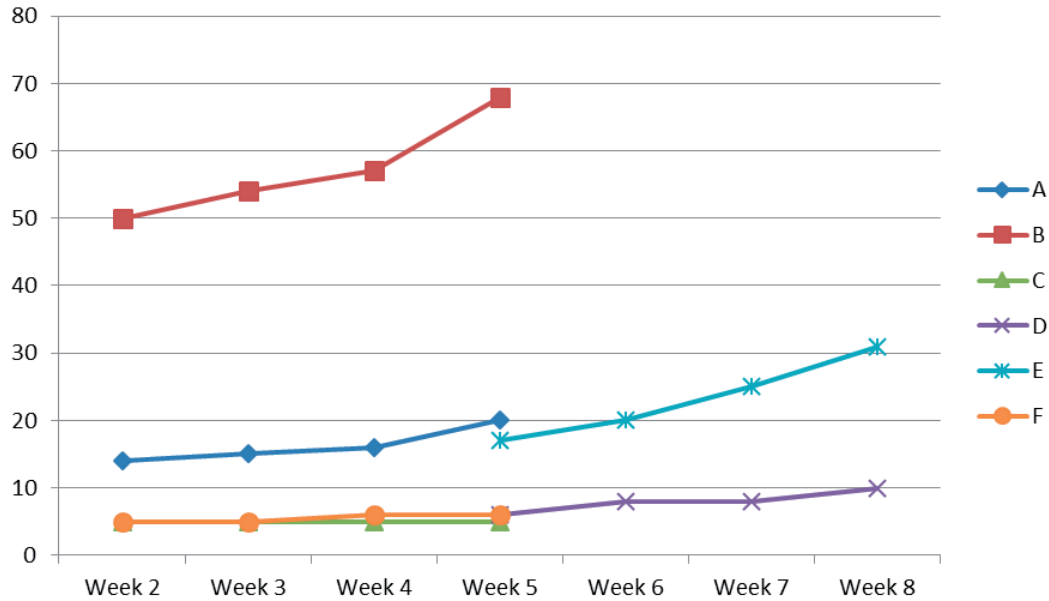


Figure 2. Mean micronucleus polychromatic erythrocyte cell (MNPCE) population among the groups across the weeks of exposure

Table 3. Comparison of Mean \pm Standard deviation of MNPCE across the various groups

Week number	Groups (Mean \pm Standard deviation of MNPCE)					
	A	A vs. B	A vs. C	A vs. D	A vs. E	A vs. F
1	-	-	-	-	-	-
2	14.13 \pm 0.56	50.45 \pm 2.31*	4.52 \pm 0.34*	-	-	4.53 \pm 0.45*
3	15.01 \pm 0.18	53.77 \pm 1.95*	4.61 \pm 0.67*	-	-	4.62 \pm 0.23*
4	16.11 \pm 0.22	56.95 \pm 2.01*	4.91 \pm 0.88*	-	-	5.63 \pm 0.45*
5	19.64 \pm 1.68	68.23 \pm 1.56*	4.82 \pm 0.75*	6.15 \pm 0.49*	17.11 \pm 1.11*	5.92 \pm 0.67*
6	-	-	-	7.85 \pm 0.98*	20.34 \pm 2.34*	-
7	-	-	-	8.01 \pm 1.01*	25.11 \pm 1.67*	-
8	-	-	-	10.07 \pm 0.67*	30.54 \pm 2.34*	-
Week number	Groups (Mean \pm Standard deviation of MNPCE)					
	B	B vs. C	B vs. D	B vs. E	B vs. F	E vs. F
1	-	-	-	-	-	-
2	50.45 \pm 2.31	4.52 \pm 0.34*	-	-	4.53 \pm 0.45*	-
3	53.77 \pm 1.95	4.61 \pm 0.67*	-	-	4.62 \pm 0.23*	-
4	56.95 \pm 2.01	4.91 \pm 0.88*	-	-	5.63 \pm 0.45*	-
5	68.23 \pm 1.56	4.82 \pm 0.75*	6.15 \pm 0.49*	17.11 \pm 1.11*	5.92 \pm 0.67*	17.11 \pm 1.11
6	-	-	7.85 \pm 0.98*	20.34 \pm 2.34*	-	20.34 \pm 2.34
7	-	-	8.01 \pm 1.01*	25.11 \pm 1.67*	-	25.11 \pm 1.67
8	-	-	10.07 \pm 0.67*	30.54 \pm 2.34*	-	30.54 \pm 2.34
Week number	Groups (Mean \pm Standard deviation of MNPCE)					
	C	C vs. D	C vs. E	C vs. F	D vs. E	D vs. F
1	-	-	-	-	-	-
2	4.52 \pm 0.34	-	-	4.53 \pm 0.45	-	4.53 \pm 0.45
3	4.61 \pm 0.67	-	-	4.62 \pm 0.23	-	4.62 \pm 0.23*
4	4.91 \pm 0.88	-	-	5.63 \pm 0.45	-	5.63 \pm 0.45*
5	4.82 \pm 0.75	6.15 \pm 0.49*	17.11 \pm 1.11*	5.92 \pm 0.67	17.11 \pm 1.11*	5.92 \pm 0.67*
6	-	7.85 \pm 0.98*	20.34 \pm 2.34*	-	20.34 \pm 2.34*	-
7	-	8.01 \pm 1.01*	25.11 \pm 1.67*	-	25.11 \pm 1.67*	-
8	-	10.07 \pm 0.67*	30.54 \pm 2.34*	-	30.54 \pm 2.34*	-

Group A – Leukaemia induction by a low dosage; Group B – Leukaemia induction by a high dosage; Group C – Negative Control; Group D – Preventive group on a low dosage of N-Nitroso-N-ethylurea; Group E – Preventive group on a high dosage of N-Nitroso-N-ethylurea; Group F – Adverse/Toxicity group. * - p significant at 0.05 ($p \leq 0.05$)

low-resource and income countries, *A. muricata* is not an exception to those qualities [12–16, 26]. Therefore, the active ingredients of the *A. muricata* ethanolic leaf extracts have been analyzed for the content of acetogenins, alkaloids, flavonoids (phenolic compounds), such as Sparteine, Anthocyanin, Sapogenin, Morphine, Phenol, Quinine, Ribalinidine, Ephedrine, Resveratrol, Catechin, Saponin, Oxalate and Quercetin [27], steroids, and saponins [28]. All the substances have specific and multiple effects on cell constituents depending on their concentration and target tissues. These abilities include, for example, antidiabetic, anticonvulsant, antioxidant, cardioprotective, antimicrobial, and anti-carcinogenic activities [23, 27].

In this study, different ENU concentrations were observed to induce pro-leukaemia with resulting leukaemia states in the models, evidenced by the increasing trend of the values of MNPCE counted per group. The ENU has been studied to possess leukaemogenetic property based on its ability to transfer alkyl to the nucleobases of cellular nucleic acid by an enzymatic reaction [9]. Therefore, this study emphasises the agent's ability and efficacy in inducing leukaemia for study and other research purposes. Furthermore, the study has proven that a required form of induction, especially the gravity of the leukaemia state, determines ENU ability to perform such a task successfully.

A. muricata has been shown to possess anticancer abilities by suppressing tumor growth and induced apoptosis of various cancer cell lines [19, 29–31]. The study further depicts its antigenotoxic and chemopreventive attributes manifested by the drastic reduction in the genotoxic effect of ENU and evidenced by the consistent reduction in the MNPCE value in the preventive groups. The protective ability of *A. muricata* leaf extract to withstand carcinogenic agents in inducing pro-leukaemic conditions and eventually full-blown leukaemia was displayed. It can be deduced from the high concentration of various acetogenins, phenols and alkaloids. The substances have been studied to possess anticancer properties. The acetogenins inhibit the mitochondrial complex I due to their bis-THF structure in vitro, thereby preventing replication of the cancerous cell lines [31]. It is characterized by its unbranched C32 or C4 fatty acid with γ -lactone

at the end of the cytoskeleton. This structure is highly reactive against cancer as it deprives the cells of ATP supply to the mitochondria, resulting in apoptosis [32–34]. On the other hand, the efficacy of alkaloids of plant derivatives has been proven in oncogenesis suppression by modulating key signalling pathways involved in proliferation, cell cycle, and metastasis [32, 33].

Furthermore, a previous study on gas chromatography-mass spectrometry (GC-MS) analysis of the essential leaf oil of *A. muricata* has further indicated terpenes, terpenoids and δ -cadinene as the significant essential oil and compounds of the leaves with 50.26% 34.24% and 22.58%, respectively. Other constituents include, amongst other sesquiterpenes, alkanes, *r*-Cadinol, esters, β -Caryophyllene, α -Copaene, Ledene oxide II, and Octadecane [37]. The phytochemicals acetogenins, flavonoids, alkaloids with the terpenes and δ -cadinene essential oil forms are the constituents suspected to be the main antigenotoxic contributors in the studied extract. The presence of these constituents severally inhibits the proliferation of MCF-7, MDA-MB-231 and 4T1 breast cell lines, initiate cytotoxicity on histiocytic lymphoma cell lines, pancreatic cancer cells, immortalised human keratinocytes, HaCat, normal human liver cells, WRL-68, and human skin malignant melanoma, A375 [38–42].

Some essential minerals such as calcium, sodium, potassium, iron, magnesium, and zinc are also abundantly present in *A. muricata* [43]. These elements generally contribute to the normal physiologic function of the cell primarily by the enzymatic catalytic system and oxidation-reduction reaction aiding cellular functions. Therefore, their presence in the leaf extracts has yielded similar outcomes in the *A. muricata* administered models hence down-regulating the induced genotoxicity.

Furthermore, this study established the ability of the mice models to tolerate *A. muricata* well enough. Hence the normal state observed with MNPCE values as seen in the negative control. Although the same leaf extract concentration was administered, the rate at which the MNPCE differed in the positive groups with the low and the high ENU dosage was also replicated in the chemopreventive groups. The fact points to consistency in the extract's ability to eradicate the leukaemic condition irrespective of the dos-

age of the ENU. This observation still affirms the anti-genotoxic ability of *A. muricata* irrespective of the extent of genotoxicity or leukaemia development.

In conclusion, the ENU-induced genotoxicity manifested by the pro-leukaemia state and detected with the bone marrow micronucleus assay in the animal model proved its capacity to induce malignancy and pose a risk factor on exposure. The studied *A. muricata* ethanolic leaf extract prevented further induction of genotoxicity and pro-leukaemia in the ENU-induced model, which was recognised by a reduced MNPCE count in the preventive groups based on the ENU dosages. The proven active antigenotoxic phytochemicals and essential oils of *A. muricata* include acetanogennins, flavonoids, alkaloids, terpenes, and δ -cadinene. The anti-genotoxic activity of *A. muricata* was also seen to be potent in the case of a high ENU carcinogenic agent dosage, with an observable tolerance of the extract when administered within the required dosage to the non-induced mice models.

Acknowledgements

We appreciate the efforts of all the Medical Laboratory Scientists of the Department of Medical Laboratory Science, LAUTECH, Osogbo, for the assisting in the study. We also appreciate the Head of the Animal House of the same institution, Mr Adegoke A., for his expertise and contributions during the experimental phase.

Conflict of interest statement

The authors declare no conflict of interest.

Funding sources

There are no sources of funding to declare.

References

1. Adalberto M, Marion P, Jacques F, Isabelle S, Alain M, Freddie B. Epidemiological patterns of leukaemia in 184 countries: a population based study. *The Lancet Haematology*. 2018;5(1):14–24.
2. Bray F, Ferlay J, Soerjomataram I, Siegel RL, Torre LA, Jemal A. Global cancer statistics 2018: gLOBOCAN estimates of incidence and mortality worldwide for 36 cancers in 185 countries. *CA J Clin*. 2018;68(6):394–424.
3. Dong Y, Shi O, Zeng Q. et al. Leukemia incidence trends at the global, regional, and national level between 1990 and 2017. *Exp Hematol Oncol*. 2020;9(14). doi.org/10.1186/s40164-020-00170-6.
4. Miranda-Filho A, Piñeros M, Ferlay J, Soerjomataram I, Monnereau A, Bray F. Epidemiological patterns of leukaemia in 184 countries: a population-based study. *Lancet Haematol*. 2018;5(1):e14–e24. doi: 10.1016/S2352-3026(17)30232-6. PMID: 29304322.
5. Paul Rawlinson (2019). Introduction to Genotoxicity In: *Genetronix*. Genetronix limited, Cheshire. <https://genetronix.co.uk/an-introduction-to-genotoxicity/>
6. Christopher W. In-Process Control Testing, In: *Separation Science and Technology*, Editor(s): Satinder Ahuja, Stephen Scypinski, Academic Press, 10, 2011:397-427. doi.org/10.1016/B978-0-12-375680-0.00010-3.
7. Aliyu A, Shaari M, Mustapha N, Sayuti N, Reduan M.F, Sithambaram S, Shaari K, and Hamzah H. Some Chemical Carcinogens for Leukaemia Induction AND THEIR Animal Models. *Annual Research and Review in Biology*. 2019;33(1):1-7.
8. Boyonoski AC, Jennifer CS, Lisa MG, Jacobs RM, Shah GM, Poirier GG, Kirkland JB. Niacin deficiency Decreases Bone Marrow Poly (ADP-Ribose) and the Latency of Ethylnitrosourea-Induced Carcinogenesis in Rats. *The Journal of Nutrition*. 2002;132(1): 108-114.
9. Aliyu A, Shaari MR, Ahmad Sayuti NS, Reduan MFH, Sithambaram S, Noordin MM, Shaari K, Hamzah H. N-Ethyl-n-Nitrosourea Induced Leukaemia in a Mouse Model through Upregulation of Vascular Endothelial Growth Factor and Evading Apoptosis. *Cancers (Basel)*. 2020;12(3):678. doi: 10.3390/cancers12030678. PMID: 32183192; PMCID: PMC7140055.
10. Chen T, Mei N, Fu PP. Genotoxicity of pyrrolizidine alkaloids. *J. Appl. Toxicol*. 2010;30:183-196.
11. Mei N, Guo X, Moore, M.M, Methods for using the mouse lymphoma assay to screen for chemical mutagenicity and photo-mutagenicity. In: Caldwell, G.W, Yan, Z. (Eds.), *Optimization in Drug Discovery: In Vitro Methods*. Humana Press, New York, 2014:561-592.
12. Nan M, Xilin L, Si C, Lei G, Xiaoqing G. Genotoxicity evaluation of nutraceuticals. In *Nutraceuticals Efficacy, Safety, and Toxicity*. In Ramesh G, Raji L. Ajay S. Second Ed. Academic Press Elsevier 2021;71:1199-1211.
13. Urruticoechea A, Alemany R, Balart J, Villanueva A, Viñals F, Capellá G. Recent advances in cancer therapy: An overview. *Current Pharmaceutical Design*. 2010;16:3-10.
14. Petrovska, BB. Historical review of medicinal plants' usage. *Pharmacogn. Rev*. 2012;6:1-5.
15. Mei N, Guo X, Ren Z, et al. Review of Ginkgo biloba-induced toxicity, from experimental studies to human case reports. *J. Environ. Sci. Health C Environ. Carcinog. Ecotoxicol. Rev*. 2017;35:1-28.
16. Akanni EO, Faremi A, Adekemi AR, Bamisaye EO, Adewumi FA, Agboola OA, Liasu OI. African Polyherbal Formulation Possesses Chemopreventive and Chemotherapeutic Effects on Benzene- Induced Leukemia in Wistar Rats. *Annual Research & Review in Biology*. 2017;16(2): 1-11.
17. Dwyer JT, Coates PM. Why Americans need information on dietary supplements. *J. Nutr*. 2018;148:1401S-1405S.

18. WHO traditional medicine strategy 2014-2023.,http://apps.who.int/iris/bitstream/10665/92455/1/9789241506090_eng.pdf?ua51. (Accessed 21 November, 2021).
19. Yang C, Gundala SR, Mukkavilli R, Vangala S, Reid MD, Aneja R. Synergistic interactions among flavonoids and acetogenins in *Graviola* (*Annona muricata*) leaves confer protection against prostate cancer. *Carcinogenesis*. 2015;36(6):656-65. doi: 10.1093/carcin/bgv046. PMID: 25863125; PMCID: PMC4566098.
20. Adewole SO, Ojewole JA. Protective effects of *Annona muricata* Linn. (Annonaceae) leaf aqueous extract on serum lipid profiles and oxidative stress in hepatocytes of streptozotocin-treated diabetic rats. *Afr J Tradit Complement Altern Med*. 2008;6(1):30-41.
21. Moghadamtousi SZ, Fadaeinasab M, Nikzad S, Mohan G, Ali HM, Kadir HA. *Annona muricata* (Annonaceae): A Review of Its Traditional Uses, Isolated Acetogenins and Biological Activities. *International journal of molecular sciences*. 2015;16(7):15625-15658. doi.org/10.3390/ijms160715625.
22. CCAC GUIDELINES. *The Canadian Veterinary Journal*, 2003;44(8):631.
23. Agu KC, Okolie NP, Eze I, Anionye JC, Falodun A. Phytochemical analysis, toxicity profile, and hemomodulatory properties of *Annona muricata* (Soursop). *The Egyptian Journal of Haematology*. 2017;42(1):36-44.
24. Schmidt W. The micronucleus test for cytogenetic analysis. In Hollaender, (ed.), *Chemical Mutagens*, Vol. 4. Plenum Press, New York, 1976;31-53.
25. Alabi OA, Bakare AA.. Genotoxicity and mutagenicity of electronic waste leachates using animal bioassays. *Tox Env Chem*.2011;93(5): 1073-1088.
26. Oyeyemi IT, Yekeen OM, Odusina PO, Ologun TM, et al., Genotoxicity and antigenotoxicity study of aqueous and hydro-methanol extracts of *Spondias mombin* L., *Nymphaea lotus* L.. and *Luffa cylindrical* L. using animal bioassays. *Interdiscip Toxicol*. 2015;8(4):184-92.
27. Onuah CL, Chukwuma CC, Ohanador R, Chukwu CN, Iruolagbe J. Quantitative Phytochemical Analysis of *Annona muricata* and *Artocarpus heterophyllus* Leaves Using Gas Chromatography-flame Ionization Detector. *Trends in Applied Sciences Research*, 2019;14:113-118.
28. Hasmila I, Natsir H, Soekamto NH. Phytochemical analysis and antioxidant activity of soursop leaf extract (*Annona muricata* Linn.) *J. Phys.: Conf. Ser*. 2019;1341(3): 20-27.
29. Roduan MR, Hamid RA, Sulaiman H, Mohtarrudin N. *Annona muricata* leaves extracts prevent DMBA/TPA-induced skin tumorigenesis via modulating antioxidants enzymes system in ICR mice. *Biomed. Pharmacother*. 2017;94:481-488. doi: 10.1016/j.biopha.2017.07.133
30. Abdulwahab SM, Jantan J, Hanque MA, Arsha L. Exploring the Leaves of *Annona muricata* L. as a Source of Potential Anti-inflammatory and Anticancer Agents. *Front. Pharmacol*. 2018;9:661.
31. Jacobo- Hernier N, Perez-Plasencia C, Castro-Torres VA, Martinez-Vazquez, Gonzalez-Esquinca AR, and Zentella-Dehesa A. Selective Acetogenins and their potential as anticancer agents. *Frontiers in Pharmacology*. 2019;10:783. PMID:31379567.
32. Syed Najmuddin SU, Romli MF, Hamid M, Alitheen NB, Nik Abd Rahman NM. Anti-cancer effect of *Annona muricata* Linn Leaves Crude Extract (AMCE) on breast cancer cell line. *BMC Complement Altern Med*. 2016;16(1):311. doi: 10.1186/s12906-016-1290-y.
33. Alali FQ, Liu XX, McLaughlin JL. Annonaceous acetogenins: recent progress. *J Nat Prod*. 1999;62(3):504-40.
34. McLaughlin JL. Paw paw and cancer: annonaceous acetogenins from discovery to commercial products. *J Nat Prod*. 2008;71(7):1311-1321.
35. Millimouno FM, Dong J, Yang L, Li J, Li X. Targeting apoptosis pathways in cancer and perspectives with natural compounds from mother nature. *Cancer Prev. Res*. 2014;7:1081-1107. doi: 10.1158/1940-6207.CAPR-14-0136.
36. Habli Z, Toumeh G, Fatfat M, Rahal ON, Gali-Muhtasib H. Emerging Cytotoxic Alkaloids in the Battle against Cancer: Overview of Molecular Mechanisms. *Molecules* (Basel, Switzerland).2017; 22(2): 250. doi.org/10.3390/molecules22020250.
37. Gyesi JN, Opoku R, Borquaye LS. Chemical Composition, Total Phenolic Content, and Antioxidant Activities of the Essential Oils of the Leaves and Fruit Pulp of *Annona muricata* L. (Soursop) from Ghana. *Biochem Res Int*. 2019;4164576. doi: 10.1155/2019/4164576.
38. Abdul Wahab SM, Jantan I, Haque Md. A, Arshad L. Exploring the Leaves of *Annona muricata* L. as a Source of Potential Anti-inflammatory and Anticancer Agents. *Frontiers in Pharmacology*.2018;9: 661.
39. Ménan H, Banzouzi, JT, Hocquette A, Péliissier Y, Blache Y, Koné, M. et al. Antiplasmodial activity and cytotoxicity of plants used in West African traditional medicine for the treatment of malaria. *J. Ethnopharmacol*. 2016;105:131-136. doi: 10.1016/j.jep.2005.10.027.
40. Osorio E, Arango GJ, Jiménez N, Alzate F, Ruiz G, Gutiérrez D, et al. Antiprotozoal and cytotoxic activities *in vitro* of Colombian Annonaceae. *J. Ethnopharmacol*. 2007;111:630-635. doi: 10.1016/j.jep.2007.01.015.
41. George VC, Kumar D, Rajkumar V, Suresh P, and Kumar RA. Quantitative assessment of the relative antineoplastic potential of the n-butanol leaf extract of *Annona muricata* Linn. in normal and immortalized human cell lines. *Asian Pac. J. Cancer Prev*. 2012;13:699-704. doi: 10.7314/APJCP.2012.13.2.699.
42. Torres MP, Rachagani S, Purohit V, Pandey P, Joshi S, Moore ED, et al. *Graviola*: a novel promising natural-derived drug that inhibits tumorigenicity and metastasis of pancreatic cancer cells *in vitro* and *in vivo* through altering cell metabolism. *Cancer letter*. 2012;323:29-40. doi: 10.1016/j.canlet.2012.03.031.
43. Elizabeth OO, Nonso IF, Adebola NI, John OJ. Comparative Study on Chemical Composition and Antioxidant Activity of *Annona muricata* Plant Parts Cultivated in Covenant University, Ota, Ogun State, Nigeria. *Curr Res Nutr Food Sci*. 2018;6(3): 807-815. doi.org/10.12944/CRNFSJ.6.3.23.

The role of TDP-43 protein in amyotrophic lateral sclerosis

Piotr Włodarczyk

Faculty of Medicine, Poznan University of Medical Sciences, Poland



Corresponding author: eedris888@yahoo.com

Mikołaj Witczak

Faculty of Medicine, Poznan University of Medical Sciences, Poland



Agnieszka Gajewska

Faculty of Medicine, Poznan University of Medical Sciences, Poland



Tomasz Chady

Faculty of Medicine, Poznan University of Medical Sciences, Poland



Igor Piotrowski

Department of Electroradiology, Poznan University of Medical Sciences, Poland; Radiobiology Laboratory, Department of Medical Physics, Greater Poland Cancer Centre, Poland

<https://orcid.org/0000-0002-4985-9321>

Keywords: Amyotrophic lateral sclerosis, ALS, TDP-43, SINE, Antisense oligonucleotides, Chaperones, autophagy enhancers

Published: 2022-12-30

How to Cite: Włodarczyk P, Witczak M, Gajewska A, Chady T, Piotrowski I. The role of TDP-43 protein in amyotrophic lateral sclerosis. *Journal of Medical Science*. 2022;91(4):e710. doi:10.20883/medical.e710



© 2022 by the author(s). This is an open access article distributed under the terms and conditions of the Creative Commons Attribution (CC BY-NC) licence. Published by Poznan University of Medical Sciences

doi: 10.20883/medical.e710

ABSTRACT

Amyotrophic lateral sclerosis (ALS) is a progressive neurodegenerative disease where both upper and lower motoneurons are damaged. Even though the pathogenesis of ALS is unclear, the TDP-43 aggregations and non-nuclear localization may be crucial to understanding this process. Despite intensive research on ALS therapies, only two lifespan-prolonging medications have been approved: Riluzole and Edaravone. Unravelling the TDP-43 pathology could help develop new ALS therapies using mechanisms such as inhibition of nuclear export, autophagy, chaperones, or antisense oligonucleotides. Selective inhibitors of nuclear export (SINEs) are drugs that block Exportin 1 (XPO1) and cause the accumulation of not exported molecules inside the nucleus. SINEs that target XPO1 are shown to slightly extend the survival of neurons and soften motor symptoms. Dysfunctional proteins, including TDP-43, can be eliminated through autophagocytosis, which is regulated by the mTOR kinase. Stimulating the elimination of protein deposits may be an effective ALS therapy. Antisense oligonucleotides (ASO) are single-stranded, synthetic oligonucleotides that can bind and modulate specific RNA: via ribonuclease H, inducing their degradation or inducing alternative splicing via blocking primary RNA transcripts. Current ASOs therapies used in ALS focus on *SOD1*, *C9ORF72*, *FUS*, and *ATXN2*, and they may be used to slow the ALS progression. Reversing the aggregation is a promising therapeutic strategy. Chaperones control other proteins' quality and protect them against stress factors. Due to the irreversible character of ALS, it is essential to understand its complicated pathology better and to seek new therapies.

Introduction

Amyotrophic lateral sclerosis (ALS), also known as Lou Gehring's disease, or Charcot's disease, is a progressive neurodegenerative disorder leading to the loss of motor neurons. Limb and bulbar onset are ALS's most common clinical phenotypes, responsible for 70% and 25% of all cases. Signs of upper and lower motor neuron (UMN and LMN) damage are required to confirm the diagnosis of ALS. UMN disruptions are presented with spasticity and weakness, in contrast to LMN malfunctions manifested by fasciculations, muscle wasting, and weakness. Dysarthria and dysphagia are bulbar signs of ALS [1]. The progressive character of ALS leads to malnutrition and respiratory failure. In Europe, the incidence of ALS varies between 2.1 and 3.8 per 100,000 person-years (2019, review) [2]. The median age of ALS diagnosis is between 54 to 69, and the median time from first symptoms to diagnosis ranges between 9 and 24 months [2]. The median survival time from the first symptoms to death or invasive respiratory ranges between 24 and 50 months [2]. However, 5–10% of patients live longer than 10 years. Older age, bulbar onset, malnutrition, psychological distress, lower forced vital capacity (FVC), and the short time delay between onset and diagnosis are related to worse clinical outcomes [3]. 30–50% of ALS patients show cognitive function deficits, and 15% meet the criteria for frontotemporal dementia (FTD) [4]. In addition, ALS and FTD share a common neurological hallmark: up to 97% of ALS and 45% of FTD patients' nervous systems have TDP-43 positive neuronal aggregates [5]. These findings support the hypothesis that ALS and FTD are two manifestations on an ALS-FTD spectrum.

The direct cause of ALS is unknown, but 10–15% of patients have a positive family record. More than 30 genes have been identified as risk factors for ALS development. Almost 70% of familial ALS (fALS) cases are associated with the mutations in superoxide dismutase 1 (SOD1), fused in sarcoma (FUS), chromosome 9 open reading frame 72 (C9ORF72), TAR DNA-binding protein 43 (TARDBP) [6, 7]. Environmental factors may relate to the more frequent onset of the sporadic form of ALS. Exposure to pesticides or low-frequency electromagnetic fields induces cellular oxidative stress, which could contribute to

the pathogenesis of many degenerative diseases [8]. Exposure to heavy metals like lead, head trauma, professional sports, intensive physical activity, and lower body mass index are all associated with a higher probability of developing ALS [8, 9]. However, the research presenting this relationship shows that the estimated probability was low. Additionally, the number of studies on environmental factors is relatively modest. Consequently, these factors are poorly established.

Although the pathomechanism of ALS is unclear, the impaired TDP-43 protein plays a crucial role in the pathogenesis of the disease. TDP-43 is a highly conserved protein belonging to the family of DNA/RNA binding ribonucleoproteins. It is mainly located in the cell nucleus [10]. In most ALS cases, TDP-43 is mislocalized from the nucleus to the cytoplasm, simultaneously forming ubiquitinated cytosolic aggregates [10, 11]. Due to ALS's progressive and irreversible character, it is essential to seek new therapies to improve patients' prognoses. Nevertheless, only two disease-modifying medications have been approved: Riluzole (possibly inhibiting glutamatergic transmission) and Edaravone (free radical scavenger; cleared by FDA but withdrawn by EMA) [12].

In this article, we present the role of impaired TDP-43 protein in the pathology of ALS and discuss current (riluzole and edaravone) and emerging ALS therapies using such methods as inhibition of nuclear export, autophagy enhancement, chaperones, antisense oligonucleotides, and inhibition of poly (ADP-ribose) polymerase.

Methodology

Papers published between 1995 and June 2022 were identified by PubMed literature searches using the terms: "amyotrophic lateral sclerosis"; "ALS"; "TDP-43 proteinopathy"; "antisense oligonucleotides"; "autophagy enhancers"; "chaperones"; "SINE"; "edaravone"; "riluzole". Additional publications were selected through the Internet from the references of those papers. Only articles in English were considered.

TDP-43 protein biology

TDP-43 is a nuclear protein encoded by the *TARDBP* gene located on chromosome 1. It was first recognized as a protein that binds to the trans-

activation response (TAR) element of the human immunodeficiency virus (HIV) and thus was named TAR DNA-binding protein-43 kDa [10]. TDP-43 is mainly concentrated in the nucleus but may perform some of its functions in the cytoplasm [13]. The primary function of the TDP-43 is RNA metabolism which includes its transcription, translation, messenger RNA (mRNA) transport and stabilization, microRNA (miRNA), and long non-coding RNA (lncRNA) processing [14].

TDP-43 is involved in forming and regulating the cytoplasmic RNA granules, termed stress granules (SGs), that appear after exposure to environmental factors, including oxidative or osmotic stressors, heat shock, or viral infections [15]. These membrane-less organelles are thought to enhance cell survival through by storing mRNAs, translation factors, and RNA-binding proteins following stress exposure. Additionally, TDP-43 residues may be significant in SGs formation in the liquid-liquid separation process [16]. Liquid-liquid phase separation of RNA-binding proteins, such as TDP-43, is a process in which membrane-less organelles are formed in cells. The abnormal phase transition of these proteins leads to the formation of insoluble protein aggregates [17]. TDP-43 proteinopathy identified as a factor in the pathogenesis of ALS and other neurodegenerative diseases develops through the depletion of the TDP-43 protein in the nucleus with its mislocalization and aggregation in the cytoplasm [18, 19]. The surge in the cytoplasmic TDP-43 concentration leads to cytoplasmic aggregation formation observed in ALS [20]. Studies suggest that the cytoplasmic mislocalization of TDP-43 induces toxicity through both the loss and gain of functions [10].

The protein consists of 414 amino acid residues composing four domains: N-terminal (NTD), two highly conserved RNA-binding domains (RRM) as well as an unstructured Carboxyl-terminal fragment (CTF) [18]. TDP-43 RRM domains bind with related RNA/DNA molecules and are involved in RNA metabolic processes [19]. Studies suggest that the RNA binding ability may be a toxic and protective mechanism of TDP-43 protein during its aggregation [19, 21]. Several mutations in the RRM domains were shown to disrupt the RNA binding capability while not significantly interfering with RNA recognition [22]. NTD is responsible for the interactions of partner proteins and the

target RNAs and may protect against cytoplasmic TDP-43 aggregation [23, 24]. Deletions or mutations in the nuclear localization signal (NLS) sequence of the NTD may cause the mislocation of TDP-43 in the cytoplasm [25].

TDP-43 aggregates in patients include its full-length form and the 35- and 25-kDa CTF, the prion-like structure of the CTF that is most important for TDP-43 neurodegenerative properties, as CTF is the dominant ALS-associated TARDBP mutation site [26–28]. Prions are self-replicating proteins that undergo conformational changes to form aggregates causing neurological infectious diseases in mammals [29]. While ALS is not an infectious disease, the misfolded structure of TDP-43 and its ability to aggregate give it prion-like properties. Moreover, there is evidence that TDP-43 aggregations can self-propagate within neuronal cells and transmit to adjacent cells. This mechanism, similar to prion replication, may be a foundation for the pathology of ALS [30].

The hyperphosphorylated and ubiquitinated CTF aggregations are found in the brain of patients with ALS. However, CTFs are rarely observed in the spinal cord of ALS patients, even the ones with remarkable degeneration of spinal motor neurons. The above suggests that TDP-43 CTFs accumulate due to additional factors influenced by regional heterogeneity in the central nervous system [29]. TDP-43 accumulation and propagation in vulnerable brain regions and the spinal cord contribute to a significant loss of motor neurons and, thus, clinical syndromes of the neurodegenerative disorder [32]. The wide range of TDP-43 protein cell functions and its post-translational modifications that include ubiquitination, phosphorylation, and acetylation indicate the diversity of biochemical mechanisms in the pathogenesis of ALS itself. (TDP-43 biology is illustrated in **Figure 1**).

Riluzole

Riluzole is the only medication approved for ALS treatment in Europe [33]. Although initial clinical trials showed that riluzole treatment increases a patient's lifespan by 2–3 months, a retrospective meta-analysis revealed that survival time could be extended by 6 to even 19 months [34].

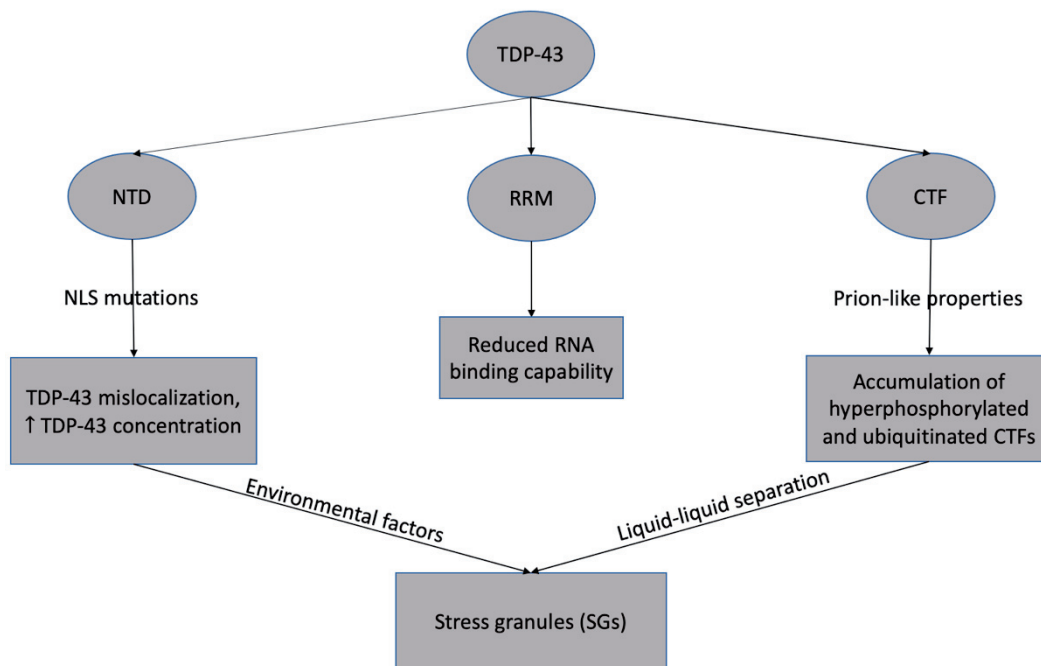


Figure 1. TDP-43 biology in ALS TDP-43 protein is composed of four domains: N-terminal (NTD), two highly conserved RNA-binding domains (RRM), and a Carboxyl-terminal fragment (CTF). Deletions or mutations in the nuclear localization signal (NLS) sequence of the NTD may cause the TDP-43 mislocalization and increased cytosol concentration. Mutations in the RRM domains result in disrupted RNA binding capability. Self-propagation of TDP-43 is mainly the result of the prion properties of CTF. Accumulation of hyperphosphorylated and ubiquitinated CTF-rich aggregations, TDP-43 cytoplasmic mislocalization, and increased concentration under stress exposure leads to stress granule formation

Riluzole moderately impacts bulbar and limb function while not influencing muscle strength [35]. Glutamate excitotoxicity is another proposed mechanism that might explain complex ALS pathology; increased glutamate levels in the cerebrospinal fluid of ALS patients support this theory [36]. It was established that riluzole could modulate glutamatergic signaling. However, a direct connection with glutamate receptors has never been shown [36]. Excitatory amino acid transporter-2 (EAAT2) is a transporter responsible for glutamate reuptake, and it is expressed in glial cells. EAAT2 mRNA transcript levels are significantly lower in TDP-43 proteinopathy leading to the accumulation of glutamate [36]. It was suggested that riluzole could inhibit the catalytic activity of protein kinase CK1 δ , preventing the formation of hyperphosphorylated TDP-43 aggregation and cytoplasmic mislocalization [36]. The preservation of TDP-43 homeostasis mediated by riluzole enables the correct maturation of mRNA transcripts and, as a result, the typical expression of the EAAT2 transporter. This phenomenon shows a connection between ALS hallmarks: glutamate excitotoxicity and TDP-43

aggregations [37]. Furthermore, riluzole can modulate TDP-43 self-interaction without changing TDP-43 expression; it may result from riluzole's antioxidative character [33]. Although most ALS patients receive riluzole after diagnosis, a recent study performed on a murine model showed that riluzole administration does not alter total levels of TDP-43 and does not affect the accumulation of TDP-43 aggregations [38]. However, little research shows that riluzole reduces TDP43 protein aggregation. Therefore, inhibition of CK1 δ kinase may be a successful approach to reduce TDP-43 aggregation.

Edavarone – free radical scavenger

Since 2001 edavarone has been used in the therapy of acute ischemic attack, and the FDA approved it in 2017 for ALS treatment [39]. Edavarone – a free radical scavenger, reduces oxidative stress, a mechanism linked to the pathology of many neurodegenerative diseases that also quickens neuron degeneration [40]. Due to the low number of studies, the direct connection between

edaravone and TDP-43 alterations needs to be clarified. Nonetheless, the antioxidative character of edavarone might impact the TDP-43 aggregation. 3-nitrotyrosine, a specific marker for oxidative stress connected with neuronal degeneration, was significantly reduced after edavarone treatment in the ALS model [41]. It has been demonstrated that reactive nitrogen species can promote TDP-43 aggregation through S-nitrosylation, leading to the formation of disulfide bonds. Additionally, enhanced nitric oxide generation and protein misfolding are caused by increased TDP-43 expression. This positive feedback loop increases nitrosative stress and protein aggregation [42]. A study conducted by Ohta et al. revealed that edavarone could modulate antioxidant cell response mediated by nuclear factor erythroid 2-related factor-2 (Nrf2) in ALS murine model [43]. Nrf2 controls cell antioxidative response. TDP-43 model demonstrated that in response to oxidative stress, the Nrf2 protein level and the expression of antioxidant genes are increased. However, the levels of glutathione (an essential antioxidant) are reduced [44]. In addition, TDP-43 alters the expression of the RNA-binding protein hnRNP K, resulting in a toxic gain of function. Aberrant hnRNP k binds to antioxidant gene transcripts affecting their translation and leading to insufficient antioxidant cell response [44]. ALS patients may find edavarone treatment beneficial by delaying the loss of physical function [45].

Selective inhibitors of nuclear export

Exportin 1 (XPO1) is involved in mediating the export of many types of proteins and RNAs out of the cell nucleus, particularly cargos with leucine-rich nuclear export signals (NES) [46, 47]. Selective inhibitors of nuclear export (SINEs) are drugs that block XPO1 and cause the accumulation of not exported molecules inside the nucleus. SINEs are shown to be helpful in patients with tumours like glioblastoma [48] and multiple myeloma, for which it is approved by the Food and Drug Administration (FDA) to be used as a 5th line of therapy [49]. Using SINEs enhanced autophagy and lysosomal regulation through Helix Loop Helix-30 (HLH-30) nuclear enrichment in SOD-1 based model of ALS in flies and nama-

todes, thus prolonged their lifespan and prevented neurodegeneration. HLH-30 is an ortholog of human Transcription factor EB (TFEB), a protein responsible for the modulation of autophagy [50]. Therefore, similar effects in ALS-affected patients might be achieved in the future. Some ALS models revealed that SINEs that target XPO1 slightly extend the cellular survival of neurons and soften motor symptoms. However, there was no evidence that one specific inhibitor could influence TDP-43 cytoplasmic levels. To prevent this, several overlapping mechanisms with multiple transporters like XPO7 or Nuclear RNA Factor 1 (NXF 1) have to target the nuclear export [51]. Some studies show that TDP-43 does not contain XPO-1-dependent NES. Therefore, the nuclear egress of TDP-43 is believed to be independent of XPO-1. The TDP-43 protein is suggested to be predominantly size-dependent and driven by passive diffusion [52].

Inhibition of poly (ADP-ribose) polymerase (PARP)

Poly (ADP-ribose) polymerase (PARP) is responsible for protein modification and DNA repair [53]. PARP-1 levels are increasing under oxidative stress conditions. The occurrence leads to an accumulation of ADP-ribose polymers, which eventually may lead to cell death. This phenomenon plays a vital role in developing ALS and other neurodegenerative diseases [54, 55]. Heterogeneous ribonucleoprotein A1 (hnRNP A1) is another RNA-binding protein that also plays a role in the pathogenesis of ALS [56]. Exaggerated response to a stressor such as a reactive oxygen species leads to the recruitment of both hnRNP A1 and TDP-43. Conversely, the decreased Poly ADP-ribosylation (PARylation) suppresses the formation of these stress granules in motor neuron-like cell lines. Therefore using PARP inhibitors, such as a drug like Olaparib used in the treatment of ovarian and breast cancer, may be a candidate for further investigation in ALS treatment [55].

Autophagy induction

Autophagocytosis is a multi-step process responsible for eliminating dysfunctional organ-

elles and proteins, including TDP-43, FUS, TAF 15, and EWSR1. Research indicates that impaired autophagy takes part in the formation of protein aggregations in eukaryotic cells such as motoneurons [57]. It may also play a role in the pathogenesis of neurodegenerative diseases. Numerous autophagosomes were found in the motoneurons of patients with both ALS forms, indicating disrupted autophagocytosis [58]. The autophagy pathway is regulated by mTOR kinase, which inhibits the entire process. The use of mTOR inhibitors, and hence the promotion of the elimination of protein deposits, could be crucial for future ALS therapy [59]. Rapamycin (Sirolimus) is a well-known and widely used immunosuppressive drug that stimulates autophagocytosis as an mTOR inhibitor. Ongoing clinical trials indicate controversial effects of Sirolimus in various genetic animal models. Additional improvement in the function of locomotor cells with TDP-43 deposits has d Rapamycin's protective effect [60]. Trehalose is a natural disaccharide that stimulates rapamycin-dependent autophagy and thus lowers the concentration of TDP-43 in spinal cord cells and motoneurons [61, 62]. It also stimulates the nuclear translocation of TFEB (transcription factor EB), which regulates the genes depending on the autophagy pathway. Trehalose treatment also induces rapid and transient lysosomal enlargement and membrane permeabilization [62]. Lithium is another element that enhances autophagocytosis, and is commonly used in treating mental diseases. Lithium also has a therapeutic effect depending on the patient's genotype. ALS patients with the UNC13A mutation benefit most from blocking the mTOR kinase pathway [63].

Antisense oligonucleotides therapies

Almost 10% of ALS cases are familial (familial amyotrophic lateral sclerosis, fALS). 70% of fALS could be explained by known mutations, the essential being: SOD1, C9ORF72, FUS, and TARDP [64]. The link between known mutations and ALS opens possibilities for personalized medicine, such as using antisense oligonucleotides (ASO). ASOs are single-stranded, synthetic oligonucleotides that can bind RNA with high speci-

ficity and could modulate gene expression in two different ways. The first mechanism involves the degradation of targeted RNA mediated by ribonuclease H, which lowers the level of the targeted protein. ASOs may also affect alternative splicing by acting as splice-switching oligonucleotides. Exon skipping and exon inclusions are two forms of splicing modification [64, 65].

Superoxide dismutase is an enzyme encoded by the SOD1 gene. Mutations in SOD1 are 10% fALS and 2% sALS (sporadic amyotrophic lateral sclerosis) cases [66]. However, The connection between the mutation in the SOD1 and the TDP-43 protein is unclear. Some authors suggest no TDP-43 aggregations in SOD1-fALS [67]. Nevertheless, others report that a high concentration of SOD1 protein may affect TDP-43 through phosphorylation and fragmentation, as a result of which SOD1 promotes nuclear-cytoplasmic mislocalization and accumulation of TDP-43 in the cytoplasm [68, 69]. Tofersen is the ASO therapy for SOD1-fALS currently in the clinical trial (BIIB067). It is an ASO that binds directly to SOD1 mRNA, stimulating its degradation via RNase H, which prevents the toxic accumulation of SOD1 [70]. Phase 1 and 2 studies have shown that tofersen in a dose of 100 mg reduces the concentration of SOD1 in cerebrospinal fluid by 36% compared to placebo [65]. Additionally, it may slow disease progression, but this requires further studies [71].

Fused in sarcoma (FUS), like TDP-43, belongs to the family of RNA binding proteins (RBP). RBPs are located mainly in the nucleus and are involved in RNA metabolism [72]. The leading cause of early-onset ALS is FUS mutations [73] which are responsible for 4% of fALS and 2% of sALS cases [74]. No TDP-43 deposits were found in FUS-fALS [67]. ION363 is an ASO designed against the 6th intron of the FUS transcript [74]. The first-in-human study showed that repeated administration of ION363 to a FUS-ALS patient reduced of FUS aggregates characteristic for FUS-fALS. The above study, combined with studies performed on murine models [74], suggests that ION363 silences the mutant FUS transcript and results in a reduction of pathological FUS aggregates and a slowing down of motor neuron degeneration [74]. However, a single-patient study cannot determine whether ION363 modifies the course of the disease. The ongoing study NCT04768972

[75] could answer the whether patients with FUS-ALS will benefit from ION363.

The increased number of the G4C2 repeats in the uncoded C9ORF72 region is the leading cause of fALS, responsible for 40% of fALS and 5–10% of sALS [76]. The expansion of G4C2 repeats in the C9ORF72 leads to specific processes such as haploinsufficiency, formation of RNA foci, and formation of dipeptide repeat proteins (DPR) [77]. Those changes are present many years ahead of the formation of TDP-43 aggregates in motor neurons, probably favouring the deposition of TDP-43 [78]. Researchers observed that DPR (polyGR) accelerates the formation of TDP-43 aggregation [77]. ASO designed selectively against V1 and V3 transcripts of C9ORF72 may lead to RNA foci and DPR reduction [78,79]. Administration of ASO on the C9ALS animal model showed a decrease of poly-GP and V3 transcript in cerebrospinal fluid [78,79]. Brown et al. were the first to apply ASO in treating C9ALS patients. The patients tolerated the therapy well, and polyGP reduction was observed [78].

The ATXN2 gene is mainly associated with spinocerebellar ataxia type 2 (SCA2), but an increased number of CUG (glutamine-encoding) repeats in ATXN2 was associated with a higher incidence of ALS [80, 81]. In addition, 4.7% of ALS patients have intermediate-length polyglutamine (polyQ) expansions in ataxin 2 [80]. Ataxin 2 is a protein involved in RNA metabolism, including stress granule assembly [82]. Intermediate-length PolyQ expansions stimulate the formation of TDP-43 aggregates in motoneurons [83]. It has been observed that lowering the concentration of ataxin 2 reduces the TDP-43 aggregation and improves survival and locomotor function in transgenic TDP-43 mice [82]. The therapy proposed by the authors is the first ASO therapy designed against a gene that is not the direct cause of neurodegenerative disease [82]. Due to crucial, physiological TDP-43 cellular functions, it is not feasible to develop an ASO therapy that directly modifies TDP-43. Therefore the primary group of ALS patients could benefit from ASO targeting ATXN2 [82, 84].

Stimulation of protein disaggregation

In ALS, both familial and sporadic, there are several abnormalities in protein synthesis, especially

TDP-43. To begin with cytoplasmic mislocalization, through the deposition of hyperphosphorylated protein in the form of aggregations, and to end with cutting off C-terminal fragments, ultimately leading to toxic protein aggregation in the patient's brain and spinal cord. Reversing protein aggregation could be a promising therapeutic strategy [85]. Thermal shock proteins (chaperones) control other proteins' quality and perform protective functions for proteins against stress factors such as temperature, chemicals, or oxidative stress. One of them, Hsp-104 isolated from *S. cerevisiae*, exhibits disaggregation abilities concerning toxic protein deposits. Studies report that genetically modified Hsp-104 can dissolve TDP-43 aggregates but does not prevent their formation [86]. Naturally occurring in the human body Hsp-70 and Hsp-90 are stimulated by a transcription factor HSF1. It was discovered that a small molecule called acrimoclomol could stimulate HSF1 [87]. Activating the HSF1 pathway reduces cell levels of TDP-43 deposits [88, 89]. However, after promising results in preclinical trials, phase III tests questioned acrimoclomol efficiency as a form of ALS treatment [90]. Hsp-90, in cooperation with its co-protein Sti1 and possibly Hsp-70, can alter TDP-43 misfolding and stabilise the TDP-43 conformation, thereby reducing TDP-43 toxicity [91]. Another function of Hsp-70 is to regulate autophagy by stimulating the binding of lysosomes to damaged proteins [92]. The Hsp-110 collaborates with the Hsp-70 protein family that functions as part of the disaggregation pathway. A study by Nagy et al. indicated that Hsp-110 could increase the survival time in the ALS murine model [93]. Serine-rich chaperone protein (SRCP-1), a novel chaperone protein that prevents protein aggregation in the cell culture of Huntington's disease, has shown controversial results in ALS models [88]. More studies and optimization are needed to evaluate its effectiveness [94]. HspA5 is a chaperone protein that binds directly to TDP-43. Recent studies indicate that up-regulation of HspA5 in ALS may increase motor neuron survival by inhibiting TDP-43 misfolding and subsequent toxicity [90].

Single chain variable fragment (scFv) obtained by molecular methods from monoclonal antibodies could be a promising approach in the treatment of neurodegenerative diseases like Huntington's disease, Parkinson's disease, and ALS. A study con-

Table 1. Summary of presented strategies and their research phase

Treatment strategy	Proposed mechanism of action in correlation with TDP-43	Clinical results
Riluzole	Riluzole inhibits the kinase CK1 δ and thus prevents the formation of hyperphosphorylated TDP-43 aggregations.	Prolongs median survival time by 3 months, compared to placebo [91].
Edavarone	Edavarone modulates antioxidant cell response mediated by Nrf2 and thus reduces oxidative stress, leading to TDP-43 aggregations.	Slows disease progression by 33% measured by ALSFRSR scale [91].
SINEs (Selective inhibitors of nuclear export)	SINEs are drugs that block XPO1 and cause the accumulation of not exported molecules inside the nucleus, including the TDP-43 protein.	Strategy in the preclinical phase.
PARP inhibitors (PARPi)	Decreasing the Poly ADP-ribosylation PARPi suppresses the formation of stress granules.	Strategy in the preclinical phase.
Rapamycin (mTOR kinase inhibitor)	Rapamycin inhibits mTOR kinase, enhances autophagocytosis, and, as a result, promotes the elimination of TDP-43 deposits.	Currently in II phase trial [92].
ASO targeting ATXN2	Antisense oligonucleotides modulate the expression of ATXN2, leading to ataxin 2 concentration lowering and, as a result, a decrease in the TDP-43 aggregation.	Strategy in the preclinical phase.
Arimoclomol	Arimoclomol activates the HSF1 pathway, stimulates HSP-70 and HSP-90 to alter TDP-43 misfolding, and stabilises TDP-43 conformation.	Arimoclomol failed in the phase II/III trial (Clinicaltrials.gov identifier NCT03491462) [84].

ducted by Tamaki et al. indicated that scFv interacts with TDP-43 directly and hastens the proteolytic degradation of its aggregations. Moreover, refolding abilities of Hsp-70 enhance the degradation of the scFv-TDP-43 complex [95]. Specific scFv can also enhance the polyubiquitin chains bound to TDP-43 and stimulate proteasomal and autophagy degradation pathways [95, 96].

Table 1 summarises presented ALS treatment strategies.

Other ongoing trials

PB-TURSO combines two compounds: phenylbutyrate (PB) and taurursodiol (TURSO). Compounds of PB-TURSO have moderating effects on endoplasmic reticulum stress (PB) and mitochondrial dysfunction (TURSO), both mechanisms known as potential pathogenic factors in ALS. The CENTAUR trial showed that introducing PB-TURSO therapy prolonged the patient's median survival by 6.5 months compared with the placebo [99].

Masitinib is a selective oral tyrosine kinase inhibitor that targets the c-KIT receptor. Experiments on the ALS model showed masitinib's ability to regulate microgliosis and neuroinflammation [100]. The study demonstrated that early introduction (before functional impairment) of masitinib could prolong a patient's survival time by 2 years compared with a placebo [101].

Reldesemtiv is a fast skeletal muscle troponin activator (FSTA) that sensitizes the sarcomere to calcium, enhancing muscular power. This phenomenon may be helpful in ALS and other neuromuscular diseases leading to muscle weakness and fatigue [102]. Reldesemtiv was tested in a phase II trial in patients with ALS. The ALS Functional Rating Scale-Revised (ALSFRSR) decrease noticed a statistically significant fall. Reldesemtiv was most beneficial for patients with faster disease progression [102].

Neurotrophic factor-secreting mesenchymal stromal cells (MSC-NTF, NurOwn) are bone marrow-derived mesenchymal stem cells. They were modified *ex vivo* to secrete neurotrophic factors such as Glial Cell Line Derived Neurotrophic Factor (GDNF) and Vascular Endothelial Growth Factor (VEGF) [103]. Unfortunately, phase 3 research on the use of MSC-NTF for ALS treatment had not reached a statistically significant response to treatment or functional improvement compared to placebo. Nevertheless, analysis of patients' cerebrospinal fluid (CSF) revealed improvements in CSF biomarkers related to neuroinflammation and neurodegeneration after using MSC-NTF whereas the placebo remained the same [104].

A platform trial is clinical research with a single master protocol that evaluates numerous therapies sequentially across one or more groups of patients and permits potential inclusion or exclusions of new therapies in the future. This model allows for faster development by evaluat-

ing many therapies simultaneously [105]. HEALEY ALS platform trial (NCT04297683) is the first for ALS patients [105]. Currently, the research includes five potential drugs: Zilucoplan, Verdiperstat, CNM-AU8, Pridopidine, and SLS-005 Trehalose. The estimated study completion date is on December 2023. This platform trial will undoubtedly accelerate the development of effective ALS therapy [Clinicaltrials.gov identifier NCT04297683].

Conclusions

Amyotrophic lateral sclerosis is a progressive, debilitating disorder that leads to a patient's death. Despite much research, approved therapies only slightly prolong patients' lives. Therefore, it is essential to understand the pathogenesis of ALS and use this knowledge to prepare new treatments. This review aims to demonstrate a new therapy approach and its possible correlation with TDP-43 proteinopathy. It is too early to choose the most promising strategy because most of the presented therapies are in the preclinical phase. It requires clinical phase trials to evaluate the safety and effectiveness of those treatments reliably. However, numerous clinical trials demonstrated that the early introduction (before functional impairment) of ALS therapies has the best response to treatment. Hopefully, further therapy development will enhance patients' prognoses.

Acknowledgements

Conflict of interest statement

The authors declare no conflict of interest.

Funding sources

There are no sources of funding to declare.

References

1. Kiernan MC, Vucic S, Cheah BC, Turner MR, Eisen A, Hardiman O, et al. Amyotrophic lateral sclerosis. *Lancet*. 2011;377:942-55. doi: 10.1016/S0140-6736(10)61156-7.
2. Longinetti E, Fang F. Epidemiology of amyotrophic lateral sclerosis: an update of recent literature. *Curr Opin Neurol*. 2019;32:771-6. doi: 10.1097/WCO.0000000000000730.
3. Chiò A, Logroscino G, Hardiman O, Swingler R, Mitchell D, Beghi E, Traynor BG, On Behalf of the Eurals Consortium. Prognostic factors in ALS: A critical

review. *Amyotrophic Lateral Sclerosis*. 2009;10:310-323. doi: 10.3109/17482960802566824.

4. Benbrika S, Desgranges B, Eustache F, Viader F. Cognitive, Emotional and Psychological Manifestations in Amyotrophic Lateral Sclerosis at Baseline and Overtime: A Review. *Front Neurosci*. 2019;13:951. doi: 10.3389/fnins.2019.00951.
5. Ling S-C, Polymenidou M, Cleveland DW. Converging Mechanisms in ALS and FTD: Disrupted RNA and Protein Homeostasis. *Neuron*. 2013;79:416-438. doi: 10.1016/j.neuron.2013.07.033.
6. van Es MA, Hardiman O, Chio A, Al-Chalabi A, Pasterkamp RJ, Veldink JH, et al. Amyotrophic lateral sclerosis. *Lancet*. 2017;390:2084-98. doi: 10.1016/S0140-6736(17)31287-4.
7. Nowicka N, Juranek J, Juranek JK, Wojtkiewicz J. Risk Factors and Emerging Therapies in Amyotrophic Lateral Sclerosis. *Int J Mol Sci*. 2019;20:2616. doi: 10.3390/ijms20112616.
8. Fang F, Ingre C, Roos P, Kamel F, Piehl F. Risk factors for amyotrophic lateral sclerosis. *Clin Epidemiol*. 2015;181. doi: 10.2147/CLEP.S37505.
9. Nguyen HP, Van Broeckhoven C, van der Zee J. ALS Genes in the Genomic Era and their Implications for FTD. *Trends Genet*. 2018;34:404-23. doi: 10.1016/j.tig.2018.03.001.
10. Suk TR, Rousseaux MWC. The role of TDP-43 mislocalization in amyotrophic lateral sclerosis. *Mol Neurodegener*. 2020;15:45. doi: 10.1186/s13024-020-00397-1.
11. Polymenidou M, Cleveland DW. The Seeds of Neurodegeneration: Prion-like Spreading in ALS. *Cell*. 2011;147:498-508. doi: 10.1016/j.cell.2011.10.011.
12. Hardiman O, Al-Chalabi A, Chio A, Corr EM, Logroscino G, Robberecht W, et al. Amyotrophic lateral sclerosis. *Nat Rev Dis Primers*. 2017;3:17071. doi: 10.1038/nrdp.2017.71.
13. Ayala YM, Zago P, D'Ambrogio A, Xu Y-F, Petrucelli L, Buratti E, et al. Structural determinants of the cellular localization and shuttling of TDP-43. *J Cell Sci*. 2008;121:3778-85. doi: 10.1242/jcs.038950.
14. Ling S-C, Albuquerque CP, Han JS, Lagier-Tourenne C, Tokunaga S, Zhou H, et al. ALS-associated mutations in TDP-43 increase its stability and promote TDP-43 complexes with FUS/TLS. *Proc Natl Acad Sci USA*. 2010;107:13318-23. doi: 10.1073/pnas.1008227107.
15. Aulas A, Vande Velde C. Alterations in stress granule dynamics driven by TDP-43 and FUS: a link to pathological inclusions in ALS? *Front Cell Neurosci*. 2015;9. doi: 10.3389/fncel.2015.00423.
16. Conicella AE, Zerze GH, Mittal J, Fawzi NL. ALS Mutations Disrupt Phase Separation Mediated by α -Helical Structure in the TDP-43 Low-Complexity C-Terminal Domain. *Structure*. 2016;24:1537-49. doi: 10.1016/j.str.2016.07.007.
17. Carey JL, Guo L. Liquid-Liquid Phase Separation of TDP-43 and FUS in Physiology and Pathology of Neurodegenerative Diseases. *Front Mol Biosci*. 2022;9:826719. doi: 10.3389/fmolb.2022.826719.
18. Chiang C-H, Grauffel C, Wu L-S, Kuo P-H, Doudeva LG, Lim C, et al. Structural analysis of disease-related TDP-43 D169G mutation: linking enhanced sta-

- bility and caspase cleavage efficiency to protein accumulation. *Sci Rep.* 2016;6:21581. doi: 10.1038/srep21581.
19. Flores BN, Li X, Malik AM, Martinez J, Beg AA, Barma-da SJ. An Intramolecular Salt Bridge Linking TDP43 RNA Binding, Protein Stability, and TDP43-Dependent Neurodegeneration. *Cell Rep.* 2019;27:1133-1150. e8. doi: 10.1016/j.celrep.2019.03.093.
 20. Neumann M, Sampathu DM, Kwong LK, Truax AC, Micsenyi MC, Chou TT, et al. Ubiquitinated TDP-43 in Frontotemporal Lobar Degeneration and Amyotrophic Lateral Sclerosis. *Science.* 2006;314:130-3. doi: 10.1126/science.1134108.
 21. Maharana S, Wang J, Papadopoulos DK, Richter D, Pozniakovskiy A, Poser I, et al. RNA buffers the phase separation behavior of prion-like RNA binding proteins. *Science.* 2018;360:918-21. doi: 10.1126/science.aar7366.
 22. Lukavsky PJ, Daujotyte D, Tollervey JR, Ule J, Stuan-ni C, Buratti E, et al. Molecular basis of UG-rich RNA recognition by the human splicing factor TDP-43. *Nat Struct Mol Biol.* 2013;20:1443-9. doi: 10.1038/nsmb.2698.
 23. Jiang L-L, Xue W, Hong J-Y, Zhang J-T, Li M-J, Yu S-N, et al. The N-terminal dimerization is required for TDP-43 splicing activity. *Sci Rep.* 2017;7:6196. doi: 10.1038/s41598-017-06263-3.
 24. Afroz T, Hock E-M, Ernst P, Foglieni C, Jambeau M, Gilhespy LAB, et al. Functional and dynamic polymerization of the ALS-linked protein TDP-43 antagonizes its pathologic aggregation. *Nat Commun.* 2017;8:45. doi: 10.1038/s41467-017-00062-0.
 25. Winton MJ, Van Deerlin VM, Kwong LK, Yuan W, Wood EM, Yu C-E, et al. A90V TDP-43 variant results in the aberrant localization of TDP-43 in vitro. *FEBS Lett.* 2008;582:2252-6. doi: 10.1016/j.febslet.2008.05.024.
 26. Van Deerlin VM, Leverenz JB, Bekris LM, Bird TD, Yuan W, Elman LB, et al. TARDBP mutations in amyotrophic lateral sclerosis with TDP-43 neuropathology: a genetic and histopathological analysis. *Lancet Neurol.* 2008;7:409-16. doi: 10.1016/S1474-4422(08)70071-1.
 27. Santamaria N, Alhothali M, Alfonso MH, Breydo L, Uversky VN. Intrinsic disorder in proteins involved in amyotrophic lateral sclerosis. *Cell Mol Life Sci.* 2017;74:1297-318. doi: 10.1007/s00018-016-2416-6.
 28. Smethurst P, Newcombe J, Troakes C, Simone R, Chen Y-R, Patani R, et al. In vitro prion-like behaviour of TDP-43 in ALS. *Neurobiol Dis.* 2016;96:236-47. doi: 10.1016/j.nbd.2016.08.007.
 29. Fraser PE. Prions and Prion-like Proteins. *Journal of Biological Chemistry.* 2014;289:19839-19840. doi: 10.1074/jbc.R114.583492.
 30. Lee S, Kim H-J. Prion-like Mechanism in Amyotrophic Lateral Sclerosis: are Protein Aggregates the Key? *Exp Neurobiol.* 2015;24:1-7. doi: 10.5607/en.2015.24.1.1.
 31. Berning BA, Walker AK. The Pathobiology of TDP-43 C-Terminal Fragments in ALS and FTLD. *Front Neurosci.* 2019;13:335. doi: 10.3389/fnins.2019.00335.
 32. Kesztycki R, Jamshidi P, Kawles A, Minogue G, Flanagan M, Zaccard C, et al. Propagation of TDP-43 proteinopathy in neurodegenerative disorders. *Neural Regen Res.* 2022;17:1498. doi: 10.4103/1673-5374.330609.
 33. Oberstadt M, Stieler J, Simpong DL, Römuß U, Urban N, Schaefer M, et al. TDP-43 self-interaction is modulated by redox-active compounds Auranofin, Chelerythrine and Riluzole. *Sci Rep.* 2018;8:2248. doi: 10.1038/s41598-018-20565-0.
 34. Andrews JA, Jackson CE, Heiman-Patterson TD, Bettica P, Brooks BR, Pioro EP. Real-world evidence of riluzole effectiveness in treating amyotrophic lateral sclerosis. *Amyotroph Lateral Scler Frontotemporal Degener.* 2020;21:509-18. doi: 10.1080/21678421.2020.1771734.
 35. Miller R, Mitchell J, Lyon M, Moore D. Riluzole for amyotrophic lateral sclerosis (ALS)/motor neuron disease (MND). In: *The Cochrane Collaboration, editor. Cochrane Database Syst Rev.* 2002, p. CD001447. doi: 10.1002/14651858.CD001447.
 36. Bissaro M, Federico S, Salmaso V, Sturlese M, Spalluto G, Moro S. Targeting Protein Kinase CK1δ with Riluzole: Could It Be One of the Possible Missing Bricks to Interpret Its Effect in the Treatment of ALS from a Molecular Point of View? *ChemMedChem.* 2018;13:2601-5. doi: 10.1002/cmde.201800632.
 37. Bissaro M, Moro S. Rethinking to riluzole mechanism of action: the molecular link among protein kinase CK1δ activity, TDP-43 phosphorylation, and amyotrophic lateral sclerosis pharmacological treatment. *Neural Regen Res.* 2019;14:2083. doi: 10.4103/1673-5374.262578.
 38. Wright AL, Della Gatta PA, Le S, Berning BA, Mehta P, Jacobs KR, et al. Riluzole does not ameliorate disease caused by cytoplasmic TDP-43 in a mouse model of amyotrophic lateral sclerosis. *Eur J Neurosci.* 2021;54:6237-55. doi: 10.1111/ejn.15422.
 39. Amekura S, Shiozawa K, Kiryu C, Yamamoto Y, Fujisawa A. Edaravone, a scavenger for multiple reactive oxygen species, reacts with singlet oxygen to yield 2-oxo-3-(phenylhydrazono)-butanoic acid. *J Clin Biochem Nutr.* 2022;70:240-7. doi: 10.3164/jcbn.21-133.
 40. Cha SJ, Kim K. Effects of the Edaravone, a Drug Approved for the Treatment of Amyotrophic Lateral Sclerosis, on Mitochondrial Function and Neuroprotection. *Antioxidants (Basel).* 2022;11:195. doi: 10.3390/antiox11020195.
 41. Sawada H. Clinical efficacy of edaravone for the treatment of amyotrophic lateral sclerosis. *Expert Opin Pharmacother.* 2017;18:735-8. doi: 10.1080/14656566.2017.1319937.
 42. Pirie E, Oh C, Zhang X, Han X, Cieplak P, Scott HR, et al. S-nitrosylated TDP-43 triggers aggregation, cell-to-cell spread, and neurotoxicity in hiPSCs and in vivo models of ALS/FTD. *Proc Natl Acad Sci USA.* 2021;118:e2021368118. doi: 10.1073/pnas.2021368118.
 43. Ohta Y, Nomura E, Shang J, Feng T, Huang Y, Liu X, et al. Enhanced oxidative stress and the treatment by edaravone in mice model of amyotrophic lateral sclerosis. *J Neurosci Res.* 2019;97:607-19. doi: 10.1002/jnr.24368.

44. Moujalled D, Grubman A, Acevedo K, Yang S, Ke YD, Moujalled DM, Duncan C, Caragounis A, Perera ND, Turner BJ, et al. TDP-43 mutations causing amyotrophic lateral sclerosis are associated with altered expression of RNA-binding protein hnRNP K and affect the Nrf2 antioxidant pathway. *Human Molecular Genetics*. 2017;26:1732-1746. doi: 10.1093/hmg/ddx093.
45. Brooks BR, Heiman-Patterson T, Wiedau-Pazos M, Liu S, Zhang J, Apple S. Edaravone efficacy in amyotrophic lateral sclerosis with reduced forced vital capacity: Post-hoc analysis of Study 19 (MCI186-19) [clinical trial NCT01492686]. *PLoS ONE*. 2022;17:e0258614. doi: 10.1371/journal.pone.0258614.
46. Fischer U, Huber J, Boelens WC, Mattajt LW, Lührmann R. The HIV-1 Rev Activation Domain is a nuclear export signal that accesses an export pathway used by specific cellular RNAs. *Cell*. 1995;82:475-83. doi: 10.1016/0092-8674(95)90436-0.
47. Wen W, Meinkoth JL, Tsien RY, Taylor SS. Identification of a signal for rapid export of proteins from the nucleus. *Cell*. 1995;82:463-73. doi: 10.1016/0092-8674(95)90435-2.
48. Green AL, Ramkissoon SH, McCauley D, Jones K, Perry JA, Hsu JH-R, et al. Preclinical antitumor efficacy of selective exportin 1 inhibitors in glioblastoma. *Neuro Oncol*. 2015;17:697-707. doi: 10.1093/neuonc/nou303.
49. Chari A, Vogl DT, Gavriatopoulou M, Nooka AK, Yee AJ, Huff CA, et al. Oral Selinexor–Dexamethasone for Triple-Class Refractory Multiple Myeloma. *N Engl J Med*. 2019;381:727-38. doi: 10.1056/NEJMoa1903455.
50. Silvestrini MJ, Johnson JR, Kumar AV, Thakurta TG, Blais K, Neill ZA, et al. Nuclear Export Inhibition Enhances HLH-30/TFEB Activity, Autophagy, and Lifespan. *Cell Rep*. 2018;23:1915-21. doi: 10.1016/j.celrep.2018.04.063.
51. Archbold HC, Jackson KL, Arora A, Weskamp K, Tank EM-H, Li X, et al. TDP43 nuclear export and neurodegeneration in models of amyotrophic lateral sclerosis and frontotemporal dementia. *Sci Rep*. 2018;8:4606. doi: 10.1038/s41598-018-22858-w.
52. Pinarbasi ES, Cağatay T, Fung HYJ, Li YC, Chook YM, Thomas PJ. Active nuclear import and passive nuclear export are the primary determinants of TDP-43 localization. *Sci Rep*. 2018;8:7083. doi: 10.1038/s41598-018-25008-4.
53. Herceg Z, Wang Z-Q. Functions of poly(ADP-ribose) polymerase (PARP) in DNA repair, genomic integrity and cell death. *Mutat Res*. 2001;477:97-110. doi: 10.1016/S0027-5107(01)00111-7.
54. Martire S, Mosca L, d'Erme M. PARP-1 involvement in neurodegeneration: A focus on Alzheimer's and Parkinson's diseases. *Mech Ageing Dev*. 2015;146-148:53-64. doi: 10.1016/j.mad.2015.04.001.
55. Duan Y, Du A, Gu J, Duan G, Wang C, Gui X, et al. PARylation regulates stress granule dynamics, phase separation, and neurotoxicity of disease-related RNA-binding proteins. *Cell Res*. 2019;29:233-47. doi: 10.1038/s41422-019-0141-z.
56. Kim HJ, Kim NC, Wang Y-D, Scarborough EA, Moore J, Diaz Z, et al. Mutations in prion-like domains in hnRNPA2B1 and hnRNPA1 cause multisystem proteinopathy and ALS. *Nature*. 2013;495:467-73. doi: 10.1038/nature11922.
57. Chen S, Zhang X, Song L, Le W. Autophagy Dysregulation in Amyotrophic Lateral Sclerosis: Autophagy Dysregulation in ALS. *Brain Pathol*. 2012;22:110-6. doi: 10.1111/j.1750-3639.2011.00546.x.
58. Chua JP, De Calbiac H, Kabashi E, Barmada SJ. Autophagy and ALS: mechanistic insights and therapeutic implications. *Autophagy*. 2022;18:254-82. doi: 10.1080/15548627.2021.1926656.
59. Palomo V, Nozal V, Rojas-Prats E, Gil C, Martinez A. Protein kinase inhibitors for amyotrophic lateral sclerosis therapy. *Br J Pharmacol*. 2021;178:1316-35. doi: 10.1111/bph.15221.
60. Mandrioli J, D'Amico R, Zucchi E, Gessani A, Fini N, Fasano A, et al. Rapamycin treatment for amyotrophic lateral sclerosis: Protocol for a phase II randomized, double-blind, placebo-controlled, multicenter, clinical trial (RAP-ALS trial). *Medicine (Baltimore)*. 2018;97:e11119. doi: 10.1097/MD.0000000000001119.
61. Wang Y, Liu F-T, Wang Y-X, Guan R-Y, Chen C, Li D-K, et al. Autophagic Modulation by Trehalose Reduces Accumulation of TDP-43 in a Cell Model of Amyotrophic Lateral Sclerosis via TFEB Activation. *Neurotox Res*. 2018;34:109-20. doi: 10.1007/s12640-018-9865-7.
62. Rusmini P, Cortese K, Crippa V, Cristofani R, Cicardi ME, Ferrari V, et al. Trehalose induces autophagy via lysosomal-mediated TFEB activation in models of motoneuron degeneration. *Autophagy*. 2019;15:631-51. doi: 10.1080/15548627.2018.1535292.
63. van Eijk RPA, Jones AR, Sproviero W, Shatunov A, Shaw PJ, Leigh PN, et al. Meta-analysis of pharmacogenetic interactions in amyotrophic lateral sclerosis clinical trials. *Neurology*. 2017;89:1915-22. doi: 10.1212/WNL.0000000000004606.
64. Amado DA, Davidson BL. Gene therapy for ALS: A review. *Mol. Ther*. 2021;29:3345-58. doi: 10.1016/j.ymthe.2021.04.008.
65. Xue YC, Ng CS, Xiang P, Liu H, Zhang K, Mohamud Y, et al. Dysregulation of RNA-Binding Proteins in Amyotrophic Lateral Sclerosis. *Front Mol Neurosci*. 2020;13:78. doi: 10.3389/fnmol.2020.00078.
66. Scoles DR, Pulst SM. Oligonucleotide therapeutics in neurodegenerative diseases. *RNA Biol*. 2018;1-8. doi: 10.1080/15476286.2018.1454812.
67. Farrarwell NE, Lambert-Smith IA, Warraich ST, Blair IP, Saunders DN, Hatters DM, et al. Distinct partitioning of ALS associated TDP-43, FUS and SOD1 mutants into cellular inclusions. *Sci Rep*. 2015;5:13416. doi: 10.1038/srep13416.
68. Zeineddine R, Farrarwell NE, Lambert-Smith IA, Yerbury JJ. Addition of exogenous SOD1 aggregates causes TDP-43 mislocalization and aggregation. *Cell Stress Chaperones*. 2017;22:893-902. doi: 10.1007/s12192-017-0804-y.
69. Jeon GS, Shim Y-M, Lee D-Y, Kim J-S, Kang M, Ahn SH, et al. Pathological Modification of TDP-43 in Amyotrophic Lateral Sclerosis with SOD1 Muta-

- tions. *Mol Neurobiol.* 2019;56:2007-21. doi: 10.1007/s12035-018-1218-2.
70. Cappella M, Pradat P-F, Querin G, Biferi MG. Beyond the Traditional Clinical Trials for Amyotrophic Lateral Sclerosis and The Future Impact of Gene Therapy. *J Neuromuscul Dis.* 2021;8:25-38. doi: 10.3233/JND-200531.
 71. Miller T, Cudkowicz M, Shaw PJ, Andersen PM, Atassi N, Bucelli RC, et al. Phase 1-2 Trial of Antisense Oligonucleotide Tofersen for SOD1 ALS. *N Engl J Med.* 2020;383:109-19. doi: 10.1056/NEJMoa2003715.
 72. Colombrita C, Onesto E, Megiorni F, Pizzuti A, Baralle FE, Buratti E, et al. TDP-43 and FUS RNA-binding Proteins Bind Distinct Sets of Cytoplasmic Messenger RNAs and Differently Regulate Their Post-transcriptional Fate in Motoneuron-like Cells. *J Biol Chem.* 2012;287:15635-47. doi: 10.1074/jbc.M111.333450.
 73. Hübers A, Just W, Rosenbohm A, Müller K, Marroquin N, Goebel I, et al. De novo FUS mutations are the most frequent genetic cause in early-onset German ALS patients. *Neurobiol Aging.* 2015;36:3117.e1-3117.e6. doi: 10.1016/j.neurobiolaging.2015.08.005.
 74. Korobeynikov VA, Lyashchenko AK, Blanco-Redondo B, Jafar-Nejad P, Shneider NA. Antisense oligonucleotide silencing of FUS expression as a therapeutic approach in amyotrophic lateral sclerosis. *Nat Med.* 2022;28:104-16. doi: 10.1038/s41591-021-01615-z.
 75. Codron P, Cassereau J, Vourc'h P. InFUSing antisense oligonucleotides for treating ALS. *Trends Mol Med.* 2022;28:253-4. doi: 10.1016/j.molmed.2022.02.006.
 76. Konopka A, Atkin J. The Emerging Role of DNA Damage in the Pathogenesis of the C9orf72 Repeat Expansion in Amyotrophic Lateral Sclerosis. *Int J Mol Sci.* 2018;19:3137. doi: 10.3390/ijms19103137.
 77. Cook CN, Wu Y, Odeh HM, Gendron TF, Jansen-West K, del Rosso G, et al. C9orf72 poly(GR) aggregation induces TDP-43 proteinopathy. *Sci Transl Med.* 2020;12:eabb3774. doi: 10.1126/scitranslmed.abb3774.
 78. Vatsavayai SC, Nana AL, Yokoyama JS, Seeley WW. C9orf72-FTD/ALS pathogenesis: evidence from human neuropathological studies. *Acta Neuropathol.* 2019;137:1-26. doi: 10.1007/s00401-018-1921-0.
 79. Liu Y, Andreucci A, Iwamoto N, Yin Y, Yang H, Liu F, et al. Preclinical evaluation of WVE-004, an investigational stereo pure oligonucleotide for the treatment of C9orf72-associated ALS or FTD. *Mol Ther Nucleic Acids.* 2022;28:558-70. doi: 10.1016/j.omtn.2022.04.007.
 80. Elden AC, Kim H-J, Hart MP, Chen-Plotkin AS, Johnson BS, Fang X, et al. Ataxin-2 intermediate-length polyglutamine expansions are associated with increased risk for ALS. *Nature.* 2010;466:1069-75. doi: 10.1038/nature09320.
 81. Lee T, Li YR, Ingre C, Weber M, Grehl T, Gredal O, et al. Ataxin-2 intermediate-length polyglutamine expansions in European ALS patients. *Hum Mol Genet.* 2011;20:1697-700. doi: 10.1093/hmg/ddr045.
 82. Becker LA, Huang B, Bieri G, Ma R, Knowles DA, Jafar-Nejad P, et al. Therapeutic reduction of ataxin-2 extends lifespan and reduces pathology in TDP-43 mice. *Nature.* 2017;544:367-71. doi: 10.1038/nature22038.
 83. Hart MP, Gitler AD. ALS-Associated Ataxin 2 PolyQ Expansions Enhance Stress-Induced Caspase 3 Activation and Increase TDP-43 Pathological Modifications. *J Neurosci.* 2012;32:9133-42. doi: 10.1523/JNEUROSCI.0996-12.2012.
 84. Ling S-C, Polymenidou M, Cleveland DW. Converging Mechanisms in ALS and FTD: Disrupted RNA and Protein Homeostasis. *Neuron.* 2013;79:416-38. doi: 10.1016/j.neuron.2013.07.033.
 85. Johnson BS, Snead D, Lee JJ, McCaffery JM, Shorter J, Gitler AD. TDP-43 Is Intrinsically Aggregation-prone, and Amyotrophic Lateral Sclerosis-linked Mutations Accelerate Aggregation and Increase Toxicity. *J Biol Chem.* 2009;284:20329-39. doi: 10.1074/jbc.M109.010264.
 86. Kim Y, Park J-H, Jang J-Y, Rhim H, Kang S. Characterization and Hsp104-induced artificial clearance of familial ALS-related SOD1 aggregates. *Biochem Biophys Res Commun.* 2013;434:521-6. doi: 10.1016/j.bbrc.2013.03.107.
 87. Kalmar B, Lu C-H, Greensmith L. The role of heat shock proteins in Amyotrophic Lateral Sclerosis: The therapeutic potential of Arimoclomol. *Pharmacol Ther.* 2014;141:40-54. doi: 10.1016/j.pharmthera.2013.08.003.
 88. Wang P, Wander CM, Yuan C-X, Bereman MS, Cohen TJ. Acetylation-induced TDP-43 pathology is suppressed by an HSF1-dependent chaperone program. *Nat Commun.* 2017;8:82. doi: 10.1038/s41467-017-00088-4.
 89. Lin P-Y, Folorunso O, Taglialatela G, Pierce A. Overexpression of heat shock factor 1 maintains TAR DNA binding protein 43 solubility via induction of inducible heat shock protein 70 in cultured cells: HSF1 Maintains TDP-43 Solubility. *J Neurosci Res.* 2016;94:671-82. doi: 10.1002/jnr.23725.
 90. François-Moutal L, Scott DD, Ambrose AJ, Zerio CJ, Rodriguez-Sanchez M, Dissanayake K, et al. Heat shock protein Grp78/BiP/HspA5 binds directly to TDP-43 and mitigates toxicity associated with disease pathology. *Sci Rep.* 2022;12:8140. doi: 10.1038/s41598-022-12191-8.
 91. Lin LT, Razzaq A, Di Gregorio SE, Hong S, Charles B, Lopes MH, et al. Hsp90 and its co-chaperone Sti1 control TDP-43 misfolding and toxicity. *FASEB J.* 2021;35. doi: 10.1096/fj.202002645R.
 92. Ormeño F, Hormazabal J, Moreno J, Riquelme F, Rios J, Criollo A, et al. Chaperone Mediated Autophagy Degrades TDP-43 Protein and Is Affected by TDP-43 Aggregation. *Front Mol Neurosci.* 2020;13:19. doi: 10.3389/fnmol.2020.00019.
 93. Nagy M, Fenton WA, Li D, Furtak K, Horwich AL. Extended survival of misfolded G85R SOD1-linked ALS mice by transgenic expression of chaperone Hsp110. *Proc Natl Acad Sci USA.* 2016;113:5424-8. doi: 10.1073/pnas.1604885113.
 94. Luecke IW, Lin G, Santarriaga S, Scaglione KM, Ebert AD. Viral vector gene delivery of the novel chaperone protein SRCP1 to modify insoluble protein in in

- vitro and in vivo models of ALS. *Gene Ther.* 2021. doi: 10.1038/s41434-021-00276-4.
95. Tamaki Y, Shodai A, Morimura T, Hikiami R, Minamiyama S, Ayaki T, Tooyama I, Furukawa Y, Takahashi R, Urushitani M. Elimination of TDP-43 inclusions linked to amyotrophic lateral sclerosis by a misfolding-specific intrabody with dual proteolytic signals. *Sci Rep.* 2018;8:6030. doi: 10.1038/s41598-018-24463-3.
 96. Pozzi S, Thammisetty SS, Codron P, Rahimian R, Plourde KV, Soucy G, Bareil C, Phaneuf D, Kriz J, Gravel C, et al. Virus-mediated delivery of antibody targeting TAR DNA-binding protein-43 mitigates associated neuropathology. *Journal of Clinical Investigation.* 2019;129:1581-1595. doi: 10.1172/JCI123931.
 97. Jaiswal MK. Riluzole and edaravone: A tale of two amyotrophic lateral sclerosis drugs. *Med Res Rev.* 2019;39:733-748. doi: 10.1002/med.21528.
 98. Mandrioli J, D'Amico R, Zucchi E, Gessani A, Fini N, Fasano A, Caponnetto C, Chiò A, Dalla Bella E, Lunetta C, et al. Rapamycin treatment for amyotrophic lateral sclerosis: Protocol for a phase II randomized, double-blind, placebo-controlled, multicenter, clinical trial (RAP-ALS trial). *Medicine.* 2018;97:e11119. doi: 10.1097/MD.00000000000011119.
 99. Paganoni S, Hendrix S, Dickson SP, Knowlton N, Macklin EA, Berry JD, Elliott MA, Maiser S, Karam C, Caress JB, et al. Long-term survival of participants in the CENTAUR trial of sodium phenylbutyrate-taurursodiol in amyotrophic lateral sclerosis. *Muscle and Nerve.* 2021;63:31-39. doi: 10.1002/mus.27091.
 100. Palomo V, Nozal V, Rojas-Prats E, Gil C, Martínez A. Protein kinase inhibitors for amyotrophic lateral sclerosis therapy. *Br J Pharmacol.* 2021;178:1316-1335. doi: 10.1111/bph.15221.
 101. Mora JS, Bradley WG, Chaverri D, Hernández-Barra M, Mascias J, Gamez J, Gargiulo-Monachelli GM, Moussy A, Mansfield CD, Hermine O, et al. Long-term survival analysis of masitinib in amyotrophic lateral sclerosis. *Ther Adv Neurol Disord.* 2021;14:175628642110303. doi: 10.1177/17562864211030365.
 102. Shefner JM, Andrews JA, Genge A, Jackson C, Lechtzin N, Miller TM, Cockcroft BM, Meng L, Wei J, Wolff AA, et al. A Phase 2, Double-Blind, Randomized, Dose-Ranging Trial Of Reldesemtiv In Patients With ALS. *Amyotrophic Lateral Sclerosis and Frontotemporal Degeneration.* 2021;22:287-299. doi: 10.1080/21678421.2020.1822410.
 103. Gothelf Y, Abramov N, Harel A, Offen D. Safety of repeated transplantations of neurotrophic factors-secreting human mesenchymal stromal stem cells. *Clinical and Translational Medicine [Internet].* 2014 [cited 2022 Oct 15];3. doi: 10.1186/2001-1326-3-21.
 104. Cudkowicz ME, Lindborg SR, Goyal NA, Miller RG, Burford MJ, Berry JD, Nicholson KA, Mozaffar T, Katz JS, Jenkins LJ, et al. A randomized placebo-controlled phase 3 study of mesenchymal stem cells induced to secrete high levels of neurotrophic factors in amyotrophic lateral sclerosis. *Muscle and Nerve.* 2022;65:291-302. doi: 10.1002/mus.27472.
 105. Gittings LM, Sattler R. Recent advances in understanding amyotrophic lateral sclerosis and emerging therapies. *Fac Rev [Internet].* 2020 [cited 2022 Oct 15];9. doi: 10.12703/b/9-12.

An overview of cord blood stem cell transplantation in Hong Kong

Chi-Kwan Leung

School of Biomedical Science, the Chinese University of Hong Kong, Shatin, Hong Kong

 <https://orcid.org/0000-0003-2140-199X>

Corresponding author: leungchikwan@cuhk.edu.hk

Published: 2022-12-30

How to Cite: Leung C-K. An overview of cord blood stem cell transplantation in Hong Kong. *Journal of Medical Science*. 2022;91(4):e741. doi:10.20883/medical.e741

 doi: 10.20883/medical.e741

Keywords: biobanking, haematopoietic stem cells, American Association of Blood Banks, Association for the Advancement of Blood & Biotherapies, Foundation for the Accreditation of Cellular Therapy, College of American Pathologists, cord blood bank, unrelated haematopoietic stem cell transplant



© 2022 by the author(s). This is an open access article distributed under the terms and conditions of the Creative Commons Attribution (CC BY-NC) license. Published by Poznan University of Medical Sciences

ABSTRACT

Haematopoietic stem cell graft derived from cord blood is standard therapy for several haematological malignancies and other diseases. The study reports cases of public and private (family) cord blood biobanking services and the related haematopoietic stem cell transplantation ever performed in Hong Kong. The published original research papers and review articles from inception to Nov 2022 have been searched for on Pubmed, Microsoft Academic Search, and Google Scholar to identify reports on existing or terminated cord blood biobanking and transplantation service in Hong Kong. Moreover, all data publicly available on the official websites of the local cord blood banks and local mainstream media has been analysed. The public Hong Kong Red Cross Blood Transfusion Service delivers the highest quantity of haematopoietic stem cell transplants. Among the private sector, HealthBaby releases the most cord blood units for clinical use in diseases in both autologous and allogeneic administration, followed by Cordlife HK. Both public and private (family) cord blood biobanks have been and continue to contribute to the Hong Kong cord blood donor registry. However, the growth of the cord blood inventory is detrimental to donor-recipient matching for lifesaving therapy.

Introduction

In France in 1989, a 5-year-old boy with Fanconi anaemia received the first cord blood transplant (CBT) using a human leukocyte antigen (HLA)-matched sibling donor [1]. Since then, CBT has developed as a standard treatment or an accepted therapeutic modality for >100 haematologic, immunologic, neurologic, and metabolic dis-

eases worldwide [2, 3]. Haematopoietic stem cell transplantation (HSCT) is the only option for curing numerous diseases, including Glanzmann's thrombasthenia, [4] relapsed B-cell acute lymphoblastic leukaemia [5], and sickle cell disease [6]. Worldwide, over 1.5 million HSCTs have been performed [7].

Cord blood represents a valuable source of HSC in addition to bone marrow (BM) and

peripheral blood (PB). Autologous or allogeneic transplantation with HLA-matched siblings, unrelated donors, and haploidentical donors has been performed on paediatric and adult patients for decades [8]. Cord blood transplant (CBT) has been widely used due to the high tolerance of HLA disparity accompanied by a low incidence of graft-versus-host disease, ease of collection, low risk of viral transmission, advancement of *in vitro* cord blood stem cell expansion and *in vivo* homing capacity, and growth of public or private (family) cord blood banks (CBB) worldwide [9, 10].

It was estimated to have over 450 CBBs worldwide; only half carry out in-house processing and storage, with the remaining outsourced to third-party facilities [11]. According to the World Marrow Donor Association, despite over 8 million cord blood units ready for transplant in public CBBs, 10,000–15,000 patients per year fail to identify a matched donor for CBT, especially for racial and ethnic minorities [12, 13]. As a result, CBBs of nation, public, and family have been calling for cord blood banking and donation to extend the inventory size for research and treatment.

Several international accrediting bodies have proposed specific, strong, and up-to-date guidelines or standards for auditing public and private (family) CBBs to ensure compliance with specified operations requirements from cord blood collection to clinical administration. These include the Foundation for the Accreditation of Cellular Therapy (FACT), the Association for the Advancement of Blood & Biotherapies, previously known as the American Association of Blood Banks (AABB), and the College of American Pathologists (CAP). FACT accreditation is the most widely-recognized and comprehensive CBB accreditation. It has been referred to as the evidence-based, objective criteria to evaluate the performance of both public and private (family) CBBs [14, 15]. The NetCord-FACT standard is the cornerstone of the FACT accreditation program for cord blood banking, as the only set of requirements to audit the clinical arm of cellular therapeutic products. As of 27 June 2022, 56 NetCord-FACT accredited CBBs have represented 23 countries on 5 continents. The NetCord-FACT standard applies to the procedures in a CBB covering cord blood donor management (for example, donor eligibility

assessment) and collection, processing, testing (for example, maternal and neonatal blood and the final cryopreserved CD34⁺-enriched cell products for HSCT), cryopreservation, storage, listing in CBB registry, search, selection, reservation, release, distribution, donor and patient informed consent or authorization and clinical administration of cord blood units (CBU) [16, 17].

The College of American Pathologists (CAP) provides an international laboratory accreditation and proficiency testing program for a broad spectrum of laboratory testing on human specimens and a biorepository to ensure testing accuracy and foster continuous modification [18]. CAP is a widely acknowledged leader in laboratory quality assurance. It accredits a suite of laboratory tests related to cord blood and stem cell processing, involving enumeration and viability of CD34⁺ stem cells and (mono) nucleated cells in the blood or related products, blood group, and HLA typing, infectious disease serology of maternal blood, and sterility.

In this study, we overview the cord blood banking industry in Hong Kong. We summarise the active and inactive public and private (family) CBBs, reporting the relevant accreditation status of individual CBBs, the total number of CB-HSCT ever performed, types of HSCT, and the variety of treated diseases. This study would contribute to understanding the ecosystem of the local cord blood banking sector and promote public awareness of the clinical significance of cord blood banking and the relevant accreditations to CBBs for demonstrating compliance with international standards.

Material and methods

The overview of the cord blood industry in Hong Kong was conducted by referencing the Preferred Reporting Items for Systematic Reviews and Meta-Analyses (PRISMA) guidelines [19]. The PRISMA statement was presented in PRISMA 2009 Flow Diagram (**Supplementary Figure 1**).

Search Method

A comprehensive search covering published original research and review articles from inception to Nov 2022 on Pubmed, Microsoft Academic Search, WiseNews, and Google Scholar was per-

formed to identify reports on active and inactive cord blood biobanking and transplantation service in Hong Kong. The keywords combinations included "haematopoietic stem cells," "American Association of Blood Banks," "Association for the Advancement of Blood & Biotherapies," "Foundation for the Accreditation of Cellular Therapy," "College of American Pathologists," "cord blood bank," "unrelated haematopoietic stem cell transplant," "stem cell transplantation," "cord blood stem cell transplantation." Moreover, all information publicly available on the official websites and annual reports of the local cord blood banks and local mainstream media have been analysed. Reference lists of identified articles were searched for additional references. The search was not restricted to any languages or publication types. Statistical analyses and graphical representation were performed using GraphPad Prism 9.3.1 (GraphPad Software, USA).

Eligibility criteria and study selection

Publications that meet the following criteria were included for analysis: (I) Peer-reviewed review, research article, or case study referring to the cord blood biobanking industry or the direct cord blood transplant in Hong Kong or oversea institutes involving locally banked cord blood units; (II) Subject: human with any indications such as Thalassaemia, hypoxic-ischemic encephalopathy, anaemia, cerebral palsy and neuroblastoma. Duplicated records were removed during the screening stage. Publications were excluded if the full-text or key data were inaccessible. A thorough literature search of the selected full-text publications was performed to determine their eligibility. All retrieved eligible publications were included and imported into EndNote 20.3 (Bld 16073) for downstream descriptive and quantitative analyses.

Results

Overview of HSCT cases released by local public and private (family) CBBs

Hong Kong has two public and seven private (family) CBBs. The first and the most extensive public CBB was established by the Hong Kong Red Cross Blood Transfusion Service (BTS) managed by the Hospital Authority, a statutory body

established on 1 December 1990 under the Hospital Authority Ordinance to manage all public hospitals in Hong Kong, introduced in utilization for processing, storage, and releasing CBU for HSCT in 1998. The CBB was renamed "The Hong Kong Red Cross Catherine Chow Cord Blood Bank" in 2007. The BTS-CBB received the NetCord-FACT accreditation in April 2013 and also became the first FACT-accredited CBB in Hong Kong. The number and other relevant clinical information on HSCT contributed by BTS is generally incomplete and non-disclosable; the data reported is primarily retrieved from the annual reports from 2015 to 2021 and peer-reviewed literature. Fifty-four HSCT cases were performed by the transplant centres using CBUs from BTS using donated cord blood collected from local public hospitals from 2015 to 2021, as the annual reports indicate. An additional 9 unrelated CBTs were delivered from 1999 to 2003, [20] with a total of 63 HSCTs confirmed (**Figure 1**). The CBT data between 2004 and 2014 are private.

Given that the mean value of HSCT within the reported years is 9, we reasonably estimated the HSCT performed in the missing period from 2004 to 2015 to be 99, adding to the cumulative HSCT cases using the CBU processed by BTS reaching 162. Mononuclear Therapeutics (MonoTx™) is a private facility receiving donations of CBU from the public Prince of Wales Hospital affiliated with the Chinese University of Hong Kong. It is intended for related and unrelated transplantation, where the donor is eligible to request autologous or related transplantation if the donated CBU is not yet released, which, however, has not been reported by MonoTx™.

Among the seven private (family) CBBs, Healthbaby delivered the highest number, with five processed CBUs for transplantation so far, followed by Cordlife HK (three cases) and Cryolife (one case). While BioCell, Smart Cells, ProStemCell, and Athena Life have not released any CBUs for HSCT. BioCell ceased the cord tissue and blood banking service in 2020, with the cryopreserved cord tissue and CBUs relocated to other private (family) CBBs for storage [21]. Smart Cells ships the collected cord blood samples overseas for further processing and storage. The local cord blood banking services of the other two private (family) CBBs (i.e., ProStemCell, and Athena Life) are either terminated or inactive.

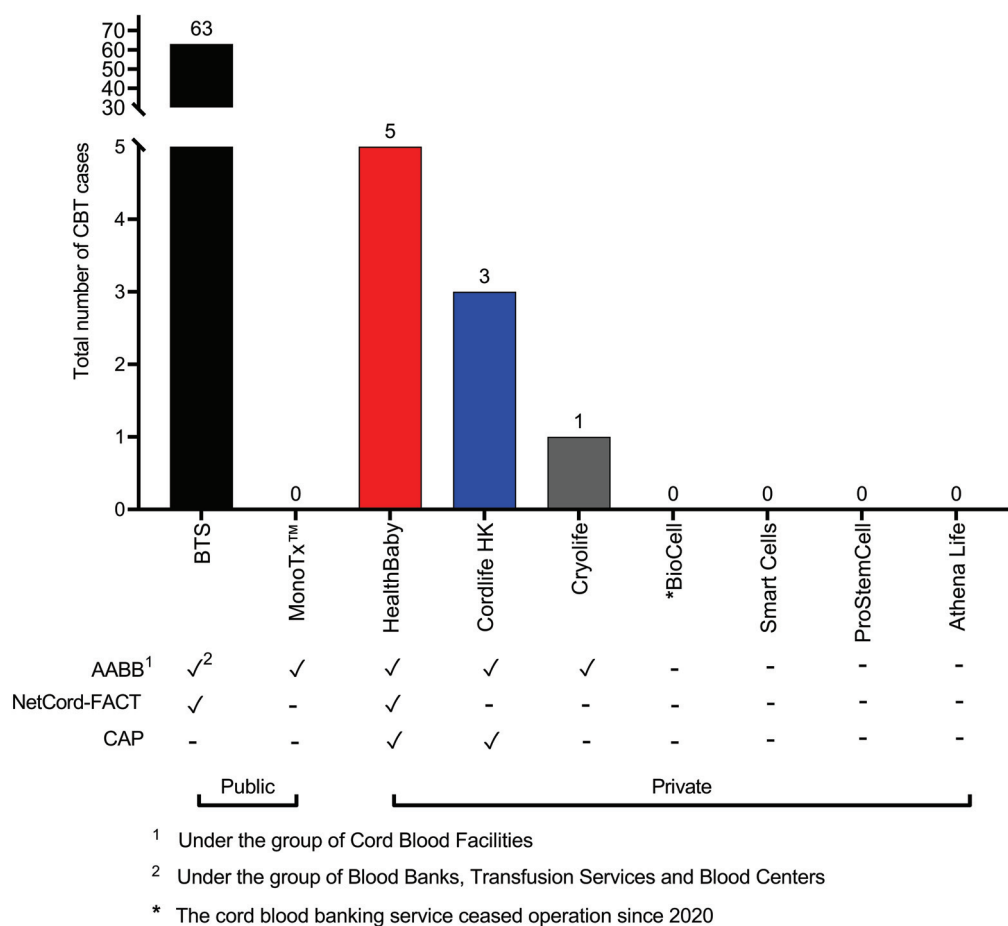


Figure 1. The number of cord blood transplant (CBT) cases of the public and private (family) cord blood banks (CBBs) and their respective accreditation status

Accreditation status awarded to CBBs

As shown in **Figure 1**, all five active public and private (family) CBBs (i.e., BTS, MonoTx™, HealthBaby, Cordlife HK, and Cryolife) are accredited by AABB. Notably, BTS is not accredited under the category of Cord Blood Facilities like the others but under the Blood Banks, Transfusion Services, and Blood Centres. The Hong Kong Red Cross Catherine Chow Cord Blood Bank, operated by BTS, is the first local CBB accredited by NetCord-FACT in March 2013, highlighting its landmark achievement in CBB provided for clinical use in the HK cord blood industry. HealthBaby is the first and only private (family) CBB accredited by the NetCord-FACT accreditation since March 2018.

Despite CAP accreditation absence, numerous medical testing services supported by the reference testing laboratories operated by BTS have been accredited by the Hong Kong Laboratory Accreditation Scheme (HOKLAS) with the ISO 15189:2012 "Medical laboratories – Require-

ments for quality and competence" (Registration No. HOKLAS 816P) followed. In categories of Clinical Microbiology and Infection, Haematology, and Medical Genetics (Molecular Genetics), they involved ABO and Rh(D) typing, haematology counting, viable CD34+, and nucleated cell enumeration, serology, bacterial surveillance tests, Nucleic Acid Amplification Test of Hepatitis B and C virus, and human immunodeficiency virus (HIV).

FACT-accredited HealthBaby and Cordlife HK are the only private (family) CBBs fully accredited under the laboratory accreditation scheme of CAP. The testing performed there is relevant to cord blood banking, covering blood group typing, serology test of maternal blood, and completed cell count with differential, viability and enumeration of CD34+ and mono(nucleated) cells in the pre-processed or processed cord blood. They also provide antimicrobial testing of the final cryopreserved cord blood products. It is worth noting that the satisfaction with the proficiency

testing (PT) requirement by CAP or other external quality assurance programs fails to represent the accreditation corresponded (Please see the Discussion for further details). In addition, HealthBaby is the only CBB in Hong Kong accredited by all three international professional bodies for cord blood banking.

Indications and transplant types of CBT

Li et al. reported that eight patients received CBTs from unrelated donors using the cord blood processed by FACT-accredited BTS (five with leukaemia, one with non-Hodgkin's lymphoma, and one with X-linked adrenoleukodystrophy) from 1999 to 2003 [20]. Other than that, the diseases and

the types of transplants treated by BTS-stored cord blood were non-disclosable.

We focused on the indications and the infusion types of CBT adopting the CBUs processed by private (family) CBBs. As **Figure 2** shows, the nine transplant cases refer to non-haematologic disorders (cerebral palsy, neuroblastoma, and hypoxic-ischemic encephalopathy (HIE)) and haematologic diseases (thalassemia major and Fanconi anaemia). HealthBaby delivered the most CBUs for nearly all indications except HIE and served as the only facility to provide CBUs for Fanconi anaemia in 2014. HealthBaby and Cordlife HK delivered CBUs for thalassemia major, neuroblastoma, and HIE, where the latter is

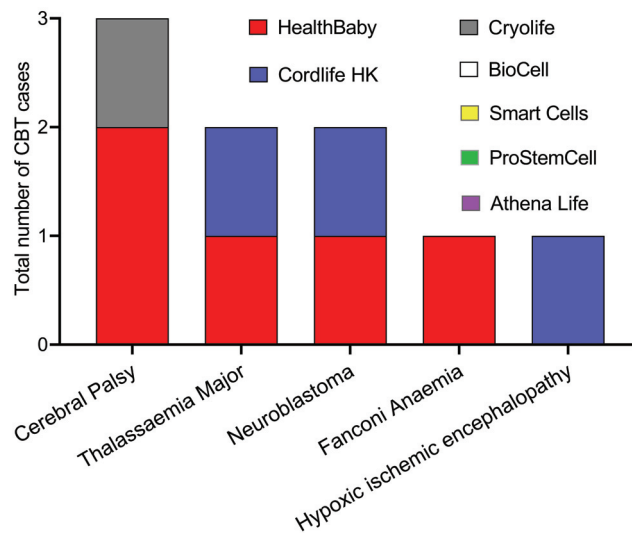


Figure 2. The number of cord blood transplant (CBT) cases for different indications using the cord blood units processed by the private (family) cord blood banks

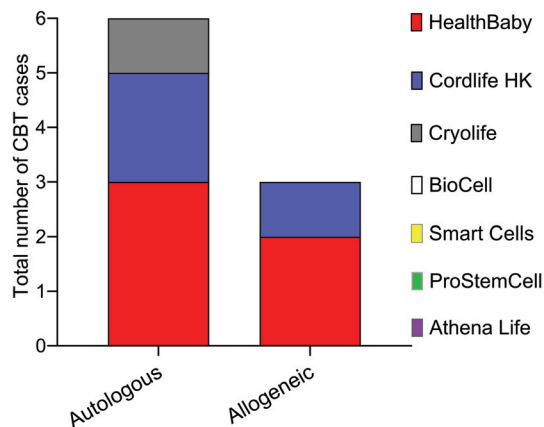


Figure 3. The number of autologous and allogeneic cord blood transplant (CBT) cases using the cord blood units processed by the private (family) cord blood banks

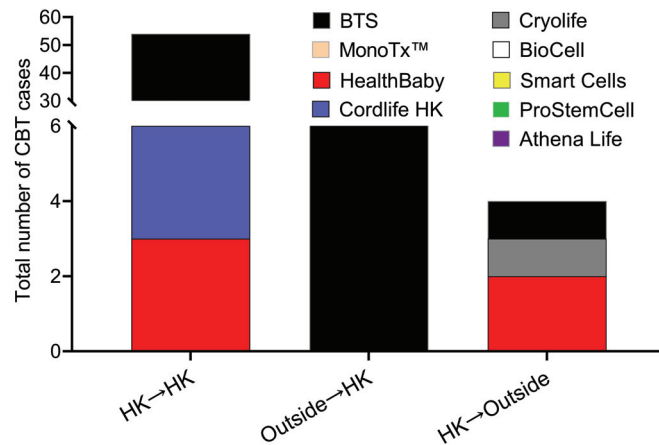


Figure 4. The number of cord blood transplant (CBT) cases using the cord blood units processed and released by the public and private (family) cord blood banks for local administration (HK→HK) or oversea administration (HKRegularOutside), or using the cord blood imported from an oversea facility for local administration

the only facility releasing CBUs for HIE in 2022. In addition, Cryolife released a CBU for cerebral palsy along with the two additional by HealthBaby.

According to **Figure 3**, both facilities released CBUs for autologous and allogeneic (related) use. Moreover, Cryolife delivered an autologous transplant for its single-release case.

Most transplants using the CBUs are performed in Hong Kong's public hospitals. **Figure 4** highlights that BTS released the most CBUs for HK→HK transplantation, with the number 48, followed by HealthBaby (three cases) and Cordlife HK (three cases). BTS is the only facility receiving CBUs from oversea facilities to provide for the six local transplantations (OutsideRegularHK). HealthBaby released three in-house processed CBUs for two oversea CBTs (HK→Outside) in the Duke University Hospital, Durham, North Carolina), and a single CBT delivered by BTS and Cryolife.

Discussion

In this study, we carried out an overview of the public and private (family) cord blood sectors in Hong Kong. We reported that the FACT- and HOKLAS-accredited public BTS released the most significant number of CBUs for allogeneic administration. HealthBaby, accredited by NetCord-FACT, AABB, and CAP, released the highest number of CBUs for autologous and allogeneic use for neurologic and hematologic disorders in

private (family) CBBs. Along with the Division of Transplantation and Immunogenetics of the public Queen Mary Hospital (CAP-accredited No.: #7175525), HealthBaby and Cordlife HK are the only CBBs in Hong Kong to offer CAP-accredited tests for cord blood testing, as are accredited by CAP, which offers the most considerable PT or external quality assessment program fulfilling the requirements of ISO/IEC 17043:2010 in the field of the PT provider (general laboratory, clinical, biochemical genetics, and anatomic pathology) granted by the leading accrediting body ANSI National Accreditation Board. Participating in the CAP PT program facilitates the evaluation of clinical laboratory performance and contributes to demonstrating a commitment to continuous modifications [22].

It must be explicitly stressed that conducting the CAP PT programme is only one of the quantities of requirements to attain full accreditation. It is accompanied by other stringent requirements not covered in the CAP PT programme and involves a quality management program, laboratory information system, competency assessment program, and document control system. All the programmes and systems are pivotal to monitoring the laboratory's performance and delivering accurate testing results. Moreover, a facility accredited by CAP does not mean that all performed tests are CAP-accredited, while only a selected panel of conducted tests is accredited. Therefore, expectant parents are highly recom-

mended to confirm and acknowledge whether the testing per se is accredited by CAP rather than the facility.

FACT-accredited BTS has continued to provide high-quality CBUs for unrelated transplants. Both AABB and FACT guide autologous and allogeneic administration. According to the AABB Standards for Cellular Therapy Services (10th Edition), effective on 1 July 2021, several reference standards apply to the autologous and allogeneic use, such as 5.12A, General Requirements for Cellular Therapy Product Donors; Reference Standard 5.12B, Clinical Evaluation and Laboratory Testing of Living Allogeneic Donors; Reference Standard 5.12C, Clinical Evaluation and Laboratory Testing of Autologous Donors; Reference Standard 5.12D, Clinical Evaluation and Laboratory Testing of Mothers of Cord Blood or Gestational Materials Donors; and Reference Standard 5.12E, Clinical Evaluation and Laboratory Testing of Cadaveric Donors. These standards are descriptive, and the facility determines the implementation of the related policy, process, and procedure, resulting in variations of standards from site to site.

On the other note, the NetCord-FACT's Cord Blood Accreditation Manual (the latest edition is the seventh) gives broader, detailed, and more specific requirements covering cord blood collection, processing, testing, cryopreservation, and storage, release, distribution, listing, and clinical administration. Distinguished from AABB, NetCord-FACT formulates detailed specification requirements pointing to CBUs for unrelated and related clinical administration in terms of the viability and cell count of both nucleated cells and CD34⁺ cells before and after cryopreservation (before release to the clinical program), HLA typing, potency test (for example, colony-forming unit), microbial screen, donor screening and testing, identity verification, labelling, accompanying documents at distribution. The corresponding explanation and example of each reference standard are provided for facilitating the establishment, implementation, and maintenance of the quality management system. In Hong Kong, only the public BTS and private (family) HealthBaby CBBs acquired accreditation from NetCord-FACT. There is no specific ordinance regulating cord blood storage in Hong Kong. However, the collection and use of cord blood are subject to regulatory control of existing ordinances under differ-

ent circumstances. The local regulatory authority recommended that FACT and AABB accreditations provide a third-party audit related to the relevant processes in CBBs and cell therapy (<https://www.advancedtherapyinfo.gov.hk>).

Compared to bone marrow, cord blood is profoundly characterised by a viable source of stem cells. The collection is non-invasive, accompanied by the more relaxed HLA matching requirement, expediting the course of transplantation, especially for ethnic and racial minorities. Nonetheless, the CD34⁺ cell count (i.e., cell dose) is limited per CBU, and the consideration of the patient's weight and HLA profiles for matching is required for clinical administration; thus, CBU is primarily adopted in paediatric patients [23, 24]. Plenty of clinical studies have supported the safety and clinical efficacy of double partially- HLA-matched CBUs graft, overcoming the inadequately dosed single-unit CBT [25]. The advanced *in vitro* cord blood stem cell expansion development has recently fueled clinical transplantation [26, 27]. Due to the insufficient availability of public clinical data on the CBT and HLA genotype and haplotype frequencies, it is intractable to determine the HLA-match likelihoods for CBT. Multi-national studies over the two decades indicated that, in the USA, UK, India, Japan, and South Korea, the probability of locating a (4/6) HLA-match CBU for transplant is nearly 100% when the inventory size reaches 100,000 CBUs [28, 29]. The likelihood of identifying a 5/6 HLA-matched unit for graft reaches over 98% in India, Japan, and South Korea [29]. A recent report released by the Institution of Guangdong Cord Blood Bank and Guangdong Women and Children Hospital indicated that 99% of patients could find a 4/6 HLA-matched CBUs for transplantation [30].

In China, the rapid growth of disease- and population-based biobanks since the late 1990s has driven scientific research and personalised medicine [31]. However, problems and challenges arising from the fast development of biobanks include the need for more implementation and enforcement of policies and laws related to sample collection and management, informed consent procedures, confidentiality, and ethical review. In addition, the policy, process, and procedures for specimen collection, logistics management, processing, storage, data management, and listing have yet to unified. Furthermore, unstable fund-

ing support for biobanks and inadequate public education campaigns, public involvement, and engagement strategies discourage sustainable development for Chinese biobanks [31–36].

In contrast, the Japanese government established the Japan Agency for Medical Research and Development (AMED) to consolidate national resources and reconstruct the funding mechanisms and management system under an initiative named National BioResource Project, to enhance the quality management of biobanks and information sharing across nations [36]. Japan's revitalization strategy and master plan development of biobanking led by AMED include the development of an open-access National Centre Biobank Network's Electronic-Catalogue-based Database for data sharing among communities for collaboration [37]. The Database provides a breadth of high-quality and up-to-date clinical data, including detailed patient's medical history, life history, disease information, and biological sample information to promote medical research and development [37]. A centralised regulatory agency is crucial to establish and enforce rules on operation, management, and information sharing among biobanks, promoting public awareness and facilitating community engagement in biobanking.

Barini et al. reported the effects of the time interval from the sample collection in a medical centre to its processing in a CBB on the CBU's quality [38]. The study found that the mean and median of the total number of nucleated cells, viable cells, and CD34⁺ cells were significantly reduced if the time between collection and processing was within 24 hr compared to 48 hr and 72 hr. Smart Cells delivers the cord blood sample to an oversea processing facility, which inevitably lengthens the turnaround time for the processing. As a result, the quality of the cryopreserved CBU may be compromised. A customer should be fully informed about the extended transport effects on the quality of the CBU.

Prior studies highlighted that the utilization rates (i.e., the ratio of transplanted to banked CBUs) in public and family CBBs are 3–4% and 0.04–0.0005%, respectively [39]. However, the local cord blood inventory information is not publicly accessible, and the utilisation rate in Hong Kong is unclear. On a related note, a recent survey report released by the Asia-Pacific Blood and Marrow Transplantation Group provided an over-

view of the transplant rate (i.e., the number of CBT per 10 million residents) in 20 countries or regions, including Hong Kong in the Asia-Pacific region [40]. The report indicated that the transplant rate in Hong Kong is 1.4, the same as China, which is lower than other developed countries such as Japan (105.3%), Singapore (16.1%), and Australia (11.2%), Korea (8.9%), and New Zealand (6.4%) [40]. Numerous cost-effective strategies have been proposed to increase therapeutic value to patients with the maximal economic sustainability of CBBs [41]. A study based on the data from the National Marrow Donor Program administered by the Health Resources and Service Administration in the USA found that the annual societal benefit, based on the estimated increment of life expectancy after CBT, is between USD 5 million and 1.5 billion. The amount is over an order of magnitude compared to the annual operational cost of running cord blood banks of USD 60–70 million [42]. Considering that more diseases are treatable by CBT and a relatively low probability for specific racial and ethnic minorities to obtain a match from other HSC sources, it is justifiable to allocate additional government sources to support the local cord blood system and infrastructure [42].

As shown in celltrials.org, the percentage of births banking cord blood in Hong Kong is 3.5%, referring to the number of units banked in the most recent year with data divided by the number of births in the same year out of the 57 examined territories. It is higher than in other developed countries such as the USA/Poland/Spain (3%), Australia (1.4%), the UK (0.3%), Japan (0.8%), Germany (0.7%), and France (0.08%). Still, it is lower than nearby territories such as Singapore (30%), Taiwan (7%) and South Korea (6.8%) (**Supplementary Table 1**). A collaborative study by the Chinese University of Hong Kong and the public Queen Elizabeth Hospital indicated that 78.2% of pregnant women are unaware of the availability of private (family) CBBs in Hong Kong. Only 20.3% of expectant women knew BTS might offer HSCT in case of medical requirements. Nearly 90% of expectant mothers agreed that the HK government should allocate more resources to cord blood banking and promote public education on the subject matter [43]. Besides, patients, transplant physicians, and the cord blood industry are encouraged to publicly provide data about the clinical outcome of

CBT to increase transparency and enable patients to make informed choices about their healthcare. The government, clinicians, and the community should work together to elevate social awareness of the clinical relevance of cord blood banking in both public and private (family) CBBs, as a crux element of antenatal care.

Numerous factors contribute to the low public awareness and willingness to cord blood banking and low utilization rates, such as employment status, educational level, uncertainty over the legitimate use of cord blood stem cell transplant, poor regulatory oversight of cord blood banking operation, cost of banking, and concern on safety and cell recovery after cryopreservation for clinical application. Therefore, it is pivotal for a government to mobilise resources to set up a regulatory body to oversee the legislation, policies, and standards implementation. These are necessary to regulate the cord blood banking business and launch education campaigns to promote the socio-economic benefits of biobanking to the general public and clinicians. In addition, it is also vital to reorganise funding mechanisms to address the economic vulnerability biobanks face to sustain the cord blood industry [44–48].

There are several limitations of this study. First, the CBT data from 2004 to 2014 delivered by BTS-CBB needed to be disclosable, and the number of HSCTs using the CBU processed by BTS was estimated. Some of the CBT information provided by other private or family CBBs may not be updated, leading to the potential under- or over-estimation of HSCT facilitated by local CBBs. Besides, a minimal amount of clinical data on individual CBT was released, impeding us from conducting a comprehensive analysis of the dosing, safety, and clinical efficacy of cord blood stem cell transplantation.

Conclusions

Public and private CBBs are the driving factor in enhancing the local inventory for potential autologous and allogeneic (related and unrelated) applications. Therefore, dedicated efforts to expand the inventory size and promote public awareness of the clinical significance of cord blood banking are crucial to nurturing the cord blood industry in Hong Kong.

Acknowledgements

Concept or design: Leung CK.
Acquisition of data: Leung CK.
Analysis or interpretation of data: Leung CK.
Drafting of the manuscript: Leung CK.
Critical revision of the manuscript for important intellectual content: Leung CK.

Leung CK had full access to the data, contributed to the study, approved the final version for publication, and took responsibility for its accuracy and integrity.

Abbreviations

HSCT: Hematopoietic stem cells transplantation; BM: Bone marrow; CBB: Cord blood bank; CBT: Cord blood transplant; CBU: Cord blood unit; PB: Peripheral blood; HLA: Human leukocyte antigens; AABB: Association for the Advancement of Blood & Biotherapies formerly known as American Association of Blood Banks; FACT: Foundation for the Accreditation of Cellular Therapy; CAP: College of American Pathologists; PT: Proficiency testing.

Conflict of interest statement

The authors declare no conflict of interest.

Funding sources

There are no sources of funding to declare.

Ethics approval

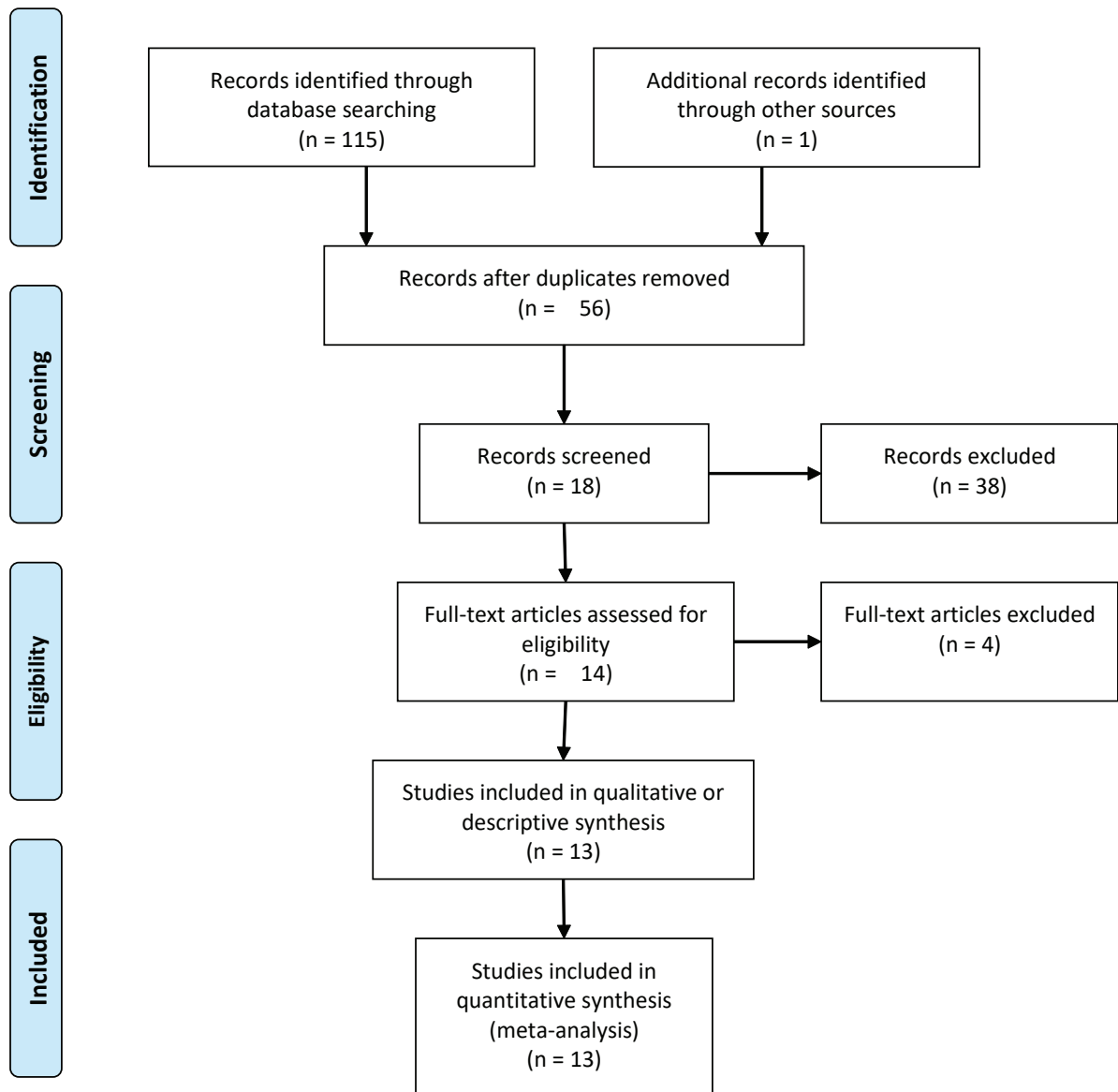
Not applicable.

References

1. Gluckman E, Broxmeyer HA, Auerbach AD, Friedman HS, Douglas GW, Devergie A, et al. Hematopoietic reconstitution in a patient with Fanconi's anemia by means of umbilical-cord blood from an HLA-identical sibling. *N Engl J Med.* 1989;321(17):1174-8.
2. Alexander T, Greco R. Hematopoietic stem cell transplantation and cellular therapies for autoimmune diseases: overview and future considerations from the Autoimmune Diseases Working Party (ADWP) of the European Society for Blood and Marrow Transplantation (EBMT). *Bone Marrow Transplant.* 2022.
3. Khaddour K, Hana CK, Mewawalla P. Hematopoietic Stem Cell Transplantation. *StatPearls.* Treasure Island (FL)2022.
4. James CCaB. Haemopoietic stem cell transplantation is a curative treatment option with minimal transplant-related complications for patients with severe Glanzmann's thrombasthenia. *Clin Med (Lond).* 2019;19(34).
5. Panz-Klapuch M, Spalek A, Duda K, Kopinska A, Wieczorkiewicz-Kabut A, Helbig G. Allogeneic hematopoietic stem cell transplantation for relapsed Bcell acute lymphoblastic leukemia after failure of autologous hematopoietic stem cell transplantation: a retrospective single-center analysis. *Pol Arch Intern Med.* 2022;132(3).
6. Khemani K, Katoch D, Krishnamurti L. Curative Therapies for Sickle Cell Disease. *Ochsner J.* 2019;19(2):131-7.

7. Granot N, Storb R. History of hematopoietic cell transplantation: challenges and progress. *Haematologica*. 2020;105(12):2716-29.
8. Xue E, Milano F. Are we underutilizing bone marrow and cord blood? Review of their role and potential in the era of cellular therapies. *F1000Res*. 2020;9.
9. Shpall EJ, Rezvani K. Cord blood expansion has arrived. *Blood*. 2021;138(16):1381-2.
10. Dumont-Lagace M, Feghaly A, Meunier MC, Finney M, Van't Hof W, Masson Frenet E, et al. UM171 Expansion of Cord Blood Improves Donor Availability and HLA Matching For All Patients, Including Minorities. *Transplant Cell Ther*. 2022.
11. Database GCBI. Global Cord Blood Industry Database, 2021. Retrieved on 15 Jun 2022.
12. Association WMD. Cord blood: the basics. 2022 Jun16.
13. Barker JN, Byam CE, Kernan NA, Lee SS, Hawke RM, Doshi KA, et al. Availability of cord blood extends allogeneic hematopoietic stem cell transplant access to racial and ethnic minorities. *Biol Blood Marrow Transplant*. 2010;16(11):1541-8.
14. Foundation PsGtCB. Accreditation Standards Retrieved on 15 Jun 2022.
15. Joris M, Paulson K, Foley L, Duffy M, Querol S, Gomez S, et al. Worldwide survey on key indicators for public cord blood banking technologies: By the World Marrow Donor Association Cord Blood Working Group. *Stem Cells Transl Med*. 2021;10(2):222-9.
16. Association TWMD. NetCord-FACT Standards. Retrieved on 15 Jun 2022.
17. Therapy FftAoC. Cord Blood Bank Standards. Retrieved on 15 Jun 2022.
18. Reese EM, Nelson RC, Flegel WA, Byrne KM, Booth GS. Critical Value Reporting in Transfusion Medicine: A Survey of Communication Practices in US Facilities. *Am J Clin Pathol*. 2017;147(5):492-9.
19. Moher D, Liberati A, Tetzlaff J, Altman DG, Group P. Preferred reporting items for systematic reviews and meta-analyses: the PRISMA statement. *PLoS Med*. 2009;6(7):e1000097.
20. Li CK, Shing MM, Chik KW, Tsang KS, Tang NL, Chan PK, et al. Unrelated umbilical cord blood transplantation in children: experience of the Hong Kong Red Cross Blood Transfusion Service. *Hong Kong Med J*. 2004;10(2):89-95.
21. Corporation HKSaTP. PUBLIC NOTICE. Retrieved on 27 Jun 2022.
22. Lopez MC, Lawrence DA. Proficiency testing experience for viable CD34+ stem cell analysis. *Transfusion*. 2008;48(6):1115-21.
23. Viswanathan C, Roy A, Damodaran D, Manira AK, Kabra P. Optimization of the inventory size of the public cord blood program--the Indian context. *J Assoc Physicians India*. 2010;58:608-11.
24. Howard DH, Meltzer D, Kollman C, Maiers M, Logan B, Gragert L, et al. Use of cost-effectiveness analysis to determine inventory size for a national cord blood bank. *Med Decis Making*. 2008;28(2):243-53.
25. Zheng CC, Zhu XY, Tang BL, Zhang XH, Zhang L, Geng LQ, et al. Double vs. single cord blood transplantation in adolescent and adult hematological malignancies with heavier body weight (≥ 50 kg). *Hematology*. 2018;23(2):96-104.
26. Scaradavou A. Cord blood beyond transplantation: can we use the experience to advance all cell therapies? *Br J Haematol*. 2021;194(1):14-27.
27. Ferreira MSV, Mousavi SH. Nanofiber technology in the ex vivo expansion of cord blood-derived hematopoietic stem cells. *Nanomedicine*. 2018;14(5):1707-18.
28. Gragert L, Eapen M, Williams E, Freeman J, Spellman S, Baitty R, et al. HLA match likelihoods for hematopoietic stem-cell grafts in the U.S. registry. *N Engl J Med*. 2014;371(4):339-48.
29. Song EY, Huh JY, Kim SY, Kim TG, Oh S, Yoon JH, et al. Estimation of size of cord blood inventory based on high-resolution typing of HLAs. *Bone Marrow Transplant*. 2014;49(7):977-9.
30. Shi CY, Wei W, Lyu LJ, Wang Q. Umbilical cord blood application analysis of Guangdong Cord Blood Bank. *Chin Med J (Engl)*. 2020;133(16):1997-8.
31. Cheng L, Shi C, Wang X, Li Q, Wan Q, Yan Z, et al. Chinese biobanks: present and future. *Genet Res (Camb)*. 2013;95(6):157-64.
32. Zhaolin Gao YH, Fei Yao and Ziyu Zhou. Public awareness and attitudes toward biobank and sample donation: A regional Chinese survey. *Front Public Health*. 2022.
33. Jiajv Chen JH, and Xuekai Xie. Legal and Ethical Challenges in the Construction of China's Biobanks. *Biotechnology Law Report*. 2021;40(5).
34. Zhang Y, Li Q, Wang X, Zhou X. China Biobanking. *Adv Exp Med Biol*. 2015;864:125-40.
35. Vaught J. Biobanking in China. *Biopreserv Biobank*. 2015;13(1):1.
36. Lee S, Jung PE, Lee Y. Publicly-funded biobanks and networks in East Asia. *Springerplus*. 2016;5(1):1080.
37. Omae Y, Goto YI, Tokunaga K. National Center Biobank Network. *Hum Genome Var*. 2022;9(1):38.
38. Barini R, Ferraz UC, Acacio GL, Machado IN. Does the time between collecting and processing umbilical cord blood samples affect the quality of the sample? *Einstein (Sao Paulo)*. 2011;9(2):207-11.
39. Lee YH. Clinical utilization of cord blood over human health: experience of stem cell transplantation and cell therapy using cord blood in Korea. *Korean J Pediatr*. 2014;57(3):110-6.
40. Minako Iida AD, Mafruha Akter, Alok Srivastava, Joon Ho Moon, Phu Chi Dung, Marjorie Rose Bravo, Aya Aya Gyi, Devinda Jayathilake, Kaiyan Liu, Bor-Sheng Ko, Amir Hamidieh, Kim Wah Ho, Aloysius Ho, Artit Ungkanont, Tasneem Farzana, Joycelyn Sim, Bishesh Poudyal, Khishigjargal Batshkh, Shin-ichiro Okamoto, Yoshiko Atsuta, Registry Committee of the Asia-Pacific Blood and Marrow Transplantation Group(APBMT). The 2016 APBMT Activity Survey Report: Trends in haploidentical and cord blood transplantation in the Asia-Pacific region. *Blood Cell Therapy*. 2021;4(2):9.
41. Rebullà P, Querol S, Pupella S, Prati D, Delgadillo J, De Angelis V. Recycling Apparent Waste Into Biologicals: The Case of Umbilical Cord Blood in Italy and Spain. *Front Cell Dev Biol*. 2021;9:812038.

42. Strong A, Gracner T, Chen P, Kapinos K. On the Value of the Umbilical Cord Blood Supply. *Value Health*. 2018;21(9):1077-82.
43. Suen SS, Lao TT, Chan OK, Kou TK, Chan SC, Kim JH, et al. Maternal understanding of commercial cord blood storage for their offspring - a survey among pregnant women in Hong Kong. *Acta Obstet Gynecol Scand*. 2011;90(9):1005-9.
44. Lu H, Chen Y, Lan Q, Liao H, Wu J, Xiao H, et al. Factors That Influence a Mother's Willingness to Preserve Umbilical Cord Blood: A Survey of 5120 Chinese Mothers. *PLoS One*. 2015;10(12):e0144001.
45. Peberdy L, Young J, Massey DL, Kearney L. Parents' knowledge, awareness and attitudes of cord blood donation and banking options: an integrative review. *BMC Pregnancy Childbirth*. 2018;18(1):395.
46. Pisula A, Sienicka A, Stachyra K, Kacperczyk-Bartnik J, Bartnik P, Dobrowolska-Redo A, et al. Women's attitude towards umbilical cord blood banking in Poland. *Cell Tissue Bank*. 2021;22(4):587-96.
47. Bhandari R, Lindley A, Bhatla D, Babic A, Mueckl K, Rao R, et al. Awareness of cord blood collection and the impact on banking. *Pediatr Blood Cancer*. 2017;64(7).
48. Shearer WT, Lubin BH, Cairo MS, Notarangelo LD, Section On HO, Section On A, et al. Cord Blood Banking for Potential Future Transplantation. *Pediatrics*. 2017;140(5).



Supplementary Figure 1. PRISMA flow diagram

Supplementary Table 1.

Country/ Region	Banking	Births	Country/ Region	Banking	Births
Singapore	30,00%	39,039	Georgia	1,00%	51,138
Greece	10,00%	88,553	Italy	1,00%	440,78
Portugal	10,00%	87,02	Japan	0,80%	918,4
Puerto Rico	9,50%	21,4	Argentina	0,70%	685,394
Romania	7,00%	188,755	Austria	0,70%	85,54
Taiwan	7,00%	181	Colombia	0,70%	649,115
South Korea	6,80%	326,9	Croatia	0,70%	36,945
Slovakia	6,00%	57,639	Ecuador	0,70%	293,139
Hungary	5,00%	89,807	Germany	0,70%	787,6
Serbia	5,00%	63,975	Peru	0,70%	60,5
Hong Kong	3,50%	53,716	Philippines	0,70%	1618,31
Montenegro	3,50%	7,264	Malaysia	0,60%	501,945
Bosnia and Herzegovina	3,00%	29,328	Ukraine	0,57%	335,874
Israel	3,00%	184,37	Denmark	0,50%	61,476
Poland	3,00%	396	Jordan	0,50%	207,917
Spain	3,00%	369,302	Norway	0,50%	55,12
United Arab Emirates	3,00%	97,738	Sweden	0,50%	115,832
United States	3,00%	3788,24	Thailand	0,50%	666,109
Macedonia	2,90%	21,333	Vietnam	0,50%	1472
Slovenia	2,70%	19,585	India	0,40%	26028,1
South Africa	2,50%	1009,07	Mexico	0,40%	2162,53
Canada	2,30%	382,533	Brazil	0,36%	2870
Albania	1,50%	28,934	Czech Republic	0,36%	114,036
Lebanon	1,50%	128,687	Turkey	0,35%	1250
Switzerland	1,50%	87,851	Belgium	0,30%	117,8
Australia	1,40%	315	Russia	0,30%	1604,34
Iran	1,20%	1366	United Kingdom	0,30%	731,21
China	1,00%	15230	France	0,08%	758

Pegylation – in search of balance and enhanced bioavailability

Dawid Łażewski

Department of Chemical Technology of Drugs,
Poznan University of Medical Sciences, Poland

 <https://orcid.org/0000-0002-9832-5094>

Marek Murias

Department of Toxicology, Poznan University
of Medical Sciences, Poland

 <https://orcid.org/0000-0002-2903-4912>

Marcin Wierzchowski

Department of Chemical Technology of Drugs,
Poznan University of Medical Sciences, Poland

 <https://orcid.org/0000-0003-2619-0466>

Corresponding author: mwierzch@ump.edu.pl

Keywords: polyethylene glycol, photodynamic therapy, anticancer therapy

Published: 2022-12-30

How to Cite: Łażewski D, Murias M, Wierzchowski M. Pegylation – in search of balance and enhanced bioavailability. *Journal of Medical Science*. 2022;91(4):e761. doi:10.20883/medical.e761



© 2022 by the author(s). This is an open access article distributed under the terms and conditions of the Creative Commons Attribution (CC BY-NC) licence. Published by Poznan University of Medical Sciences

 doi: 10.20883/medical.e761

ABSTRACT

In the process of finding better therapeutics, thousands of new molecules are synthesised every day. Many of these can be poorly soluble in water, leading to a potentially promising drug being rejected during testing due to its poor solubility. Polyethylene glycol (PEG) has become known as an excellent modification to remedy this and was initially used to increase circulation time and reduce the immunogenicity of therapeutic proteins. Thus significantly increasing their safety and range of use. Another group of compounds in which significant benefits of pegylation have been seen are photosensitisers. Used in photodynamic therapy, they are often characterised by very high hydrophobicity. Pegylation of their structure significantly increases their affinity for cancer cells and facilitates their penetration through cell membranes. Classical small-molecule drugs can benefit from temporary combinations hydrolysed in the body or very short PEG chains. This approach allows a significant increase in the bioavailability of the drug while avoiding the disadvantages of small molecule pegylation. However, the most common motive for pegylation recently is the creation of drug carriers. Liposomes and nanoparticles make it possible to exploit the advantages of PEG to stabilise their structure and increase circulation time while not modifying the structure of the active compound. Unfortunately, PEGs also have their drawbacks. The first is their high molecular weight range, especially for longer chains, which poses difficulties in purification. Another is the emergence of antibodies directed against PEG. Nevertheless, pegylation is still an up-and-coming method for modifying pharmaceutically active molecules.

Introduction

One of the significant challenges in drug design is the poor solubility of many compounds in water. Organic molecules used in medicine are mainly hydrophobic. However, not all of them require or

can benefit from increased solubility. According to the BCS (Biopharmaceutics Classification System), there are four classes of drugs. They are segregated according to their solubility (high vs. low) and intestinal permeability (high vs low). Drugs from class 1 are highly soluble and absorb

well; ideally, all drugs would eventually have such desirable properties. Classes 2 and 3 comprise drugs with either low solubility or low permeability, while class 4 drugs with the weakest parameters have the poorest bioavailability. Most modifications to the structure aimed at increasing their solubility in water rely on introducing hydrophilic functional groups (e.g. hydroxyl, amine) into their structure or giving these molecules an electric charge by introducing quaternary ammonium groups or quickly dissociating groups (such as sulfonyl or carboxyl groups). There are several disadvantages to using this approach. Such hydrophilic compounds are not easily transported across biological membranes, mostly lipid in structure. Therefore, such modification will move a drug from BCS class 2 to class 3, not improving overall bioavailability. Additionally, acidic groups such as carboxyl or sulfonyl groups generally increase water solubility only under primary conditions where they can ionise. One of the solutions to improve this is 'pegylation'. It offers the possibility of increasing the solubility and, consequently, bioavailability of drugs in a wide range of applications. Polyethylene glycol (PEG) consists of units containing alternating ethylene groups and oxygen atoms, giving it an amphiphilic structure. The structure is very advantageous from the point of view of penetration through biological membranes because it has an affinity for both the aqueous environment of body fluids and lipid cell membranes. These properties make it a fascinating modification, as it can result in modified drugs transitioning to a higher BCS class, thereby improving their therapeutic usability. One of the most significant advantages of pegylation is that

it can improve solubility and permeability at the same time with the use of only one modification. However, due to the variety of substituents and methods of linking them to active molecules, different drugs require a different approach to this up-and-coming method.

PEG can be attached to the target in many ways (**Figure 1**). Due to their large size and slightly negative charge owing to the oxygen atoms, they can be adsorbed on the surface of nanoparticles. In the case of liposomes, PEG is often incorporated into the membrane by adding it to the mixture during formulation. Alternatively, some of the lipid chains in phospholipids can be exchanged with PEG chains. When modifying molecules, a covalently bonding target with PEG is the preferred method and can be used on its own or as a linker to another molecule or carrier. This mini-review will focus on modification utilizing covalent bonds. There are two possible methods of pegylation of small molecules, permanent attachment of the glycol chain or temporary, as in the case of pro-drugs. Nevertheless, only one is preferred for macromolecules. The irreversible method is most commonly used in protein and photosensitiser modification. It provides stability and structure invariability even after drug administration. Still, unfortunately, it can reduce efficiency compared to the original molecule if the size of the PEG chain is too large. The most commonly used PEG chains contain functional groups that react irreversibly with those in the modified compound. Amine, hydroxyl, or thiol groups are common targets of this reaction. The first can create connections, e.g., amide, urethane, secondary or tertiary amine and imine. On the other hand, the

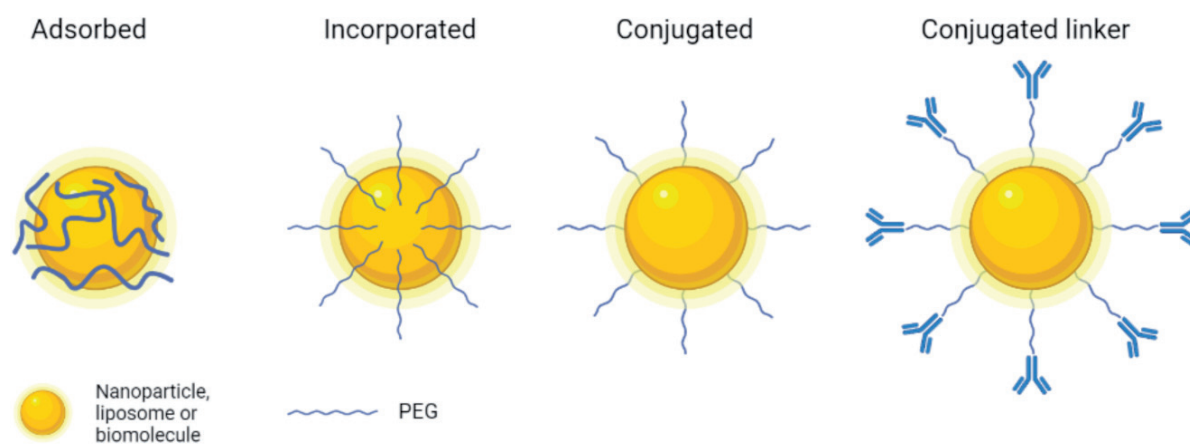


Figure 1. Possible ways of attaching PEG (created with BioRender.com)

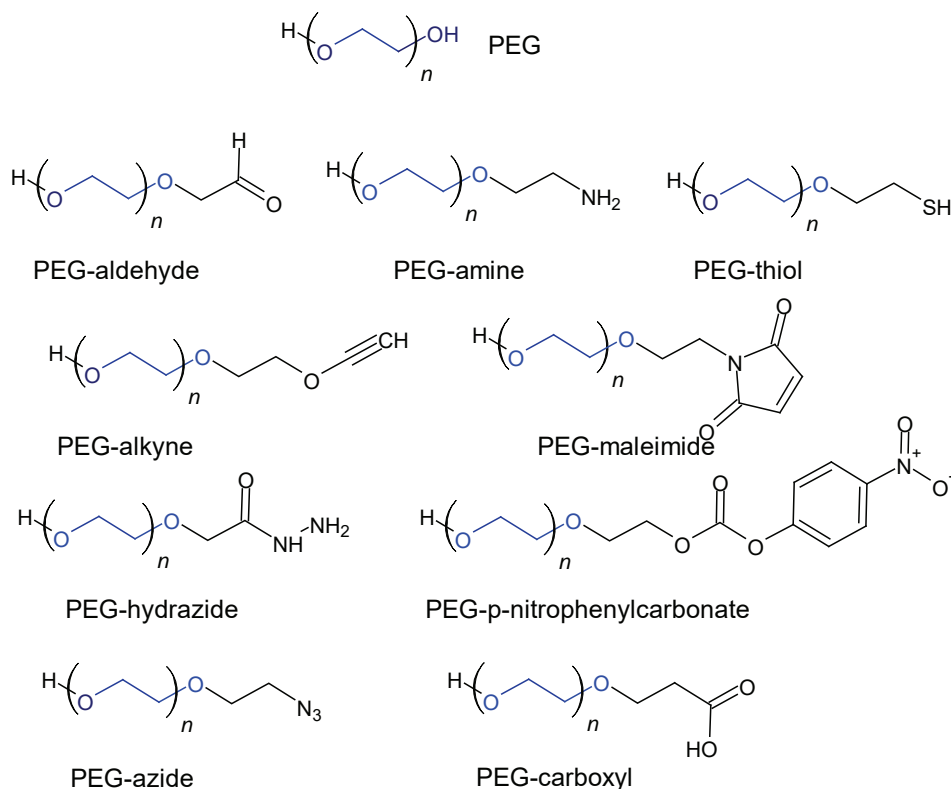


Figure 2. Examples of reagents for introducing PEG chain into molecules

hydroxyl and thiol groups most often form ether and thioether connections. The pro-drug method is based on the temporary attachment of a glycol chain through bonds that undergo gradual hydrolysis (biotransformation) in the patient's body. Ester bonds are mainly used for this, ensuring better solubility and bioavailability at the formulation and administration stage while not reducing the effect of the original molecule. The disadvantage of this approach, however, is the lower stability of such combinations, especially during more extended storage, and the high dependence of the rate of hydrolysis on the patient's conditions [1, 2].

Proteins and enzymes

Until now, pegylation is most often used to modify proteins and enzymes. Several of them have already completed the clinical trial phase and have been approved by the European Medicines Agency (EMA) and US Food and Drug Administration (FDA) (**Table 1**). The primary purpose of protein pegylation is to increase the time they cir-

culate in the body. The pegylated proteins introduced for treatment include interferons used in melanoma and viral hepatitis [3, 4] and filgrastim to manage bone marrow suppression induced by chemotherapy [5]. There are also clinical trials of pegylated enzymes such as arginase and asparaginase in treating leukaemia [6, 7]. PEGylated proteins and enzymes are the groups with the most prominent and heaviest PEG substituents. They usually have a mass of several tens of thousands of Da and are very often branched chains. An additional advantage of protein pegylation is that it usually lowers the immunogenicity of the primary protein, which reduces the body's immune response to the administered drug [4].

Drug carriers

Efforts to increase the bioavailability of drugs have given rise to many forms of drug carriers and delivery systems. The two main groups currently receiving the most attention are liposomes and nanoparticles [15]. At the same time incorporating polyethylene glycol into the structure of drug

Table 1. Pegylated drugs approved by FDA [8–14]

Brand name	Active molecule	Attached PEG	Therapeutic target	Year of approval
Adagen	Adenosine deaminase	5 kDa – multiple chains	Severe combined immunodeficiency disease	1990
Oncaspar	Asparaginase	5 kDa – multiple chains	Acute lymphoblastic leukaemia	1994
Doxil	Liposomal doxorubicin	2 kDa	Ovarian cancer, multiple myeloma	1995
PegIntron	Interferon α -2b	12 kDa	Hepatitis C	2001
Pegasys	Interferon α -2a	40 kDa – branched	Hepatitis C	2001
Neulasta	Filgrastim	20 kDa	Neutropenia	2002
Somavert	Growth hormone receptor antagonist	4–6 x 5 kDa	Acromegaly	2003
Macugen	Anti-VEGF aptamer	40 kDa – branched	Macular degeneration	2004
Mircera	Epoetin- β	30 kDa	Chronic kidney disease-associated anaemia	2007
Cimzia	Anti-TNF Fab	40 kDa – branched	Rheumatoid arthritis and Crohn's disease	2008
Asclera	Dodecyl alcohol	400 Da	Varicose veins	2010
Krystexxa	Uricase	9–11 x 10 kDa	Chronic gout	2010
Sylatron	Interferon α -2b	12 kDa	Melanoma	2011
Omontys	Erythropoietin-mimetic homodimeric peptide	40 kDa – branched	Chronic kidney disease-associated anaemia	2012
Movantik	Naloxone	339 Da	Opioid-induced constipation	2014
Plegridy	Interferon β -1a	20 kDa	Multiple sclerosis	2014
Adynovate	Coagulation factor VIII	20 kDa	Haemophilia A	2015
Rebinyon	Coagulation factor IX	40 kDa	Haemophilia B	2017
Jivi	Coagulation factor VIII	60 kDa	Haemophilia A	2018
Palynziq	Phenylalanine ammonia-lyase	20 kDa	Phenylketonuria	2018
Revcovi	Adenosine deaminase	80 kDa	Adenosine deaminase severe combined immunodeficiency	2018
Asparlas	L-asparaginase	31–39 x 5 kDa	Leukaemia	2018
Udenyca	G-CSF	20 kDa	Infection during chemotherapy	2018
Ziextenzo	G-CSF	20 kDa	Infection during chemotherapy	2019
Esperoct	Coagulation factor IX	40 kDa	Haemophilia A	2019
Nyvepria	G-CSF	20 kDa	Chemotherapy associated neutropenia	2020
Empaveli	Compstatin	40 kDa	Paroxysmal nocturnal hemoglobinuria	2021
Skytrofa	Human growth hormone	4 x 10 kDa	Growth hormone deficiency	2021
Besremi	Interferon α -2b	40 kDa	Polycythemia vera	2021

carriers such as liposomes and nanoparticles is gaining more and more popularity. Such usage does not require modification of the active compound structure. PEG in liposomes is usually an additive to the formulation, while in nanoparticles, it depends on their nature. In the case of metallic nanoparticles, it can be a covalent bond that is very durable, or it can be adsorption based. In PEG liposomes, they most often play a stabilizing and protective role [16]. PEG-containing liposomes significantly improve pharmacokinetic parameters over conventional liposomes and free drugs. PEGs with molar masses in the range of 2–5 kDa are best suited for application [17]. Nawalany et al. have conducted a comparison study in which they test pegylated porphyrin against a non-pegylated

compound enclosed in pegylated liposomes. They note that both approaches reduce the dark cytotoxicity but liposomes retain higher activity when exposed to light. The liposomes also internalize the non-pegylated porphyrin into cells faster and in higher concentrations than pegylated porphyrin on its own [18]. The EU and US have approved pegylated liposomal formulation of doxorubicin for treating various cancers for over 25 years. Better pharmacokinetic profile, longer circulation time and lower toxicity are characteristics of the formulation [19]. Pegylation can also significantly improve liposome stability during long-term storage without any negative impact on the delivery of the therapeutic, as shown by Knudsen et al. in their study. Wherein pegylated liposomes con-

taining calcipotriol – a synthetic vitamin D analogue used in psoriasis treatment, were examined and compared with normal ones [20]. Unfortunately, pegylation is not always a perfect solution, as demonstrated during the development of liposomal formulations of vincristine. One of the big problems is its high leakage through the membranes outside the liposomes. It was demonstrated that adding PEG slows down this process, although further studies are necessary for clinical application [21]. Due to their nature, nanoparticles are often accumulated by the phagocytic system and thus removed from circulation. Aggregation, which can lead to the congestion of capillaries, is still another problem. Therefore, it is necessary to protect them by coating them with various molecules, out of which PEG is the most often used [22]. Covering the surface of nanoparticles prevents aggregation and the response of the phagocytic system. As a result, the time they stay in the bloodstream increases. The most frequently used PEGs for this purpose have a mass of several thousand Da [23]. Pegylation can also increase the circulation time of nanoparticles made from biodegradable polymers like PLGA (poly lactic-co-glycolic acid), an emerging material in controlled drug release systems. Adding PEG to the polymer shields it from hydrolysis and enables copolymer to form micelles for drug transport [24]. Similarly, the nanoparticles made from mesoporous materials have gained much interest recently. Although not fault-free, pegylation can help overcome them. Zhu et al. showed one of the examples in their work on pegylated mesoporous silica nanoparticles as drug carriers. They demonstrate, as many others, better stability and dispersity in aqueous conditions as well as lower toxicity of nanoparticles themselves. Simultaneously, when loaded with doxorubicin, the pegylated carriers exhibit higher cellular uptake and stronger cytotoxic activity against cancer cells than free doxorubicin [25].

PDT and photosensitisers

Photodynamic Therapy (PDT) uses various light-absorbing dyes as photosensitisers (PS) and their ability to produce singlet oxygen or other Reactive Oxygen Species (ROS) to kill cancer cells or pathogenic microorganisms. PS can

be applied topically or intravenously, and after it builds up in the cells, it is irradiated with visible light. Illumination activates the photosensitiser, which can then transfer its surplus energy to a molecule such as oxygen and form ROS or directly to the building blocks of cells such as DNA, proteins, and structural elements like membrane, mitochondria and cell walls. The main goal of PDT is to induce oxygen to its reactive singlet state, which then reacts with cellular mechanisms causing damage and leading to apoptosis [26, 27].

Photosensitisers, by their nature, are often compounds with many conjugated double bonds, making them usually highly hydrophobic molecules with poor water solubility. The feature is very unfavourable for its usefulness in photodynamic therapy. One of the main challenges in successful PDT is the even distribution of photosensitiser within a tumour and selectivity against cancer cells. Only a few photosensitisers have been clinically approved, and a few more are in the clinical trial phase [28]. The quaternisation of pyridyl or amino groups, sulfonation, carboxylation and pegylation are typical modifications to increase photosensitisers solubility in water [29]. Another possibility is to enclose photosensitisers in liposomes, which allows them to be dispersed in an aqueous medium. Liposomes can also be modified to increase the ability of compounds to target cancer [16].

One of the more promising modifications of the photosensitiser molecule is pegylation, which links PS to polyethylene glycol chains to increase the water solubility of such conjugates [30]. Other advantages of pegylation include increased stability and better bioavailability. The most common method of photosensitiser pegylation is the permanent introduction of polyethylene glycol chains into the photosensitiser molecule via a stable covalent bond. The vast majority of clinically used photosensitisers have the structure of pyrrole macrocycles [31]. Macrocyclic pyrrole-derived compounds, includes porphyrins, benzoporphyrins, chlorins, porphyrazines, phthalocyanines, naphthalocyanines, corroles and others. These are molecules that usually consist of four pyrrole molecules. The core of these macrocyclic molecules is strongly hydrophobic and mostly soluble in non-polar solvents or insoluble. Numerous solution attempts are being made to

incorporate PEG chains or linkers into their structure. Pavlíčková et al. demonstrated a pegylated derivative of purpurin 18 that exhibits significantly higher photodynamic activity against many cancer cell lines compared to the parent molecule, even with a lower quantum yield of singlet oxygen generation (**Figure 3**) [32]. Zhdanova et al. presented the synthesis of various asymmetric pegylated porphyrins in their work. They show an easy method to obtain many compounds for high throughput studies (**Figure 3**) [33].

PEG chains are universal linkers, as demonstrated by Darwish et al. In their work on phthalocyanine conjugated to a monoclonal antibody directed against multiple myeloma. They achieved good photodynamic activity in the nanomolar range [34]. Purushothaman et al. report their success in creating self-assembled nanoparticles of hydrophobic porphyrin and biotin with a PEG linker and encapsulated doxorubicin. They show synergistic effects of combining traditional chemotherapy and PDT (**Figure 4**) [35].

Such amphiphilic molecules can be more easily tested in aqueous solutions exhibiting different photophysical properties than in organic solvents. Mandal et al. demonstrated this in their publications on unsymmetrical porphyrins, chlorins and bacteriochlorins. The authors extensively study the photophysical properties of water-soluble compounds from these groups ready to be combined with other molecules or

carriers [37–39]. Natural protoporphyrin IX can be very easily modified with PEG chains by esterification, which significantly increases its photodynamic activity. At the same time, pegylation substantially improves the therapeutic index, thus increasing the safety of use (**Figure 4**) [36]. The literature mentions the ability to form nanoparticles in the self-assembly of compounds with PEG chains in their structure without using additional stabilizers or surfactants [35, 40, 41]. In addition, the complexing properties of metals by these macrocycles make them excellent candidates for use in radio imaging with the help of radioactive isotopes such as copper ^{64}Cu [42]. The length and number of PEG chains have a significant influence on the properties of the final compounds. Mewis et al. noted that direct comparison is difficult because many authors publish compounds with a different number of substituents and largely non-uniform PEG chain length [43]. Kępczyński et al. Carried out studies of a hydrophobic porphyrin with one very long PEG chain with a mass of 8 kDa, including studies of aggregation, dissociation and interaction with liposomes. The authors note that adding PEGylated porphyrin increases the liposomes' size slightly while increasing their stability [44]. Later, in their work, a part of the same team compared the different porphyrin chain lengths and their in vitro efficacy. It is noteworthy that increasing the chain length increases the cytotoxicity in the light without affecting the

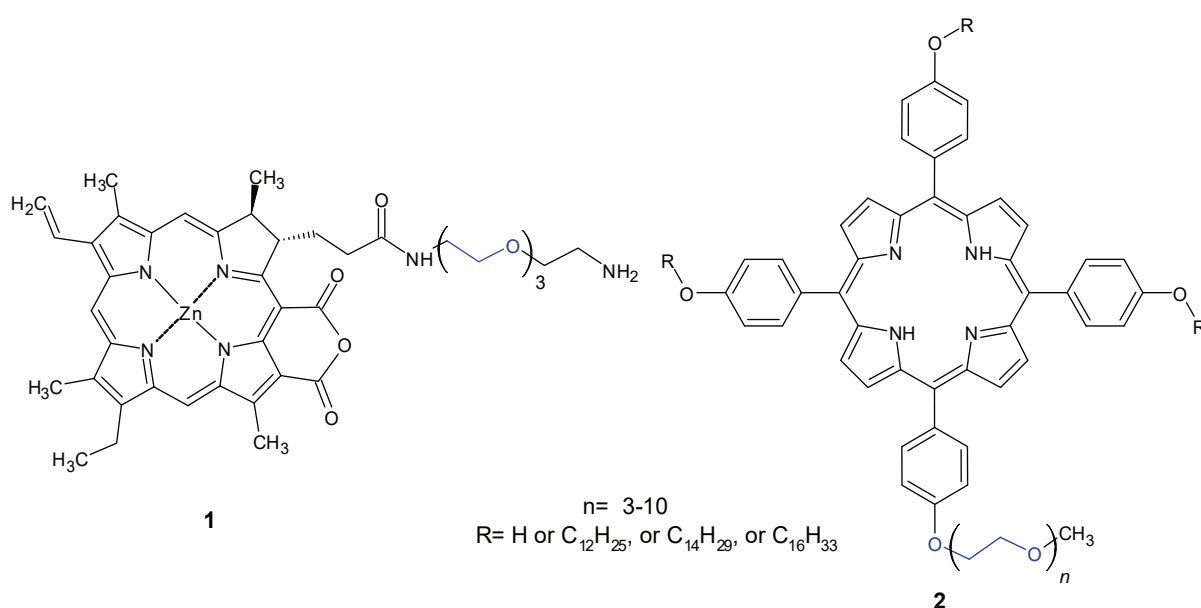


Figure 3. Purpurin 18 derivative designed by Pavlíčková et al. – 1 [32] and porphyrin derivatives – 2 designed by Zhdanova et al. [33]

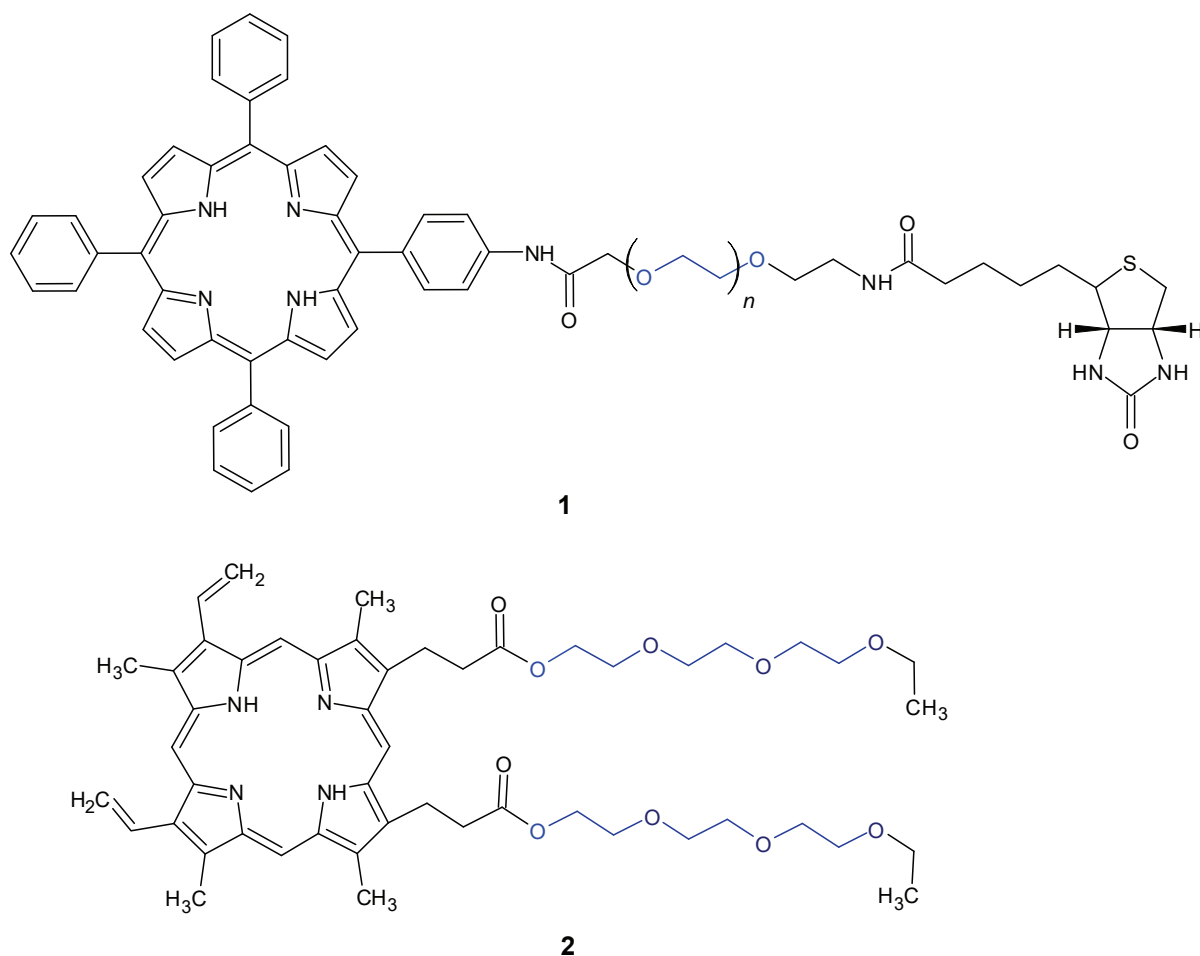


Figure 4. Porphyrin biotin conjugate with PEG linker – 1 [35], protoporphyrin IX PEG ester – 2 [36]

cytotoxicity in the dark. However, too long a chain reduces the efficacy of the compound. Therefore, PEG with a mass of approx. 2 kDa turned out to be the most optimal [45]. There is, however, a growing body of research in using short PEG chains below 1000Da, utilizing their small size to achieve similar results as their bigger brothers. Their main advantage is size uniformity which allows for much greater precision when tailoring the amphiphilic balance of the studied compound [46]. At the same time, it is worth noting that more is only sometimes better. For example, Sibrian-Vazquez et al. investigated the penetration of porphyrins modified with various amounts of polyethylene glycol chains inside the cell. They noticed that the presence of one and two chains in the molecule promotes the penetration of the test compound into the cells. Conversely, 3–4 chains significantly reduce their ability to penetrate the membranes [47]. On the other hand, in the literature, there are examples of numerous substituted

phthalocyanines containing up to 8 short chains of PEG, which achieve excellent activity against cancer cells and viruses at the same time [48].

Classic therapy and small molecule drugs

The drugs most commonly used in traditional therapies are small molecules that target receptors or active sites in enzymes. Contrary to photodynamic therapy, traditional drugs must fit into small spaces present in macromolecules to modify their action. The placement of large functional groups, as PEG chains very often are, can have positive and negative consequences. Hamidi et al. reviewed several advantages, such as increased circulation time of PEG-modified drugs in the blood, alteration of the elimination profile towards biliary elimination instead of renal filtration, and accumulation in neoplastic cells [49].

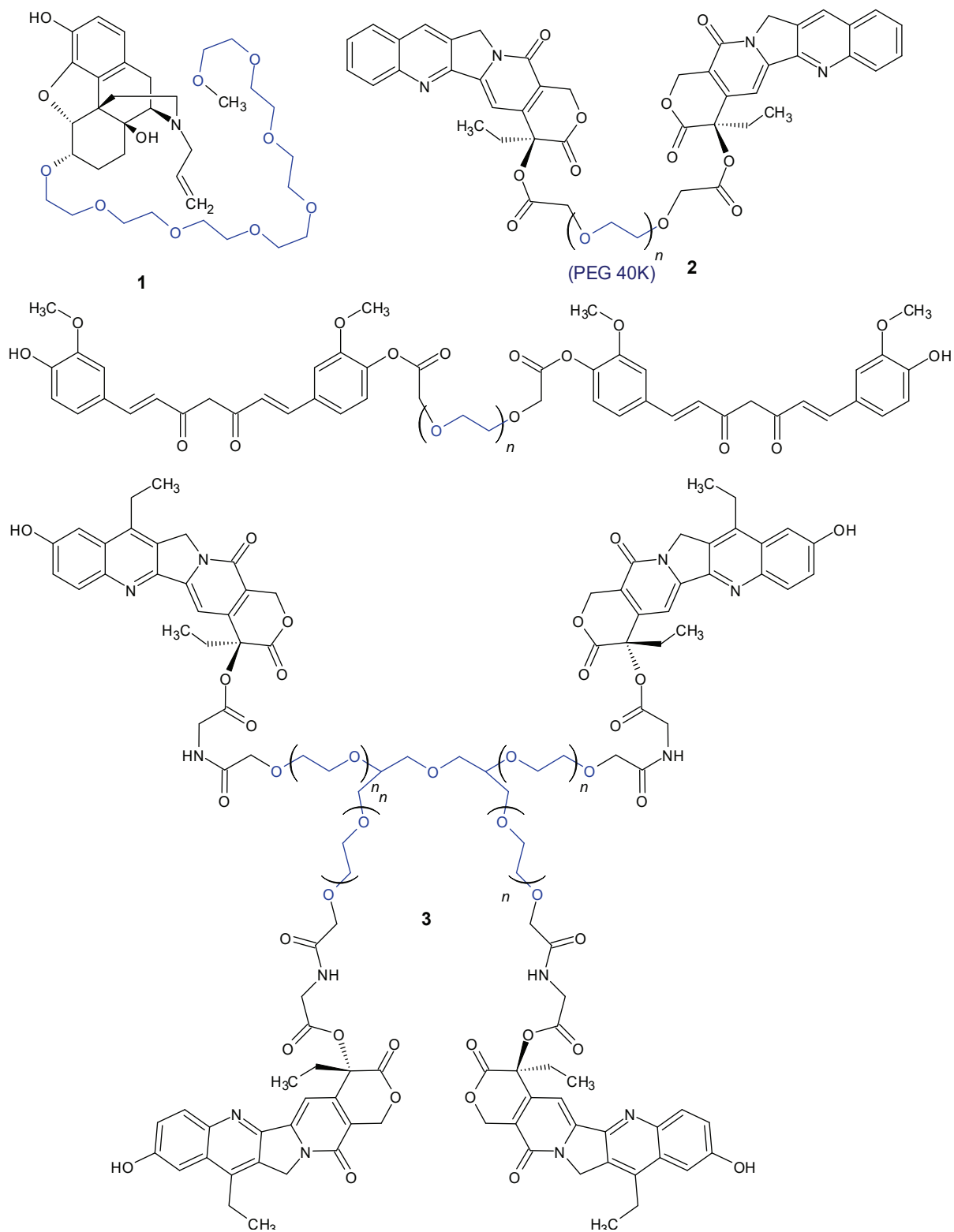


Figure 5. Structures of pegylated naloxol – 1 [54], pegylated camptothecin derivative – 2 [53] and camptothecin derivative with multibranching PEG – 3 [53]

An excellent example of the problems associated with small molecule pegylation is the research by Greenwald et al. Carried out in the 1990s. The taxol modifications they obtained became much more soluble in water, but unfortunately, they lost a significant part of their anticancer activity [50]. So far, most research has focused on the pegylation of large molecules such as proteins and enzymes. In modifying small molecule drug candidates, a few, including pegylated derivatives of irinotecan, camptothecin (**Figure 5**), doxorubicin and docetaxel, have proceeded to Phase III clinical trials [7, 51, 52]. Many other molecules, often PEG-modified cytostatic drugs in use today, are at an earlier stage. These include paclitaxel, carboplatin (**Figure 6**), gemcitabine, methotrexate and lamellarin derivatives (**Figure 6**). There are also reports on pegylated drugs from other therapeutic groups like e.g. acyclovir, gentamicin, zidovudine and amphotericin B [53]. In 2014, the EMA and the FDA approved a pegylated derivative of naloxol for treating constipation caused by opioids (**Figure 5**) [9].

An interesting pegylation variation is combining active particles with crown ethers (**Figure 6**). These cyclic versions of polyethylene glycol can complex metal ions such as sodium and potassium. They can also lock small molecules of drugs inside them. Thus, they can significantly facilitate the penetration of the lipid membranes of cells.

Their use for creating non-ionic liposomes by combining with a lipophilic molecule, e.g. cholesterol, has also been described [55].

Problems to be solved

Despite its very many desirable properties, the use of PEG is not free of drawbacks. In the last 20 years, reports have begun to emerge about the opposite of the expected effects of molecules in combination with PEG – shortening of circulation time, no reduction or even increased binding of drugs by proteins, and reduced ability to penetrate membranes. Studies of new combinations of therapeutics with PEG very often test only one type of PEG of a particular length or introduce a certain amount of PEG chains into the modified molecule without systematically comparing the effect of varying their amount on the properties of the resulting conjugate. Due to the production method, it is natural for the distribution of PEG molecular masses to span even often several thousand Da. The above contradicts the assumptions of bringing strictly formulated therapeutics with a defined structure to the market. The discovery of antibodies directed against PEG has become another problem. They pose a serious challenge because they can significantly affect the efficacy of all pegylated therapeutics admin-

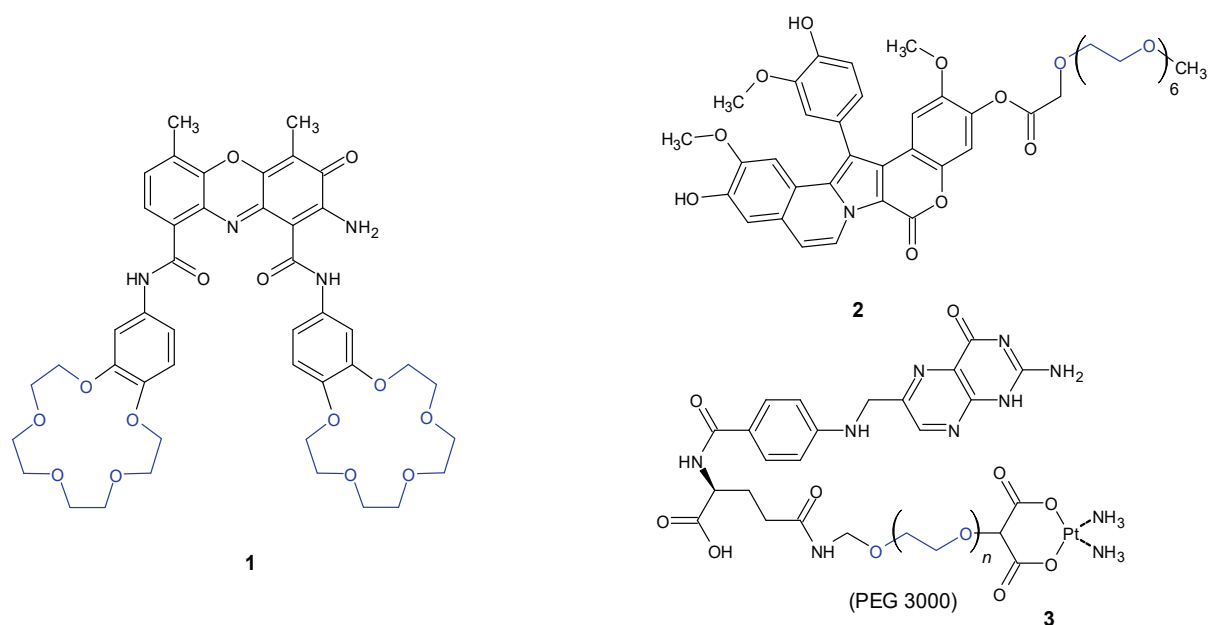


Figure 6. Antinocin conjugated with crown ethers – 1 [55], pegylated lamellarin derivative – 2 [53] and carboplatin with PEG linker and folate designed to target cancer cells – 3 [53]

istered subsequently, regardless of whether they are directed at treating different ailments [56, 57]. One of the challenges in using PEG is finding the appropriate balance in the amount. Adding too much PEG to the liposomes or copolymer nanoparticles results in too fast a release of the transported drug leading to a burst increase in concentration which can, of course, cause toxic effects. Depending on the modified particle and PEG chain chosen, liposomes and nanoparticles exhibit shorter circulation times and accumulate in the liver in the same way as non-pegylated versions. One possible explanation for this is the particle size increase after pegylation, making them easier to capture by RES (reticuloendothelial system) macrophages [56, 58–60]. A notable drawback of PEG is that while it is considered biocompatible, it is not biodegradable. Some pegylated drugs have been shown to accumulate in cytoplasmic vacuoles. Moreover, while currently, there are no known toxicological effects of this phenomenon, it still warrants further research. Especially as long-term consequences are completely unknown. An additional concern relates to the big size of PEG pendants in proteins and small molecules. While protecting them from elimination they can significantly lower their activity, by as much as 93% [61]. Most of this effect stems from the same shielding property of PEG as it can interfere with the therapeutic binding either to the active site where it is supposed to act or block the access of substrates to the active site of the pegylated enzyme [62]. Many of these concerns stem from no detailed research on the effects of the PEG chain length on the modified particle. The number of substitutions or the amount of PEG in a formulation is the second most important consideration.

Summary

Progress in medicine and pharmacy causes a constant increase in the number of therapeutics containing polyethylene glycol chains in their structure. An increasing representation of this compound type appears in the second and third clinical trial phases. Literature reports confirm that more and more new compounds are designed from scratch, taking into account the favourable properties of PEG. The emerging difficulties in the

purification and response of the immune system are a reason to consider the direction of these modifications. Pegylation can also offer opportunities for the return to therapy of drugs that may have been discontinued due to their pharmacokinetic properties. It also improves the properties of currently used drugs that do not have an alternative in the form of newer drugs. Pegylation also opens up new possibilities for emerging compounds that might not proceed to the further research phase due to problems with formulation or bioavailability. In conclusion, pegylation is an excellent modification method, but more detailed studies are needed comparing the effects of different lengths and numbers of chains.

Acknowledgements

Conflict of interest statement

The authors declare no conflict of interest.

Funding sources

There are no sources of funding to declare.

References

1. Greenwald RB, Choe YH, McGuire J, Conover CD. Effective drug delivery by PEGylated drug conjugates. *Adv Drug Deliv Rev.* 2003;55(2):217–50.
2. D'souza AA, Shegokar R. Polyethylene glycol (PEG): a versatile polymer for pharmaceutical applications. *Expert Opin Drug Deliv [Internet].* 2016;13(9):1257–75. doi: 10.1080/17425247.2016.1182485.
3. Herndon TM, Demko SG, Jiang X, He K, Gootenberg JE, Cohen MH, et al. U.S. Food and Drug Administration Approval: Peginterferon-alfa-2b for the Adjuvant Treatment of Patients with Melanoma. *Oncologist [Internet].* 2012 Oct 1;17(10):1323–8. Available from: <https://academic.oup.com/oncolo/article/17/10/1323/6400884>.
4. Jevševar S, Kunstelj M, Porekar VG. PEGylation of therapeutic proteins. *Biotechnol J.* 2010;5(1):113–28.
5. Vogel CL, Wojtukiewicz MZ, Carroll RR, Tjulandin SA, Barajas-Figueroa LJ, Wiens BL, et al. First and subsequent cycle use of pegfilgrastim prevents febrile neutropenia in patients with breast cancer: A multicenter, double-blind, placebo-controlled phase III study. *J Clin Oncol.* 2005;23(6):1178–84.
6. Dinndorf PA, Gootenberg J, Cohen MH, Keegan P, Pazdur R. FDA Drug Approval Summary: Pegaspargase (Oncaspar®) for the First-Line Treatment of Children with Acute Lymphoblastic Leukemia (ALL). *Oncologist.* 2007;12(8):991–8.
7. Mishra P, Nayak B, Dey RK. PEGylation in anti-cancer therapy: An overview. *Asian J Pharm Sci [Internet].* 2016;11(3):337–48. doi: 10.1016/j.ajps.2015.08.011.
8. FDA Approved PEGylated Drugs Up To 2022 | Biopharma PEG [Internet]. [cited 2022 Oct 18]. Available from: <https://www.biochempeg.com/article/58.html>

9. Park EJ, Choi J, Lee KC, Na DH. Emerging PEGylated non-biologic drugs. *Expert Opin Emerg Drugs* [Internet]. 2019;24(2):107–19. doi: 10.1080/14728214.2019.1604684.
10. Swierczewska M, Lee KC, Lee S. What is the future of PEGylated therapies? *Expert Opin Emerg Drugs* [Internet]. 2015;20(4):531–6. doi: 10.1517/14728214.2015.1113254.
11. Yadav D, Dewangan HK. PEGYLATION: an important approach for novel drug delivery system. *J Biomater Sci Polym Ed* [Internet]. 2021;32(2):266–80. doi: 10.1080/09205063.2020.1825304.
12. Hoy SM. Pegcetacoplan: First Approval. *Drugs* [Internet]. 2021;81(12):1423–30. doi: 10.1007/s40265-021-01560-8.
13. Sravanthi S, Kumari MM, Sharma JVC, Peg R. A Critique View On Skytrofa. 2021;4(11):188–91.
14. Aschenbrenner DS. New Treatment for Polycythemia Vera. *AJN, Am J Nurs* [Internet]. 2022 Mar;122(3):18–9. Available from: <https://journals.lww.com/10.1097/01.NAJ.0000822968.37066.5c>
15. Jadach B. From the carrier of active substance to drug delivery systems. *J Med Sci*. 2017;86(3):231–6.
16. Ghosh S, Carter KA, Lovell JF. Liposomal formulations of photosensitizers. *Biomaterials* [Internet]. 2019;218(April):119341. doi: 10.1016/j.biomaterials.2019.119341.
17. Allen TM. Long-circulating (sterically stabilized) liposomes for targeted drug delivery. *Trends Pharmacol Sci*. 1994;15(7):215–20.
18. Nawalany K, Rusin A, Kepczyński M, Mikhailov A, Kramer-Marek G, Śnietura M, et al. Comparison of photodynamic efficacy of tetraarylporphyrin pegylated or encapsulated in liposomes: In vitro studies. *J Photochem Photobiol B Biol*. 2009;97(1):8–17.
19. Duggan ST, Keating GM. Pegylated Liposomal Doxorubicin. *Drugs* [Internet]. 2011 Dec;71(18):2531–58. Available from: <http://link.springer.com/10.2165/11207510-000000000-00000>.
20. Knudsen NØ, Rønholdt S, Salte RD, Jorgensen L, Thormann T, Basse LH, et al. Calcipotriol delivery into the skin with PEGylated liposomes. *Eur J Pharm Biopharm*. 2012;81(3):532–9.
21. Wang X, Song Y, Su Y, Tian Q, Li B, Quan J, et al. Are PEGylated liposomes better than conventional liposomes? A special case for vincristine. *Drug Deliv* [Internet]. 2016;23(4):1092–100. doi: 10.3109/10717544.2015.1027015.
22. Amoozgar Z, Yeo Y. Recent advances in stealth coating of nanoparticle drug delivery systems. *Wiley Interdiscip Rev Nanomedicine Nanobiotechnology*. 2012;4(2):219–33.
23. Jakerst JV, Lobovkina T, Zare RN, Gambhir SS. Nanoparticle PEGylation for imaging and therapy. *Nanomedicine*. 2011;6(4):715–28.
24. Locatelli E, Franchini MC. Biodegradable PLGA-b-PEG polymeric nanoparticles: Synthesis, properties, and nanomedical applications as drug delivery system. *J Nanoparticle Res*. 2012;14(12):1–17.
25. Zhu Y, Fang Y, Borhardt L, Kaskel S. PEGylated hollow mesoporous silica nanoparticles as potential drug delivery vehicles. *Microporous Mesoporous Mater* [Internet]. 2011;141(1–3):199–206. doi: 10.1016/j.micromeso.2010.11.013.
26. Kübler AC. Photodynamic therapy. *Med Laser Appl*. 2005;20(1):37–45.
27. MACDONALD IJ, DOUGHERTY TJ. Basic principles of photodynamic therapy. *J Porphyrins Phthalocyanines* [Internet]. 2001 Feb;05(02):105–29. Available from: <http://www.worldscientific.com/doi/abs/10.1002/jpp.328>.
28. Baskaran R, Lee J, Yang SG. Clinical development of photodynamic agents and therapeutic applications. *Biomater Res*. 2018;22:1–8.
29. Luciano M, Bruckner C. Modifications of porphyrins and hydroporphyrins for their solubilization in aqueous media. Vol. 22, *Molecules*. 2017.
30. Milton Harris J, Martin NE, Modi M. Pegylation: A novel process for modifying pharmacokinetics. *Clin Pharmacokinet*. 2001;40(7):539–51.
31. Gunaydin G, Gedik ME, Ayan S. Photodynamic Therapy for the Treatment and Diagnosis of Cancer—A Review of the Current Clinical Status. *Front Chem*. 2021;9(August):1–26.
32. Pavličková V, Rimpelová S, Jurášek M, Záruba K, Fährnich J, Křížová I, et al. PEGylated purpurin 18 with improved solubility: Potent compounds for photodynamic therapy of cancer. *Molecules*. 2019;24(24):1–25.
33. Zhdanova KA, Cherepanova KS, Bragina NA, Mironov AF. New pegylated unsymmetrical meso-arylporphyrins as potential photosensitizers. *Macroheterocycles*. 2016;9(2):169–74.
34. Darwish WM, Bayoumi NA, El-Shershaby HM, Allahloubi NM. Targeted photoimmunotherapy based on photosensitizer-antibody conjugates for multiple myeloma treatment. *J Photochem Photobiol B Biol* [Internet]. 2020;203(January):111777. doi: 10.1016/j.jphotobiol.2020.111777.
35. Purushothaman B, Choi J, Park S, Lee J, Samson AAS, Hong S, et al. Biotin-conjugated PEGylated porphyrin self-assembled nanoparticles co-targeting mitochondria and lysosomes for advanced chemophotodynamic combination therapy. *J Mater Chem B*. 2019;7(1):65–79.
36. Wierzychowski M, Łażewski D, Tardowski T, Grochocka M, Czajkowski R, Sobiak S, et al. Nanomolar photodynamic activity of porphyrins bearing 1,4,7-trioxanonyl and 2-methyl-5-nitroimidazole moieties against cancer cells. *J Photochem Photobiol B Biol* [Internet]. 2020;202(October 2019):111703. doi: 10.1016/j.jphotobiol.2019.111703.
37. Mandal AK, Sahin T, Liu M, Lindsey JS, Bocian DF, Holten D. Photophysical comparisons of PEGylated porphyrins, chlorins and bacteriochlorins in water. *New J Chem* [Internet]. 2016;40(11):9648–56. doi: 10.1039/C6NJ02091G
38. Zhang N, Jiang J, Liu M, Taniguchi M, Mandal AK, Evans-Storms RB, et al. Bioconjugatable, PEGylated hydroporphyrins for photochemistry and photomedicine. Narrow-band, near-infrared-emitting bacteriochlorins. *New J Chem* [Internet]. 2016;40(9):7750–67. doi: 10.1039/C6NJ01155A

39. Liu M, Chen CY, Mandal AK, Chandrashaker V, Evans-Storms RB, Pitner JB, et al. Bioconjugatable, PEGylated hydroporphyrins for photochemistry and photomedicine. Narrow-band, red-emitting chlorins. *New J Chem* [Internet]. 2016;40(9):7721–40. doi: 10.1039/C6NJ01154C
40. Ding F, Li C, Xu Y, Li J, Li H, Yang G, et al. PEGylation Regulates Self-Assembled Small-Molecule Dye-Based Probes from Single Molecule to Nanoparticle Size for Multifunctional NIR-II Bioimaging. *Adv Healthc Mater*. 2018;7(23):1–9.
41. Hou W, Xia F, Alves CS, Qian X, Yang Y, Cui D. MMP2-Targeting and Redox-Responsive PEGylated Chlorin e6 Nanoparticles for Cancer Near-Infrared Imaging and Photodynamic Therapy. *ACS Appl Mater Interfaces*. 2016;8(2):1447–57.
42. Cheng L, Jiang D, Kamkaew A, Valdovinos HF, Im HJ, Feng L, et al. Renal-Clearable PEGylated Porphyrin Nanoparticles for Image-Guided Photodynamic Cancer Therapy. *Adv Funct Mater*. 2017;27(34):1–10.
43. Mewis RE, Savoie H, Archibald SJ, Boyle RW. Synthesis and phototoxicity of polyethylene glycol (PEG) substituted metal-free and metallo-porphyrins: Effect of PEG chain length, coordinated metal, and axial ligand. *Photodiagnosis Photodyn Ther*. 2009;6(3–4):200–6.
44. Kepczyński M, Nawalany K, Jachimska B, Romek M, Nowakowska M. Pegylated tetraarylporphyrin entrapped in liposomal membranes. A possible novel drug-carrier system for photodynamic therapy. *Colloids Surfaces B Biointerfaces*. 2006;49(1):22–30.
45. Nawalany K, Rusin A, Kepczynski M, Filipczak P, Kumorek M, Kozik B, et al. Novel nanostructural photosensitizers for photodynamic therapy: In vitro studies. *Int J Pharm* [Internet]. 2012;430(1–2):129–40. doi: 10.1016/j.ijpharm.2012.04.016.
46. Lazewski D, Kucinska M, Potapskiy E, Kuzminska J, Tezyk A, Popenda L, et al. Novel Short PEG Chain-Substituted Porphyrins: Synthesis, Photochemistry, and In Vitro Photodynamic Activity against Cancer Cells. *Int J Mol Sci*. 2022;23(17).
47. Sibrian-Vazquez M, Jensen TJ, Vicente MGH. Synthesis and cellular studies of PEG-functionalized meso-tetraphenylporphyrins. *J Photochem Photobiol B Biol*. 2007;86(1):9–21.
48. Sobotta L, Wierzchowski M, Mierzwicki M, Gdaniec Z, Mielcarek J, Persoons L, et al. Photochemical studies and nanomolar photodynamic activities of phthalocyanines functionalized with 1,4,7-trioxanonyl moieties at their non-peripheral positions. *J Inorg Biochem* [Internet]. 2016;155:76–81. Available from: <http://www.sciencedirect.com/science/article/pii/S0162013415301112>.
49. Hamidi M, Azadi A, Rafiei P. Pharmacokinetic consequences of pegylation. *Drug Deliv*. 2006;13(6):399–409.
50. Greenwald RB, Pendri A, Bolikal D. Highly Water Soluble Taxol Derivatives: 7-Polyethylene Glycol Carbamates and Carbonates. *J Org Chem* [Internet]. 1995 Jan 1;60(2):331–6. Available from: <https://pubs.acs.org/doi/abs/10.1021/jo00107a010>.
51. Parveen S, Arjmand F, Tabassum S. Clinical developments of antitumor polymer therapeutics. *RSC Adv*. 2019;9(43):24699–721.
52. Zhang X, Wang H, Ma Z, Wu B. Effects of pharmaceutical PEGylation on drug metabolism and its clinical concerns. *Expert Opin Drug Metab Toxicol*. 2014;10(12):1691–702.
53. Li W, Zhan P, De Clercq E, Lou H, Liu X. Current drug research on PEGylation with small molecular agents. *Prog Polym Sci* [Internet]. 2013;38(3–4):421–44. doi: 10.1016/j.progpolymsci.2012.07.006.
54. Floettmann E, Bui K, Sostek M, Payza K, Eldon M. Pharmacologic profile of naloxegol, a peripherally acting μ -opioid receptor antagonist, for the treatment of opioid-induced constipation. *J Pharmacol Exp Ther*. 2017;361(2):280–91.
55. Chehardoli G, Bahmani A. The role of crown ethers in drug delivery. *Supramol Chem* [Internet]. 2019;31(4):221–38. doi: 10.1080/10610278.2019.1568432.
56. Verhoef JJF, Anchoroquy TJ. Questioning the use of PEGylation for drug delivery. *Drug Deliv Transl Res*. 2013;3(6):499–503.
57. Armstrong JK, Hempel G, Koling S, Chan LS, Fisher T, Meiselman HJ, et al. Antibody against poly(ethylene glycol) adversely affects PEG-asparaginase therapy in acute lymphoblastic leukemia patients. *Cancer* [Internet]. 2007 Jul 1;110(1):103–11. Available from: <https://onlinelibrary.wiley.com/doi/10.1002/cncr.22739>.
58. Sebak AA. Limitations of pegylated nanocarriers: Unfavourable physicochemical properties, biodistribution patterns and cellular and subcellular fates. *Int J Appl Pharm*. 2018;10(5):6–12.
59. Xu J, Gattacceca F, Amiji M. Biodistribution and Pharmacokinetics of EGFR-Targeted Thiolated Gelatin Nanoparticles Following Systemic Administration in Pancreatic Tumor-Bearing Mice. *Mol Pharm* [Internet]. 2013 May 6;10(5):2031–44. Available from: <https://www.ncbi.nlm.nih.gov/pmc/articles/PMC3624763/pdf/nihms412728.pdf>
60. Rafiei Pedram HA. IJN-121881-docetaxel-loaded-plga-and-plga-peg-nanoparticles-for-intrave. *Int J Nanomedicine*. 2017;12:935–47.
61. Zalipsky S, Harris JM. Introduction to Chemistry and Biological Applications of Poly(ethylene glycol). Vol. 680, ACS Symposium Series. 1997. 1–13 p.
62. Zhang F, Liu MR, Wan HT. Discussion about several potential drawbacks of PEGylated therapeutic proteins. *Biol Pharm Bull*. 2014;37(3):335–9.

A case of symmetrical drug-related intertriginous and flexural exanthema

Sweta Subhadarshani

Department of Dermatology, University of Cincinnati, Cincinnati, OH, United States

 <https://orcid.org/0000-0003-1199-8075>

Anisha P. Valluri

Joan C. Edwards School of Medicine, Huntington, WV, United States

 <https://orcid.org/0000-0002-7924-1581>

Corresponding author: valluri4@marshall.edu

Keywords: drug-induced rash, Symmetrical drug-related intertriginous and flexural exanthema, Amoxicillin

Published: 2022-12-30

How to Cite: Subhadarshani S, Valluri AP. A case of symmetrical drug-related intertriginous and flexural exanthema. *Journal of Medical Science*. 2022;91(4):e742. doi:10.20883/medical.e742

 doi: 10.20883/medical.e742



© 2022 by the author(s). This is an open access article distributed under the terms and conditions of the Creative Commons Attribution (CC BY-NC) license. Published by Poznan University of Medical Sciences

ABSTRACT

Symmetrical drug-related intertriginous and flexural exanthema (also known as Baboon syndrome) is a skin eruption in the intertriginous areas. It is believed to be a delayed-type hypersensitivity response to the drug which occurs secondary to systemic absorption of agents after cutaneous sensitization. Our case provides high quality clinical images to aid in clinical diagnosis of this uncommon skin eruption.

A 55-year-old woman presented to the clinic with a 3-day history of a pruritic macular rash that began in the inguinal area. There were no other constitutional symptoms. The rash developed two days after the first dose of amoxicillin 500 mg thrice daily, used as a presurgical prophylaxis. Six months prior, the patient had taken a five-day amoxicillin course for an upper respiratory tract infection. On examination, she had a symmetrical, erythematous, macular rash in the groins, on the buttocks, inframammary area, and in the cubital and popliteal fossa (**Figure 1 a–c**). After discontinuing the drug, the lesions resolved without treatment within five days. In addition, symmetrical drug-related intertriginous and flexural exanthema (SDRIFE) was diagnosed.

SDRIFE is a skin eruption in intertriginous areas. It is believed to be a delayed-type hypersensitivity response to the drug occurring secondary to systemic absorption of agents after cutaneous sensitization [1]. Drug interactions are most common with beta-lactam antibiotics, especially amoxicillin. Various medications, including antifungals, antihypertensives, chemotherapy, and monoclonal antibodies, can trigger this reaction [1]. The rash has a characteristic morphology i.e sharply demarcated erythema of the gluteal area or V-shaped erythema of the inguinal region, symmetry of affected areas, involvement of at least one other intertriginous site/flexural fold, and the absence of systemic symptoms and signs, which occurs after system-

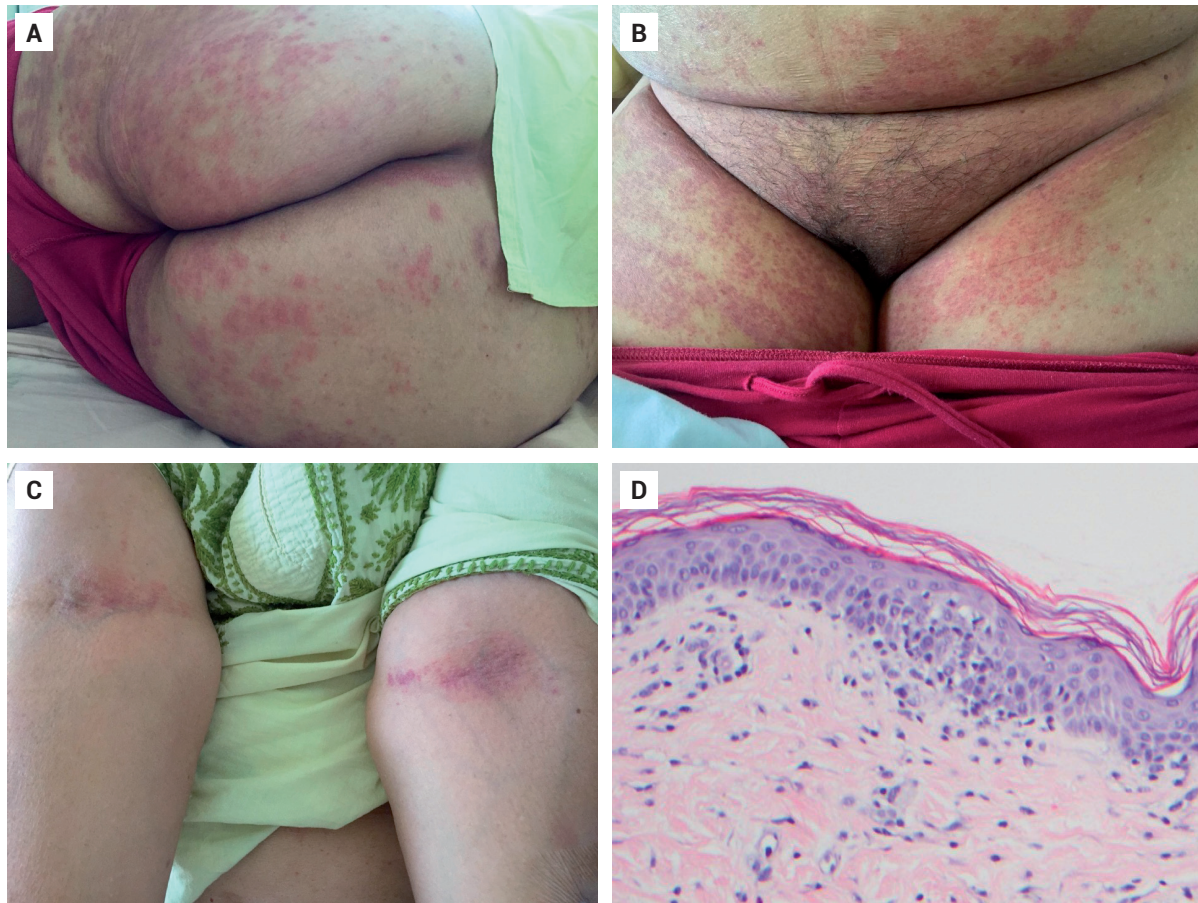


Figure 1. Symmetrical, erythematous, macular rash involving the buttocks, groin, and the cubital and popliteal fossa. (A-C) Histopathological evidence of perivascular infiltrates of lymphocytes and eosinophils (D)

ic exposure to the drug [2]. The case patient met all the criteria.

Histopathological findings include perivascular infiltrates of lymphocytes and eosinophils. However, histopathology is not needed to confirm the clinical diagnosis.

Acknowledgements

Conflict of interest statement

The authors declare no conflict of interest.

Funding sources

There are no sources of funding to declare.

References

1. Harbaoui S, Litaïem N. Symmetrical Drug-related Intertriginous and Flexural Exanthema. [Updated 2021 Oct 9]. In: StatPearls [Internet]. Treasure Island (FL): StatPearls Publishing; 2022 Jan-. Available from: <https://www.ncbi.nlm.nih.gov/books/NBK539750>.
2. de Risi-Pugliese T, Barailler H, Hamelin A, Amsler E, Gaouar H, Kurihara F, Jullie ML, Merrill ED, Barbaud A, Moguelet P, Milpied-Homsî B, Soria A. Symmetrical drug-related intertriginous and flexural exanthema: A little-known drug allergy. *J Allergy Clin Immunol Pract*. 2020 Oct;8(9):3185-3189.e4. doi: 10.1016/j.jaip.2020.04.052.

Journal of Medical Science (JMS) is a PEER-REVIEWED, OPEN ACCESS journal that publishes original research articles and reviews which cover all aspects of clinical and basic science research. The journal particularly encourages submissions on the latest achievements of world medicine and related disciplines. JMS is published quarterly by Poznan University of Medical Sciences.

ONLINE SUBMISSION:

Manuscripts should be submitted to the Editorial Office by an e-mail attachment: nowinylekarskie@ump.edu.pl. You do not need to mail any paper copies of your manuscript.

All submissions should be prepared with the following files:

- Cover Letter
- Manuscript
- Tables
- Figures
- Supplementary Online Material

COVER LETTER: *Manuscripts* must be accompanied by a *cover letter* from the author who will be responsible for correspondence regarding the manuscript as well as for communications among authors regarding revisions and approval of proofs. The cover letter should contain the following elements: (1) the full title of the manuscript, (2) the category of the manuscript being submitted (e.g. Original Article, Brief Report), (3) the statement that the manuscript has not been published and is not under consideration for publication in any other journal, (4) the statement that all authors approved the manuscript and its submission to the journal, and (5) a list of at least two referees.

MANUSCRIPT: Journal of Medical Science publishes Original Articles, Brief Reports, Review articles, Mini-Reviews, Images in Clinical Medicine and The Rationale and Design and Methods of New Studies. From 2014, only articles in English will be considered for publication. They should be organized as follows: Title page, Abstract, Introduction, Materials and Methods, Results, Discussion, Acknowledgments, Conflict of Interest, References and Figure Legends. All manuscripts should be typed in Arial or Times New Roman font and double spaced with a 2,5 cm (1 inch) margin on all sides. They should be saved in DOC, DOCX, ODT, RTF or TXT format. Pages should be numbered consecutively, beginning with the title page.

Ethical Guidelines

Authors should follow the principles outlined in the Declaration of Helsinki of the World Medical Association (www.wma.net). The manuscript should contain a statement that the work has been approved by the relevant institutional review boards or ethics committees and that all human participants gave informed consent to the work. This statement should appear in the Material and Methods section. Identifying information, including patients' names, initials, or hospital numbers, should not be published in written descriptions, illustrations, and pedigrees. Studies involving experiments with animals must be conducted with approval by the local animal care committee and state that their care was in accordance with institution and international guidelines.

Authorship:

According to the International Committee on Medical Journal Ethics (ICMJE), an author is defined as one who has made substantial contributions to the conception and development of a manuscript. Authorship should be based on all of the following: 1) substantial contributions to conception and design, data analysis and interpretation; 2) article drafting or critical advice for important intellectual content; and 3) final approval of the version to be published. All other contributors should be listed as acknowledgments. All submissions are expected to comply with the above definition.

Conflict of Interest

The manuscript should contain a conflict of interest statement from each author. Authors should disclose all financial and personal relationships that could influence their work or declare the absence of any conflict of interest. Author's conflict of interest should be included under Acknowledgements section.

Abbreviations

Abbreviations should be defined at first mention, by putting abbreviation between brackets after the full text. Ensure consistency of abbreviations throughout the article. Avoid using them in the title and abstract. Abbreviations may be used in tables and figures if they are defined in the table footnotes and figure legends.

Trade names

For products used in experiments or methods (particularly those referred to by a trade name), give the manufacturer's full name and location (in parentheses). When possible, use generic names of drugs.

Title page

The first page of the manuscript should contain the title of the article, authors' full names without degrees or titles, authors' institutional affiliations including city and country and a running title, not exceeding 40 letters and spaces. The first page should also include the full postal address, e-mail address, and telephone and fax numbers of the corresponding author.

Abstract

The abstract should not exceed 250 words and should be structured into separate sections: Background, Methods, Results and Conclusions. It should concisely state the significant findings without reference to the rest of the paper. The abstract should be followed by a list of 3 to 6 Key words. They should reflect the central topic of the article (avoid words already used in the title).

The following categories of articles can be proposed to the Journal of Medical Science:

ORIGINAL RESEARCH

Original articles: Manuscripts in this category describe the results of original research conducted in the broad area of life science and medicine. The manuscript should be presented in the format of Abstract (250-word limit), Keywords, Introduction, Material and Methods, Results, Discussion, Perspectives, Acknowledgments and References. In the Discussion section, statements regarding the importance and *novelty of the study* should be presented. In addition, the limitations of the study should be articulated. The abstract must be structured and include: Objectives, Material and Methods, Results and Conclusions. Manuscripts cannot exceed 3500 words in length (excluding title page, abstract and references) and contain no more than a combination of 8 tables and/or figures. The number of references should not exceed 45.

Brief Reports: Manuscripts in this category may present results of studies involving small sample sizes, introduce new methodologies, describe preliminary findings or replication studies. The manuscript must follow the same format requirements as full length manuscripts. Brief reports should be up to 2000 words (excluding title page, abstract and references) and can include up to 3 tables and/or figures. The number of references should not exceed 25.

REVIEW ARTICLES

Review articles: These articles should describe recent advances in areas within the Journal's scope. Review articles cannot exceed 5000 words length (excluding title page, abstract and references) and contain no more than a combination of 10 tables and/or figures. Authors are encouraged to restrict figures and tables to essential data that cannot be described in the text. The number of references should not exceed 80.

A THOUSAND WORDS ABOUT... is a form of Mini-Reviews. Manuscripts in this category should focus on *latest achievements of life science and medicine*. Manuscripts should be up to 1000 words in length (excluding title page, abstract and references) and contain up to 5 tables and/or figures and up to 25 most relevant references. The number of authors is limited to no more than 3.

OTHER SUBMISSIONS

Invited Editorials: Editorials are authoritative commentaries on topics of current interest or that relate to articles published in the same issue. Manuscripts should be up to 1500 words in length. The number of references should not exceed 10. The number of authors is limited to no more than 2.

Images in Clinical Medicine: Manuscripts in this category should contain one distinct image from life science or medicine. Only original and high-quality images are considered for publication. The description of the image (up to 250 words) should present relevant information like short description of the patient's history, clinical findings and course, imaging techniques or molecular biology techniques (e.g. blotting techniques or immunostaining). All labeled structures in the image should be described and explained in the legend. The number of references should not exceed 5. The number of authors is limited to no more than 5.

The Rationale, Design and Methods of New Studies: Manuscripts in this category should provide information regarding the grants awarded by different founding agencies, e.g. National Health Institute, European Union, National Science Center or National Center for Research and Development. The manuscript should be presented in the format of Research Project Objectives, Research Plan and Basic Concept, Research Methodology, Measurable Effects and Expected Results. The article should also contain general information about the grant: grant title, keywords (up to five), name of the principal investigator and co-investigators, founding source with the grant number, *Ethical Committee permission number*, code in clinical trials (if applicable). Only grant projects in the amount over 100,000 Euro can be presented. Manuscripts should be up to 2000 words in length (excluding references) and can include up to 5 tables and/or figures. The abstract should not exceed 150 words. The number of authors is limited to the Principal Investigator and Co-investigators.

Acknowledgements

Under acknowledgements please specify contributors to the article other than the authors accredited. List here those individuals who provided help during the research (e.g., providing language help, writing assistance or proof reading the article, etc.). Also acknowledge all sources of support (grants from government agencies, private foundations, etc.). The names of funding organizations should be written in full.

References

All manuscripts should use the 'Vancouver' style for references. References should be numbered consecutively in the order in which they appear in the text and listed at the end of the paper. References cited only in Figures/Tables should be listed in the end. Reference citations in the text should be identified by Arabic numbers in square brackets. Some examples:

- This result was later contradicted by Smith and Murray [3].
- Smith [8] has argued that...
- Multiple clinical trials [4–6, 9] show...

Journal names should be abbreviated according to Index Medicus. If available always provide Digital Object Identifier (DOI) or PubMed Identifier (PMID) for every reference.

Some examples

Standard journal articles

1. Petrova NV, Kashirskaya NY, Vasilyeva TA, Kondratyeva EI, Marakhonov AV, Macek Jr M, Ginter EK, Kutsev SI, Zinchenko RA. Characteristics of the L138Ins (p.Leu138dup) mutation in Russian cystic fibrosis patients. *JMS* [Internet]. 2020 Mar 31;89(1):e383. doi: 10.20883/medical.383.

Books

Personal author(s)

1. Rang HP, Dale MM, Ritter JM, Moore PK. *Pharmacology*. 5th ed. Edinburgh: Churchill Livingstone; 2003.

Editor(s) or compiler(s) as authors

2. Beers MH, Porter RS, Jones TV, Kaplan JL, Berkwitz M (editors). *The Merck manual of diagnosis and therapy*. 18th ed. Whitehouse Station (NJ): Merck Research Laboratories; 2006.

Chapter in the book

1. Phillips SJ, Whisnant JP. Hypertension and stroke. In: Laragh JH, Brenner BM, editors. *Hypertension: pathophysiology, diagnosis, and management*. 2nd ed. New York: Raven Press; 1995. p. 465–478.

TABLES: Tables should be typed on sheets separate from the text (each table on a separate sheet). They should be numbered consecutively with Arabic numerals. Tables should always be cited in text (e.g. table 2) in consecutive numerical order. Each table should include a compulsory, concise explanatory title and an explanatory legend. Footnotes to tables should be typed below the table body and referred to by superscript lowercase letters. No vertical rules should be used. Tables should not duplicate results presented elsewhere in the manuscript (e.g. in figures).

FIGURES: All illustrations, graphs, drawings, or photographs are referred to as figures and must be uploaded as separate files when submitting a manuscript. Figures should be numbered in sequence with Arabic numerals. They should always be cited in text (e.g. figure 3) in consecutive numerical order. Figures for publication must only be submitted in high-resolution TIFF or EPS format (*minimum 300 dpi resolution*). Each figure should be self-explanatory without reference to the text and have a concise but descriptive legend. All symbols and abbreviations used in the figure must be defined, unless they are common abbreviations or have already been defined in the text. Figure Legends must be included after the reference section of the Main Text.

Color figures: Figures and photographs will be reproduced in full colour in the online edition of the journal. In the paper edition, all figures and photographs will be reproduced as black-and-white.

SUPPLEMENTARY ONLINE MATERIAL: Authors may submit supplementary material for their articles to be posted in the electronic version of the journal. To be accepted for posting, supplementary materials must be essential to the scientific integrity and excellence of the paper. The supplementary material is subject to the same editorial standards and peer-review procedures as the print publication.

Review Process

All manuscripts are reviewed by the Editor-in-Chief or one of the members of the Editorial Board, who may decide to reject the paper or send it for external peer review. Manuscripts accepted for peer review will be blind reviewed by at least two experts in the field. After peer review, the Editor-in-Chief will study the paper together with reviewer comments to make one of the following decisions: accept, accept pending minor revision, accept pending major revision, or reject. Authors will receive comments on the manuscript regardless of the decision. In the event that a manuscript is accepted pending revision, the author will be responsible for completing the revision within 60 days.

Copyright

The copyright to the submitted manuscript is held by the Author(s), who grants the Journal of Medical Science (JMS) a nonexclusive licence to use, reproduce, and distribute the work, including for commercial purposes.